

PL-TR-94-2291

# **THE MULTI-FACTOR MODEL OF MAGNITUDE RESIDUALS AND THE PROBLEM OF THE PRECISE DETERMINATION OF MAGNITUDE**

**T. G. Rautian  
V.I. Khalturin**

**Columbia University in the City of New York  
Box 20  
Low Memorial Library  
New York, NY 10027**

**October, 1994**

**DTIC QUALITY INSPECTED 4**

**Scientific Report No. 4**

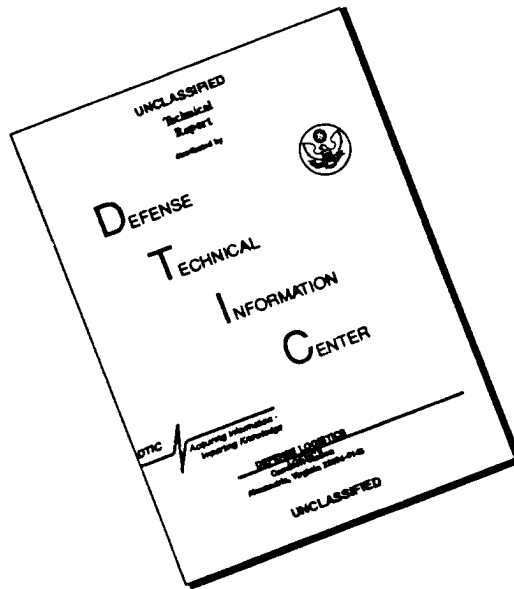
**19960705 088**

**Approved for public release; distribution unlimited**



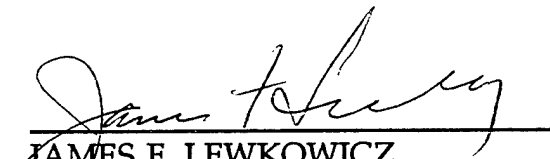
**PHILLIPS LABORATORY  
Directorate of Geophysics  
AIR FORCE MATERIEL COMMAND  
HANSCOM AIR FORCE BASE, MA 01731-3010**

# DISCLAIMER NOTICE



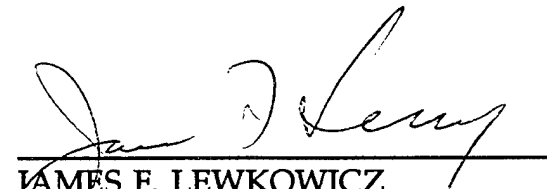
THIS DOCUMENT IS BEST QUALITY AVAILABLE. THE COPY FURNISHED TO DTIC CONTAINED A SIGNIFICANT NUMBER OF PAGES WHICH DO NOT REPRODUCE LEGIBLY.

This technical report has been reviewed and is approved for publication.



---

JAMES F. LEWKOWICZ  
Contract Manager  
Earth Sciences Division



---

JAMES F. LEWKOWICZ  
Director  
Earth Sciences Division

This report has been reviewed by the ESC Public Affairs Office (PA) and is releasable to the National Technical Information Service (NTIS).

Qualified requestors may obtain additional copies from the Defense Technical Information Center. All others should apply to the National Technical Information Service.

If your address has changed, or if you wish to be removed from the mailing list, or if the addressee is no longer employed by your organization, please notify PL/IM, 29 Randolph Road, Hanscom AFB, MA 01731-3010. This will assist us in maintaining a current mailing list.

Do not return copies of this report unless contractual obligations or notices on a specific document requires that it be returned.

# REPORT DOCUMENTATION PAGE

Form Approved  
OMB No. 0704-0188

Public reporting burden for this collection of information is estimated to average 1 hour per response, including the time for reviewing instructions, searching existing data sources, gathering and maintaining the data needed, and completing and reviewing the collection of information. Send comments regarding this burden estimate or any other aspect of this collection of information, including suggestions for reducing this burden, to Washington Headquarters Services, Directorate for Information Operations and Reports, 1215 Jefferson Davis Highway, Suite 1204, Arlington, VA 22202-4302, and to the Office of Management and Budget, Paperwork Reduction Project (0704-0188), Washington, DC 20503.

1. AGENCY USE ONLY (Leave blank)		2. REPORT DATE October, 1994		3. REPORT TYPE AND DATES COVERED Scientific Report No. 4	
4. TITLE AND SUBTITLE The Multi-Factor Model of Magnitude Residuals and the Problem of the Precise Determination of Magnitude				5. FUNDING NUMBERS PE 61102F PR 7600 TA 09 WU BK	
6. AUTHOR(S) T. G. Rautian V. I. Khalturin				Contract F19628-90-K-0059	
7. PERFORMING ORGANIZATION NAME(S) AND ADDRESS(ES) Lamont-Doherty Earth Observatory of Columbia University Palisades, NY 10964				8. PERFORMING ORGANIZATION REPORT NUMBER	
9. SPONSORING/MONITORING AGENCY NAME(S) AND ADDRESS(ES) Phillips Laboratory 29 Randolph Road Hanscom AFB, MA 01731-3010  Contract Manager: James Lewkowicz/GPEH				10. SPONSORING/MONITORING AGENCY REPORT NUMBER  PL-TR-94-2291	
11. SUPPLEMENTARY NOTES					
12a. DISTRIBUTION/AVAILABILITY STATEMENT  Approved for public release;  distribution unlimited				12b. DISTRIBUTION CODE	
13. ABSTRACT (Maximum 200 words)  Station corrections for hundreds of stations and seismic waves dynamic data in many regions were jointly analyzed to study the statistical structure of seismic magnitude deviation. The multi-factor model of station residuals is proposed. It was found that total deviation of magnitudes (0.4 magn. units for EQs and 0.34 for UNEs) is formed by a set of components: 1) Site effects component S1 is equal to 0.10. 2) Area of observation component S2 is equal to 0.14. 3) The influence of the earthquake (EQ) zone is described by the component S3 which is also equal to 0.14. 4) The path effect component S4 is equal to 0.19. 5) The random component S5 is influenced by a variety of factors which are unknown. This component varies from 0.28 for EQs and 0.18 for UNEs. The real accuracy of magnitude depends not only on the number of stations used, but mostly on different areas and types of paths. Based on dispersion analysis of magnitude, a technique for realistic error estimates is proposed. The efficiency of station corrections is discussed. Our observations show, that even in cases when all factors are corrected, the lower limit of magnitude error is 0.07.					
14. SUBJECT TERMS Magnitudes, Station correction, Seismic coda, UNEs, Multi-Factors model, Path and site effects				15. NUMBER OF PAGES 182	
				16. PRICE CODE	
17. SECURITY CLASSIFICATION OF REPORT Unclassified	18. SECURITY CLASSIFICATION OF THIS PAGE Unclassified	19. SECURITY CLASSIFICATION OF ABSTRACT Unclassified	20. LIMITATION OF ABSTRACT SAR		



## THE TABLE OF CONTENTS

SUMMARY .....	xvi
INTRODUCTION .....	1
1. SEISMIC STATIONS AND OBSERVATIONS .....	4
1.1. The seismic stations used in this study .....	4
1.2. The standard instrumentation .....	4
1.3. Frequency band-pass seismic station (ChISS) .....	6
2. CALIBRATION SCALES AND CATALOGS OF SEISMIC DATA IN THE FUSSR .....	15
2.1. Surface wave magnitude MLH .....	15
2.2. Body wave magnitude MPV .....	16
2.3. Energy class K .....	17
2.4. Coda magnitude Mc .....	19
2.5. Catalogs of seismic data in ther FUSSR .....	21
3. THE PROBLEM OF ACCURACY OF MAGNITUDE DETERMINATION; THE MULTI-FACTOR MODEL OF MAGNITUDE RESIDUALS .....	24
3.1. The accuracy of magnitude and station corrections ..	24
3.2. Factors, creates the magnitude deviations .....	31
3.2.1. The observation area effect .....	31
3.2.2. Local conditions (the site effect) .....	32
3.2.3. The epicentral zone effect .....	32
3.2.4. The path effect .....	33
3.2.5. Random component of deviation .....	34
3.2.6. Total deviation .....	34
3.2.7. The path effect for surface magnitude .....	35
3.2.8. Basic magnitude .....	35
3.3. The multi-factor model and the method of estimation the errors.....	35
3.4. The calculation of errors and the accuracy problem..	37
3.5. Some notes from the geophysical side of the problem	38
4. THE MAGNITUDE RESIDUALS CONNECTED WITH LOCAL CONDITIONS, OBSERVATION AREA AND EPICENTRAL ZONE EFFECTS .....	39
4.1. The local and area deviations .....	39
4.1.1. Data from 12 Soviet SKD-stations .....	39
4.1.2. Data of 27 Soviet SKM-stations .....	41
4.1.3. North's data from World Network (mb magn.) ..	42
4.1.4. Marshall's data from World Network (mb magn.)	42
4.1.5. Data from 8 Caucasus SK-station .....	44
4.1.6. Data from 9 Turkmenia SKM-stations .....	44
4.1.7. Data from 12 SKM stations of Garm Network ...	45
4.2. The total and random deviations .....	46
4.3. The zone effect .....	46
4.4. The small scale variation of zone effect due to complexity of geological structure in the vicinity of the source .....	47
4.5. The summary of data .....	48

5. THE INSTABILITY OF THE AMPLITUDE-DISTANCE CURVES AS A SOURCE OF THE MPV DEVIATION DUE TO PATH EFFECT .....	50
5.1. The general A/T-D curve from our data .....	50
5.2. The path effect from "source-station" couples .....	53
5.3. The path effect obtained from the A/T-D curves: profile observation .....	54
5.4. Small-scale path effect, at the distance range 8,000 -11,000 km .....	56
5.5. The path effect obtained from the A/T-D curves: regional observations .....	61
5.5.1. A/T-D curves for eight epicentral zones .....	61
5.5.2. A/T-D curves for four observational areas ...	63
5.6. The summary of estimations of path component of deviation .....	65
6. THE PATH EFFECT IN SURFACE WAVE MAGNITUDE RESIDUALS AND METHOD OF CORRECTION .....	66
6.1. Comparing the MLH magnitude residuals from different sets of data .....	66
6.2. The effect of the "Pacific-Continental Asia" boundary on MLH residuals .....	69
6.3. The variations of the MLH residuals connected with the Black Sea depression .....	73
6.4. Small-scale variations of the MLH residuals at the epicentral distances of 100 - 500 km ....	80
6.5. The MLH residuals connected with crossing Tibet ....	81
7. THE USE OF SEISMIC CODA TO DETERMINE THE STATION CORRECTIONS FROM REGIONAL AND LOCAL OBSERVATIONS .....	85
7.1. The properties of coda, important when using it for determining the station correction .....	85
7.1.1. The basic definitions .....	85
7.1.2. Coda envelope as a calibration curve for coda magnitude .....	86
7.2. The method of the determination the station magnitude residual from coda .....	89
7.3. The values of the station residuals obtained from coda .....	89
7.3.1. Station residuals for stations of Garm Network determed by coda method .....	89
7.3.2. Station residuals of three local networks of SKM-instruments .....	91
7.4. The station residuals of direct S waves and coda ...	92
7.5. The common system of station corrections for whole Soviet Central Asia .....	94
7.5.1. Data and method used for estimation the station magnitude corrections .....	95
7.5.2. Magnitude station residuals for stations installed on hard rocks and on sediments ..	98
7.5.3. The coda level for vertical and horizontal components .....	98
7.5.4. Efficiency of coda method for estimation the station magnitude corrections at	

local networks and seismic array .....	99
8. THE SPECTRAL ASPECT IN MAGNITUDE DETERMINATION AND CORRECTION .....	100
8.1. The ratios of A/T of P waves and coda level on short-period (SKM) and long-period (SKD) instruments records and its dependence on magnitude .....	101
8.1.1. A/T ratio of P waves on SKM and SKD records..	101
8.1.2. The difference between SKM and SKD coda magnitudes as a characteristic of source spectra .....	104
8.2. The station spectral corrections determination from ChISS records of coda waves .....	107
8.2.1. ChISS coda as an instrument for study very local site effect .....	107
8.2.2. Spectral station residuals for ChISS stations at Central Asia and Kazakhstan obtained by coda method .....	110
9. THE SOURCE SPECTRA AND SPECTRAL ZONING .....	119
9.1. The mapping of low- and high-frequency earthquakes based on spectral content of coda .....	120
9.2. The method of determination of the source spectra from ChISS-coda .....	120
9.3. The regional difference of the source spectra .....	123
9.4. The effect of attenuation in epicentral area on the teleseismic data .....	129
10. THE ESTIMATION OF REALISTIC ERRORS OF MAGNITUDES AND STATION CORRECTIONS .....	131
10.1. Values of standard deviations correspondent to main factors and total deviation of magnitude determination .....	131
10.2. Estimation the station correction error dB .....	131
10.3. Calculation the precision of magnitude determination	132
10.4. Zone effect, strategy of diminishing and lower limit of the magnitude error .....	133
CONCLUSIONS .....	134
REFERENCES .....	139
APPENDIX 1. LIST OF STATIONS .....	143
APPENDIX 2. THE REGIONAL STATION MAGNITUDE CORRECTIONS ....	147
APPENDIX 3. STATION MAGNITUDE RESIDUALS .....	151

## List of Figures

FIGURE		PAGE
1	Typical magnification curves of the standard broad-band instruments used in the FUSSR .....	5
2	ChISS station characteristics, version for local events registration. There are eight channels with central frequencies $f_c$ from 0.6 Hz to 40 Hz; top - the magnification curves; bottom - the time responses on the delta input signal .....	7
3	The ChISS record of the first Soviet UNE from STS (Degelen), Oct 11, 1961, 07:40, mb=4.81, st. Talgar, D=735 km. The central frequencies from top-to-bottom are 0.7, 1.4, 2.7, 5.7 and 11 Hz .....	8
4	The ChISS record of the Soviet UNE from STS (Degelen), Dec 30, 1976, 03:57, mb=5.08, Talgar station, D=730 km. The central frequencies from top-to-bottom are 18, 10, 5, 2.5, 1.25, 0.62 Hz. The calibration signal corresponds to 0.5 mcm/sec of ground velocity .....	9
5	The ChISS record of the Soviet UNE from STS (Degelen) by instrument with low gain, Nov 30, 1977, 04:57, mb=6.0, Talgar station, D=745 km. The central frequencies from top- to-bottom are 27, 18, 10, 5, 2.5, 1.25, 0.62 Hz. Calibration signal corresponds to 0.5 mcm/sec of ground oscillation velocity .....	10
6	The ChISS record of the three Soviet ONES from Orenburg (51.3N; 53.3E), Oct 7, 1983, 04:02, mb about 5.3 for each of them, Zerenda station, D=1100 km. The central frequencies from top-to-bottom are 5, 2.5, 1.25, 0.62, 0.31 Hz .....	11
7	The ChISS records of the quarry blast from North Kazakhstan. Oct 2, 1989, Zerenda station, D=20 km. The central frequencies from top to bottom - left : 5, 2.5, 1.25, 0.62 Hz; right: 40, 27, 18, 10 Hz .....	12

8	The ChISS records of the earthquake from Sayan (55.1N, 93.1 E), Feb 27, 1972, MPV=4.7, Semipalatinsk station (ink record), D=1060 km. The central frequencies from top-to-bottom: 2.8, 1.0, 0.47, 0.35, 0.07 Hz .....	13
9	The local earthquake at South Tien Shan region recorded by high-frequency version of Talgar ChISS station, Aug 15, 1992, D = 28 km. The central frequencies from top-to-bottom: 204, 136, 90, 60, 40 Hz; the relative width of channels $df/f_c$ is 0.22 .....	14
10	The nomogram for determining K from $A_p + A_s$ amplitudes at SKM records. Note that the distance scale is not exactly logarithmic, but is deformed to make the amplitude curve a straight line. K is proportional to $\log(A_p + A_s)/0.56$ .....	18
11	The nomogram for determining coda magnitudes $M_c$ from records of SKM standard instruments. The example of magnitude determination is shown: the crosses and open circles are the measured coda amplitudes at two stations of the same earthquake. The magnitude $M_c(\text{SKM})$ calculated from these 15 measurements is 5.35 with their scattering of 0.06 .....	20
12	The correlation between MLH (from Soviet Bulletin) and $M_c(\text{SKM})$ , calculated from single station GAR. The diamond are for shallow earthquakes, Xs for deep (80-250 km) ones. Note the saturation for large magnitudes (5.5-7.0) for both groups of earthquakes ....	22
13	The correlation between surface waves magnitude MLH (from Soviet Bulletin) and coda magnitude $M_c(\text{SKD})$ , calculated from SDD-records of single station GAR .....	23
14	Comparing the station corrections $d\text{MPV}(\text{SKD})$ by Vanek [1983] and Feofilaktov [1970] for the same stations, earthquakes from Alaska and Aleutian .....	28
15	The correlation between magnitude $m_b$ determination for Semipalatinsk UNES made by NORSAR and AWRE .....	29
16	The difference $d_m$ between magnitudes $m_b$ from ISC and $m_b$ from NORSAR (or from AWRE, or their average if they both are available) versus NORSAR (AWRE) magnitude. Notice that for small events ( $m_b < 4.4$ ) the ISC magnitudes are systematically overestimated .....	30

- 17 The mapping of  $dm = mb - m(Lg)$  for a cluster of UNES in the Balapan subarea [Kirichenko, 1993]. The  $dm$  changes strongly depending on the position of source and on its distance from the main fault zone inside this small (about 25 km) subarea ..... 50
- 18 Our regional A/T-D curve (1) compare with the USCGS curve (2) and the standard curve used in the USSR network (3). Numbers near the points of (1) mean the number of observations included in these points ..... 51
- 19 The A/T-D curves obtained from the Big Profile of SKM-stations "Pamir-Baykal". Seven earthquakes were used: a - from Aden Gulf (## 1, 2), b - from Persian Gulf (## 3 and 4) and c - from Far East (## 5 - 7). The list of earthquakes is given in Table 15. The absolute level of curves corresponds to  $MLH = 5.0$  ..... 55
- 20 Two A/T-D ongoing curves, obtained from observations along the Big Profile "Pamir-Baykal". (1) is the curve from records of Altay-Baykal earthquakes by North Tien Shan stations and (2) - from records of North Tien Shan earthquakes by stations in Baykal area, compare with our general curve (3). The absolute level of curves corresponds to  $MLH = 5.0$ . The local residuals were corrected, the area ones remain the same ..... 57
- 21 The magnitude residuals for single station Mondy (MOY) versus distance for two profile of epicenters with their azimuths 0-30 degrees and 90-120 degrees. Notice the distance range: from 8,600 to 11,000 km ..... 58
- 22 The space distribution of magnitude  $mb$  station residuals for UNES from Nevada TS at temporal stations of Kokchetav network. The average epicentral distances is about 10,000 km. Note, the big scattering of residuals (till 0.7 magn. units) even for close stations ..... 60
- 23 The A/T-D curves built separately for the earthquakes from each epicentral zone, using all the 12 stations in each case; the station residuals were corrected. Epicentral zones: a - Africa; b - Far East; c - Arctic zone; d - Baykal; e - Tien Shan, Mongolia, China; f - Mediterranean, Iran, Pamir; g - India, Burma, Indonesia. Numbers near the points of (1) mean the number of observations included in these point. The absolute level of curves corresponds to  $MLH = 5.0$ . Dashed lines are the amplitude curves for each epicentral zone; the solid lines are our general curve ..... 62

24	The A/T - D curves for four observation areas: Russian platform (Moscow), Central Asia, North Tien Shan and Baykal. The data of several nearby stations inside each area were combined after correcting their local residuals. Numbers near the points mean the number of observations included in these point. The absolute level of curves corresponds to MLH = 5.0 .....	64
25a	Comparing the station corrections dMLH by Vanek [1983] and Landyрева [1968 and 1974] for the same stations, earthquakes from Japan .....	67
25b	Comparing the station corrections dMLH by Vanek [1983] and Landyрева [1968 and 1974] for the same stations, averaged for all epicentral zones .....	68
26a	The surface magnitude MLH station residuals versus distance for earthquakes from three West Pacific epicentral zones: Japan, the Kuril and Aleutian. The residuals are negative and increase with distances from -0.60 near the epicentral zone to about zero for distances more then 40 degrees .....	70
26b	The surface magnitude MLH station residuals versus distance for earthquakes from Mediterranean zone .....	71
26c	The surface magnitude MLH station residuals versus distance for earthquakes from three zones : Central Asia, Alaska and Indonesia .....	72
27	The map of the ray traces of Rg waves crossing and not crossing the Black Sea from two earthquakes, #35 in North-West Turkey and #51, Vrancea. The values of the residuals are shown in a middle of the ray traces, triangles are the seismic stations, the solid circles are the epicenters used in this study. The residuals are great and negative when crossing the deep part of the sea .....	75
28	The map of the ray traces of Rg waves crossing and not crossing the Black Sea from the epicentral zone #6. The values of residuals are shown in a middle of the ray traces. The residuals are great and negative when crossing the deep part of the sea and small or positive when past .....	76
29	The map of the ray traces of Rg waves crossing and not crossing the Black Sea from the epicentral zone #2 and 4. The values of residuals are shown in a middle of the ray traces. The residuals are great and negative when crossing the deep part of the sea and small or positive when past .....	77

30	The map of the ray traces of Rg waves crossing and not crossing the Black Sea from the distant epicentral zones. The ray traces are not shown completely. The code of the station and the values of residual are shown near each ray trace. Again, the negative residuals are at traces crossing the deep part of the Black Sea .....	78
31	The small-scale dMLH residuals at GAR SKD station depending on the epicenter position .....	82
32	The small-scale dMLH residuals at TLG SKD station depending on the epicenter position .....	83
33	Example of damage of the surface wave train crossing the northern border of Tibet. The vertical line corresponds to the group velocity 3.0 km/sec. Records of Semipalatinsk ChISS station, $f_c=0.07$ Hz. A - traces, going westerly of Tibet; C - traces easterly of Tibet; B1 - traces, on the direction to Tibet, from epicenters localized northerly the Tibet border; B2 - epicenters localized inside Tibet, or southerly .....	84
34	The examples of envelopes on teleseismic events recorded by SKD station Rio Carpintero, Cuba. Look at the different shape of envelopes of Rg waves, early coda and late coda .....	87
35	The regional SKM-coda envelopes: 1 - Altai and Sayans; 2 - Fergana Valley and Peter the Great Range; 3 - Southern and Central Tien Shan; 4 - Crimea; 5 - Caucasus; 6 - Kuril; 7 - Kamchatka; 8 - Cuba; 9 - Baykal. All curves are compared with Tien-Shan one (dotted line). Note that the curves for two regions (5 and 6) decrease much more than for others, exposing the low-Q zone beneath these regions .....	88
36	Examples of envelopes of the local earthquakes at stations with different site conditions. The lower curves correspond to station in the tunnel in hard rock, upper curves correspond to stations installed on the soft soil .....	90
37	Comparing the station corrections for Garm network obtained from S wave and from coda SKM records of local and Hindu Kush earthquakes .....	93
38	Envelopes of SKD-coda at VTS (Bulgaria) station and Central Asian stations VAN, GRM, CHL, CHD and TLG. The earthquakes used are: #11-North Africa; #7-West Iran; #12-Hindu Kush, $h=200$ km; #4-South Iran; #15-Gazli;	



- # 2-South Tien Shan. Note, that the late coda is close to the standard envelope (bold line), whereas the coda close to max Rg wave varies in shape. The distances from VTS to VAN - 2700 km, to GAR, CHL, CHD-3600 km, to TLG-4300 km ..... 96
- 39 Examples of envelopes of ChISS coda level at Garm and VAN stations, 1100 km between. Three events are taken: A - in Kopet-Dag, close to VAN; B - in the Caspian Sea; C - in Hindu Kush, close to Garm. Horizontal line indicate the absolute amplitude level (in micron/sec) for both stations data. Note that the level of coda on both stations is near the same at all frequencies from 0.3 till 10 hz ..... 97
- 40 The dependence of  $b = MPV(SKD) - MPV(SKM)$  upon distance for Talgar (1) and Garm (2) stations. The period  $T_0$  of SKM instruments are 1.2 sec at Talgar and 2.0 sec at Garm. The numbers of individual measurements are shown near each point ..... 102
- 41 The difference  $b$  between  $\log(A/T)$  of P wave on long-period SKD and short-period SKM records (TLG station) versus magnitude MLH ..... 103
- 42 Comparing the MPVA (top) and mb (bottom) with surface wave magnitude MLH. Note the nonlinear character of the dependence for both cases. For the same MLH, the mb values are 0.20-0.25 smaller than MPVA ..... 105
- 43 The correlation between the coda magnitudes  $M_c(SKD)$  and  $M_c(SKM)$  determined at single station Garm for shallow earthquakes. The relation between them is :  $M_c(SKM) = 0.91 + 0.83 M_c(SKD)$  ..... 106
- 44 Comparing the level of ChISS coda envelopes of the same event at two close points of Chusal valley - at the tunnel in the granite (point #1, Z component, solid circle), and at the soft sediments 60 m thickness (point #5, Z - open circle and EW component-crosses). The frequency from top to bottom:  $f=0.62, 2.5$  and  $10$  Hz ..... 108
- 45 Comparing the level of ChISS coda envelopes of the same event at two close points of Chusal valley - at the tunnel in the granite (point # 1, Z component, solid circle), and at the soft sediments 40 m thickness (point #3, Z - open circle and EW - crosses). The frequency from top-to-bottom - at left:  $0.62, 1.25, 2.5, 5$  Hz and at right:  $10, 18$  and  $27$  Hz ..... 109

- 46 The average spectral ratios in different points of observation (## 1-5), referenced to the basic point. The vertical components were used. Note that the spectral ratios are near the same for P, S, coda and microseismic noise ..... 111
- 47 The monitoring of spectral ratio of coda level of the same earthquakes at two stations Chusal and Garm during the 1988 at 1.25 Hz (top) and 0.62 Hz (bottom). Note the small scattering of individual ratios: standard deviation is 0.10 log. units ..... 112
- 48 The spectral ratios of coda level of the same earthquakes on the records of two ChISS stations of the Garm network : Chusal/Garm (top) and Chil Dora/Garm (bottom). The solid circles are the data from individual earthquakes ..... 113
- 49 The spectral station residuals for three ChISS stations installed in tunnel on Paleozoic rocks : Gezan and Chuyan-Goron (Tadjikistan), and Talgar (North Tien Shan) ..... 115
- 50 The spectral station residuals for two ChISS stations: Arzhinak (Tadjikistan) and Vannovskaya (Mesozoic limestone, Kopet-Dag) ..... 160
- 51 The spectral station residuals for three ChISS stations installed in tunnel on Mesozoic sedimentary rocks: Chil-Dora, Nurek, Gissar ..... 117
- 52 The spectral station residuals for three ChISS stations installed on thick sediments: Shahartuz and Bogi-Zagon (Tadjik Depression) and Sufi-Kurgan (Alai Valley) ..... 118
- 53 The map of  $dM = Mc(SKM) - Mc(SKD)$ . The diamonds are epicenters of low-frequency earthquakes, with  $dM < -0.13$ ; the crosses are high-frequency ones, with  $dM > 0.13$  ..... 121
- 54 The source spectra  $\log DIS(f)$  of four earthquakes obtained by coda method, using the data of 3 - 5 stations for each. The station spectral corrections were used. Note the small scattering of the different stations data ..... 124
- 55 The example of the source spectra of displacement (squares), velocity (crosses) and acceleration (triangles) for Alay earthquake (Nov 1, 1978, 38.5N, 72.6E,  $M_s=6.8$ ) obtained by ChISS-coda method from

	records of Garm station (R=200 km). Spectrum has simple shape with single corner frequency. The f-square slope observed between 7sec and 18 Hz without fmax. Source parameters are: log Mo=19 (in N*m), To=6 sec, log E= 15.7 (in J), apparent stress is 170 bars .....	125
56	The velocity source spectra for earthquakes with different depth:triangles are for events deeper than 100 km in Pamir and Hindu Kush and more then 12 km in Tadjik Depression). The squares are for the shallow events at three zones .....	126
57	The displacement source spectra of eight Central Asian earthquakes obtained by Rautian's method from data of 1 - 4 stations each. Station spectral correction were used. Note the clear flat part of spectra and high frequency slopes agree to the omega-square model .....	127
58	Map of spectral ratios 2.5/0.5 Hz at P wave ChISS spectra of teleseismic events. More then 700 earthquakes of mb = 4.5 - 5.5 were used. All data obtained from Semipalatinsk ChISS station records. The values of these ratios were referenced to epicenters and then smoothed .....	130

# List of Tables

TABLE		PAGE
1	The List of Seismic Stations Used for Estimate Station Corrections .....	143
2	The Band Pass of ChISS Filters and Their Central Frequencies $f_c$ .....	6
3	The Station Magnitude Corrections for MPV (Short-Period Instrument SKM) Obtained from Different Sets of Data .....	25
4	The Station magnitude Corrections for MPV (Long-Period Instrument SKD) Obtained from Different Sets of Data .....	26
5	The Total Station Residuals (TSR), Area (AR), Local Residuals (LR) and the Standard Deviations Obtained from 12 Stations Data (SKD-Instrument) .....	40
6	The Total Station Residuals (TSR), Area (AR), Local Residuals (LR) and the Standard Deviations after Vanek et al. [1979] .....	41
7	The Area Residuals and Local Standard Deviations from North [1977] Data for Eight Observation Areas .....	42
8	The Total Station Residuals (TSR), the Area ones, the Local and Area Deviations for 17 Areas from Marshall's Data [Richards, 1993] .....	43
9	The Stational Residuals (SR), Referenced to YER, the Local Residuals (LR), Referenced to Average Magnitude, and Random Standard Deviations in Caucasus Network of SKD Stations after [Vanek, Tskhakaya, 1967] .....	44
10	The Station Residuals of MPV Magnitude for Regional Earthquakes in South Turkmenia .....	45
11	The Station Deviations at Garm Local Network of Short-Period Instruments SKM .....	46
12	The Summary of Local, Area and Random Components of Total Deviation of the Magnitude Station Correction ....	48
13	The Mean Magnitude MPV Residuals for the South Tien Shan Group of Stations .....	53
14	The Standard Deviations of Station Residuals for Different Epicentral Zones After North [1977] and Number N of Zones Used for Each Station .....	54

15	The List of the Earthquakes Used for Plotting the Profile A/T - D Curve (Figure 19) .....	54
16	The Standard Deviation of the Zone A/T - D Curves Relatively the Standard Calibration Curve .....	63
17	The Shape Deviations of A/T - D Curves of 12 Stations ..	63
18	Path Standard Deviations for Different Sets of Data ....	65
19	Regional Station Corrections dMLH (Horiz. Component) by Landireva [1974] for Six Epicentral Zones .....	147
20	Regional Station Corrections dMLH (Horiz. Component) by Landireva [1974] for Seven Epicentral Zones .....	148
21	Regional Station Corrections dMLH (Horiz. Component) from Vanek et al.[1980] for Five Epicentral Zones .....	149
22	Regional Station Corrections dMLV (Vertical Component) from Vanek et al.[1980] for Five Epicentral Zones .....	159
23	The MLH Magnitude Residuals for Different Seismic Traces After the Data of the Earthquakes on the Alpine Band and Number N of Traces Used .....	74
24	The Magnitude Residuals dMLH for Close and Distant from Black Sea Stations for Earthquakes from Distant Epicentral Zones for Two Types of Ray Traces .....	79
25	Station Corrections dMLH for the Main Soviet Stations Which Should be Taken Into Account the Black Sea Effect for Earthquakes from Nine Epicentral Zones .....	80
26	The Log-Amplitude Residuals dlogAc of Seismic Coda and Their Standard Deviations s for Garm Network Stations for Different Type of Instruments .....	91
27	The Station Magnitude Corrections dMc for SKM Stations of Altay, Uzbekistan and Crimea Local Networks Obtained from Seismic Coda Records .....	92
28	The Comparing the Station Residuals dlogA and Their Standard Deviations s Obtained Separately for S Waves and Seismic Coda at Garm Network SKM Stations .....	94
29	Station Magnitude Residuals dM and Their Standard Deviations s for Horizontal (H) and Vertical (V) Components from SKM and SKD Records at Hard Rocks and Sediments Obtained by Coda Method for Stations of Regional Networks at Central Asia and Caucasus .....	151

30	The Mean Values of Residuals for Stations at Hard Rocks and at Sediments Depending on Region and Instrument ....	98
31	The Log-Difference (DlgA) of H and V Components of Coda Amplitudes at SKM and SKD Records, and Standard Deviations s of Individual Earthquake Data .....	99
32	Station Spectral Residuals of Seismic Coda Level for Central Asia and Kazakhstan ChISS Stations; Garm was Taken as a Basic Station .....	114
33	The Values of Transform Functions $d(f)$ , $v(f)$ and $a(f)$ Which were Used for Calculation the Source Spectrum from Coda Spectrum at 100 Sec .....	122
34	The Example of Coda Spectral Content $\log A_{100}(f)$ at Several Stations Before the Correcting and Average Value and Its Standard Deviation After Adding the Station Spectral Corrections for Earthquake Feb 20, 1988 .....	123
35	Apparent Stress Values of Earthquakes From Some Epicentral Zones .....	128
36	The Upper Limits of Dynamic Apparent Stress $h_s$ at Some Epicentral Zones of Central Asia .....	128
37	The Standard Deviations, Correspondent to Different Factors Responsible for Total Magnitude Deviation .....	131

## SUMMARY

The goal of this work was to find the origins of magnitude deviations, their contribution in total errors of magnitude determination and the ways to correct them. The multi-factor model of magnitude deviation was proposed. It allowed to estimate a realistic precision of magnitude values of UNE and earthquakes as well as the accuracy and efficiency of station correction. The estimation of errors was made for different situations and the results are in a good accordance with real errors obtained from observed data.

Using the multi-factor model of magnitude residual the total magnitude deviation  $S$  is considered as a squared sum of partial deviations, which originates from five independent factors. They are:

- local station condition;
- condition in area of observation;
- path effect;
- conditions in epicentral zone;
- random scattering of data.

These partial deviations describe the contribution of each factor into the total residual. The sixth factor is not a geophysical one, but is also responsible for an error of magnitude. It is a way to choose the basic magnitude when creating the system of station corrections.

The data of our study as well as the data of several Soviet and Western authors were analyzed. The average value of each partial deviation ( $S_i$ ) and average total deviation  $S$  (for P wave magnitude) were found (in magnitude units):

local component	$S(\text{loc})$	0.12 ;
area component	$S(\text{area})$	0.15 ;
path component	$S(\text{path})$	0.18 ;
zone component	$S(\text{zone})$	0.15 .

Total deviation  $S$  found from over world observation data is equal to 0.38 for earthquakes and 0.32 for UNES. The random component was calculated as:

$$S(\text{rand})^2 = S^2 - S(\text{loc})^2 - S(\text{area})^2 - S(\text{path})^2 .$$

$S(\text{rand})$  is equal 0.27 for earthquakes and 0.18 for UNES.

The definitions of each component were taken as follows.

Area effect means the average station residual of stations, localized in some area, which can be considered as homogeneous (platform, shield, orogenic zone, rift zone, etc).

Local effect calculated as a difference between the station residual inside the area and the area residual.

The path effect is measured as the difference between the station residual for earthquake from some epicentral zone and the average station residual calculated from earthquakes in "all" epicentral zones.

The data shows that the area effect originates due to existence (or absence) of the low-Q volume beneath the area of observation. The zone effect is of the same cause and has to be of the same value. But, zone effect is invisible by observation of teleseisms, because the seismic rays from a earthquake penetrate this volume and are lost (or are not lost) near the same part of energy when crossed it. The zone effect is significant but can be measured only using independent information about event (like yield for UNE or local magnitude from local network data, which do not feel attenuation in upper mantle).

The random component of deviation includes the effects which cannot be easily corrected. They are the source radiation pattern; the effect of geological structure in vicinity of the source, transforming the time-history, the variations of an individual spectral content of source radiation. Some artifacts play a serious role too: that is, systematical overestimation of magnitude of small events, the instability of instrument magnification and so on.

To obtain the realistic estimation of magnitude errors,  $dM$  and/or errors of station correction  $dB$ , one needs to take into account the values of each partial deviation, and not only the common number of station or earthquakes -  $N(rand)$ , but the numbers of realization for each factor taking part in a particular case: numbers  $N(loc)$ ,  $N(area)$ ,  $N(zone)$ ,  $N(path)$ .

To estimate the error of magnitude  $dM$  for an earthquake recorded by many stations, localized in several areas, one has to take into account the numbers  $N(rand)=N(st)$ ;  $N(area)$ ;  $N(path)=N(area)$  and  $N(zone)=1$ . If no station correction is available,

$$dM = \frac{S(rand)^2}{N(st)} + \frac{S(loc)^2}{N(st)} + \frac{S(area)^2}{N(area)} + \frac{S(path)^2}{N(area)} + \frac{S(zone)^2}{1} \quad (1)$$

It is clear from the formula, that if hundreds or even thousands of stations were used, but most of them are localized in few areas, only the two first terms became small. Two next terms decrease much less, and the last term does not change at all. So, one needs various strategy to diminish each partial deviation.

When the station corrections were determined from records of  $N(eq)$  earthquakes,  $N(rand)=N(eq)$ ,  $N(path)=N(zone)$ , the error  $dB$  is estimated as follow:



$$dB = \frac{S^2(\text{rand})}{N(\text{eq})} + \frac{S^2(\text{zone})}{N(\text{zone})} + \frac{S^2(\text{path})}{N(\text{zone})} \quad (2)$$

Again, if even a thousand earthquakes were used from only a few epicenter zones  $N(\text{zone})$ , the station correction cannot be precise for any other zones. If calculating the magnitude using the station corrections, it does not mean, that the corresponding term in (1) disappeared; it just becomes less,  $S(\text{st})$  being replaced by  $dB$  found from (2).

The monitoring of UNE from presumable test sites is a case when the precise magnitude determination is most important. In determinate the station corrections for seismic stations installed at each Test Site separately, such correction includes the local, area and path effects. The random factor can be decreased by the regular way, using as many stations as possible. But zone effect limited the accuracy. If not using a zone correction, the relative accuracy can be good, but all events from this test site will have the same systematic error from zone effect. It can be corrected, but to get zone correction the independent information is necessary. A few possible ways to find zone correction are considered.

When small events are monitored, only a few stations data are usually available, mostly at distances about several hundreds km. To reach a high accuracy in this case, it can be recommended to use not only P wave, but Pg, Sn, Lg waves, and seismic coda, and calculate the magnitude from few frequency bands independently. The random component is really produced by instability of condition in the near vicinity of source. It displays as a variation of the relation between P and S waves, and between different parts of spectrum. The use of different waves and different frequency bands to calculate magnitude smooths the random component. From our experience, it is possible to get the accuracy about 0.05 when using 2-4 stations, 2-4 wave groups and 3-5 frequency bands.

The coda is a much easier and most precise tool to obtain the local component of residual, and is especially recommended for small networks and arrays. It was found that the station residuals obtained from coda and from S (Lg) waves differ no more than 0.05. To get the homogeneous system of station corrections from coda, only 10-15 common earthquakes are needed, whereas to get the residuals from Lg wave with the same accuracy, the number of earthquakes must be 10 times more.

The residuals of the surface-wave magnitudes were analyzed for two great inhomogeneities making the shadow. It was found, that in correcting these residuals, the system of corrections differ from that for MPV. The values of corrections depends on the relative position of seismic ray and the inhomogeneity and on the distance between the station and the inhomogeneity.

# THE MULTI-FACTOR MODEL OF MAGNITUDE RESIDUALS AND THE PROBLEM OF THE PRECISE DETERMINATION OF MAGNITUDE

## INTRODUCTION

Do we really need high accuracy in the determination of magnitude? Perhaps the errors are not very important for earthquakes. But if the goal is the monitoring of nuclear explosions, the accuracy is not only a scientific, but an important political problem.

Today, there are thousands of seismic stations operating the world over. It might be seen that there is no problem in measuring seismic magnitudes with high accuracy, say, to one-hundredth or even one-thousandth of a magnitude unit. Even if records are available from only a few stations, the use of station corrections is supposed to solve the accuracy problem.

Is this really true? What is the accuracy of station corrections? Are the station residuals the same for all azimuth and for different epicentral regions? Are magnitude residuals the same for all epicentral zones? If not, what is the maximum size of a zone for which we can use the same station correction? How many different corrections have to be estimated for each station? Is the station correction the same for all types of waves: P, S, Lg, surface and coda waves? Is it the same for vertical and horizontal components? How do station corrections depend on the response of the instrument we use?

Other problems arise with the concept of basic magnitude: the size of the network, and the size of the epicentral zone we want to monitor. There is a major difficulty in determining absolute values of station magnitude deviation (and thus the value of magnitude correction): it depends on what is chosen as the "true" or "basic" magnitude - averaged magnitude of all stations, or magnitude from one station or group of stations (the base set), or some other procedure.

Even if we choose a particular definition of basic magnitude, but apply it to different regions or different sizes of network, results can be different. We may say, the results depend on the meaning of "all stations". All in the world? In a region of size about 1000-2000 km? Stations of a small local network (100-200 km)? Or even a small array? Also important is the distance to the earthquakes under consideration. If they are closer than 200 km, the seismic waves sampled only the upper part of the crust. For teleseismic signals inhomogeneity in the upper mantle can reveal itself as an "area" effect. Station corrections obtained by different authors for the same stations can seriously differ if they use earthquakes from different

regions, different distances, and use different definitions of base magnitude.

If one is interested in not only magnitude, but also the spectrum of signals, especially in the high frequency range, we have to keep in mind that station residual is a function of frequency and, therefore, instrument response. The higher the frequency we study, the more unpredictable residuals appear.

This is only a brief sample of the questions that arise regarding magnitude residuals and corrections. We may, nonetheless, identify a few main factors creating residuals in magnitude:

- local conditions in the station area; this can be a very local effect, literally a site condition;
- area effect depending on the crust and upper mantle of the area of observation;
- conditions in the epicentral zone;
- conditions along the seismic wave path;
- the spectral content due to the spectrum of seismic radiation;
- the frequency band of the instruments.

There is no general rule to divide residuals into partial residuals connected with each of the factors mentioned above. This will depend on size of network and size of seismic zone, as well as on the goal: are we interested in local, regional, or teleseismic signals? There are two ways to approach the problem. We can try to find the geological structure creating the magnitude residuals; or, we can attempt to prescribe a stable system of magnitude determination without overtly complicated procedures.

There are situations in which we need to find the structure of a strong inhomogeneity to create good corrections. We will consider two examples: the Black Sea and the border between the Pacific Ocean and the Asian continent. The inhomogeneities like that produce the "shadow" as large as 1000 km with the magnitude residuals about 0.3-0.7. Tibet generates an even stronger effect, completely killing the Lg waves when their ray traces crosses its border.

In this study, we do not try to get "the best" version of station corrections. We would like to show the complexity of the problem and how we tried to optimize our study depending on the situation. We will describe mainly our data and compare them with data of some other authors, and discuss our results for local, regional and teleseismic observations.

We will not look at the problem from the point of view of wave propagation in inhomogeneous media; no wave theory. Our goal is to find what factors are really important and what is the contribution of each of them to the scatter of the data.

Conclusions about the mechanism responsible for effects observed will be drawn and discussed only if the influence is clearly seen from observations.

We will examine the spectral aspect of the problem by studying station corrections for different standard instruments used in the former USSR (FUSSR) - both short and long period. We also estimate station correction as a function of frequency for many places where CHISS seismic stations were installed.

The magnitude errors can be considered as consisting of a few components, created by factors mentioned above. The components were assumed to be independent from each other. It is a basis of simple statistical multi-factor model to calculate the error of magnitude and of station corrections. This model shows realistic predictions of the accuracy which can be reached, depending on the character of the data used.

We found that seismic coda can be a very effective tool to study the local effect. It is the best method to obtain magnitude and spectral corrections for local and regional networks, especially for arrays. This method allows us to obtain high accuracy of corrections using a comparatively small volume of data.

Taking account of these factors, the report consists of the following parts:

1. Description of the instruments and seismic stations for which the corrections were determined.
2. The calibration scales used in FUSSR and their relations with  $M_s$  and  $m_b$ .
3. The definition of systematic and random components of magnitude residuals and the method of their determination. The problem of accuracy in the case of multi-factor origin of residuals.
4. The definition and estimation the magnitude residual components connected with local conditions, observational area and epicentral zone.
5. Data on the variability of amplitude-distance curves for P-waves, due to inhomogeneities of the Earth's interior, as one of the main sources of magnitude residuals.
6. Summary of the surface wave magnitude MLH station residuals for the FUSSR network. A detailed study of the effect of the Black Sea and the boundary between oceanic and continental crust on the amplitudes of the surface waves.
7. Comparing mean station corrections obtained for the same stations from different volumes of data.
8. The seismic coda as a tool to determine the local component of station correction.
9. Station residuals from short- and long - period instrument records. Method and results of the determination of the spectral station corrections from the CHISS-coda.

10. The method and the results of source spectra determination from the ChISS-coda and spectral zoning.

11. Quantitative estimation of main factors contribution to magnitude deviation.

12. Errors of magnitude estimated by multi-factor model in different situations.

## 1. SEISMIC STATIONS AND OBSERVATIONS

### 1.1. The Seismic Stations Used in This Study

In this study, we used data from stations of the seismic network of the FUSSR, called ESSN. ESSN is a Russian abbreviation meaning United System of Seismic Observations. We also used the data of regional networks of Tadjikistan, Kyrgyzia, Khazakhstan, Turkmenia, Uzbekistan, Armenia, Georgia and Azerbaidjan. In addition, we used data from temporary and permanent local networks, and separate stations installed by CSE (Complex Seismological Expedition of the Institute of the Physics of the Earth, Russian Academy of Science) in different regions of Central Asia and Kazakhstan. Finally, we reviewed data obtained by other (mostly Russian) authors. These authors used records from stations of the ESSN and stations in Eastern Europe. A complete list of seismic stations, their locations and the instruments for which the station correction was determined, are shown in Table 1 (see Appendix 1).

### 1.2. The Standard Instrumentation

Two main types of instrumentation were used in the FUSSR as a standard: long-period (SKD or SK) and short-period (SKM or VEGIK). All recorded ground displacement, but in different frequency bands. From 1950-1970, the "long-period instrument" was SK. It had a magnification of about 1000-1500 and a flat magnification curve between 0.3 and 12 sec. Later, SK was replaced by SKD with the flat part of the magnification curve prolonged to 20 sec. "Short-period instrument" SKM has magnification of about 20,000-60,000 at periods from 0.1 to 1.5 sec. At some stations, the other short-period instrument, called VEGIK, was installed. It was standard in the 1950s and was later replaced by SKM. VEGIK magnification was about 10,000-20,000 in a period band from 0.1 to 0.8 sec. While this may seem to be very similar to SKM, the difference between them becomes important when both 1.5 and 0.8 sec periods are within the high-frequency slope of the seismic signal spectrum.

Typical magnification curves of the standard broad-band instruments used in the FUSSR are shown in Figure 1.

# THE RESPONSE CURVES OF THE STANDARD SOVIET BROAD-BAND INSTRUMENTS

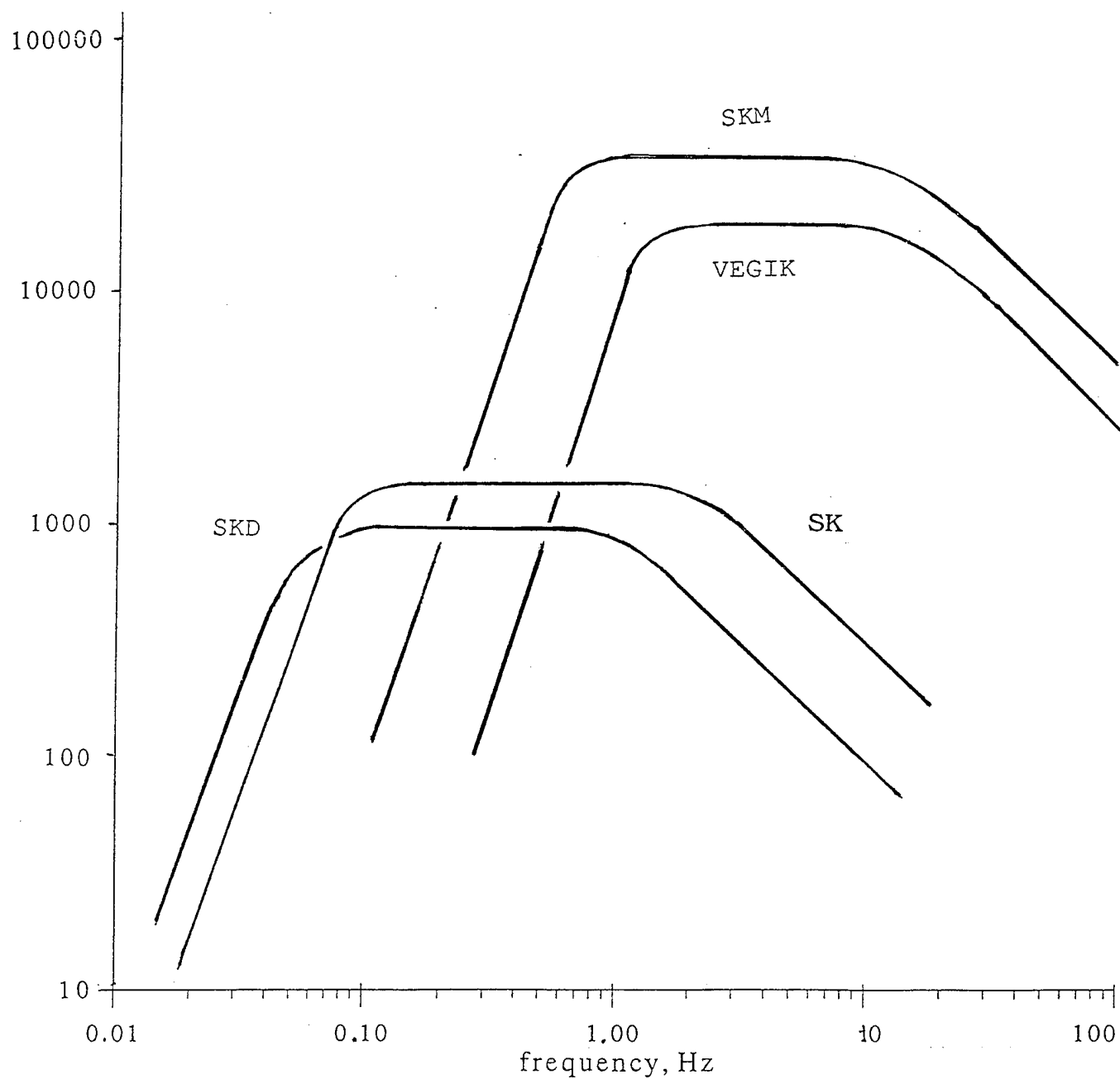


Figure 1. Typical magnification curves of the standard broad-band instruments used in the FUSSR .

### 1.3. Frequency Band-Pass Seismic Station (ChISS)

The ChISS station [Zapolsky, 1971] was used for spectral study. "ChISS" is a Russian abbreviation meaning "frequency band-pass filter system". The overall frequency range was wide (from 60 sec to 40 Hz) and divided into a maximum of 13 channels. The ChISS station analyzes ground velocity. Most stations have only 7-9 channels with central frequencies  $f_c$  from 0.3 or 0.6 Hz to 27 or 40 Hz (Figure 2 and Table 2).

Table 2. The Band Pass of ChISS Filters ( $f_1 - f_2$ ) and Their Central Frequencies  $f_c$

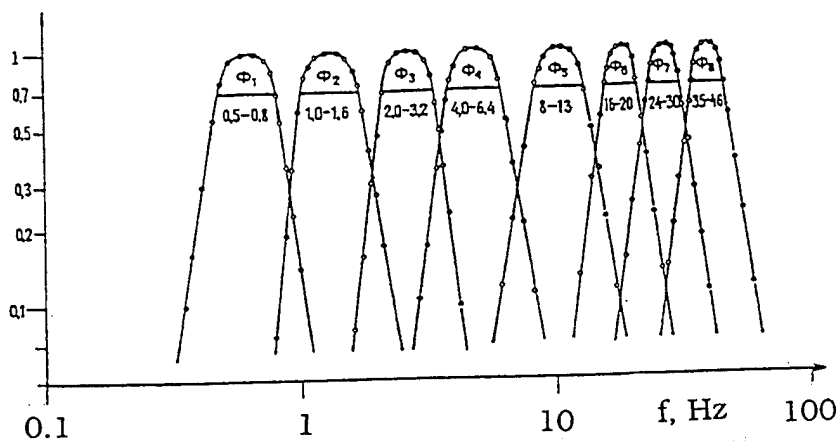
Band $f_1 - f_2$ , hz	$f_c$ hz	Band $f_1 - f_2$ , hz	$f_c$ hz
0.016 - 0.032	0.022	2.0 - 3.2	2.5
0.032 - 0.064	0.045	4.0 - 6.4	5.0
0.050 - 0.10	0.07	8.0 - 13	10
0.10 - 0.20	0.14	16 - 20	18
0.25 - 0.40	0.31	24 - 30	27
0.5 - 0.8	0.62	36 - 45	40
1.0 - 1.6	1.25		

The relative width of the band-pass filters is  $k = df/f_c$ , the absolute width  $df=f_2-f_1$ , and  $f_c$  is the central frequency of the filter (the square root of  $f_2 \cdot f_1$ ). ChISS stations with long-period filters (range  $T_c=3-40$  sec) have  $k=0.7$  (one octave), mid-frequency ranges (0.6-10 Hz) have  $k=0.48$  (two-thirds of octave), and the high-frequency ranges, 18-40 Hz, have narrower bands with  $k = 0.23$  (one-third of octave). These filter widths are narrow enough to describe the frequency content, but wide enough to preserve the temporal structure of seismic waves. When  $k=0.5$ , the response to a delta-like input pulse is 2 cycles of oscillation, so the time history of the seismic signal is not obscured. The pulse response consists of 1.5, 2 or 4.5 cycles corresponding to  $k=0.7$ , 0.5 and 0.23.

The ChISS instrumentation in the GAR, TLG, ZRN, NSB, CHU and CHD stations was operated for a long period, at some other stations only temporarily. Examples of ChISS records are shown in Figures 3 - 8.

Lately, the frequency range was widened up to 200 Hz by additional channels with  $f_c$  40, 60, 90, 136 and 204 Hz (Figure 9). Not many records were obtained, but it is important that some local events were recorded at  $f=200$  Hz.

## ChISS amplitude response



## ChISS impulse response

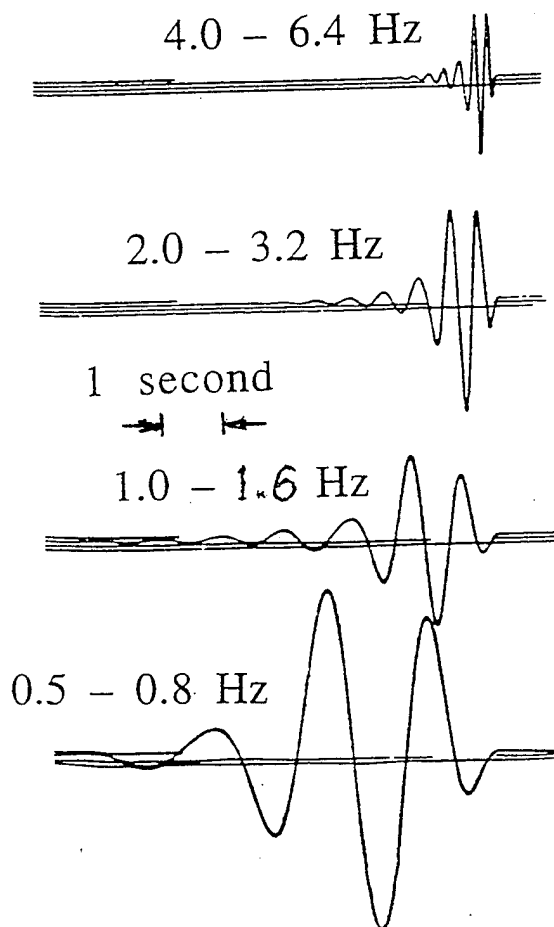


Figure 2. ChISS station characteristics, version for local events registration. There are eight channels with central frequencies  $f_c$  from 0.6 Hz to 40 Hz; top - the magnification curves; bottom - the time responses on the delta input signal.



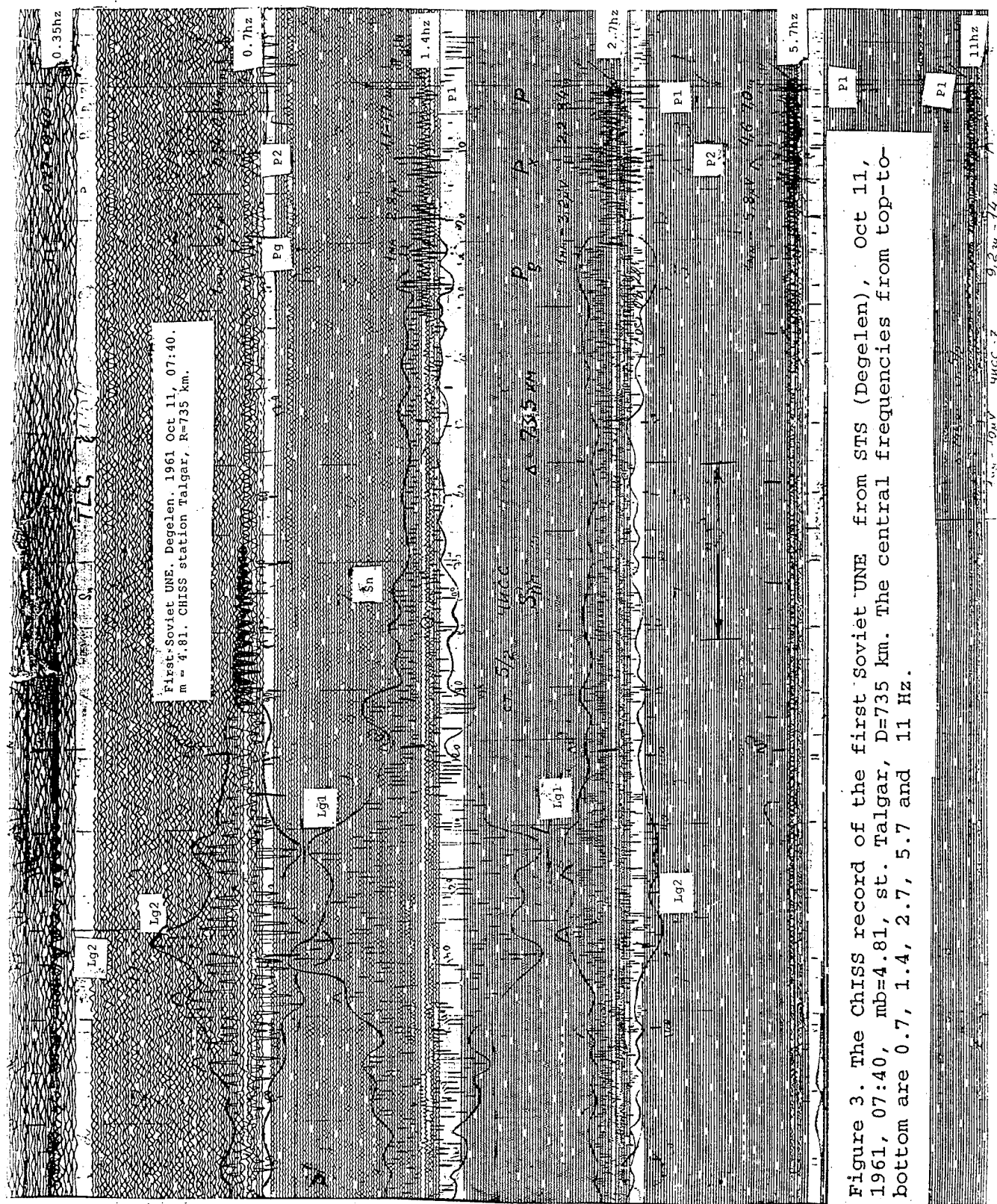


Figure 3. The ChISS record of the first Soviet UNE from STS (Degelen), Oct 11, 1961, 07:40, mb=4.81, st. Talgar, D=735 km. The central frequencies from top-to-bottom are 0.7, 1.4, 2.7, 5.7 and 11 Hz.

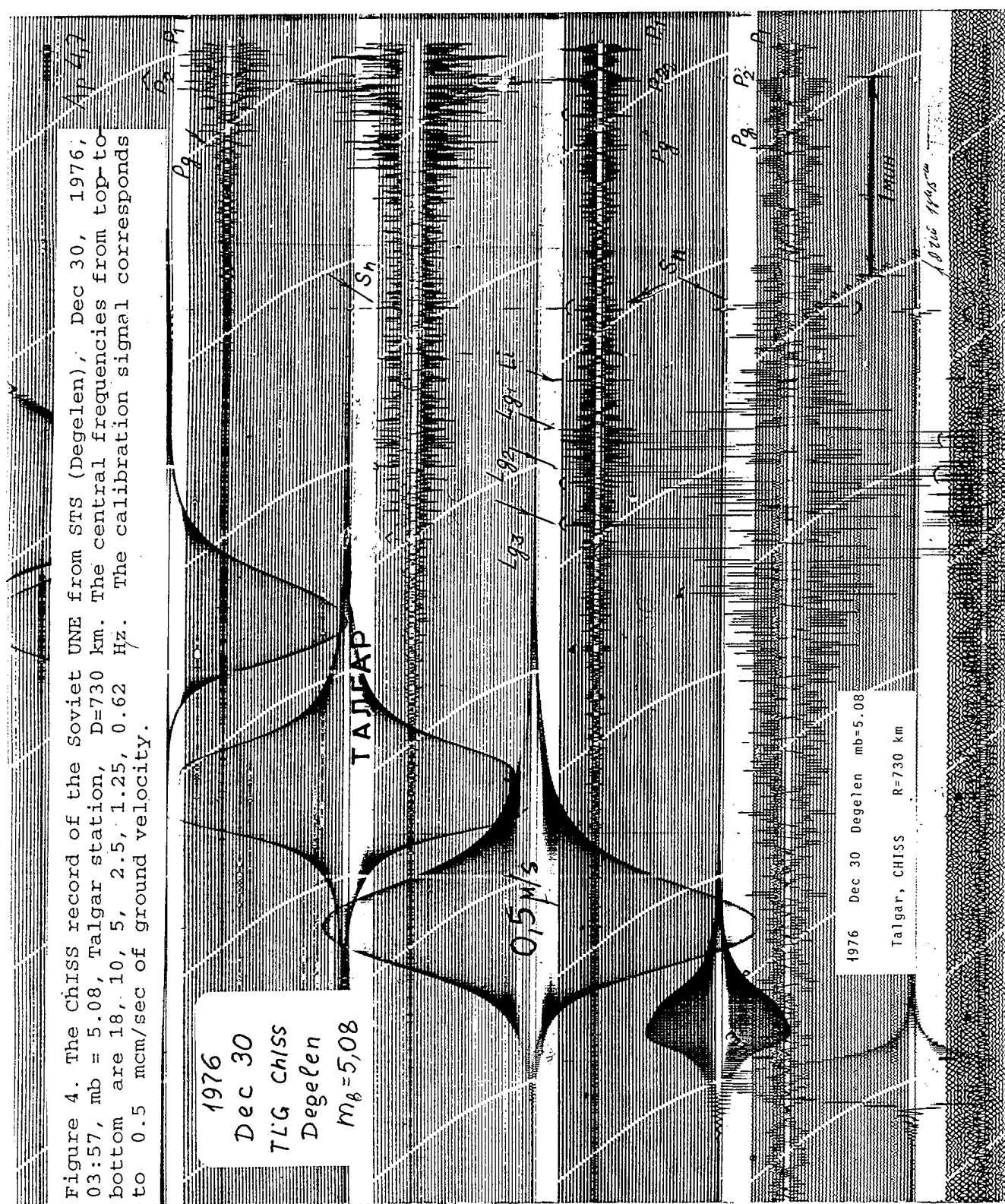


Figure 4. The CHISS record of the Soviet UNE from STS (Degelen), Dec 30, 1976, 03:57, mb = 5.08, Talgar station, D=730 km. The central frequencies from top-to bottom are 18, 10, 5, 2.5, 1.25, 0.62 Hz. The calibration signal corresponds to 0.5 mcm/sec of ground velocity.

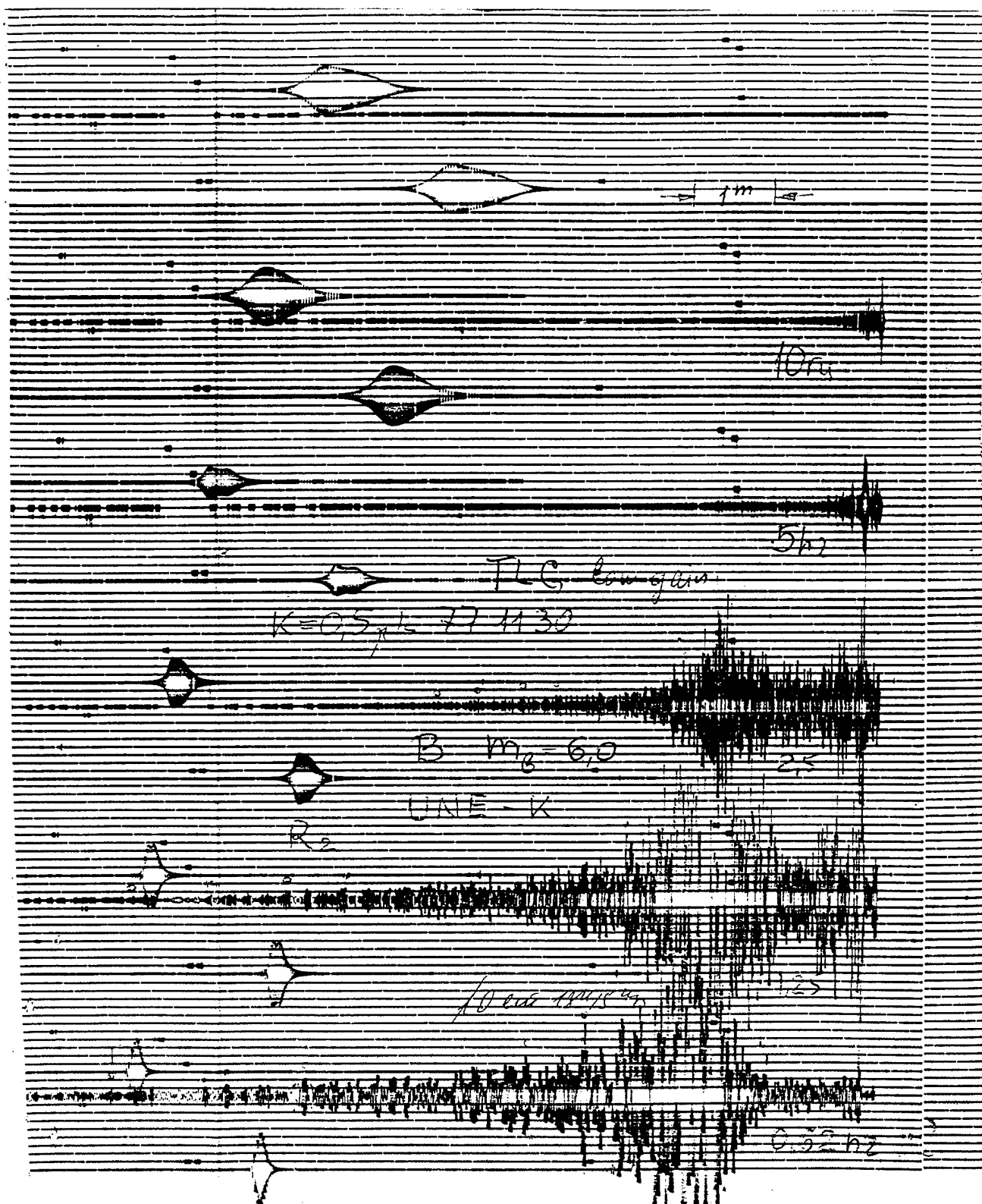


Figure 5. The ChISS record of the Soviet UNE from STS (Degelen) by instrument with low gain, Nov 30, 1977, 04:57,  $m_b = 6.0$ , Talgar station,  $D=745$  km. The central frequencies from top-to-bottom are 27, 18, 10, 5, 2.5, 1.25, 0.62 Hz. Calibration signal corresponds to 0.5 mcm/sec of ground oscillation velocity.

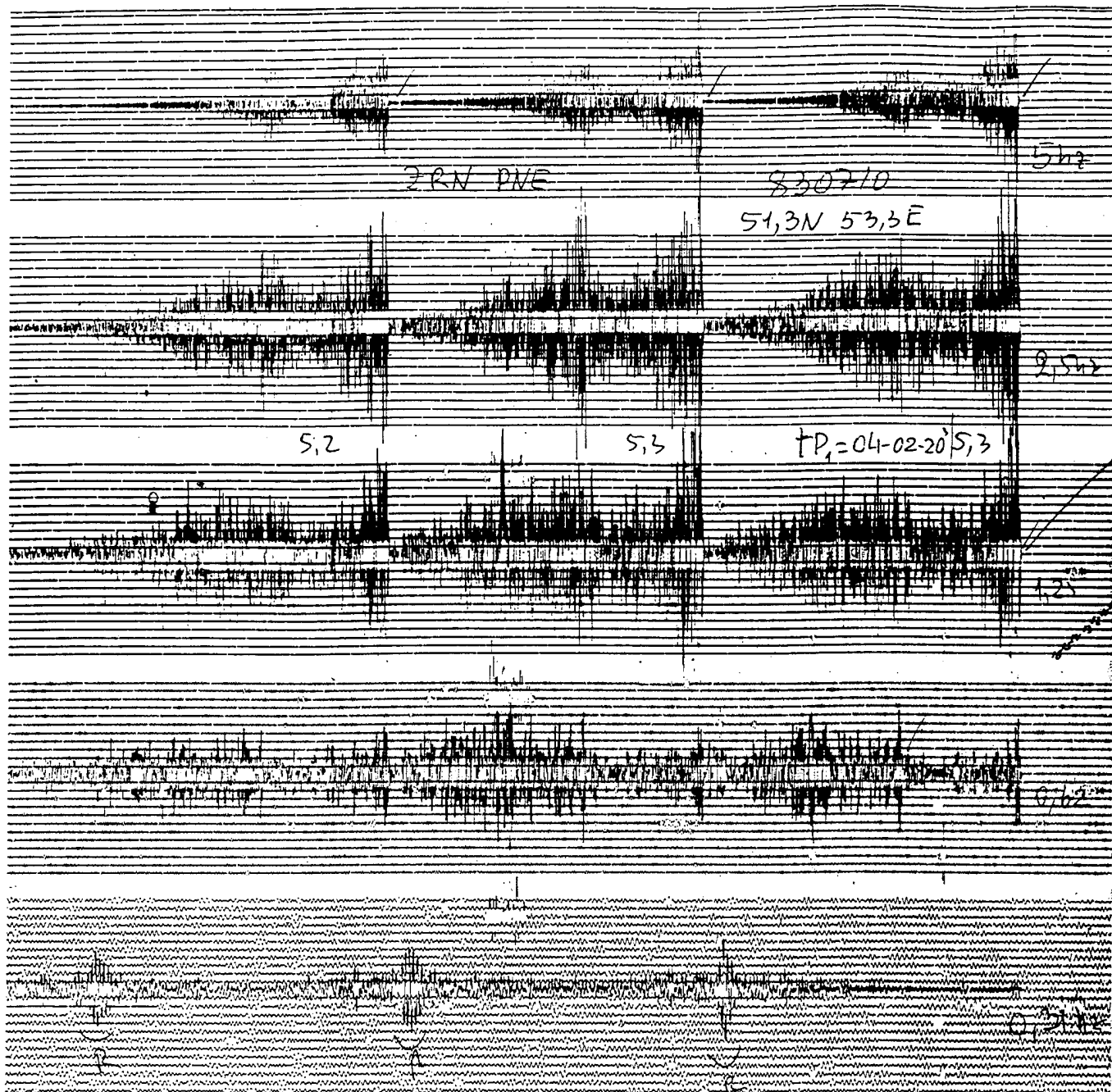


Figure 6. The ChISS record of the three Soviet ONEs from Orenburg (51.3N; 53.3E), Oct 7, 1983, 04:02, mb about 5.3 for each of them, Zerenda station, D = 1100 km. The central frequencies from top-to-bottom are 5, 2.5, 1.25, 0.62, 0.31 Hz.

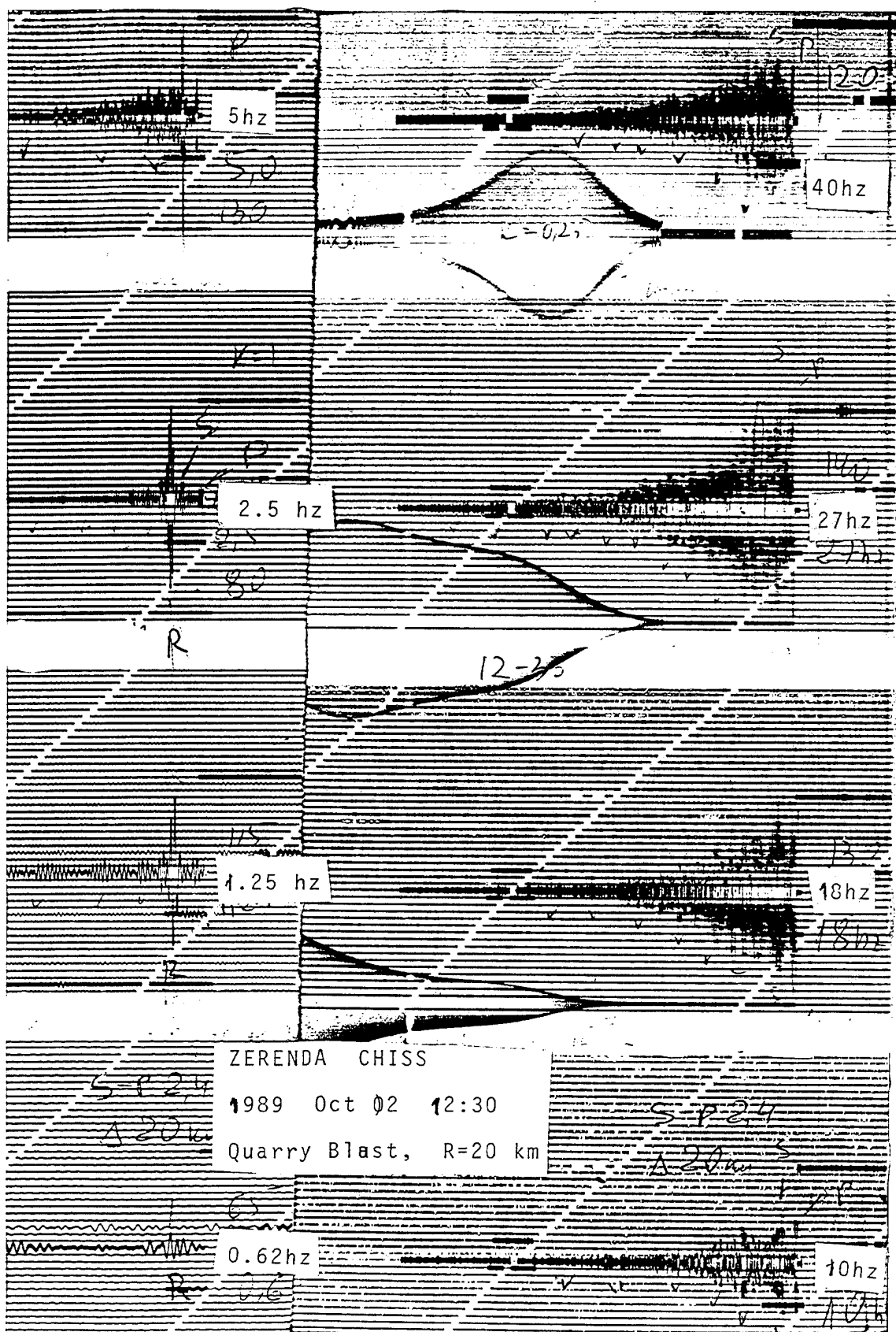


Figure 7. The ChISS records of the quarry blast from North Kazakhstan, Oct 2, 1989, Zerenda station, D = 20 km. The central frequencies from top-to-bottom - left : 5, 2.5, 1.25, 0.62 Hz; right: 40, 27, 18, 10 Hz.

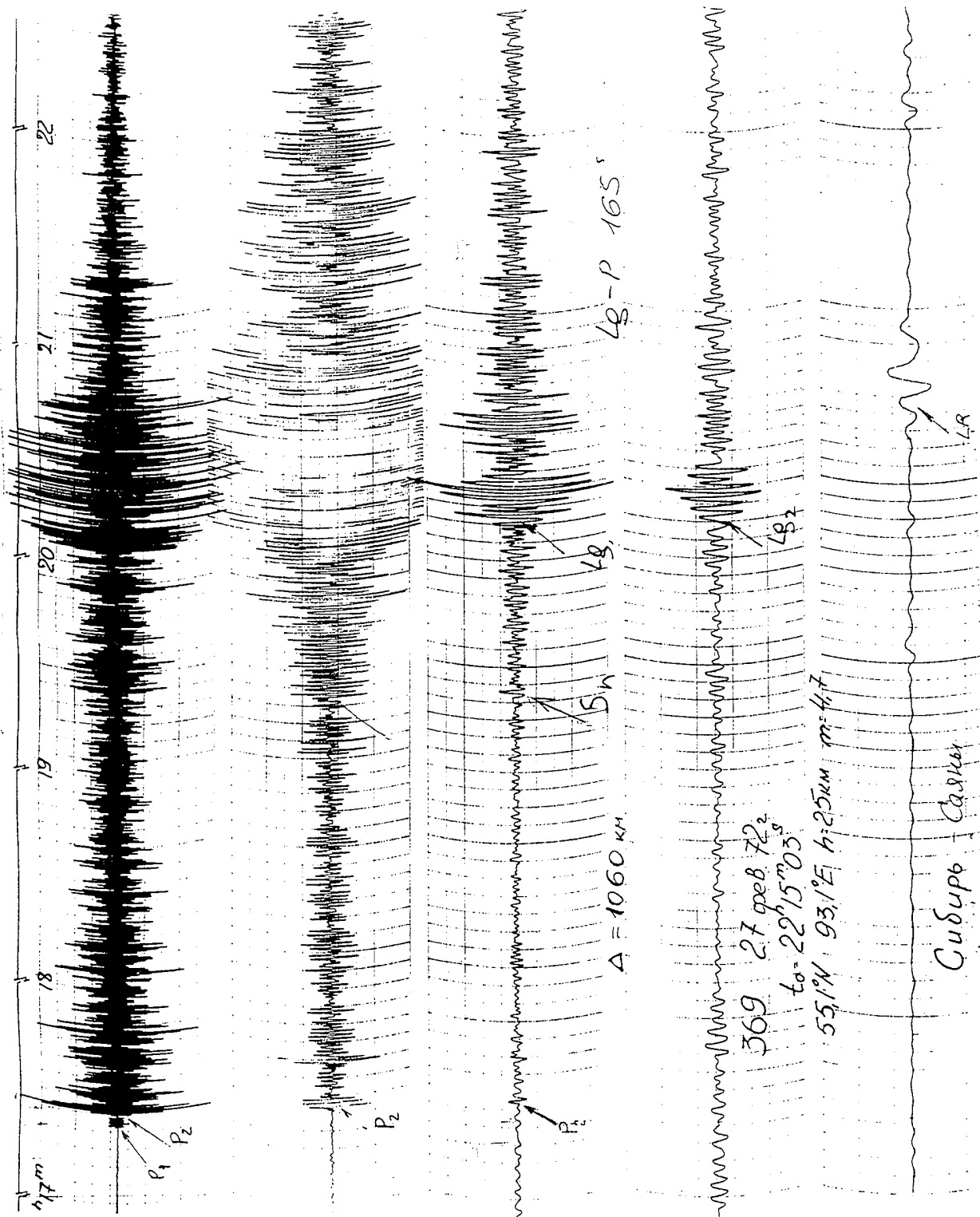


Figure 8. The Chiss records of the earthquake from Sayan (55.1N, 93.1E), Feb 27, 1972, mb = 4.7, Semipalatinsk station (ink record), D = 1060 km. The central frequencies from top-to-bottom: 2.8, 1.0, 0.47, 0.35, 0.07 Hz.



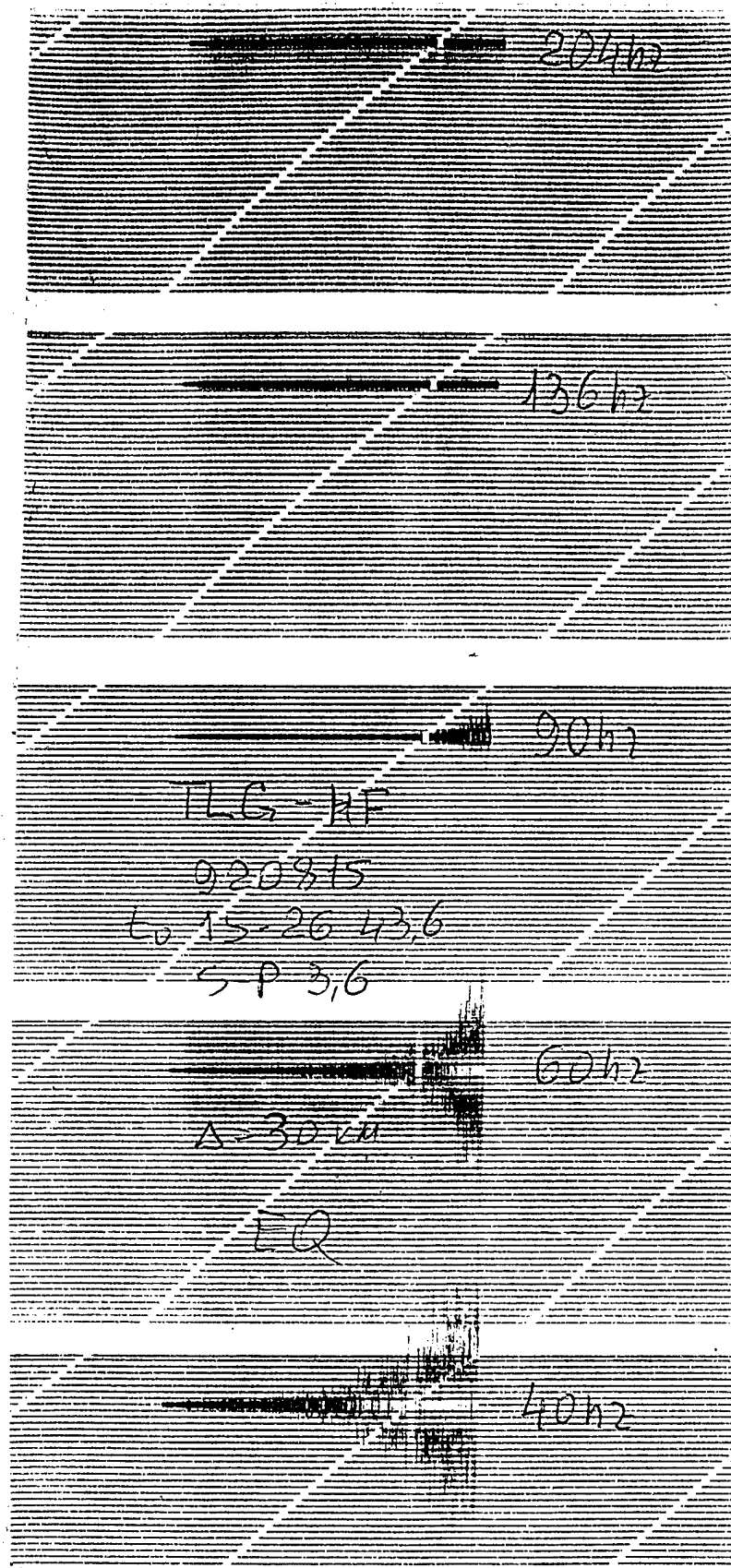


Figure 9. The local earthquake at South Tien Shan region recorded by high-frequency version of Talgar ChISS station, Aug 15, 1992,  $D = 28$  km. The central frequencies from top-to-bottom: 204, 136, 90, 60, 40 Hz; the relative width of channels  $df/f_c$  is 0.22.

## 2. CALIBRATION SCALES AND CATALOGS OF SEISMIC DATA IN THE USSR

Specific magnitude scales were used in the FUSSR as a standard. They were MLH (and MLV), MPV and energy class K. The coda wave scale, Mc, was proposed in the last decade [T.Rautian et al., 1981]. It has not yet become standard, but we consider it the most preferable. The national network, dealing mostly with teleseismic distances and for earthquakes with  $M > 4$  used the surface wave magnitudes MLH and MLV, and P wave magnitude MPV. These correspond to  $M_s$  and  $m_b$  used in US, but there are some differences.

### 2.1. Surface Wave Magnitude MLH

The magnitude MLH used in the FUSSR is defined as

$$MLH = \log(A/T) + 1.66 \log D + 3.3, \quad (2.1)$$

where  $A/T$  is the maximum of this quantity in the surface wave train on the horizontal component of SKD or SK records (see Section 1),  $A$  is measured in micrometers,  $T$  period in sec,  $D$  distance in degree [Gutenberg, 1945; Vanek et al., 1962]. LH is the usual magnitude used for moderate and large events. At times MLV (calculated in the same way from the vertical component of surface waves) were published, but MLV did not become an official scale. It was found that MLH and MLV gave very similar values, so publication of MLV values in bulletins ceased.

The MLH scale gives nearly the same values as the  $M_s$  magnitude scale used by Western seismologists. It was shown [V.Khalturin, 1974] that there is a relation between these magnitudes in the magnitude range from 5 to 7.5 :

$$MLH = M_s + C. \quad (2.2)$$

The mean  $C$  value is 0.15. It varies slightly depending on epicentral zone:

Far East (Alaska, Aleuts, Kuril,	
Kamchatka, Japan)	0.30
Indonesia, Fiji, New Guinea, Tonga	0.00
Continental Asia	0.10

A change in the name of this scale was made in 1988, instead of MLH it was called " $M_s$ ". Our opinion is that it was a wrong step, because of the difference in the definition of  $M_s$  and MLH. So, when looking at catalogs since this change, Western seismologists have to remember an old adage: "If 'Buffalo' is written at the cage of the lion - do not believe your eyes".



## 2.2. Body Wave Magnitude MPV

In a routine procedure MPV determination was standard and used the same calibration function as mb for all stations, regions and instruments, for distances greater than 2000 km. In some studies MPH (from horizontal component records) was also considered.

Magnitude MPV is similar to the mb scale and used the same calibration function, but there are some differences because of the instruments. Values of mb are obtained from a short-period Benioff instrument ( $f_0=1.3$  Hz), whereas MPV are determined from SKD ( $f_0=0.05$  Hz) and SKM ( $f_0=0.7$  Hz) instruments, using the same calibrating curve for both instruments. Instrument differences were at first denoted by MPVA (for SKM) and MPVB (for SK or SKD). Since 1988, the names of the scales were changed to MPSP (for the short-period instrument) and MPLP (for long-period).

For teleseismic events MPLP is slightly larger than MPSP in average on 0.25-0.3 mag. units. Their difference increases with magnitude [Magnitude..., 1974; Rautian, Khalturin et al., 1981] as:

$$\text{MPLP} = 1.16 \text{ MPSP} - 0.50 .$$

The methods of measuring mb and MPV scales are also different. The Western tradition is to make measurements in the beginning part of P wave records. This is a natural and good procedure for nuclear explosions and small earthquakes with a short duration of the source process. But for large earthquakes, the maximum amplitudes can be radiated late. In that case the amplitude measured near the first arrival will not be the maximum. An additional effect arises at regional distances, from hundreds of km up to 2,000 km: the max of A/T can be late in the wave train not only due to the duration of the source process, but also due to the complexity of the wave form of regional phases.

The Russian procedure is to measure A/T at a moment of time, when there is a maximum of the wave on displacement records. It is not easy to say how important the contribution of this difference in measurement technique is in comparing magnitudes from Soviet and World Wide seismic networks, but we expect differences in magnitude values due to this differences in procedure.

Another aspect is connected with the frequency, at which the measurement conducts. It was shown [K.K.Zapolsky et al., 1973 and 1974] that correspondingly to initial Gutenberg's definition of magnitude, the measurements have to be done at frequency, which is at the maximum of velocity spectrum. The frequency on records belongs to high-frequency slope of

velocity spectra, being limited by corner frequency  $f_0$  of instrument magnification curve. The values  $f_0$  are different at Benioff (1.3 Hz) and SKM (0.7 Hz). It makes the magnitude  $m_b$  less than MPV by about 0.25. Thus, MPV from records of SKM is less than from SKD, especially for large earthquakes.

### 2.3. Energy Class K

The energy class K [Rautian, 1960, 1964, 1974] was used routinely since the 1960s as a scale for regional networks in all continental regions of the USSR. K is based on the sum of maximum amplitudes of P and S (or P and Lg) waves. The sum ( $A_p + A_s$ ) is more stable to variations due to radiation pattern and propagation factors. There are two versions of the calibration curves, depending on the instrument used, SKM or SKD. In practice the SKM measurement was commonly used.

The calibration curve was determined in the distance range 5 to 3000 km. The K value was intended to be a measure of seismic energy radiated by the source

$$K = \log E, \quad (E \text{ in J}). \quad (2.3)$$

It was found later, that the energy class is a little more, than  $\log E$ : in average for the whole Central Asia it is about

$$K = \log E + 0.30. \quad (2.4)$$

Figure 10 shows the nomogram for determining K from SKM amplitudes. Note that the distance scale is not exactly logarithmic, but is deformed to make the amplitude curve a straight line. K is proportional to  $\log(A_p + A_s)/0.56$ . Note that the SKM instrument records displacement, not velocity of ground motion; thus, a dominant period of ground oscillation is implicitly assumed. However, the coefficient of  $\log(A_p + A_s)$  is 0.56, not 0.50, indirectly taking into account that the period (which is not measured) of the maximum amplitude of the phases increase with increasing.

MPV scale is not used practically in studying regional seismicity because A/T-D is very unstable at distances up to 2,000 km; the main scales are MLH and K. The standard equation between them is [Rautian, Khalturin et al., 1981]:

$$MLH = 0.67K - 3.53. \quad (2.5)$$

The  $K=15$  approximately corresponds to  $MLH=6.5$ ;  $K=13$  to  $MLH=5.1$ ;  $K=10$  to  $MLH=3.2$ .

The relation between K and  $m_b$  was found to be for UNE from STS [Khalturin, Rautian, Richards, 1993]:

$$m_b = 0.44K - 0.53. \quad (2.6)$$

# THE NOMOGRAM FOR ENERGY CLASS K DETERMINATION FROM SKM RECORDS

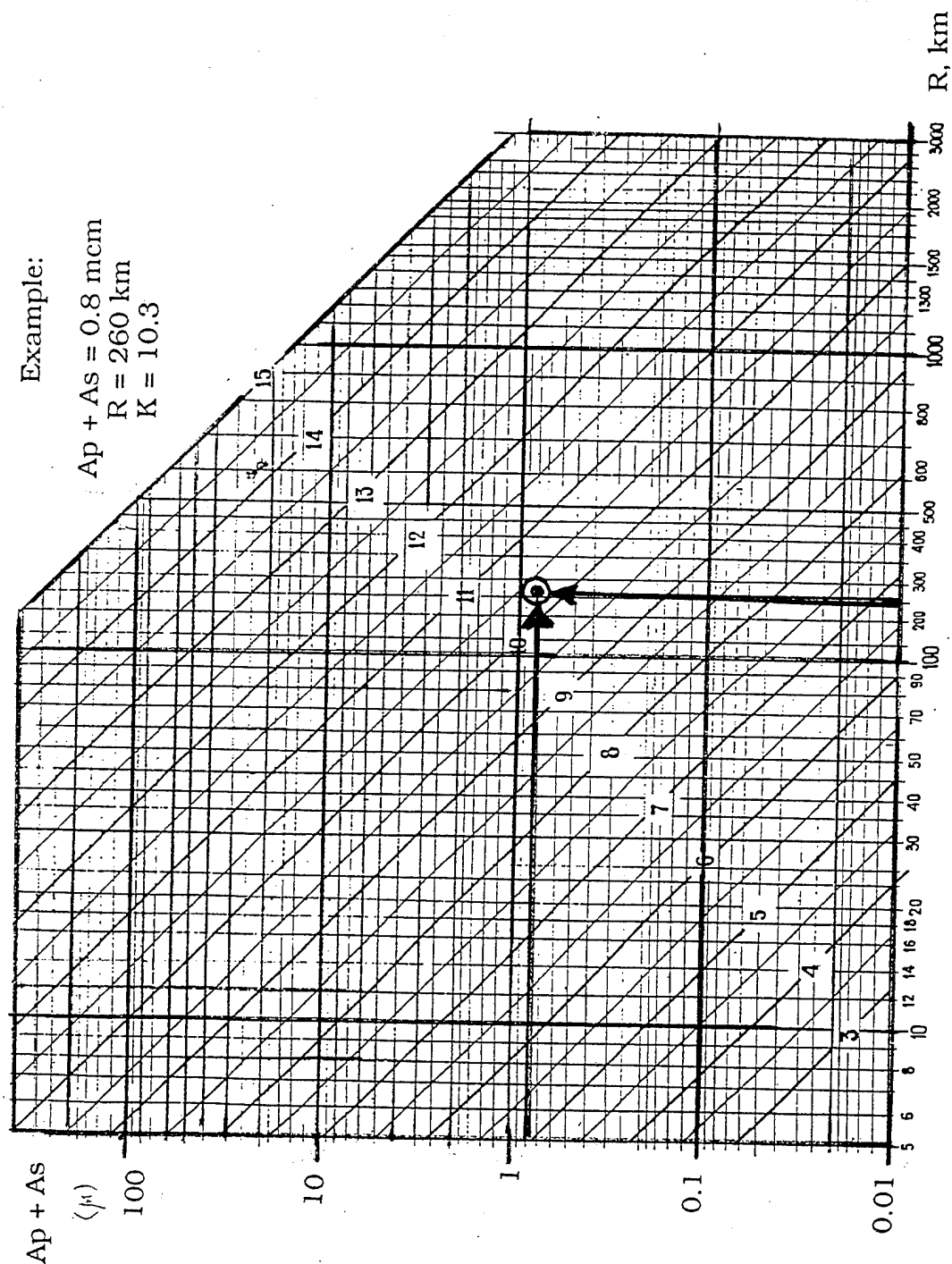


Figure 10. The nomogram for determining  $K$  from  $A_p + A_s$  amplitudes at SKM records. Note that the distance scale is not exactly logarithmic, but is deformed to make the amplitude curve a straight line.  $K$  is proportional to  $\log(A_p+A_s)/0.56$ .

For earthquakes the equation between MPSP and logE (in J) was found [Rautian, Khalturin et al., 1981]:

$$\text{MPSP} = 0.415 \cdot \log E - 0.05 \quad (2.7)$$

Taking into account (2.4) we get

$$\text{MPSP} = 0.415 \cdot K - 0.17 \quad (2.8)$$

#### 2.4. Coda Magnitude $M_c$

Our scale  $M_c$  [Rautian, Khalturin et al., 1981] uses the amplitude of coda, but not its duration. We use the coda envelope (amplitude versus lapse time) obtained from observation as a calibrating curve.

It was found from studying coda, that coda amplitudes vary from amplitudes predicted from a generalized envelope much less than direct wave amplitudes vary from generalized amplitude curves. This is because scattered waves illuminate the earth medium in all directions, so inhomogeneities in a substantial volume take part in creating the coda. Thus, coda averages source factors through scattering of direct waves over many points and directions, removing variability due to these factors. The only factor causing differences in the level of coda envelope for the same earthquake at different stations is the local station condition.

That prompted us to create the magnitude scale  $M_c$  for earthquakes at regional distances. Two versions of  $M_c$  were proposed, for records by SKD and SKM instruments. The level of the coda envelope at a certain lapse time was taken as a measure of coda intensity. For SKM records the level of coda at  $t-t_0=100$  sec was used, for SKD records:  $t-t_0=1000$  sec. Coda magnitude  $M_c$  was defined to be the same value as MLH when  $\text{MLH}=5.00$ . The defining formulas are

$$M_c(\text{SKM}) = \log A_{100}^{\text{SKM}} + 3.8 \quad (2.9)$$

and

$$M_c(\text{SKD}) = \log A_{1000}^{\text{SKD}} + 4.7 \quad (2.10)$$

Figure 11 shows the example of nomograms for determining coda magnitudes (from records of SKM standard instrument). The crosses and open circles are the amplitude of coda, measured at two stations, GAR and CHS for the same earthquake. One can see the small scattering of amplitudes. The magnitude from this data are estimated as 5.33 with standard deviation of individual measurements 0.055 only.

# THE NOMOGRAM FOR CODA MAGNITUDE $M_c$ DETERMINATION

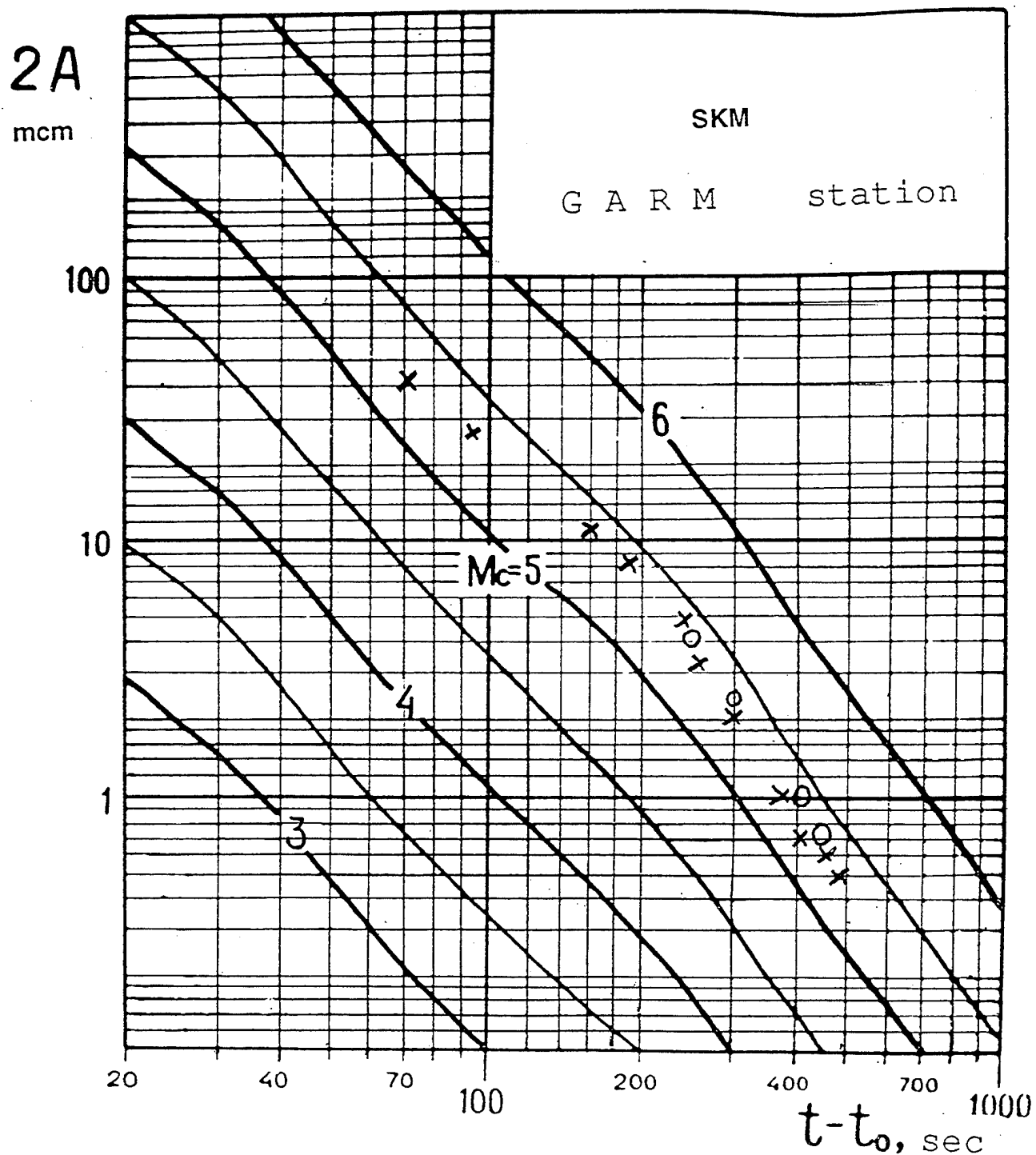


Figure 11. The nomogram for determining coda magnitudes  $M_c$  from SKM. The example of magnitude determination is shown: the crosses and open circles are the measured coda amplitudes of the same earthquake at two stations. The magnitude  $M_c(\text{SKM})$  calculated from these 15 measurements is 5.35 with their scattering of 0.06

Figure 12 shows the correlation between MLH and  $M_c(SKM)$ . Two groups of earthquakes were used: the deep (50-250 km) and the shallow ones. The MLH for deep earthquakes were calculated from amplitudes measured in the part of seismograms, corresponding to the group velocity 3.0-2.9 km/sec. In Figure 13 one can see that the same intensity of short-period coda corresponds to significantly bigger MLH at shallow events, then for deep ones.

Comparing two short-period scales (K and  $M_c(SKM)$ ) the correlation between them is the same for shallow earthquakes and for deep ones:

$$K = 1.73 M_c(SKM) + 4.14$$

or

$$M_c(SKM) = 0.78 K - 2.40 .$$

Coda magnitude was not used as a standard scale, but we prefer it as the most accurate for regional networks.  $M_c$  can be used successfully when only a few, even only single-station, data are available.

## 2.5. Catalogs of Seismic Data in the FUSSR

There were three main sources of seismic information which were published in the FUSSR.

Since the 1950s, data for earthquakes in the FUSSR territory as well as the rest of the world were published in "Preliminary Catalog of events" (first source) for each 10-day period. About 1,000-1,500 events per year were reported. The lower limit of magnitude was about 4.0 for Central Asia, 4.5 for other parts of the FUSSR, 5-5.5 for Eurasia, 5.5-6 for other regions of the World. The Catalog included origin time to, region of epicenter, coordinates and depths, magnitudes MLH (Ms) and MPV from SP and LP records, and some macroseismic data about strong events.

The "Seismic Bulletin" (second source) included reviewed epicenter parameters, the number of stations used and parameters of ellipse of error. Some station data (arrival times, amplitudes and periods of main phases) were also published. The Bulletin was also issued every 10 days.

Annually, "Earthquakes in the USSR" published lists of local and regional earthquakes. The lists included earthquakes from  $K=9$  (corresponding to  $M_s=2.8$ ) separately for each of the regions: Carpathian, Crimea, Caucasus, Kopetdag, Central Asia (including Pamirs-Hindu Kush zone), North Tien Shan, Altai-Sayan, Baikal, East Siberia, Sakhalin, Kamchatka, Arctic.

The energy class K was estimated for all earthquakes.

# COMPARING MAGNITUDES MLH and Mc(SKM)

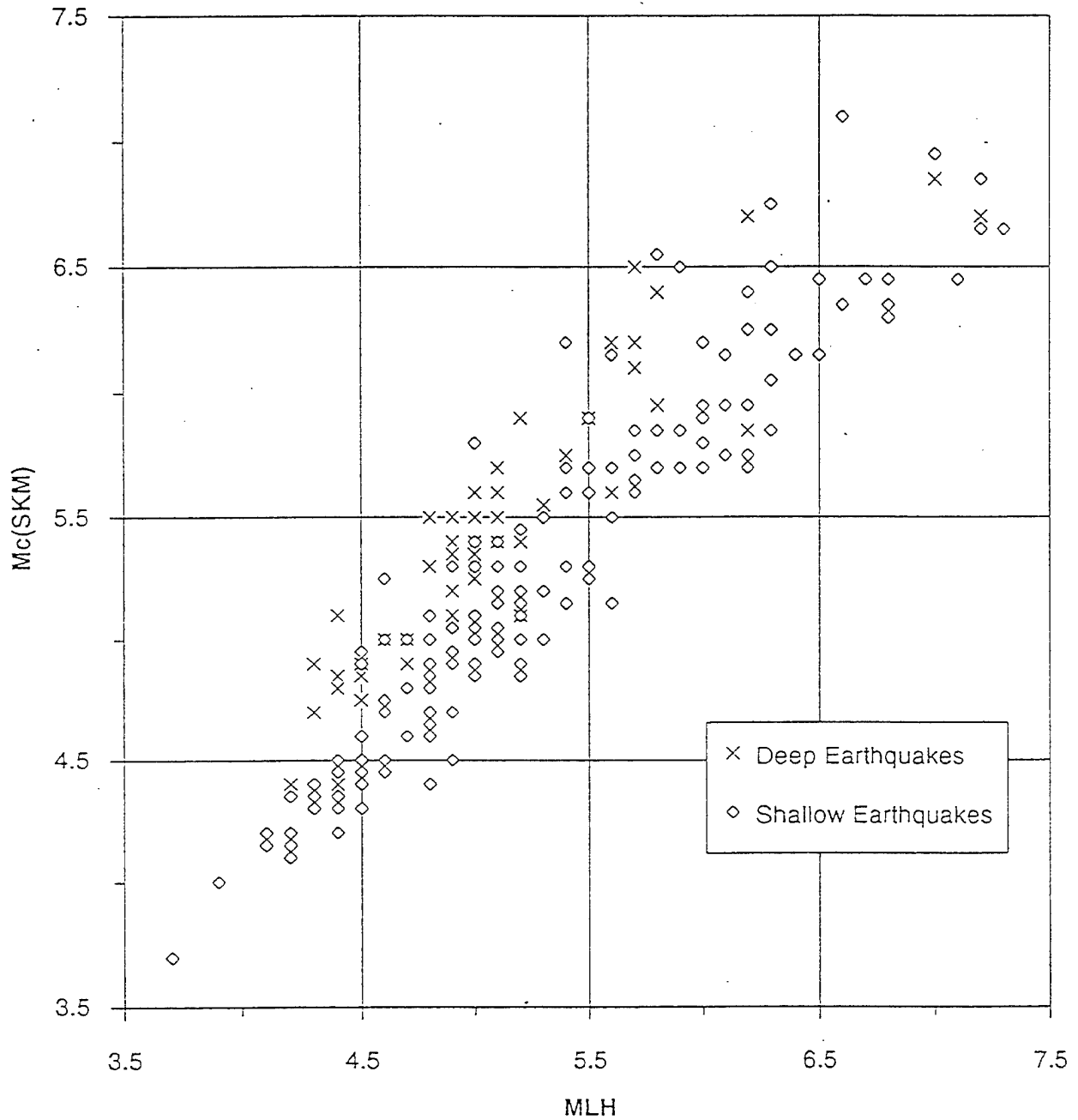


Figure 12. The correlation between MLH (from Soviet Bulletin) and Mc(SKM), calculated from single station GAR. The diamond are for shallow earthquakes, Xs for deep (80 - 250 km) ones. Note the saturation for large magnitudes (5.5 - 7.0) for both groups of earthquakes.

# COMPARE MLH AND Mc(SKD)

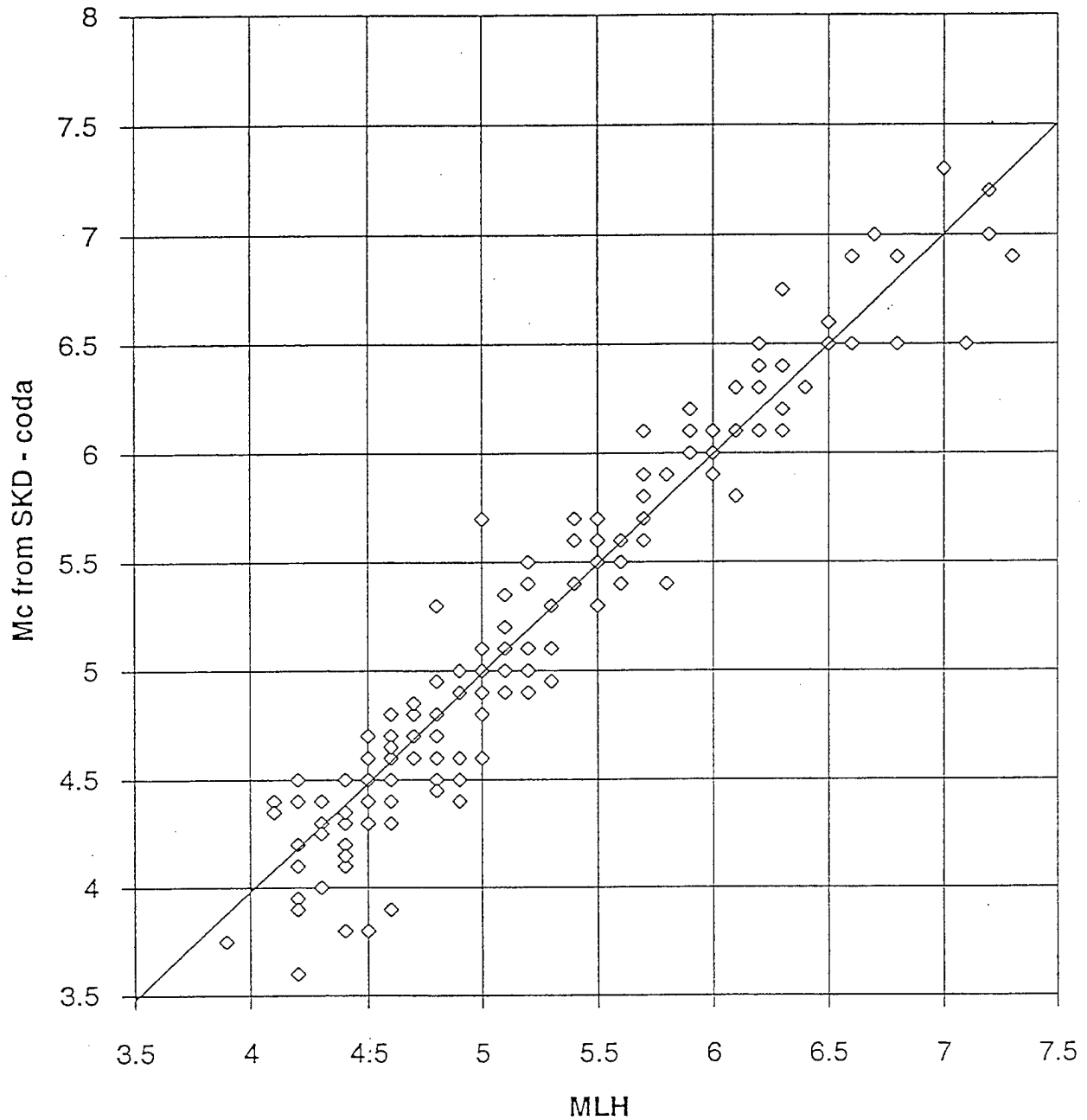


Figure 13. The correlation between surface waves magnitude MLH (from Soviet Bulletin) and coda magnitude  $Mc(SKD)$ , calculated from SDD-records of single station Garm.



The Annual summarized the long-term seismicity of each of the regions mentioned above. Macroseismic data for earthquakes were described in regional papers. During the last decade fault plane solutions, source spectra and source parameters (seismic moments, seismic energy, apparent stress, etc.) were also published for some regions.

### **3. THE PROBLEM OF ACCURACY OF MAGNITUDE DETERMINATION; THE MULTI-FACTOR MODEL OF MAGNITUDE RESIDUALS**

#### **3.1. The Accuracy of Magnitude and Station Corrections**

Authors define the errors of their calculations as a standard deviation of individual estimations divided by the square root of the number of the data used. If the data from all the world were available and huge numbers of earthquakes were used, the error calculated by this method would, naturally, be extremely small. For example, North [1985] found that in his study the standard deviations of station residuals obtained from separate earthquakes vary from 0.24 (PRU) to 0.50 (BNG). Having divided these values by the square root of the number of the earthquakes investigated, he estimated the error of the station corrections which varied from 0.0052 (MOX station) to 0.0174 (CAN). On the average, it is 0.0099. In [Vanek et al., 1983], the number of earthquakes was not too great (from about 10 to 200-230), the error of the correction was estimated by them about 0.02-0.075.

The same situation is with errors of magnitude determination. The values of magnitudes for UNEs are published with three decimals and with announced errors about 0.01 or less. But is the real error so small? The simplest way to check it is to compare the station correction obtained independently for the same stations by different authors.

The station corrections made by different authors were compared. The data obtained using short-period instruments are in Table 3, the data of the long-period ones are in Table 4.

The sources of information for this table are:

"Marsh" and "Ring" - Marshall and Ringdall. Their data were taken from [Richards, 1993].

"North" - the data from [North, 1977].

"Feof" - [Feofilaktov, 1970]. He studied station correction using the data of 20 Aleutian earthquakes 1961-1963 with the MPV between 5.8 - 6.8. He used the recordings at 17 basic seismic stations with SK instruments (1-10 sec).

"Tskh" - [Vanek and Tskhakaya, 1967]. They studied the station corrections for 8 stations operating in the Caucasian region. The residuals were referred to the Yerevan station. 268 distant earthquakes ( $D = 60 - 80$  degrees) were studied.

The calculated accuracy of these corrections varied from 0.031 (BKU, 56 obs.) to 0.007 (TBL, 178 obs).

"Khalt" - [Antonova, Aptikaev, Khalturin et al., 1968]. The station correction was referred by the level of the station amplitude-distance curves to our own general curve obtained by generalizing many station and regional curves. These are data from 12 stations, mentioned above.

"Pas" - [Pasechnik, 1962]. He determined the station corrections using the data of the underground nuclear explosions on the Nevada Test Site recorded at 34 Soviet seismic stations. Here we quoted his data for the stations we used.

"Vanek" - A team of Soviet and East European seismologists [Vanek, Kondorskaya, Christoskov, 1967, 1974, 1978, 1979, 1980, etc]. They are studying the amplitude curve together with the station residuals to obtain an "Optimized Homogeneous Magnitude System".

Table 3. The Station Magnitude Corrections for MPV (Short-Period Instrument SKM) Obtained from Different Sets of Data

St.	Marsh	Ring	North Vanek	St.	Marsh	Ring	North Vanek
ALE		.22	-.04	KRA		.32	.22
ASP		.09	-.05	KRV	.00		.35
BHA		-.25	-.28	KTG		-.07	.02
BKR	.40	.38		LAO	-.1	.04	-.10
BMO	-.3	-.28	-.29	LOR		-.08	.06
BNG		.01	-.07	LPS		.12	.04
BOD	.00	-.02		MBC		.09	.14
BUL		-.05	-.07	MOX		.07	.02
CAN		.11	-.02	MOY	.10	.12	
CAR		.14	.13	NAO		-.10	-.09
CLK		-.24	-.27	NDI		.30	.33
CLL		.16	.20	NEW	-.2	-.07	.05
COL		.07	.01	NUR	.2	.11	.19
CPO	.2	-.02	-.07	OBN	.30	.39	
DUG	-.1	-.04	-.15	PET	.20		.04
EDM	.3	.43	.37	PMG		.27	.10
EKA		.00	.00	PMR		-.11	-.08
EKT	.40	.37		POO		.19	.17
ELT	.20	.15		PRE		-.08	-.07
EUR	-.20	-.36	-.24	PUL	.30		.05
FRU	.40	.35	.01	PYA	.30		.09
GDH		-.05	.00	RES		.04	.13
GRF		.25	.24	SEM	.10		.32
HFS		.13	.05	SHL		.22	.11
HYB		.26	.19	SJG		.19	.24
ILT	.10	.08	.33	SOC	.30		.06
IRK	-.10	-.03		TIK	.10	.03	.27
KBL	.20	.15		TUC	-.2	-.17	-.14

Table 3. (continued)

St.	Marsh	Ring	North Vanek	St.	Marsh	Ring	North Vanek
KEV	.00	.05	.02	TUL		.21	.21
KHE	.30	.37	.02	UBO		-.13	-.11
KHC		.03	.10	VLA	.20		.32
KHO	.60	.59		YAK	.40	.43	
KJF	.10	.16	.09	YSS	.10	.20	.41
KOD		.18	.06	ZAK	-.10	-.11	.33

In [Richards, 1993], the average difference between the station corrections by [North, 1977] and [Ringdal, 1985] for 48 common stations was found to be 0.074. It seems a good value; however, it is much more than the expected difference 0.014.

We borrowed the station corrections from [Ringdal, 1985] and [Marshall, 1979] for 27 stations. The standard deviations for difference between them is similar to that of North/Ringdal: 0.089. In both publications the global data were used, the calculating system of corrections was the same, and in both cases the very many earthquakes in over the world locations were taken to calculate each station correction. That is why they obtain so small absolute values of station residual discrepancy. But even these small values are four times greater than the expected ones if based on announced errors.

In comparing their residuals with Vanek - Kondorskaya ones, the difference was found much more. From 13 common stations the standard deviation of difference between Vanek and Marshall data is 0.25, with systematic difference being as small as 0.007. The standard deviation of station corrections for long-period (SKD) recordings are listed in Table 4.

Table 4. The Station Magnitude Corrections for MPV (Long-Period Instruments SKD) Obtained from Different Sets of Data

Stat.	Pasech	Tskha	Vanek	Feofil	Khalt
AND	-.45				-.27
APA			-.05	.00	
ASH				.00	
ATA	.06				-.21
GAR	-.12				
GRS		.12	.09	-.05	
FRU	-.25		.06	.21	-.06
IRK	.03		.30	-.29	-.34
KBL	.06				.21
KRV		.06	.04	-.07	
KYH	.10			-.02	.21
MAK		.16	.13	-.22	

Table 4. (continued)

Stat.	Pasech	Tskha	Vanek	Feofil	Khalt
PUL			.26	-.37	
PYA		.30	.05		
RYB	.20				.06
SEM			.22	.22	
SIM			.15	.20	
SOC		.24	.13		
TAS		-.25	-.07	-.14	.08
TLG	-.07				.06
VLA			.30	.32	
YSS			.21	-.30	

From these data the standard deviation of difference between residuals, obtained by the authors for the same station is large too: 0.195 (Figure 14). Again, it is much greater than announced errors.

We think that there are two causes for so significant a discrepancy. First, all Soviet data obtained from earthquakes from lesser epicentral zones than data by North, Ringdall and Marshall. Thus, zone effect, as well as path effect, being not smoothed enough badly created the scattering of residuals. Second, is a different basic magnitude. For instance, Vanek et al. take OBN as the basic station with a zero correction. But from [Ringdall, 1985] data, the OBN has a great positive residual (0.39) in relation to the mean magnitude.

Thus, the main reason is that magnitude residual is not the random value in a simple sense. It is created by several factors, which can be random or systematical depending on a situation, and has a different degree of freedom.

Even comparing so carefully calculated data as magnitudes of UNE, the discrepancy between determined magnitudes and station correction is too great. Look, for example, on the correlation between magnitudes for Semipalatinsk UNE made by NORSAR and AWRE (Figure 15). The difference between them is about 0.10. In comparing the magnitude  $M(\text{ISC})$  with AWRE or NORSAR data (or with their average), the standard deviation  $\text{dm}$  of the difference is even more: 0.15 (Figure 16). And what is important, for small events ( $\text{mb} < 4.4$ ) the ISC magnitudes are systematically overestimated. This overestimation originates due to the loss of the data from stations with negative residuals. This threshold effect was discussed in [Khalturin, 1974]. The special system of its correction was proposed [North, 1977].

So the real errors of the magnitudes and of the station corrections are much more than the announced ones. The deviation of measured values depends on several factors, being

# STATION CORRECTIONS $dMPV(SKD)$ BY TWO AUTHORS EARTHQUAKES FROM ALASKA AND ALEUTIAN

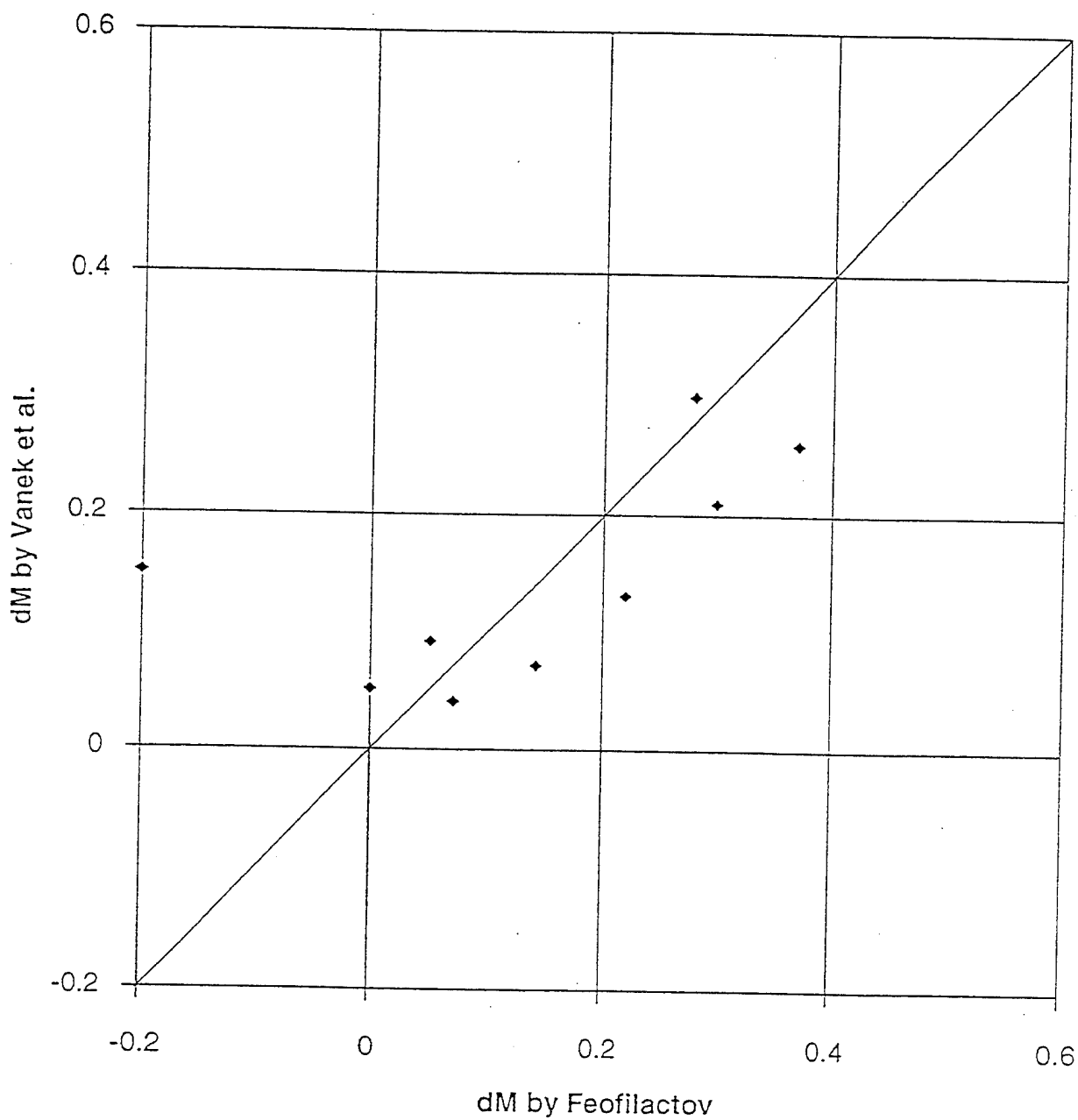


Figure 14. Comparing the station corrections  $dMPV(SKD)$  by Vanek [1983] and Feofilaktov [1970] for the same stations, earthquakes from Alaska and Aleutian

### Magnitudes of UNE from SEMI TS

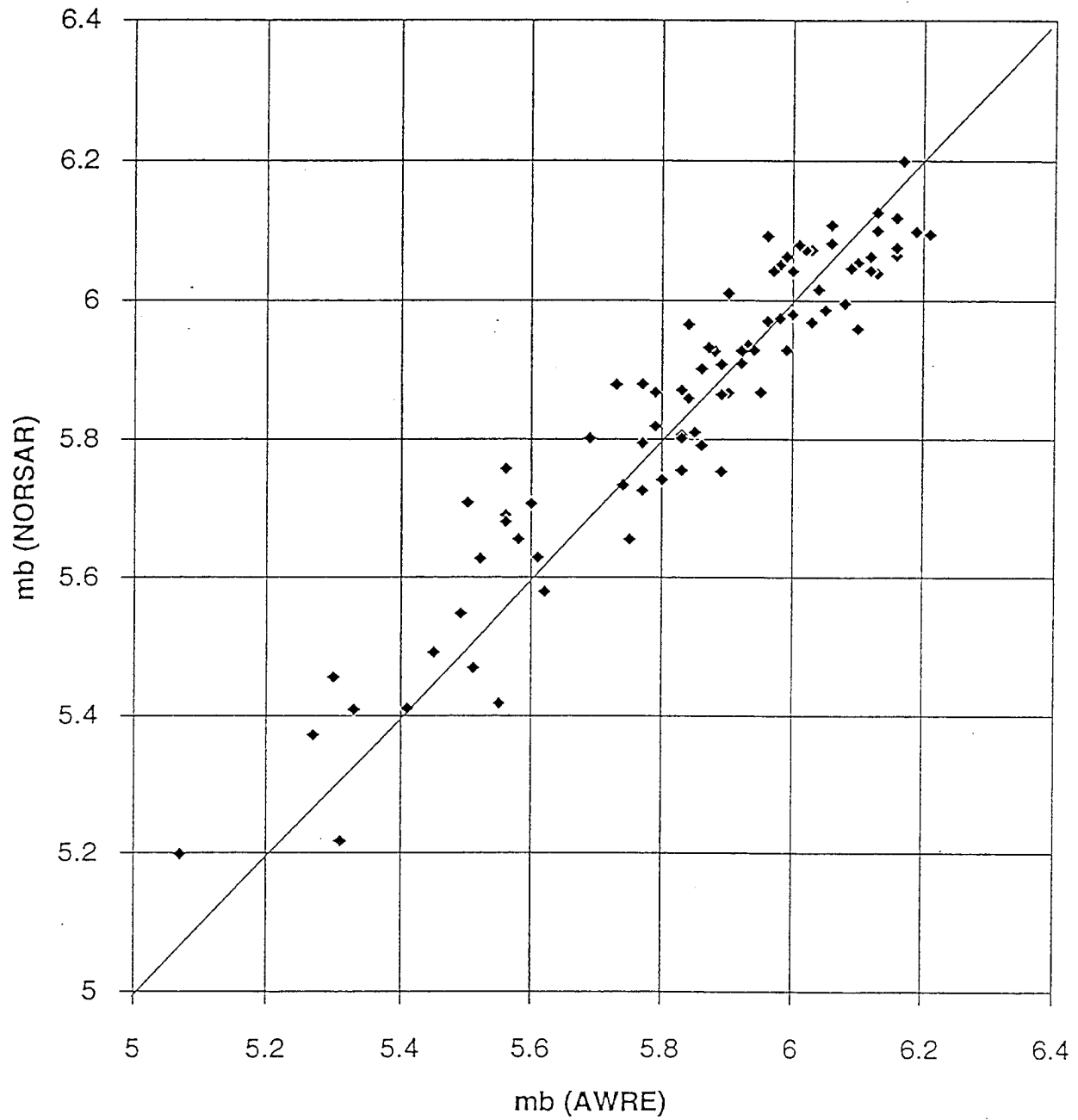


Figure 15. The correlation between magnitude mb determination for Semipalatinsk UNEs made by NORSAR and AWRE.

# UNEs from SEMIPALATINSK

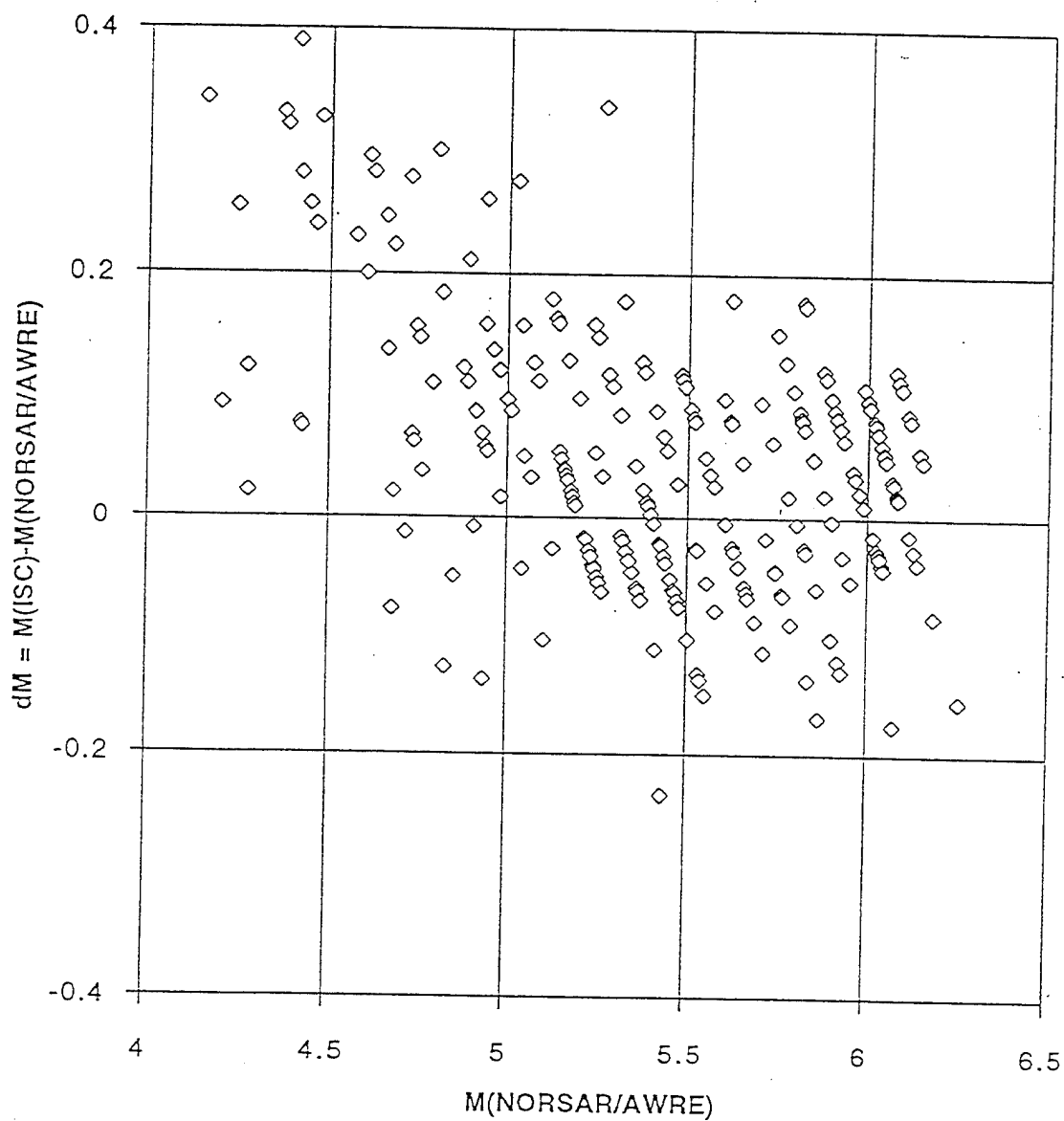


Figure 16. The difference  $dm$  between magnitudes  $m_b$  from ISC and  $m_b$  from NORSAR (or from AWRE, or their average if they both are available) versus NORSAR (AWRE) magnitude. Notice that for small events ( $m_b < 4.4$ ) the ISC magnitudes are systematically overestimated.

random or systematical in different situations.

### 3.2. Factors, Creates the Magnitude Deviations

To get realistic estimation of errors, which appear from some factors, one needs a base on multi-factor model of magnitude residual. It is important to find the contribution of random and systematic factors into the common scattering of magnitude estimation in each particular case. It means, the multi-factor models have to be used with the definition of degree of freedom for each of them.

First of all, let us define the factors which can be considered formally in the problem as a part of multi-factor model. Second, let us discuss our 'terminology'. We call "area" the territory of observation, which seems to be homogeneous from a geological point of view. The groups of nearby events will be called an "epicentral zone", or simply "zone". The splitting of one zone from another as well as one area from another was made by geological reason.

The "region" will be used to point to the part of the Earth where all stations and earthquakes studied were localized. Or, say, it is a territory, covered by seismic ray traces for stations and events, used in the study. For example, our data described in part 4 the "region" includes the USSR territory, the North-West Pacific, North-West Asia, Mediterranean. The region studied by North is all of the globe. In our study "areas" are the Baykal, Central Asia, North Tien Shan, Russian Platform. The epicentral "zones" are, for example, Persian Gulf, Baykal, and so on.

What factors seem to be important?

#### 3.2.1. The Observation Area Effect

This component is connected with the peculiarity of a comparatively large region which seems to be homogeneous from the tectonic point of view - such as wide depressions, platforms or the shields, orogen zones, volcanic area and so on. Among them, the low-Q zones in the mantle are most important. It means that if there is a low-Q zone in the upper mantle, it changes the amplitudes of records at a group of nearby stations. They have the common component of station residuals, for all stations, localized in that area. We call it the residual component originated from whole area of observation, or just "area component". To estimate the area effect for a particular area, the average residual for all stations has to be calculated.

To get the statistical description of the area effect the data from many areas have be studied. The area deviation is defined as a standard deviation of many area residuals.



The area residual can be corrected.

### 3.2.2. Local Conditions (the Site Effect)

The local residual of a particular station is defined as the difference between the area residual and the residual of this station. The local standard deviation is calculated from the local deviations of many stations in the same area. It is connected with the upper part of the crust (and the ground, or even the seismometer-basement contact). This effect can vary significantly with the position of the receiver moving a small distance - a few km or even a few tens of meters.

Earthquakes at small distances can "see" only the very local upper part of the crust. In the observation conducted by small groups, the difference of magnitude residuals between these stations is created by local conditions. Surely, these local situations really create the difference, depending on the frequency content of input signal, on the direction of seismic wave coming, on the component of oscillation. This dependence is more significant in a case of the complicated relief. But formally we separate as a local effect only mean one, sending all its variations into the random component.

Local residuals can be corrected.

### 3.2.3. The Epicentral Zone Effect

From geophysical point of view an epicentral zone effect is symmetrical to one of observation area. But it is "invisible" by teleseismical observation. The ray traces to all stations cross the same sample of lower crust and upper mantle. And if there is a low-Q volume, the whole-world stations record equally reduced amplitudes. That is why it is not easy to get a realistic estimation of zone effect for certain epicentral zone.

Two ways can be proposed. First, is to use independent data about sources. It can be the value  $Y$  of yields for UNEs. The important information can be taken from the data which is obtained from local network observation. The local records are not always influenced by the upper mantle. If seismic energy, calculated from source spectra or energy class  $K$ , is available, the low  $Q$  displays itself as too small teleseismic magnitude compared with expected ones from general correlation  $K$  and  $MPV$ .

Secondly, if there is a network of seismic stations in the epicenter zone under consideration, the area effect of these stations can be taken as a zone effect.

If no one source of such information is available, geophysical and geological information about absence or

existence of low-Q in considered zone (even expert's opinion about it) is useful. The zone residual can be taken of the same value, as was found in other zones with similar conditions. We believe, that it will be much better than nothing and can prevent heavy errors in UNE magnitudes.

The zone effect can be corrected.

#### 3.2.4. The Path Effect

There are three distance intervals which are known as producing strong variations of the shape of A/T - D curve. They relate to the three strongest boundary (or narrow transitional layers) in the Earth's interior: the first two are in the mantle at depths about 400 and 700 km, the third one is in the transition zone between the lower mantle and core.

These zones are inhomogeneous, the boundaries change somehow in different places of the globe, being up or down the mean depth, and vary the relation of velocities. It produces the focusing and defocusing of seismic rays at the Earth surface. It makes the positive and negative residuals from mean A/T-D curve of different values and at different distances. The path effect looks like the difference between the value of A/T-D for any particular couple "source-receiver" and the expected ones from standard calibration function at the distance, corresponding to this couple. It appears because the calibration function is not absolutely valid anywhere in the globe.

When analyzing the observational data, it is found that the variations of the maxima and minima of A/T-D curve change their position on the distance scale and their amplitudes. As a result, the station magnitude residuals versus distance oscillate in unpredictable ways. We define these oscillations as a path effect.

The path effect for a particular couple "source-receiver" can be observed as station residual, which do not stay at zero after correction for area, local and zone residuals. It looks like the variation of magnitude residuals when distance and azimuth to epicenter change.

The statistical description of path effect can be made as a standard deviation of path residuals many stations epicentral and many epicentral zones for each. It can be found as a second term of cross-correlation function between calibration A/T-D function and the A/T-D curve obtained from profile observation. It can be the observation by a single station and profile of epicenters, or the epicenter from a small zone, recorded by profile of stations. The first term of cross-correlation is supposed to be zero, being corrected by local, area and zone corrections.

The path effect cannot be corrected so simply as the station residual or as the zone effect.

### 3.2.5. Random component of deviation

There is one more component of deviation - the random one. It describes the component of scattering, connecting with factors which are unknown, or which we can not or will not control. It includes source radiation pattern or spectral content of the wave arrived, depending on source spectra and/or on the Q beneath epicentral zone, etc. But this problem is not studied yet good enough to talk about its correcting.

### 3.2.6. Total Deviation

We suppose, that all these factors are independent. It means, that total deviation is a squared sum of all partial components created by these factors. The random scattering of data exists and put its own contribution into total residual.

Three factors, local, area and zones, can work like systematical residuals when we deal with one station, (with stations from the same area; with earthquakes from the same epicentral zone). The goal is to find these values and use them for magnitude correction. The path effect is a more complex factor - it can not be described by some figure - it can be described as a function of pair points on the globe, or as a function of distance and azimuth from particular station.

There is no absolutely valid way to divide the total scattering into this components. It depends on how we boulder the regions, whether or not the stations are in a similar ground (or tectonic) conditions and so on. If we install all stations in a similar site condition and they are close to each other, (for example, installing an array on hard rock in tunnels), the station component will decrease. The path effect becomes the same for these stations and stays "invisible" for this set of data only. But it exists, and it will create part of an error, if using the stations of array for determination of magnitudes of distant earthquakes or explosions. If using more detailed rationalization, the scattering "moves" from random to area and/or zone component, from local factor to area one.

The statistical description of deviation can be made very formally to see, what is an order of errors value we meet. When we get these values for many stations (areas, zones), we find how much they differ from each other and can distribute it statistically as random factors, independent from each other. When getting one factor as a systematical value, others play the role of random noise, but have a different degree of freedom.

### 3.2.7. The Path Effect for Surface Waves Magnitude

For surface-wave magnitude like MLH, the path effect responds more easily to the inhomogeneities of the crust. The large sized inhomogeneities, like boundaries between oceanic and continental crust, create the shadow in surface wave amplitudes. The length of the shadow can be as long as twice or more the size of the origin of the shadow.

That is why the path effect of surface (Rg and Lg) waves can be corrected. But the correction must be connected not with the station or epicentral zone itself, but with the position of the ray trace, if it crosses or not the particular origin of the shadow. The distance between this crossing and station is important too.

### 3.2.8. Basic Magnitude

It is important to keep in mind one more factor, which is not natural, but originates from a method of calculation we choose. It is a so-called basic magnitude. People use, as a basic, the average magnitude and the average station condition. This is not something absolute. It depends on what station conditions (as well as zone conditions) are predominate in the set of data used.

This factor plays an important role in magnitude discrepancies when they are obtained by different authors and from different data, as well as it seems responsible for non-sufficiency of the magnitude correction systems. It is the factor which can (and must) be governed. Our opinion is that it is important to create objective and valid criteria of basic magnitude and basic station condition.

### 3.3. The Multi-Factor Model and the Method of Estimation the Errors

To estimate the total deviation as a result of all factors, the use of dispersion analysis is necessary. A case more simple than ours was studied in [Rautian and Pisarenko, 1965]. The two-factor model was used to create the method of estimation of accuracy. In that case, the deviation depends on two factors plus the random scattering. The realistic circumstance was taken into account, that the part of meshes of 2-D table can be empty, other ones contained the different number of the data. The exact formula was very complicated, even for that 2-D case.

The most important conclusion from that work was, that the accuracy of result in two-factor problem is significantly different from the simplest (single-factor) case. It was shown also how to optimize the strategy to get the better accuracy.

The exact formula was very complicated, even in the 2-D problem. Our case is an extremely more complicated one. We have four factors plus the random scattering; thus, we need to keep the rules of multi-factor deviations. Realistically, only a simplified version of the model can be created. In our 4-D case we are of necessity to use simplified approximate model. Formally, it means we assume that the total deviation is a sum of only squared partial deviations, created by each factor separately. From our experience we know, that approximate calculations give the result inside the 10 % from exact one.

Our approach corresponds to (3.1)-(3.4). When considering individual measuring of magnitude without any corrections, all these factors work like random ones, independent from each other:

$$S^2 = S(\text{area})^2 + S(\text{loc})^2 + S(\text{zone})^2 + S(\text{path})^2 + S(\text{rand})^2. \quad (3.1)$$

The last term in (3.1) called "random" is the only factor, which cannot be determined from the right observation. It can be calculated, after the total standard deviation  $S$  and all factor components will found. Then:

$$S(\text{ran})^2 = S^2 - \{S(\text{area})^2 + S(\text{loc})^2 + S(\text{zone})^2 + S(\text{path})^2\}. \quad (3.2)$$

The random factor is only one, which cannot be corrected.

Based on it, we will design a formula for calculating the error in any problem. The error of result depends not only on the total number  $N$  of data, but on numbers of realization of all factors: stations, areas of observation, epicentral zones and paths.

Deviation became less, when we used more data. Our model allowed us to calculate the realistic errors if the deviation due to all factors are not found. The number of realization of each factor have to be taken into account. Let us sign the numbers of various factors:

the number of earthquakes	is $N(\text{eq})$ ;
the number of stations used	is $N(\text{st})$ ;
the total number of observation	is $N(\text{rand})$ ;
the number of observ. areas	is $N(\text{area})$ ;
the number of epicentral zones	is $N(\text{zone})$ ;
the number of paths	is $N(\text{path})$ .

When we determine the station correction from data of many earthquakes,  $N(\text{rand})=N(\text{eq})$  and  $N_{\text{path}}=N_{\text{zone}}$ . In determining the magnitude of a particular event,  $N(\text{rand}) = N(\text{st})$  and  $N_{\text{path}} = N_{\text{area}}$ . Practically  $N(\text{zone}) < N(\text{eq})$  and  $N(\text{area}) < N(\text{st})$ .

### 3.4. The Calculation of Errors and the Accuracy Problem

There are two ways to get a higher accuracy of magnitude: to use as many individual measurements as possible and to use the system of corrections. Looking on formula (3.1) one can see that the efforts must be applied to all terms.

What is an error of magnitude of some earthquake, if we use  $N$  observations without any corrections and the standard calibration curve? In this case  $N(\text{rand}) = N(\text{st})$  and

$$dM^2 = \frac{S_{\text{rand}}^2 + S_{\text{loc}}^2}{N_{\text{st}}} + \frac{S_{\text{area}}^2 + S_{\text{path}}^2}{N_{\text{area}}} + S_{\text{zone}} \quad (3.3)$$

It is clear from (3.3), that when we use more and more stations in the same areas, the area and path deviations stay the same. So when the first two terms become smaller then the others, the total error  $dM$  stops to decrease. Its value depends on path and area and zone components only. The zone deviation term does not change at all. It means that the error  $dM$  of magnitude has a lower limit, depending mostly on the Q-condition beneath epicentral zone and on path effect.

The common opinion is, that station correction can make the error of magnitude determination much less. Based on the multi-factor model of deviation, one can estimate the errors of magnitude in different situations. Let us see first what is an error  $dB$  of station correction  $B$  :

$$dB^2 = \frac{S_{\text{rand}}^2}{N_{\text{eq}}} + \frac{S_{\text{zone}}^2 + S_{\text{path}}^2}{N_{\text{zone}}} \quad (3.4)$$

It is clear from (3.4), that using more and more events do not guarantee small error of station correction, because only one term became smaller. The other two terms can be diminished only if we use earthquakes from different zones and azimuths. If we obtain the very many earthquakes from all zones with the paths covering all the globe by representative ways, we will obtain the best station correction. But it is at best an average for any event on any epicenter position. But for each particular epicenter zone, the path effect and the zone conditions stay uncorrected!

If the station correction was obtained from data, predominant for one epicentral zone, the station correction will differ from "global mean" zone. It will include the path effect and so will be "better" for this zone - but worse for other zones.

If the well-averaged station correction is used, the terms dependent on area and local effects disappear. But we have to replace them by value of dB :

$$dM = \frac{S(rand)^2 + dB(loc)^2}{N(st)} + \frac{dB(area)^2 + S(path)^2}{N(area)} + S(zone)^2 \quad (3.5)$$

Again, the accuracy of magnitude is limited by influence of zone deviation and path effect. The corrections of a zone conditions seems to be even more important, because it cannot be diminished by using more observation. We expect that zone correction can be found. It is equal to the area residual of stations, localized in zone under consideration. Thus, if correct, the total error will decrease significantly. If we use zone correction Z, the error of magnitude can be estimated

$$dM = \frac{Srand^2 + dB^2}{Nst} + \frac{Spath^2}{Nzone} + dZ^2 \quad (3.6)$$

The path effect can not be corrected so simply. But if the goal is to monitor some small zone, where UNE are produced or supposed to be done, the corrections have to be found for each station for that particularly zone. In such cases the path effect turns out to be included in station correction. Then, the error of magnitude will be less:

$$dM = \frac{Srand^2}{Nst} + \frac{dB^2}{Nst} + dZ^2 \quad (3.7)$$

We looked at the problem from a formal point of view, only statistically. Really, there are many sides of the problem, which have be studied; one way is geophysical.

### 3.5. Some Notes from the Geophysical Side of the Problem

Dividing the total scattering into components is not absolutely valid. It depends on how we demarcate the regions, whether our stations are in a similar ground (or tectonic) conditions. If we install all stations in similar site conditions and they are close to each other, (for example, installing an array on hard rock in tunnels), the station component will decrease. The path effect becomes the same for these stations and stays "invisible" from this set of data. But it exists, and will create that part of an error if using the stations of array for determining magnitudes of

distant earthquakes or explosions. If using more detailed rationalization, the scattering partly "moves" from random to area and/or zone component, from local to area one and so on.

The important part of error is the way people choose the basic magnitude and the basic station. From a statistical point of view, there is no problem. But consider it geophysically; we came to the opinion that the "normal" kind of conditions taken as basic seem to be preferable. We will return to this problem later.

For surface-wave magnitude ( $M_s$  or  $MLH$ ), the path effect effect can easily respond to the inhomogeneities of the crust. The large sized inhomogeneities, like boundaries between oceanic and continental crust, create the shadow in surface wave amplitudes. The length of the shadow can be as long as twice the size of the origin of the shadow.

That is why the path effect of surface ( $R_g$  and  $L_g$ ) waves can be corrected. But the correction must be connected not with station or epicentral zone itself, but with the position of ray tracing, even if it crosses or not the particular origin of the shadow. The distance between this crossing and the station is important too.

#### **4. THE MAGNITUDE RESIDUALS CONNECTED WITH LOCAL CONDITIONS, OBSERVATION AREA AND EPICENTRAL ZONE EFFECTS**

In this section we describe the data obtained from several sets of observations in the southern part of FUSSR, and some data from other regions. There is a different size of area, different way to choose the basic magnitude, number of seismograms vary from hundreds for Garm local network to millions in Ringdal's world wide data. But we found that the values of area and local deviations are in pretty good agreement in all these sets of data.

##### **4.1. The Local and Area Deviations**

###### **4.1.1. Data from 12 Soviet Stations (SKD Instruments)**

Let us look first to the data we obtained from 12 Soviet stations, localized in four different areas. In Table 5 the total station residuals (TSR) are shown. The area residuals (AR), local residuals (LR) and their standard deviation were calculated.



Table 5. The Total Station Residuals (TSR), Area (AR), Local Residuals (LR) and the Standard Deviations Obtained from 12 Stations Data (SKD-instrument)

Stations	The Station Residual		
	TSR	AR	LR
Moscow	0.46		
I. CENTRAL ASIA			
Andizhan	0.27		0.21
Tashkent	-0.09		-0.15
Frunze (Bishkek)	0.06		0.00
Garm	0.01		-0.05
Area residual		0.062	
Local stand. deviation			0.131
II. NORTHERN TIEN-SHAN			
Alma-Ata	0.21		0.175
Talgar	-0.06		-0.105
Stchel Dalnaya	-0.03		-0.075
Rybachye	0.06		0.015
Area residual		0.045	
Local stand. deviation			0.109
III. BAYKAL			
Irkutsk	-0.34		-0.09
Kabansk	-0.21		0.04
Kyakhta	-0.21		0.04
Area residual		-0.25	
Local stand. deviation			0.061

The Central Asia and Tien Shan area residuals vary around zero. The distance between Talgar and Alma-Ata is about 25 km only but their station residuals differ significantly. It is because the Talgar station is installed in a tunnel within a hard rock, whereas the Alma-Ata station is situated on a layer of sediments, about 1 km thick. So that is exclusively the local effect.

The lowest negative area residual, -0.25 is for the stations in the Baykal area. It seems that near the Baykal area there is a regional low Q-zone connected with the young Baykal rift. That is why the amplitudes at the Baykal stations decrease when crossing this zone. The Q value is known to be very high on the Russian Platform, it is less in the orogenic area of the Alpine Belt. That is very likely the cause of area residuals.

The highest positive residual is at the Moscow station. Unfortunately, only this station was available for the Russian Platform area, so we cannot divide the local residual from the area for the Moscow station.

We calculated two versions of area deviation: including MOS with assumption, that station residual for MOS is area residual and excluding Moscow at all. In calculating the local deviation, two versions were done; one included Moscow data with the assumption that MOS residual is created by local conditions and one excluded MOS.

Without MOS:

Area stand. deviation (without MOS)	0.15
Local stand. deviation (without MOS)	0.108
Total station stand. dev.(without MOS)	0.185

Including MOS:

Area stand. deviation (includ. MOS)	0.26
Local stand. deviation (including MOS)	0.134
Total station stand. dev.(includ. MOS)	0.282

#### 4.1.2. Data of 27 Soviet Stations (SKM Instrument)

The next set of data are the station residuals of MPV magnitude determined at 27 seismic stations (SKD instrument) from 9 areas by Kondorskaya, Vanek et al. [1979].

Table 6. The Total Station Residual (TSR), Local (LR) and Area (AR) Residuals of MPV(SKD) after Vanek et al.[1979].

St.	TSR	AR	LR	St.	TSR	AR	LR
1. EAST EUROPE				6. THE CAUCASUS			
CLL	-.17		.07	BKR	.07		.12
KRA	-.38		-.14	GRO	.04		.09
MOX	-.22		.02	GRS	-.09		-.04
PRU	-.39		-.15	KRV	-.04		.01
SOF	-.03		.21	MAK	-.13		-.08
Area residual	-.24			PYA	-.05		.00
Local stand. deviat.			.135	SOC	-.13		-.08
				Area residual	-.05		
				Local stand. deviat.			.070
2. RUSSIAN PLATFORM				7. CENTRAL ASIA			
OBN	0.00		-.13	PRZ	-.02		-.02
PUL	.26		.13	FRU	-.06		-.06
Area residual	.13			TAS	.07		.07
Local stand. deviat.			.13	Area residual	.00		
				Local stand. deviat.			.055
3. ARCTIC				8. THE FAR EAST			
KHE	-.17		.05	MAG	-.25		.02
ILT	-.25		-.02	PET	-.30		-.03
TIK	-.28		-.05	YSS	-.21		.06
Area residual	-.23			VLA	-.30		-.03
Local stand. deviat.			.042	Area residual	-.27		
				Local stand. deviat.			.038
4. THE BAYKAL				9. THE CRIMEA			
IRK	-.30		-.06	SIM	-.15		
ZAK	-.18		.06				
Area residual	-.24						
Local stand. deviat.			.06				
5. THE KOLA PENINSULA							
APA	.05						

From these data we found that the average area residual is not zero, but -0.11. That is probably because of basic station OBN, which does not correspond to total average conditions in these regions. Thus, we calculate the area residual as a difference from that value -0.11 to obtain the standard deviations:

Area stand. deviation	0.139
Local stand. deviation	0.085
Total station stand. dev.	0.163.

These values are similar to the previous case (Table 5).

#### 4.1.3. North [1977] Data from World Network (mb Magnitude)

We took station residuals data from North's [1977] maps and divided them into 8 areas of observation. In Table 7, the number N of stations used in each area, the area residuals for each area, and local standard deviation inside each area are shown. We divided the total station residuals onto the local and area components (Table 7). Standard deviation of total station residuals from these two component can be calculated :

$$\sqrt{0.14^2 + 0.11^2} = 0.18$$

which corresponds to 0.175, obtained from all North's data of station residuals. We are sure that it is the correct way to calculate total error by a squared sum of its components.

Table 7: The Area Residuals and Local Standard Deviations from North [1977] Data for Eight Observation Areas

The Areas	Number Stat.	Area Residual	Local St.Dev.
East Africa	5	-0.256	0.022
Western US	11	-0.19	0.135
Australia	5	0.074	0.138
India	5	0.114	0.059
Scandinavia	8	0.075	0.121
Canada, Alaska	15	0.041	0.110
Europe	14	0.126	0.123
Eastern US	6	0.130	0.167
Area standard deviation		0.142	
Local standard deviation			0.109

#### 4.1.4. Marshall's Data from World Network (mb Magnitude)

Marshall's data of station corrections were taken from his figures 8 and 9 in [Richards, 1993]. We divided Marshall's region of observation into 17 areas. The residuals and the standard deviations are shown in Table 8.

Table 8. The Total Station Residuals (TSR), the Area ones, the Local and Area Deviations for 17 Areas from Marshall's Data.

St.	TSR	St.	TSR	St.	TSR
I. CANADA		V. SOUTH USA		X. FAR EAST	
PG	-0.1	KC	0.1	MAT	0.0
FSJ	-0.1	FLO	0.1	YSS	0.1
PHC	0.0	ACO	0.3	VLA	0.2
VIC	0.0	PCO	0.5	PET	0.2
PNT	0.1	TUL	0.1	Area res.	0.12
CW	0.0	LUB	0.1	Local dev.	0.08
SES	0.3	WLO	0.5		
JP	-0.1	GV	0.3	XI. YAKUTIA	
EDM	0.3	DAL	0.2	SEY	0.2
Area res.	0.044	JCT	-0.2	YAK	0.4
Loc. dev.	0.15	SJ	0.2	Area res.	0.3
		OXF	0.2	Local dev.	0.10
II. WEST US-1		JE	0.3		
MSD	-0.1	BI	0.1	XII. BAYKAL	
BOZ	0.0	BLA	0.1	BOD	0.0
HY	-0.3	ATL	0.0	IRK	-0.1
RCD	0.2	AX	0.1	ZAK	-0.1
LAO	-0.10	TQ	0.3	MOY	0.1
Area res.	-0.06	SHA	0.3	Area res.	-0.02
Loc. dev.	0.16	BE	0.3	Local dev.	0.083
		Area res.	0.20		
		Loc. dev.	0.156		
III. WEST US-2		VI. EAST USA		XIII. KAZAKH PLATFORM	
LON	-0.4	MIM	-0.1	SEM	0.1
COR	0.1	SBM	0.1	NVS	0.1
NEW	-0.2	IRM	-0.1	ELT	0.2
BMO	-0.3	WES	-0.1	Area res.	0.13
MO	-0.4	AGM	0.1	Local dev.	0.05
HL	-0.2	EMM	0.1		
WI	-0.3	DH	0.1	XIV. CENTRAL ASIA	
MV	-0.3	UCT	-0.1	ASH	0.5
MN	-0.3	BCT	-0.2	TAS	0.5
BMN	-0.2	OCD	-0.2	SAM	0.6
EVR	-0.2	BGO	0.0	KHO	0.6
OB	-0.2	GEO	0.0	FRU	0.4
GSC	-0.1	SVP	-0.1	GAR	0.3
TF	-0.2	Area res.	-0.04	AND	0.3
CP	-0.3	Loc. dev.	0.07	PRZ	0.3
Area res.	-0.20	VII. EURASIAN NORTH		TLG	-0.2
Loc. dev.	0.14			KAB	0.2
		KBS	0.0	QUE	0.2
IV. WEST US-3		KEK	0.0	Area. res.	0.34
TUC	-0.2	APA	0.0	Local dev.	0.218
FM	-0.1	KHE	0.3		
TFO	-0.3	TIK	0.1	XV. CAUCASUS	
DUG	-0.1	ILT	0.1	BKR	0.4
UBO	-0.1	Area res.	0.08	KRV	0.0
JR	-0.2	Loc. dev.	0.107	PYA	0.0
KN	0.0			GRS	0.1
PM	-0.2	VIII. SCANDINAVIA		Area res.	0.20
BDW	-0.1	UPP	0.5	Local dev.	0.16
FK	0.2	KIR	0.6		
GOL	-0.3	KJF	0.1	XVI. RUSS. PLATFORM	
DR	-0.3	NUR	0.2	OBN	0.3
ALO	-0.4	Area res.	0.35	ARU	0.4
LC	-0.2	Loc. dev.	0.21	SVE	0.4
MSO	-0.1			PUL	0.3
Area res.	-0.16	IX. THE GREAT LAKES		Area res.	0.35
Loc. dev.	0.14	RK	0.1	Local dev.	0.05
		LNC	0.1		
		NC	0.0	XVII. CARPATHIANS	
		AR	0.0	UZG	0.1
		AAM	0.1	PVL	0.0
		Area res.	0.06	KDZ	0.0
		Local dev.	0.05	Area res.	0.03
				Local dev.	0.05
Area standard deviation				0.17	
Average local standard deviation				0.12	

Notice, we chose the areas arbitrarily, not based on geological and geophysical data. That is why some deviations formally described as a local one, really can originate from a changing geological situation. The example is Talgar. We include this station in a wide area of Central Asia. Talgar has a large negative residual, looking as a local one, but it originates due to low-Q zone of small size in the upper mantle [Khalturin, Molnar, 1975].

#### 4.1.5. Data from Eight Caucasus Stations (SKD Instrument)

Tskhakaya and Vanek [1967] studied the station correction for eight Caucasian stations. Some stations with large values of residuals, like Leninakan, did not take part in the determination of station corrections. All corrections in Table 9 are positive, because the basic station (YER) is not correspondent to "mean conditions": amplitudes at all stations are less, then at YER.

Table 9. The Station Residuals (SR), Referenced to YER, the Local Residuals (LR), Referenced to Average Magnitude, and Random Standard Deviation in Caucasian Network of SKD Stations after [Vanek, Tskhakaya, 1967]

Stat.	N	SR	LR	Random Dev.
TBL	248	-0.23	-0.07	0.115
GRS	204	-0.12	0.04	0.270
SOC	198	-0.25	-0.09	0.126
MAK	200	-0.16	0.00	0.164
KRV	53	-0.06	0.10	0.153
PYA	139	-0.30	-0.14	0.157
BKU	117	-0.15	0.01	0.259
YER		0.00	0.16	
Average		-0.16	0.0	0.178

The average station residual is not area residual, because the only Caucasian area was under consideration. To obtain local residual for each station in this case, we recalculated the corrections from references to YER (TSR) and references to average magnitude (local residual).

One can expect that area residual have to be negative. We think so, because there are some evidences that there is a low-Q volume in Caucasus lower crust and upper mantle. It is known from strong coda attenuation, correspondent to Q (1 Hz) is as small as 150 [Khalturin, 1989], strong attenuation of macroseismic intensity [Rautian, 1980]. There is a Quaternary volcanic zone and high heat flow here.

#### 4.1.6. Data from Nine SKM-stations at Turkmenia Region

The station residuals in the Turkmenia area were studied by [Rakhimov et al., 1983] for 9 seismic stations with short - period SKM instruments. The residuals responding to average magnitude for earthquakes were used in this study. The earthquakes studied were at regional distances, and no more than 400 km. The data are shown in Table 10.

Table 10. The Station Residuals of MPV Magnitude for Regional Earthquakes in South Turkmenia

Station	dMPV
Ashgabad	0.21
Gyaurs	0.12
Kisil-Atrek	0.12
Nebit-Dag	0.08
Ovadan-Tepe	0.06
Kara-Kala	0.03
<hr/>	
Station	dMPV
Kaushut	-0.08
Manysh	-0.10
Vannovskaya	-0.31
<hr/>	
Local stand. dev	0.15

Turkmenia is very special. In other areas of Central Asia stations are mostly installed in hard rocks. In Turkmenia, only one station, VAN is at the south-west side of Kopetdag fault, where hard rocks are exposed on the surface. Other stations are at the opposite side of the fault, on depression, with different thickness of sediment. The average local conditions here are the typical sedimental ones, whereas in Kyrgyzia they are the typical hard rock ones.

The total scattering of data found by Rakhimov et al., is 0.34. This is not total scattering in a rigid sense, because no area and path effects take part in creating the scattering in this case. Formally calculated random scattering is

$$0.34 - 0.15 = 0.30$$

#### 4.1.7. Data from Twelve SKM Stations of Garm Network

The residuals for Garm network of short - period SKM stations were obtained from about 100 local events ( $D < 100$  km) and under-crust earthquakes from Pamir-Hindu Kush zone. The station residuals were calculated from the deviations of log amplitudes of S wave, normalized to standard distance (Table 11).

Table 11. The Station Deviations at Garm Local Network of Short Period Instruments SKM

Stat.	Local Residual	Random Stand.Dev.	Stat.	Local Residual	Random Stand.Dev.
TDR	0.18	0.20	TRT	-0.06	0.15
ISH	0.11	0.20	SNG	-0.07	0.21
GAR	-0.11	0.14	KFG	-0.15	0.18
YAL	-0.18	0.14	CHD	0.10	0.19
JFR	0.03	0.15	KHT	0.02	0.21
CHS	-0.18	0.17	LNG	0.18	0.22

The random component of standard deviation from these data is in average 0.18. Local standard deviation is 0.117.

#### 4.2. The Total and Random Deviation

As described above, the random deviation was defined as a difference between total deviation and all other components, created by factors. Not every set of data can be considered as a source of information about total and random deviation. To find them, one has to be sure that the observed deviation includes the influence of all factors. The most representative are the data obtained from global distributed earthquakes and seismic stations, such as North's data, which we obtained from [Richards, 1993].

The 72 stations over the World were used to calculate the deviations. The station residuals vary from -0.28 to +0.37, with the standard deviation 0.17, including both local and area effects. Standard deviation of individual magnitude variations for each station in average is 0.36, which includes the path effect and the random scattering. Thus, the total deviation observed by North can be calculated as

$$S(\text{total}) = \sqrt{0.17^2 + 0.36^2} = 0.40$$

This value does not include an influence of condition in the epicentral zone.

#### 4.3. The Zone Effect

A zone effect (if it is created by high or low attenuation beneath the epicenter zone) cannot be detected from the data of teleseismic observations, because all the seismic rays to all distant stations over the globe penetrate this zone and are lost, or do not approach the same part of energy. To see this effect, one needs to compare the independent data about

the sources.

The first example of such effect is the difference of magnitudes obtained for UNEs with the same yields, but made in different regions. It is known that the magnitudes of the Semipalatinsk UNEs exceed the Nevada UNEs of the same yield by approximately 0.32. The difference seems to be due to a lower Q value in the crust and the upper mantle in Nevada in contrast to high Q at the Kazakh platform. This value (0.32) is in a good agreement with the area residuals -0.20 for West US and +0.13 for Kazakh platform and Altai (our estimations after Marshall's data, Table 8).

The second example is the Baykal region. The area residual for Baykal network stations was found to be 0.25. We can expect the negative zone effect on the seismic waves radiated by the Baykal earthquakes. The local determinations of energy class K gives information about the source. K is not influenced by upper mantle attenuation. The ray traces to local stations from the distances not greater than a few hundred kilometers do not penetrate the low-Q zone below the Moho boundary.

We have evidence about the existence of low Q zone in the upper mantle in the vicinity of Baykal. The spectral content of Baykal earthquakes is similar to that of North Tien Shan and Altai-they all have an intensive high-frequency component; but in studying the records at distant stations, the Baykal earthquakes look like low-frequency signals. We found that the teleseismic magnitudes MPV of Baykal earthquakes (with known K value) are by 0.22 mag. units smaller than the expected ones as it follows from the standard equation for K and MPV obtained from many other regions:

$$MPV = 0.415 K - 0.17 .$$

It is in good agreement with the area residual of Baykal stations (-0.25). It lets us believe that residual for the particular zone can be taken as equal to the area residual found from observations by stations, localized in this zone. If so, the zone standard deviation can be taken as the same as area deviation  $S_{zone} = 0.156$ . We must keep in mind, that zone effect can differ for the earthquakes and the UNE. Explosion signals of higher frequency attenuate faster than low-frequency signals from the earthquakes.

#### 4.4. The Small Scale Variation of Zone Effect due to Complexity of Geological Structure in the Vicinity of the Source

The signal radiated from the seismic event source influenced by local, small scale geological structures. As a result, the time history as well as maximum amplitudes became



distorted. This effect is analogous to the local site effect near the station. Some data about it are known now.

The first example of such effect is a different station correction which the NORSAR array needs for the events from the Balapan and Degelen sub-areas. The observation of the NORSAR shows that the residuals of the Norsar stations differ by about 0.35 for the events from Degelen and Balapan. The distance between these two parts of the Test Site is about 50 km only. Their general geological conditions are very similar. So even for such small distances the variations of the station residual can be significant. These observations are very important to understand what kind of difficulties can be met when monitoring distant test sites and trying to obtain accurate magnitudes by special correction system.

The second example shows the difference for an even smaller scale. From the observation of UNE at the Semipalatinsk Test Site, it was discovered [Kirichenko,1993] that the seismic efficiency of UNE in the same type of rocks depends also on the geological conditions in the vicinity of the source, (outside the "inelastic zone"). He studied the  $dm = mb - mLg$  for a cluster of UNES in the Balapan sub-area and showed that this  $dm$  is strongly dependent on the distance from the main fault zone inside the sub-area with its size about 20 km, (Fig.17). One can see from this map that close UNE with epicenters about 10-15 km from each other have their  $mb - mLg$  different till 0.35 mag. units. It means that P-waves are much more sensitive to the tectonic conditions in the source vicinity than Lg-waves.

The small scale influence of geological conditions near the source can be recognized only for UNES, with a known position of epicenter and detailed data of geology. As an everyday seismological practice, this effect looks like a random one and cannot be corrected.

#### 4.5. The Summary of Data

Summarizing the area and local deviations from above data are shown in Table 12.

Table 12. The Summary of Local, Area and Random Components of Total Deviation of the Magnitude Station Correction

Data Set	Number of		Standard Deviation			
	Areas	Stations	Local	Area	Random	Total
12 SKD st	4	12	0.108	0.150	-	-
Vanek	9	28	0.085	0.139	-	-
North	8	69	0.109	0.14	-	0.40
Marshall	17	129	0.12	0.170	-	-
Tskhakaya	1	8	0.097	-	-	-

Table 12. (continued)

Data Set	Number of		Standard Deviation			
	Areas	Stations	Local	Area	Random	Total
Turkmenia	2	8	0.15	-	0.30	-
Garm CSE	1	12	0.116	-	0.18	-
Average			0.114	0.150	0.24	0.41

The station deviation (due to both area and local effects) is in average 0.19:

$$S_{st} = S_{area} + S_{loc} = 0.114 + 0.156 = 0.188$$

These data are not concluded as absolute or the best value, but it seems they are good enough to be used for estimating the errors in different situations. Later, we will see the difference between the error, following from a single-factor model and a multi-factor model, and prove that the multi-factor model gives the realistic values of errors.

#### 5. THE INSTABILITY OF THE AMPLITUDE-DISTANCE CURVES AS A SOURCE OF THE MPV DEVIATION DUE TO PATH-EFFECT

One of the most important sources of the station residuals is the so-called path effect, meaning the instability of the amplitude-distance curve. We studied this problem for P waves observed at distances from 1,000 to 11,000 km.

##### 5.1. The General A/T-D Curve from Our Data

The regional A/T-D curve was built, using all data from 12 Soviet stations (Table 5) mostly located in the Central Asia and Khazakhstan. In Figure 18 the A/T-D curve obtained from all these data is compared with the standard curve used in the USSR and USA networks.

For the distances less than 2000 km our generalized curve oscillates. It has the local maxima when waves Pn1, Pn2 and Pn3 appear [Nersesov, Rautian, 1964]. The 20-degree maximum changes its position. The East European data [Ruprechtova, 1960; Vanek, 1964] show a distance corresponding to this maximum equal to 2,170 km. Our maximum is more wide and flat, and is located between 2,100 and 2,780 km.

The minimum of 800 - 1600 km exists everywhere in the World. But its "depth", in comparison with the maximum near 2,000 km, is the most variable part of the amplitude curves. It is the deepest, 1.4 log units for the Gutenberg's curve

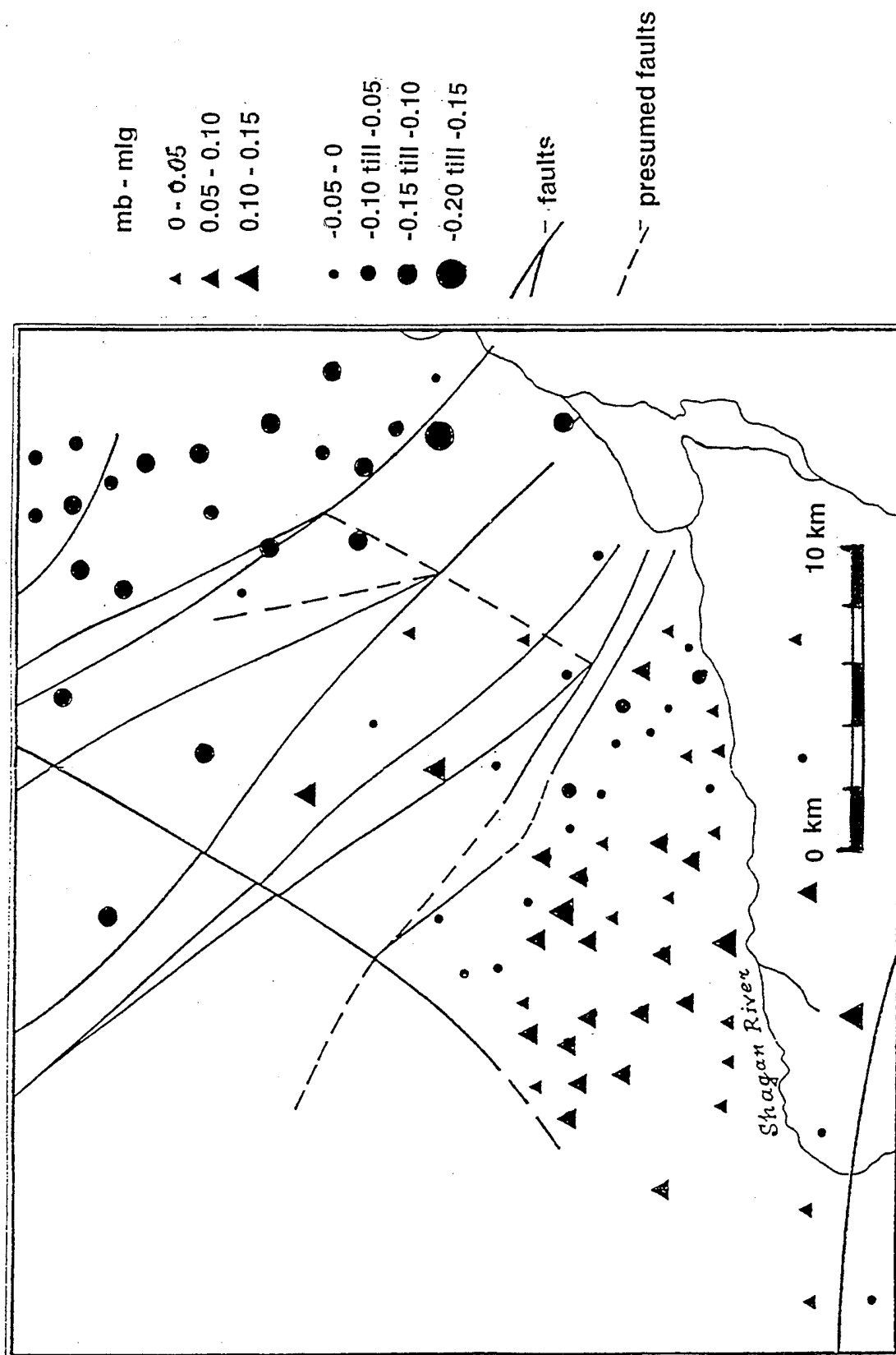


Figure 17. The mapping of  $dm = mb - m(Lg)$  for a cluster of UNEs in the Balapan subarea [Kirichenko, 1993]. The  $dm$  changes strongly depending on the position of source and on its distance from the main fault zone inside this small (about 25 km) subarea.

# P WAVE CALIBRATION CURVES

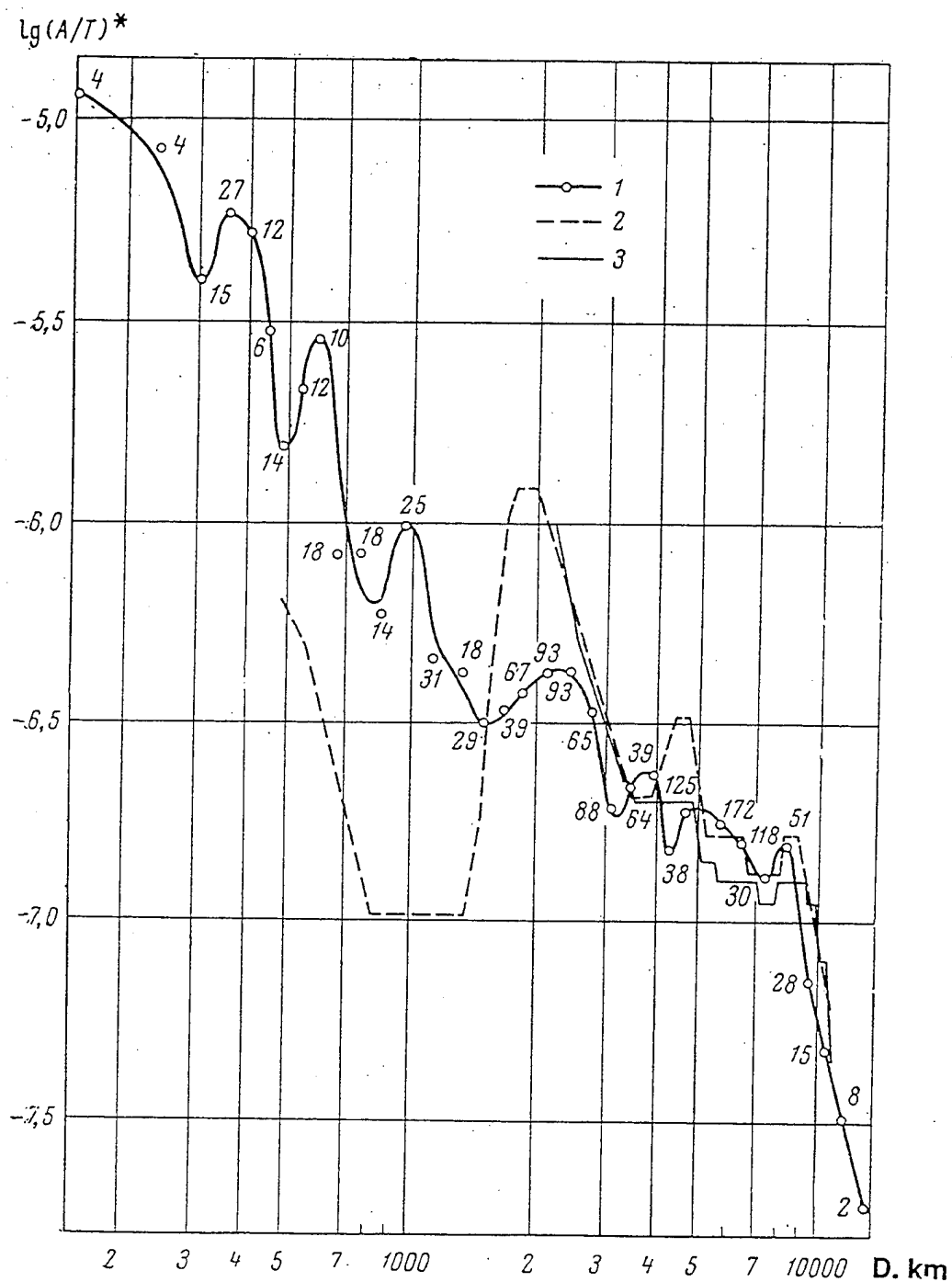


Figure 18. Our regional A/T - D curve (1) compare with the USCGS curve (2) and the standard curve used in the USSR network (3). Numbers near the points of (1) mean the number of observations included in these points.

[Gutenberg, Richter, 1956]. All the other data have higher amplitudes in this distance range. In log units the difference between the minimum (about 800 km) and maximum (about 2,000 km) is at our general curve 0.8-1.0; Solovyev and Solovyeva [1964] (for Far East) give it 0.8-1.0 also; Vanek and Radu [1964] and Ruprechtova [1958, 1960] (both for Europe) 0.4-0.5. The regional instability of A/T-D curves at distances less than 2,000 km is well-known.

The Gutenberg curve has the following three main maxima - near 4,500, 5,800 and 9,000 km. The maxima of our general curve have shifted to shorter distances, 4,000, 5,000-5,500 and 8,000 km respectively. A significant decrease in the amplitudes connected with the core boundary begins earlier, from 8300 km (in the Gutenberg curve it begins from 9000 km).

There are three distance intervals of strong variation of the shape of A/T-D curve. They relate to the three strongest boundaries (or narrow transitional layers) in the Earth's interior: two are in the upper mantle at depths of 400 and 700 km. The third is the transition zone between the lower mantle and core surface. The change of velocity of wave propagation near these boundaries produces the focusing and defocusing of seismic rays at the Earth surface.

These zones are inhomogeneous, the boundaries change a little in different places of the globe, being up or down the mean depth, and vary the relation of velocities. Due to such variations, the maxima and minima of A/T-D curve change their position on the distance scale and their amplitudes. As a result, the station magnitude residuals versus distance oscillate. This oscillation we definite as a path effect.

To describe the oscillation quantitatively, the squared difference between the particular A/T-D curve and standard curve was taken. This difference originates from the path effect, but is weaker, because it is smooth to some degree. Thus, we call that difference between partial and standard curve as the deviation of shape of A/T-D curves. The value we get is called  $S(sh)$ . One can expect that  $S(sh)$  always is less than the whole path effect.

To estimate the components of the magnitude residuals due the pure path effect, we used several selections of data:

- residuals, obtained for one station, but separately for several "station - epicentral zone" paths with the various distances between;

- the A/T-D curves, obtained from profile system of observation: one station or a group of stations in a small area and profile of epicenters;

- the A/T-D curves, obtained from earthquakes in a small zone recorded by profile of stations;

- the A/T curves, obtained from data of a single station recorded the earthquakes at different azimuths and distances;

the A/T-D curves obtained from data of events in a small zone and recorded by many stations in different distances and azimuths.

The last two selections of data show the path effect more or less smooth, because earthquakes from different zones and paths can turn out to be at the same distances. In such cases, the variations due to path effect move to a random component of deviation.

Table 13. The Mean Magnitude MPV Residuals for the South Tien Shan Group of Stations

Epicentral Zones	Magnitude Residuals	Epicentral Zones	Magnitude Residuals
Alaska	0.05	The Persian Gulf	0.05
The Aleutian	0.15	Iran, Iraq	0.05
The Ryukyu	0.00	Turkey	0.20
Mongolia	0.15	The Mediterranean	0.20
Japan	0.10	Greenland	0.05
The Philippines	-0.05	Indonesia	0.00
The Red Sea	-0.30	The Hindu Kush	-0.15
India	-0.55		
Standard deviations due to path effect			0.19

## 5.2. The Path Effect from "Source-Station" Couples

Antonova et al. [1974], used the North Tien Shan group of stations and obtained the mean residual for this group separately for different epicentral zones. The local effects, peculiar for each station were smoothed out, so the path effect became clearer (Table 14). It was found that the residuals are different depending on the positions of the epicentral zones.

Some data about the station residuals for different zones were obtained by North [1977, in his Table III]. The residuals in this table was calculated from mean value for all zones. To get the path effect, we have to clean the data from local and area effect. It was done by calculating the deviations from average residual for a particular station. After doing so we obtain the values of standard deviation which correspond to path effect (Table 14).

Table 14. The Standard Deviations of Station Residuals for Different Epicentral Zones After North [1977] and Number N of Zones Used for Each Station

Stat.	N of Zones	Stand. Dev.
Germany		
BNS	4	0.05
CLL	5	0.13
FUR	6	0.12
GRF	3	0.04
MOX	6	0.10
STU	3	0.11
East Africa		
BHA	4	0.10
CIR	4	0.07
CLK	4	0.18
KRR	4	0.07
Western USA		
DUG	4	0.11
EUR	7	0.11
TFO	5	0.10
TUC	3	0.14
UBO	7	0.06
Average stand. dev.		0.10

### 5.3. The Path Effect Obtained from the A/T-D Curves: Profile Observation

The Big Profile of the temporary SKM-stations installed in 1961-62 extended from the Pamir to the Baykal region with the stations at distances of about 100 km from each other. In Figure 19 the A/T-D curves obtained from the profiles of stations are shown. Seven earthquakes were used with their data marked with different signs. The list of earthquakes is given in Table 15.

Table 15. The List of the Earthquakes Used for Plotting the Profile A/T-D Curve (Figure 19)

N	Date 1962	Time	Region	Ms	Distances km
1.	Jun 4	15:08	The Red Sea	5.0	3940 - 6700
2.	Jul 6	02:12	The Gulf of Aden	5.0	3400 - 6540
3.	Oct 1	12:13	The Persian Gulf	5.5	2410 - 5190
4.	Nov 9	01:11	Zagros	5.3	2350 - 5140
5.	Feb 6	18:17	Kamchatka	5.5	3600 - 6850
6.	Nov 20	07:32	Kamchatka	5.0	3380 - 6850
7.	May 15	19:32	Kamchatka	5.0	3310 - 6560

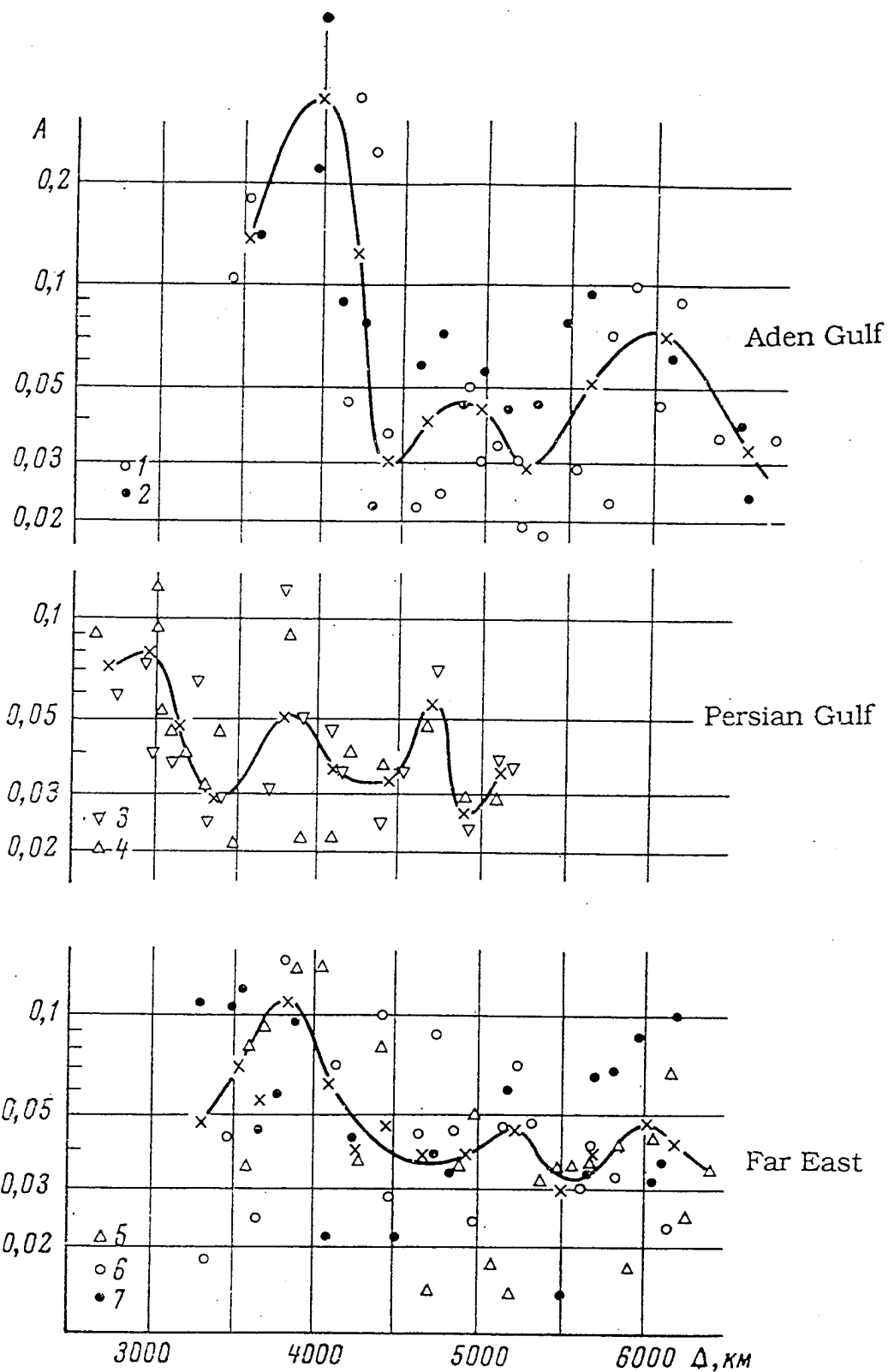


Figure 19. The  $A/T - D$  curves obtained from the Big Profile of SKM stations "Pamir-Baykal". Seven earthquakes were used: a - from Aden Gulf (## 1, 2), b - from Persian Gulf (##3 and 4) and c - from Far East (## 5 - 7). The list of earthquakes is given in Table 15. The absolute level of curves corresponds to  $MLH = 5.0$ .



It is remarkable that for the earthquakes from the Red Sea and the Aden Gulf, the large maximum of A/T-D curve is at a distance of about 4,000 km with its pick-pick amplitude being more than 1.0 log unit, whereas for the earthquakes not far from the former ones at the Persian Gulf, it is only 0.2 log units and is shifted to 3,800 km. Thus, if we observe the amplitude-distance data in more detail, the difference in the curve shapes became more distinct.

The epicenter profiles were taken extending along the Big Profile "Pamir - Baykal". In Figure 20, two curves are shown. One is from data recorded by stations in the Baykal area, the other from stations in North Tien Shan area. The epicenter profile includes the earthquakes from the North Tien Shan, Dzungaria, the Altai, the Sayan and the Baykal. The station residuals were corrected only by referring to the average value inside each group of stations. Thus, the area component of residuals, common for a group of stations, is shown in the Figure 20. Two curves correspond to the same profile with the waves propagating in opposite directions.

The path deviations calculated from profile observations vary from 0.07 to 0.25; the path standard deviation at the distances  $D < 2000$  km is 0.20, whereas at  $D > 2000$  km is 0.12.

An interesting and important result showing instability of amplitude-distance curves at distances near 10,000 km was obtained by Antonova et al. [1974]. They studied, depending on distance, the magnitude residuals for single station Mondy for earthquakes from two narrow sectors of azimuths of epicenters: 0-30 degrees and 90-120 degrees. The distance range studied is from 8,600 to 11,000 km.

One can see from Figure 21 that the station residual increased very rapidly at northern azimuths by about 0.4 log units near the distance of 10,000 km. The residuals in other directions of wave propagation remained practically the same and did not change with distance. The corresponding standard deviation is about 0.30.

#### 5.4. Small-Scale Path Effect at the Epicentral Distance Range Around 8,000-11,000 km

Large scale inhomogeneities of the amplitude fields were considered above. Let us observe two examples of special situations. There is evidence that the small scale path effect exists also, producing the variations of the magnitude at nearby stations. This effect is observed at distances more than 8,500 km at the interval of distances where A/T-D curve becomes unstable (see Section 5.3).

Small-scale inhomogeneities of P wave amplitudes at

$(A/T)_p$

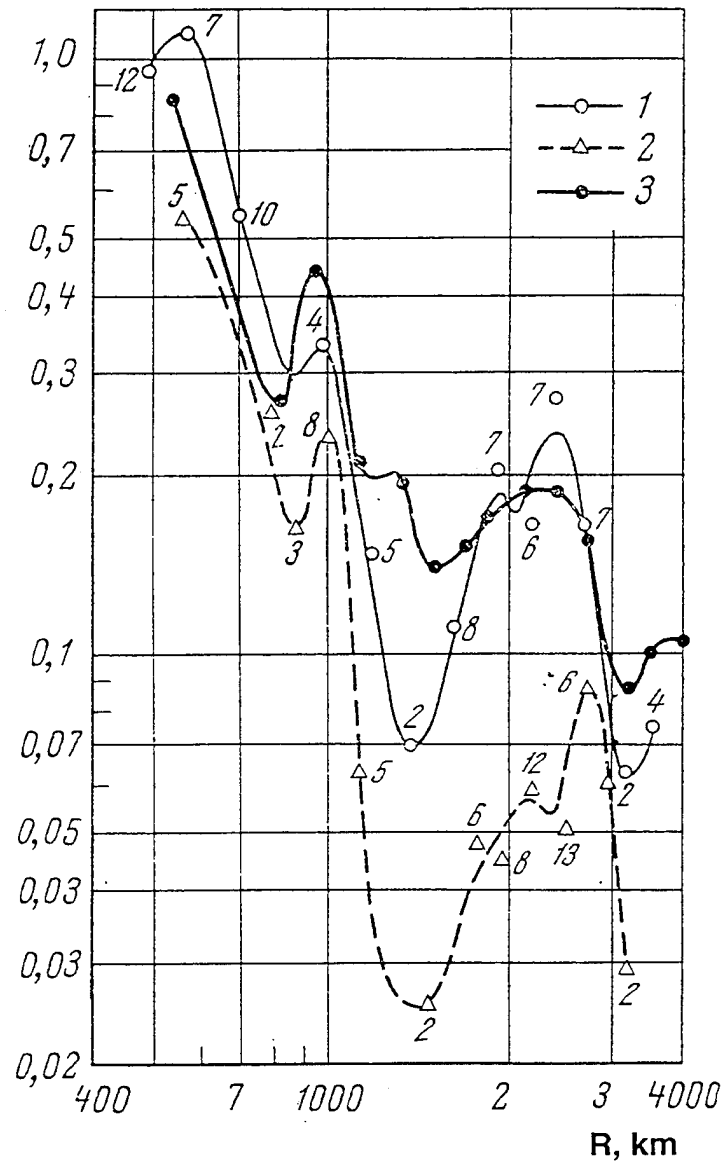


Figure 20. Two  $A/T - D$  ongoing curves, obtained from observations along the Big Profile Pamir-Baykal. (1) is the curve from records of Altay-Baykal earthquakes by North Tien Shan stations and (2) - from records of North Tien Shan earthquakes by stations in Baykal area, compare with our general curve (3). The absolute level of the curves corresponds to  $MLH = 5.0$ . The local residuals were corrected, the area ones remain the same.

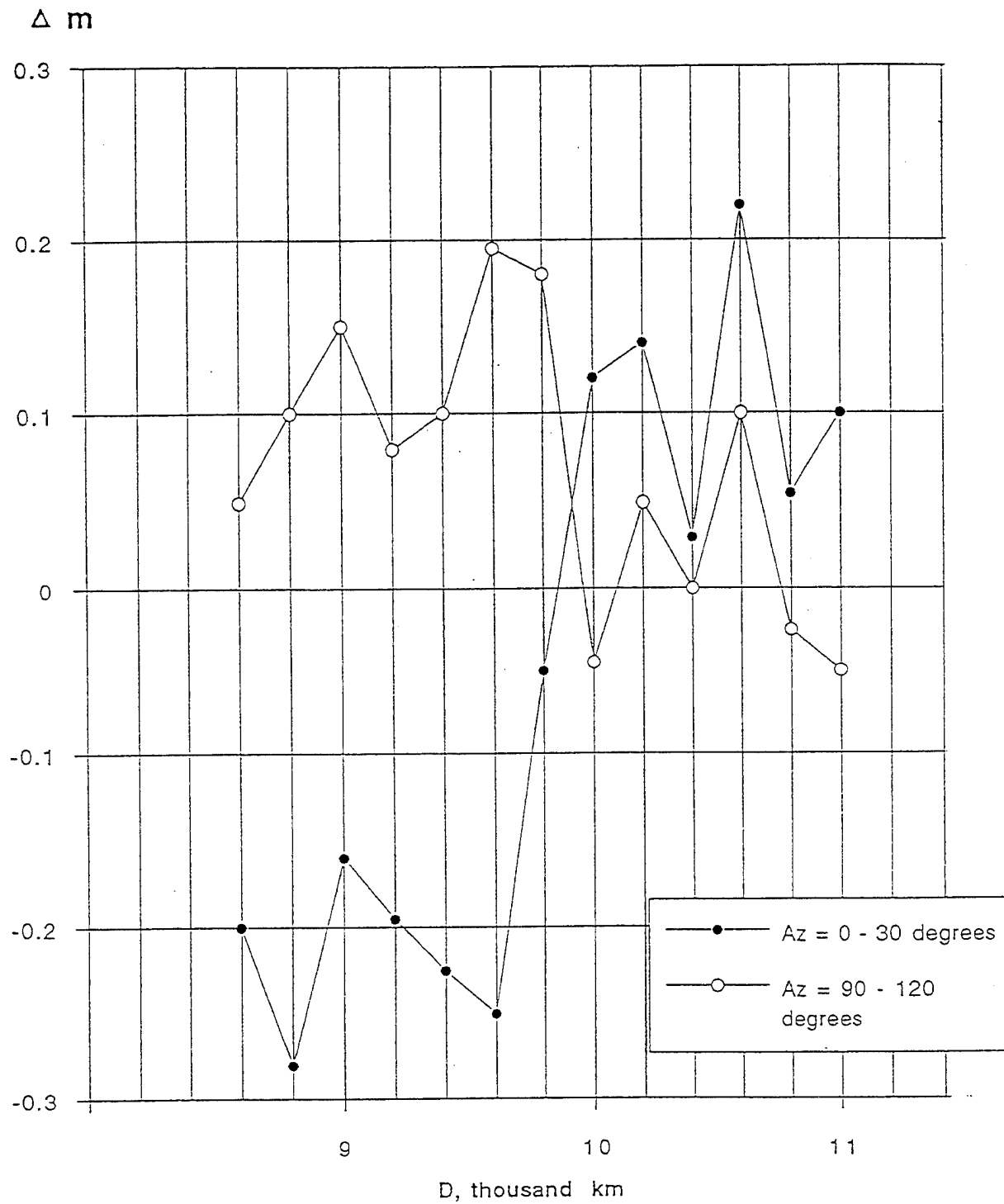


Figure 21. The magnitude residuals for single station Mondy (MOY) versus distance for two profile of epicenters with their azimuths 0-30 degrees and 90-120 degrees. Notice the distance range : from 8,600 to 11,000 km.

teleseismic distances were studied by using UNES from Nevada Test Site as a stable seismic source of many seismic signals with an approximately constant position of the epicenter and approximately similar radiation pattern. The seismic stations (Kokchetav network) were installed by CSE in the Zerenda-Borovoye region (Northern Kazakhstan) to monitor the UNES from Nevada TS. The network covered a comparatively small area, about 200 x 400 km (52 - 54N and 67 - 72E).

Station residuals for the Nevada UNES in the Zerenda-Borovoye network are an example of the instability of A/T-D curves at close stations, when the epicentral distances are within the interval 8,000-10,000 km. The distances in this case were 10,070 - 10,230 km.

The residuals were calculated as a difference between mb at each station and mb from the ISC data. Since we used many UNES (from 15 to 60 for different stations) with a similar radiation pattern and near the same epicenter position, the mean station residuals were obtained with high confidence. The space distribution of station residuals are shown in Figure 22. It exposes a remarkable picture. The stations are clustering on the map with small areas with very high positive values of the residuals, 0.40-0.65, whereas at very close stations the residuals are as small as 0.10-0.20.

It is known that in this region very hard unbroken and old rocks are everywhere on the Earth's surface. The surface conditions are similar for all stations. So there is absolutely no possibility to explain the variations of magnitude residual as an effect of local site.

The residuals obtained for these stations from closer events in different epicentral zones and distances differ from those from the Nevada events. Those are much more similar to each other. The origin of the residual for the events from Nevada is not local and is not usual for a regular teleseismic situation. It is specific for that particular epicentral zone, and for a particular range of epicentral distances of about 8,500 - 10,500 km where the shadow zone from the Earth's core begins. To obtain the value of path-effect, one has to exclude the area residual, which is in average +0.24, then the small-scale path deviation is 0.23.

The data, considered above (Figure 21) for Mondy station confirm that the significant variations of the amplitudes are typical for distances of about 8,500-10,500 km.

From the point of view of our main goal, this opens an opportunity to find the best position for installing the monitoring station (or an array). The best position can be found, keeping in mind not only the epicentral distance, local conditions and the regional tectonic situation. It sounds like a paradox, but the possibility to find a place

# Magnitude station residuals dmb at Kokchetav network for UNEs from Nevada TS

N

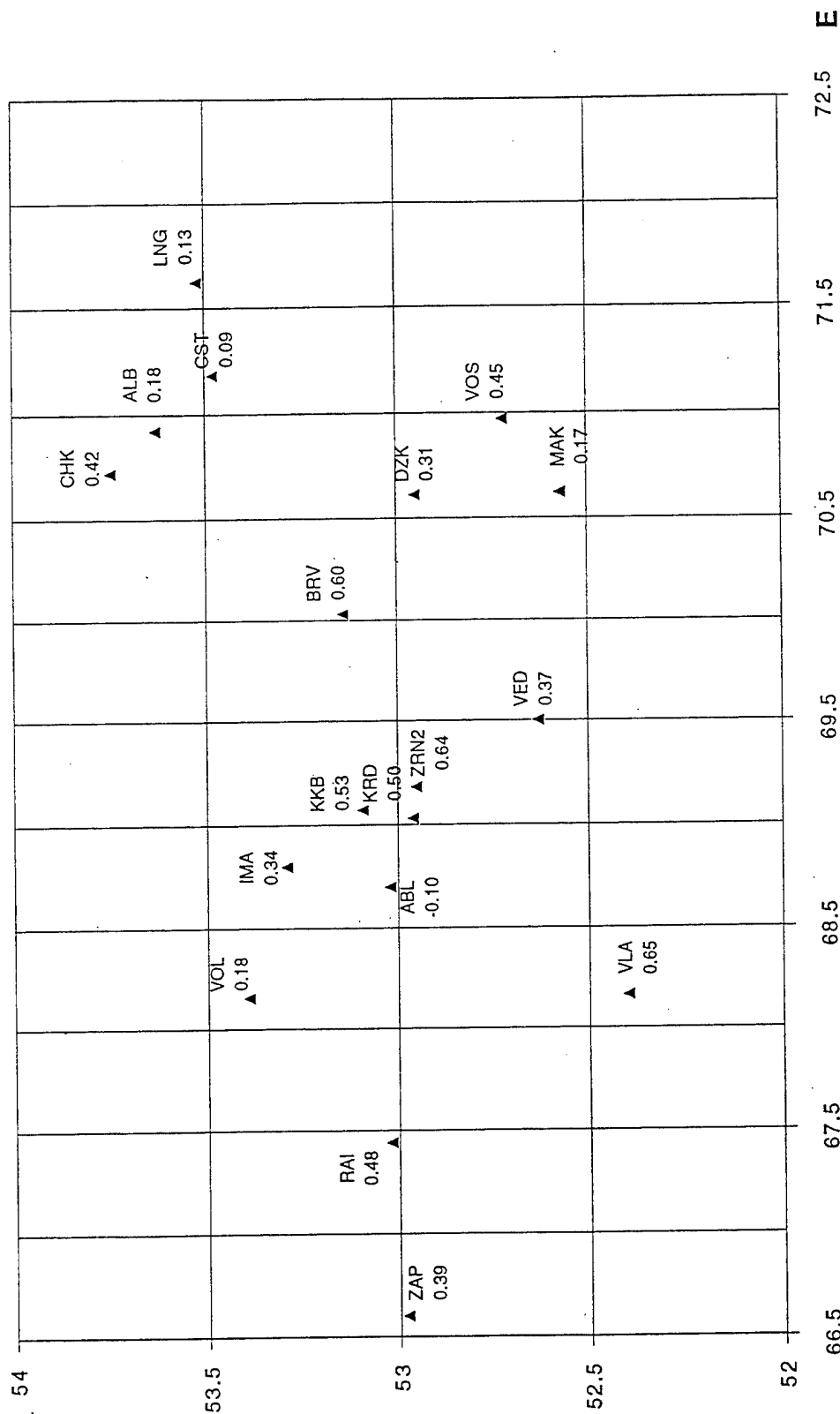


Figure 22. The space distribution of magnitude mb station residuals for UNEs from Nevada TS at temporal stations of Kokchetav network. The average epicentral distances is about 10,000 km. Note, the big scattering of residuals : till 0.7 magn. units) even for close stations.

with better sensitivity on a particular epicentral zone is bigger at 8,500-10,500 km interval than at 6,000-8,500 km. Practically, it is not easy to find such a point because we have no evidence about it on the surface. It will take a lot of time and field observations.

Looking at all these determinations, we see that the standard path deviations vary from 0.10 to 0.24, depending on how wide beams of seismic ray traces were taken. The wider they are, the path effect is stronger and smooth and the larger part of it moves into random component. The path variations of residual distribution seems not to be normal. The standard deviation is not terribly large, but there are many cases with a large residual. Examples for traces are India - North Tien Shan and the case for Mondy station.

#### 5.5. The Path Effect Obtained from the A/T - D Curves: Regional Observations

The next two sets of data are the curves A/T-D, obtained from observing the earthquakes from different zones, distances and azimuths, recorded by one particular station, or earthquakes from one small zone, recorded by 12 stations at different areas, azimuths and distances.

We built the A/T-D curve, plotting the A/T values of each earthquake as a function of distance D, both in log scale. The A/T values were previously reduced to MLH=5.0 by equation:

$$\log (A/T) = \log (A/T) - k*(MLH-5). \quad (5.1)$$

The parameter k was estimated experimentally from observations and was taken 0.63 for SKD records, 0.53 for SKM records at Garm ( $T_0 = 2.0$  sec), and 0.49 for SKM records at Talgar ( $T_0 = 1.2$  sec). There is a natural period of SKM instruments seismometers at both stations.

##### 5.5.1. A/T - D curves for Eight Epicentral Zones

The earthquakes from eight epicentral zones were taken. The station correction was used, and then "A/T-D" curves were built separately for the earthquakes for each epicentral zone, using all the 12 stations in each case (Figure 23).

When comparing the curves of the nearby zones on the Asian continent, the positions of the maxima do not vary significantly, but their difference with curves of some other zones is more noticeable. In some cases the curves have even opposite signs of extremes. For example, at the distance of 7000 km there is a maximum in the curve for Indonesian earthquakes and a minimum in the Far East recorded in Central Asian stations. At a distance of 5,000-5,500 km there is the deep minimum for the continental Asia and a

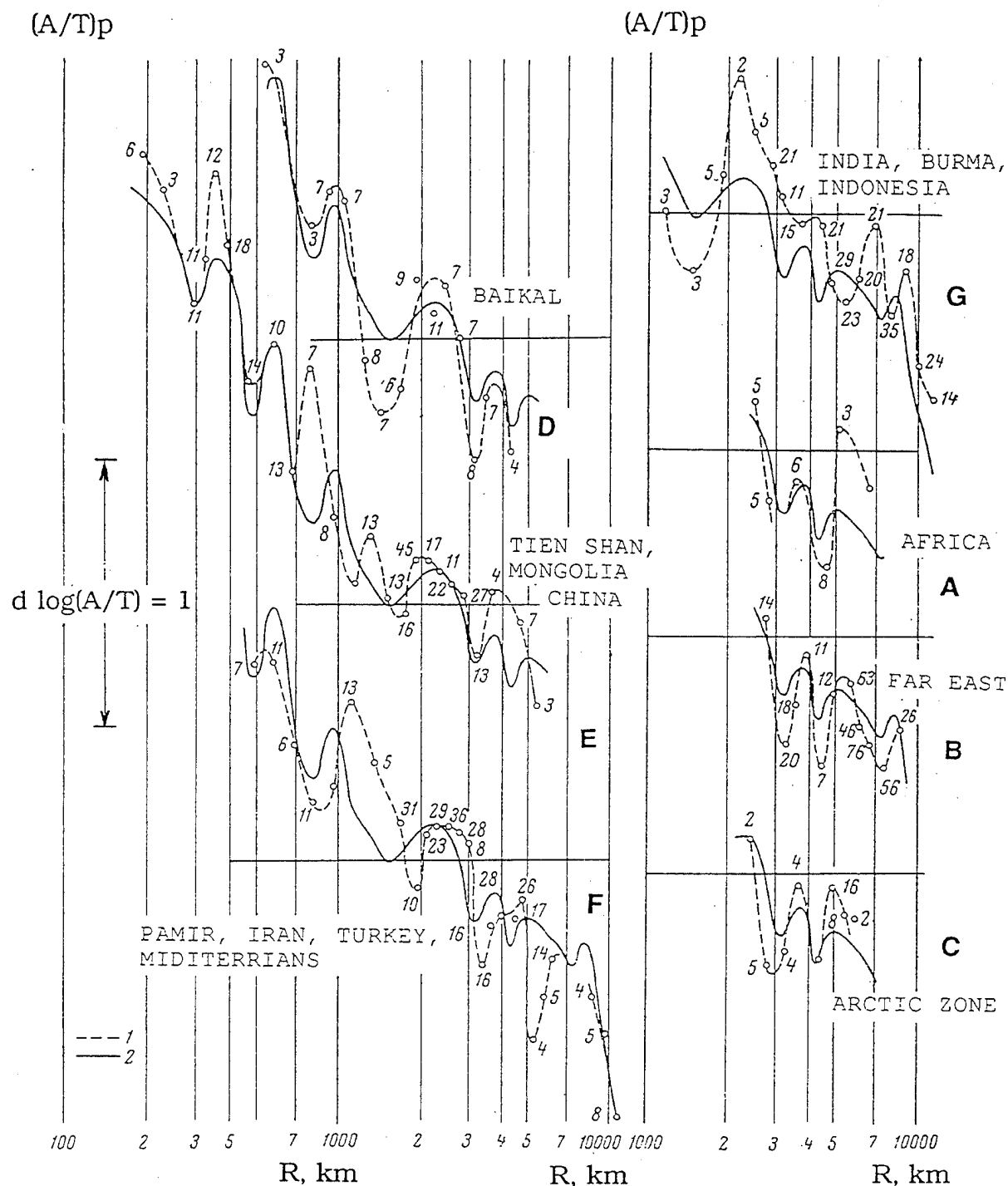


Figure 23. The A/T-D curves built separately for the earthquakes from each epicentral zone, using all the 12 stations in each case; the station residuals were corrected. Epicentral zones: a - Africa; b - Far East; c - Arctic zone; d - Baykal; e - Tien Shan, Mongolia, China; f - Mediterranean, Iran, Pamir; g - India, Burma, Indonesia. Numbers near the points of (1) mean the number of observations included in these point. The absolute level of curves corresponds to  $MLH = 5.0$ . Dashed lines are the amplitude curves for each epicentral zone; the solid lines are our general curve.

maximum in curve for Far Eastern and African earthquakes.

The amplitude of the oscillation of the difference between partial zone A/T curves and standard one reaches 0.3-0.4 in some part of the distance scale (see Table 16) whereas in general it is 0.12. It is not so small a deviation for a partly smoothed effect.

Table 16. The Standard Deviations of the Zone A/T-D Curves Relatively the Standard Calibration Curve

The Epicenter Zone	Stand. Dev. of Shape
The Baykal, the Sayan	0.288
Japan, the Kuril, the Aleutian	0.048
The Tien Shan, Mongolia, China	0.084
Africa, Arabia	0.117
The Mediterranean, Iran, the Pamir	0.093
The Arctic	0.088
India, Burma, Indonesia	0.106
The mean shape deviation	0.118

#### 5.5.2. A/T - D Curves for Four Observational Areas

Combining the A/T-D curves of several nearby stations, corrected by local and area effects, we obtained the curves for four observation areas: Russian platform (Moscow), Central Asia, North Tien Shan and Baykal. The curves are shown in Figure 24, the standard deviation of A/T-D shapes is 0.14. One can see the difference in the details the curve shapes and in the general attenuation. The difference is more significant at distance ranges 2000-3000 km than at 5000-7000 km.

Table 17. The Shape Deviations of A/T-D Curves of 12 Stations

Stations	Stand. Dev.	Stations	Stand. Dev.
Moscow	0.044	Talgar	0.168
Andizhan	0.119	Stchel Dalnaya	0.177
Tashkent	0.135	Rybachye	0.100
Frunze (Bishkek)	0.168	Irkutsk	0.162
Garm	0.143	Kabansk	0.125
Alma-Ata	0.150	Kyakhta	0.174

The variation of shape of A/T - D curves from data of Table 17 is 0.14 magn. units.

One can see that the shape deviations in these two cases (0.12 and 0.14) are smaller than the standard deviation due



$\log(A/T)$

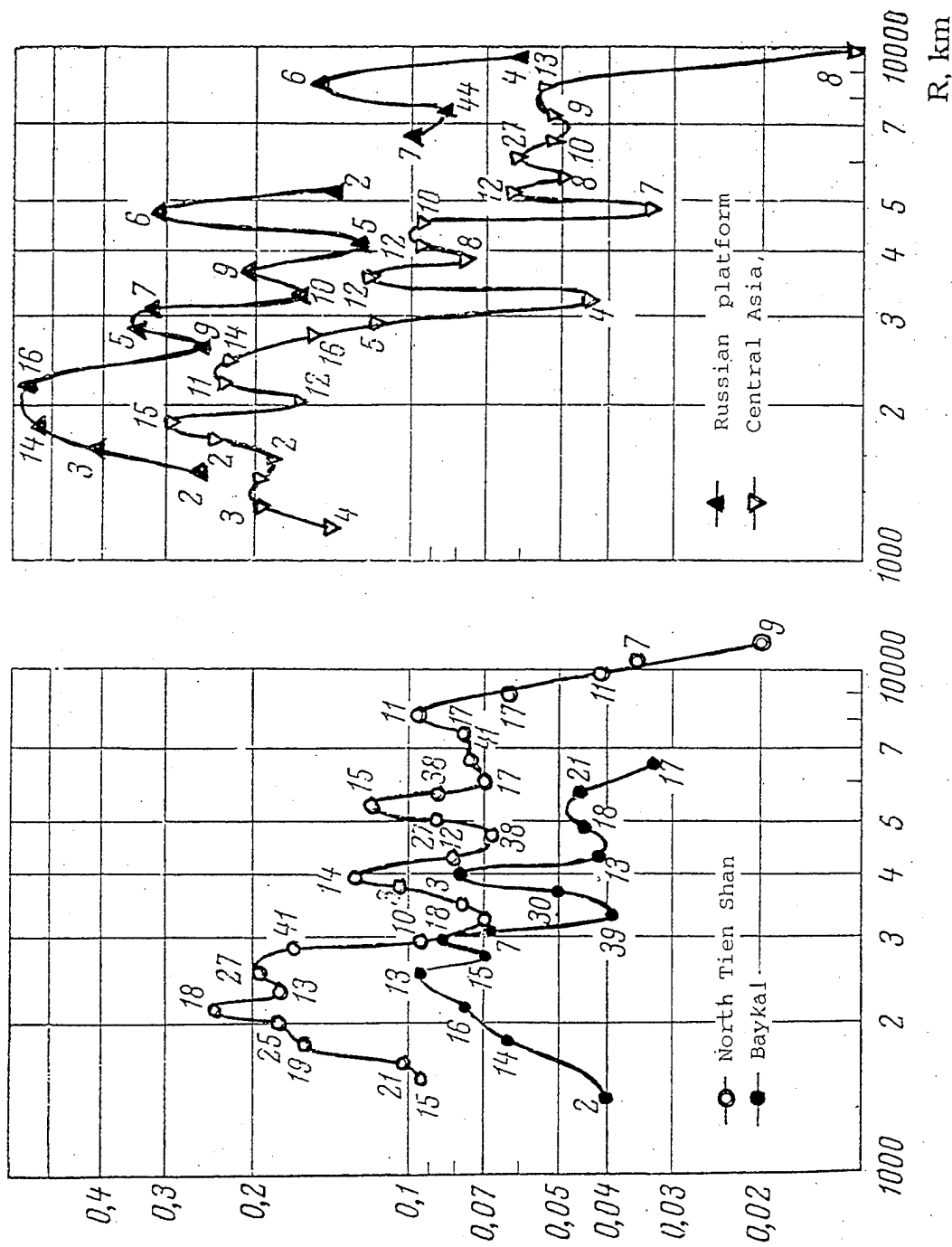


Figure 24. The A/T - D curves for four observation areas: Russian platform (Moscow), Central Asia, North Tien Shan and Baykal. The data of several nearby stations inside each area were combined after correcting their local residuals. Numbers near the points mean the number of observations included in these point. The absolute level of curves corresponds to  $MLH = 5.0$ .

to path effect obtained from profile observations or from couple "area-zone" (0.18). But nevertheless, it is significant.

#### 5.6. The Summary of Estimation of Path Component of Deviation

We saw above, that the values of path effect are different depending how "pure" was the data selection. If the ray traces covered a wide territory, the path effect smooths and the value obtained seems to be less then path effect. Part of it moves into the random component.

Other systematical difference depends on interval of distance. That is why, in our summary, we calculated the path-effect standard deviation separately for distances  $D < 2,000$  km,  $2,000 < D < 8,500$  km and  $D > 8,500$  km. The data, obtained from "station curves" and "zone curves" were not used when the path-effect deviation was calculated. The summary and average data are shown in Table 18.

Table 18. Summary Path Standard Deviation of A/T-D Curves for Different Sets of Data

Set of Data	Path Stand. Dev.
Couples "area-zone"	
Antonova, 1974	0.19
Marshall, 1993	0.10
Profile of stations	
Aden Gulf	0.289
Persian Golf	0.121
Kamchatka	0.152
Profile of epicenters	
North Tien Shan area $D < 2000$ km	0.178
8500km $> D > 2000$ km	0.070
Baykal area $D < 2000$ km	0.252
8500km $> D > 2000$ km	0.150
Small-scale path effect	
Mondy station $D > 8500$ km	0.30
Semipalatinsk network $D > 8500$ km	0.23
Average standard deviation:	
$D < 2000$ km	0.22
8500 km $> D > 2000$ km	0.15
$D > 8500$ km	0.26

The values obtained from different sets of data vary strongly, even inside the distance intervals mentioned above. We do not think that allows a precise estimation of averages. Our opinion is that 0.18 can be taken as a reliable value to describe the average variations of a path effect.

Of course, it is impossible to create the over the world

correction system for any path effect (from "each epicentral zone" to "each station"). But if the problem is to monitor some zone, where UNE were conducted or supposed to be, the special station correction for each particular small area have to be obtained. Such correction includes not only local and area effect, but path effect as well. As was mentioned above the zone effect can be corrected too. If so, the origin of error becomes only random component.

## **6. THE PATH EFFECT IN SURFACE WAVE MAGNITUDE RESIDUALS AND METHOD OF CORRECTION**

It is known that the accuracy of the magnitude estimation for the surface waves is higher than for the body P waves. The station residuals  $\Delta MLH$  are more stable too. The amplitude curve used for the magnitude MLH determination agrees with the observation data almost everywhere in the world. That is because of the long periods of the surface wave, and because they propagate in the Earth's crust on the whole whereas the P wave curve oscillates joining with the boundaries in the crust, the mantle and even the core surface.

The MLH scale is one basis in seismic observation in FUSSR. It can be used as a part of information used in creating the Ms- $\Delta mb$  (MLH-MPV) discriminant in the problem of UNES monitoring. That is why we consider, as an important problem, the MLH residuals and the way to correct them. We suggest starting from the table of correction and the data itself. Three sets of data were used. These are the summaries [Landyreva, 1967, 1974] and [Vanek et al., 1974, 1978] and our own studies of the effect of large inhomogeneities like Black Sea or Tibet on the surface-wave amplitudes. The method of correcting this kind of pass effect is proposed.

### **6.1. Comparing the MLH Magnitude Residual from Different Sets of Data**

Some studies were conducted to find the station residuals and corrections for MLH. Now we compare data by Landyreva [1967, 1974] and Vanek et al. [1974, 1978]. There were only 14 stations common in both studies. Figure 25 shows the correlation between MLH corrections by Vanek and Landyreva. The straight line corresponds to the identity of their estimations. Standard deviation of difference between Landyreva's and Vanek's estimations is 0.171. Only two stations deviate more than 0.35.

The data evidences that station correction significantly varies when different sets of data are used. This discrepancy cannot be due to random scattering only. It is not just error; actually, there are factors which do not allow obtaining a high accuracy by only increasing a number of stations.

MLH STATION CORRECTIONS dMLH BY TWO AUTHORS  
EARTHQUAKES FROM JAPAN

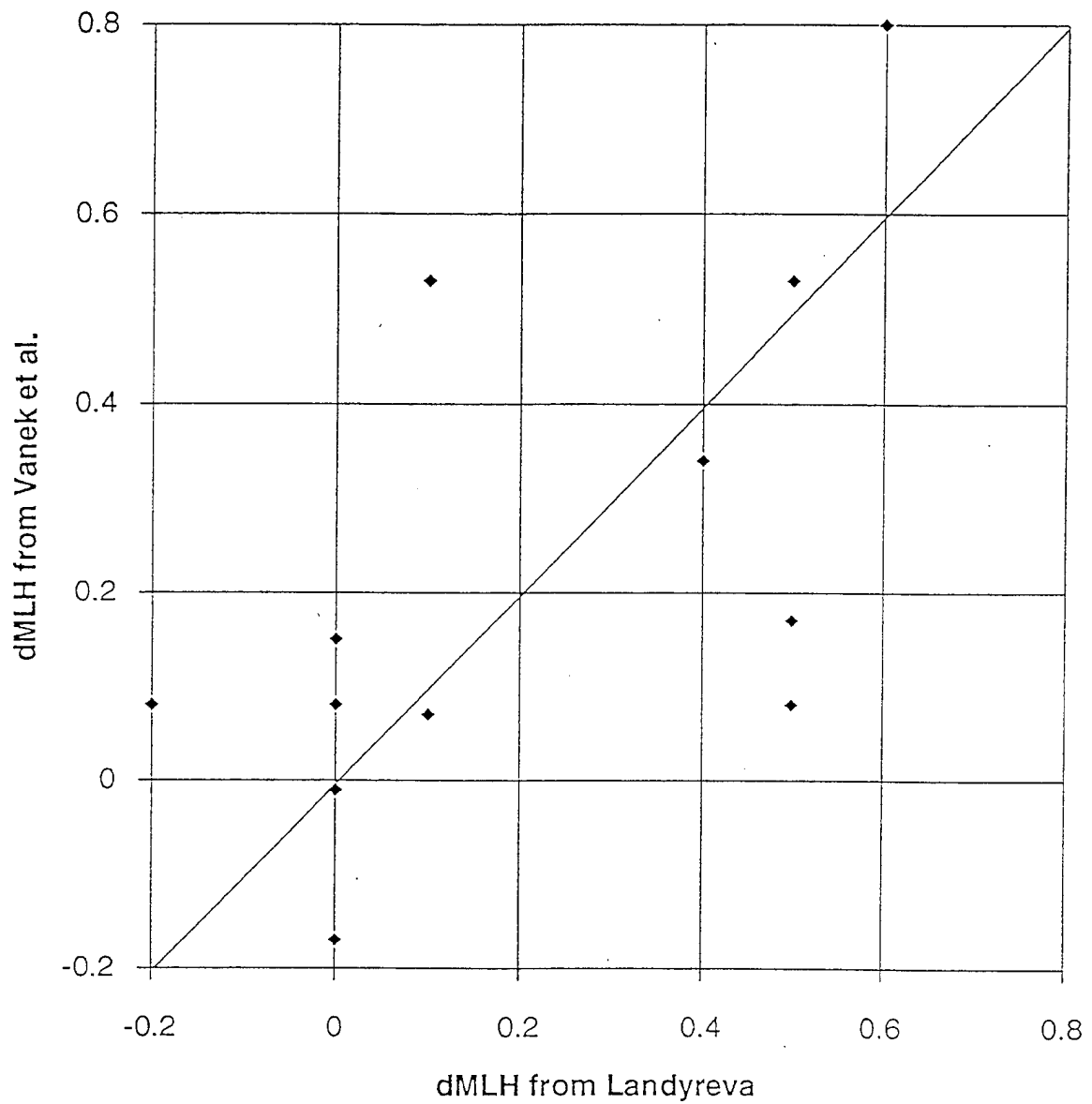


Figure 25a. Comparing the station corrections dMLH by Vanek [1983] and Landyrev [1968 and 1974] for the same stations, earthquakes from Japan.

# MLH STATION CORRECTIONS dMLH BY TWO AUTHORS EARTHQUAKES FROM SEVERAL EPICENTRAL ZONES

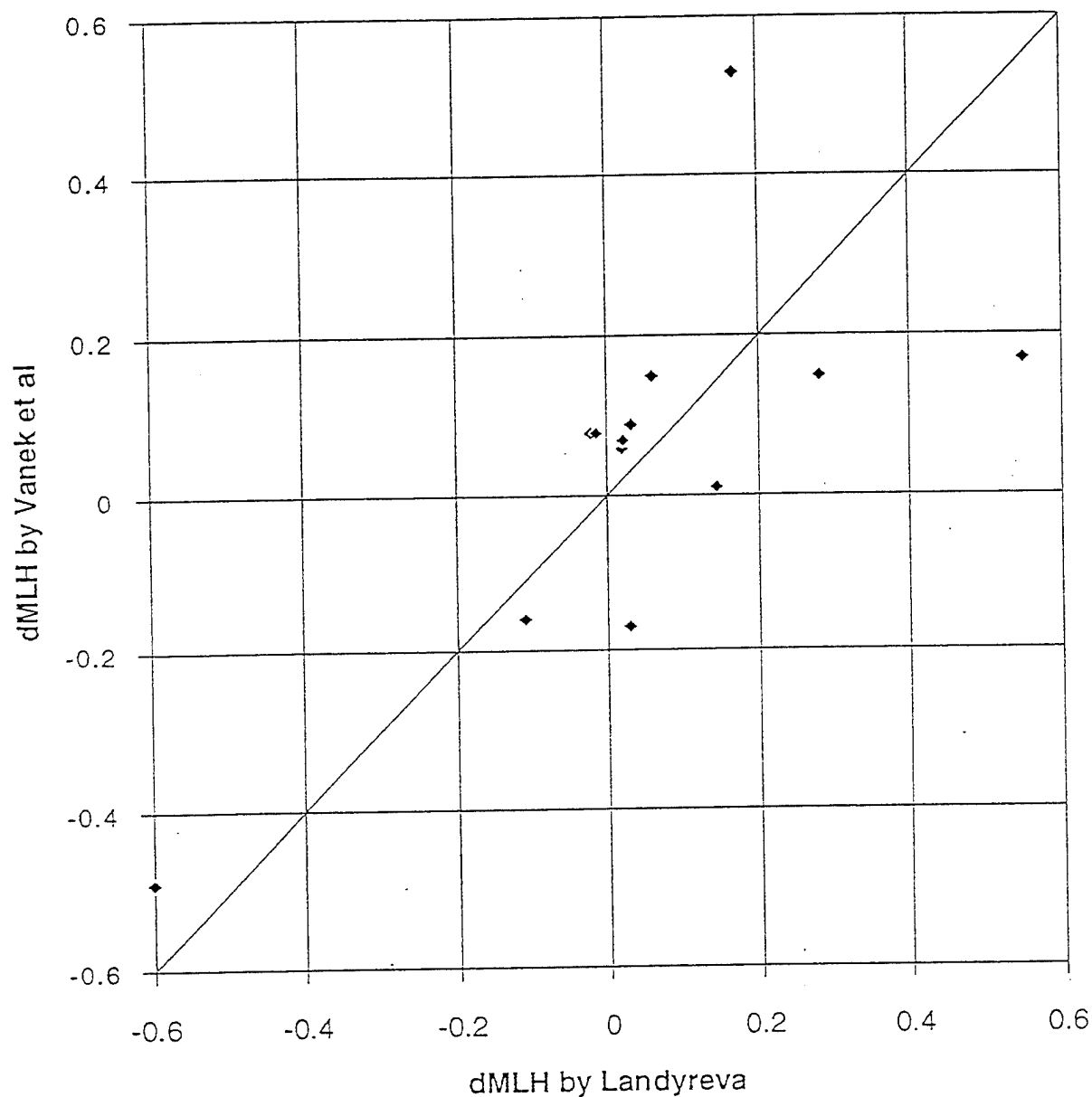


Figure 25b. Comparing the station corrections dMLH by Vanek [1983] and Landyrev [1968 and 1974] for the same stations, averaged for all epicentral zones.

There is a peculiarity of surface wave, which makes it easier to find the sources of magnitude residual-much easier, than to find the path-effect for P-waves. The intensity of the surface wave depends on large inhomogeneities of the Earth's crust which create "shadows" in the wave field. The most important inhomogeneity is the boundary between the ocean and the continental crust. We will see some data on it.

## 6.2. The Effect of the "Pacific-Continental Asia" Boundary on MLH Residuals

The effect of the ocean-continent boundary on MLH residuals was studied by Landyрева [1967, 1974] for 42 Soviet seismic stations, for each of 10 epicentral zones separately. The station corrections obtained are shown in Tables 19 and 20 (Appendix 2). Another study of the MLH residual was made by data from Vanek, Kondorskaya et al [1980, 1983]. Their results are given in Tables 21 and 22 (Appendix 2).

One can see from the tables that the station residuals in the same station are different depending on the epicentral regions. For example, the stations of the Far East need positive corrections (0.3-0.7 mag.units) for the earthquakes from the Aleutian, Kamchatka, the Kuril, Japan, but negative corrections for the earthquakes from the Mediterranean and Iran. The stations in the Caucasus need negative corrections for the Far East earthquakes, and positive corrections for the Mediterranean.

It seems that the amplitudes of the surface waves are smaller when they pass from an area with the oceanic crust to a continental one. Penetrating the boundary between the oceanic and the continental crust, the surface waves decrease their amplitudes significantly. But if the distance between this boundary and the station becomes longer, the amplitude becomes "normal" and the residuals acquire values scattered around the zero.

Figure 26 shows the variation of station corrections with the distance for the Eurasian paths of earthquakes from the "oceanic" zones (Japan, the Kuril, the Aleutian, the Mediterranean, Alaska, the Philippines and Indonesia). The corrections, on the average, are about zero when the distance is 4,000 km and longer. Thus, it seems that the station corrections depend on the distance, and the standard calibration curve does not agree with the data of observations.

Note that this effect is obvious only when the surface waves cross the "ocean - continent" boundary. But if the ray traces are completely continental (like the ray paths from the Central Asia earthquakes to the Far East stations),

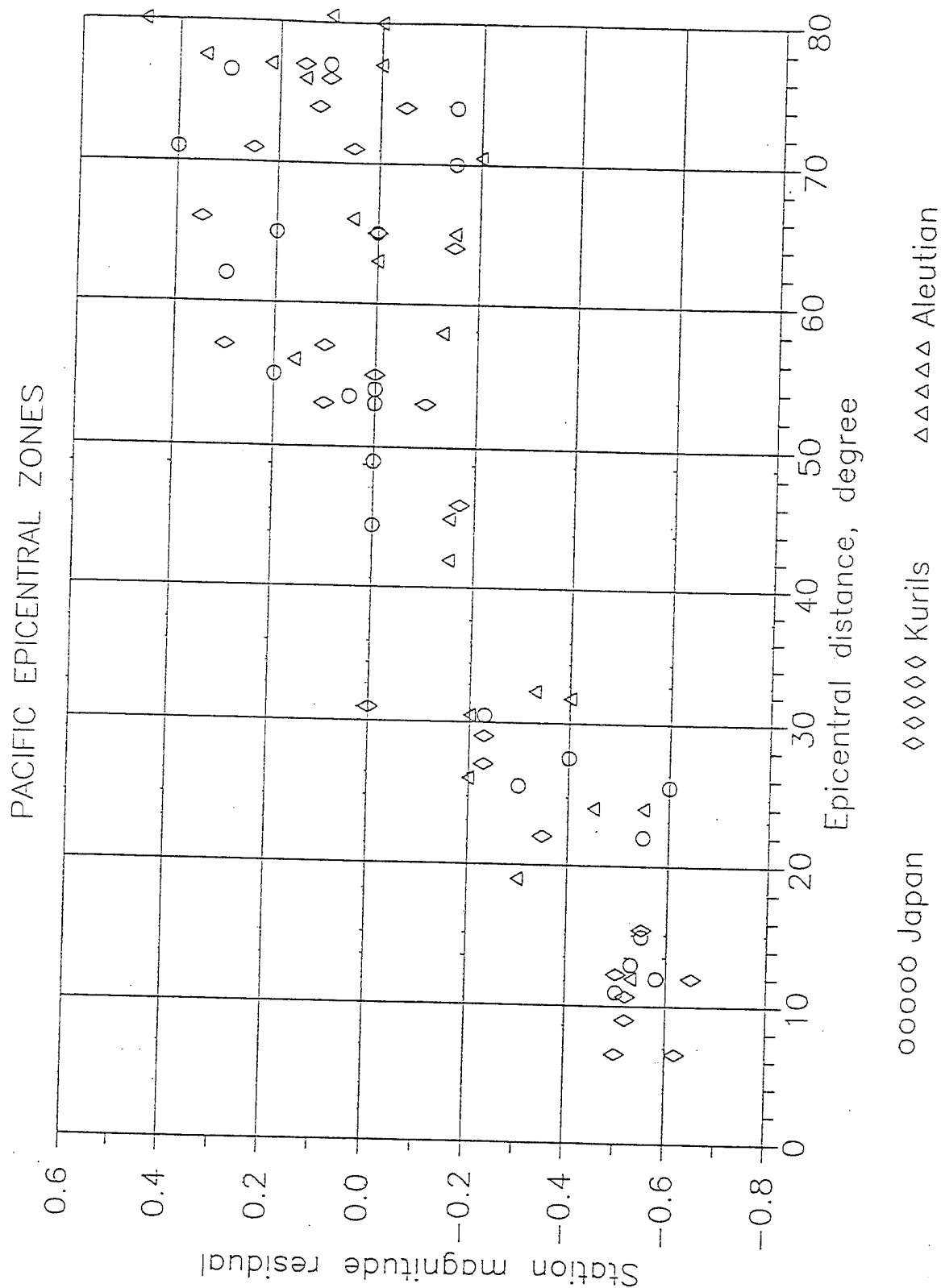


Figure 26a. The surface waves magnitude MLH station residuals versus distance for earthquakes from three West Pacific epicentral zones: Japan, the Kuril and Aleutian. The residuals are negative and increase with distances from  $-0.60$  near the epicentral zone to about zero for distances more than 40 degrees.

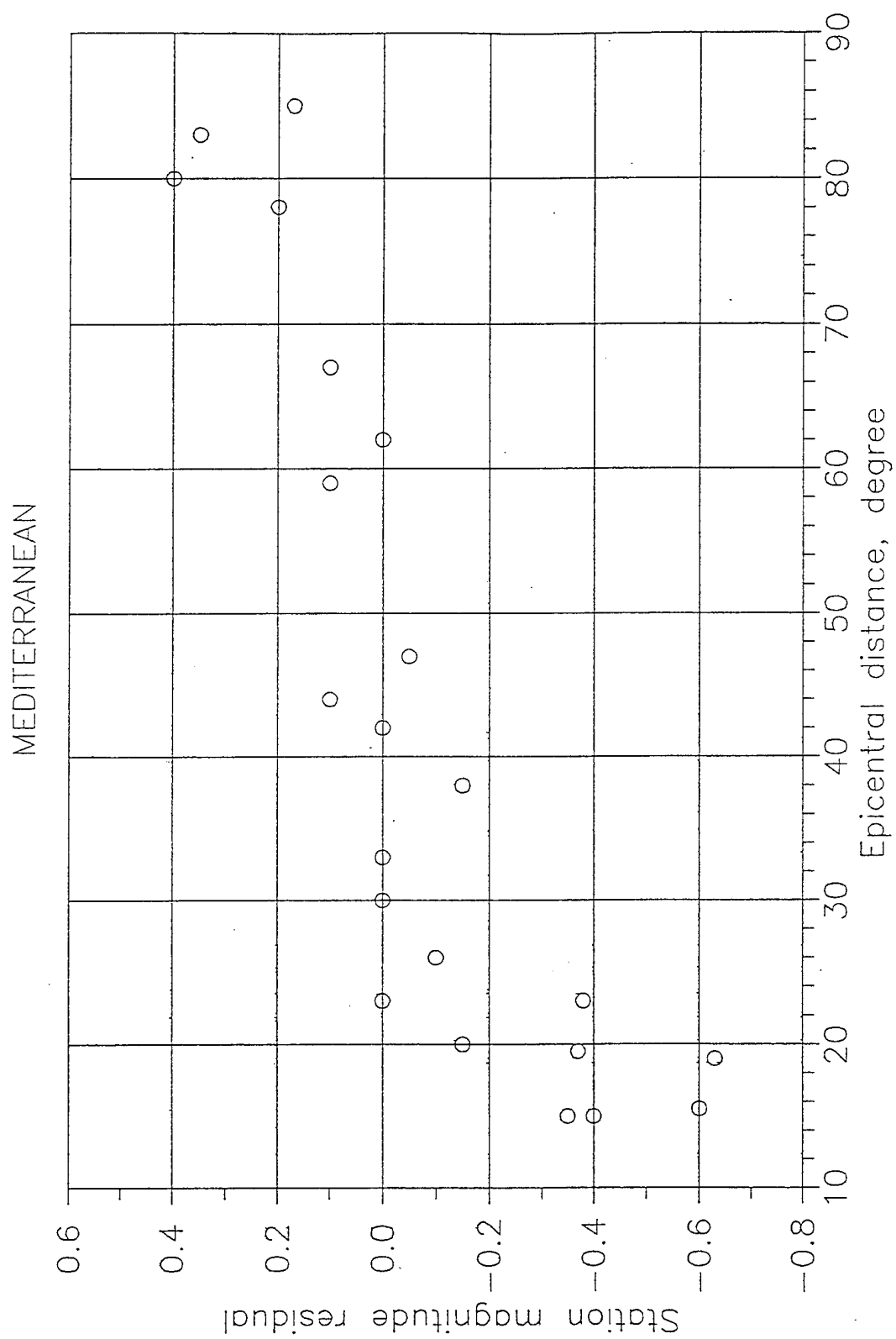


Figure 26b. The surface waves magnitude MLH station residuals versus distance for earthquakes from Mediterranean zone.



# CENTRAL ASIA, ALASKA, INDONESIA

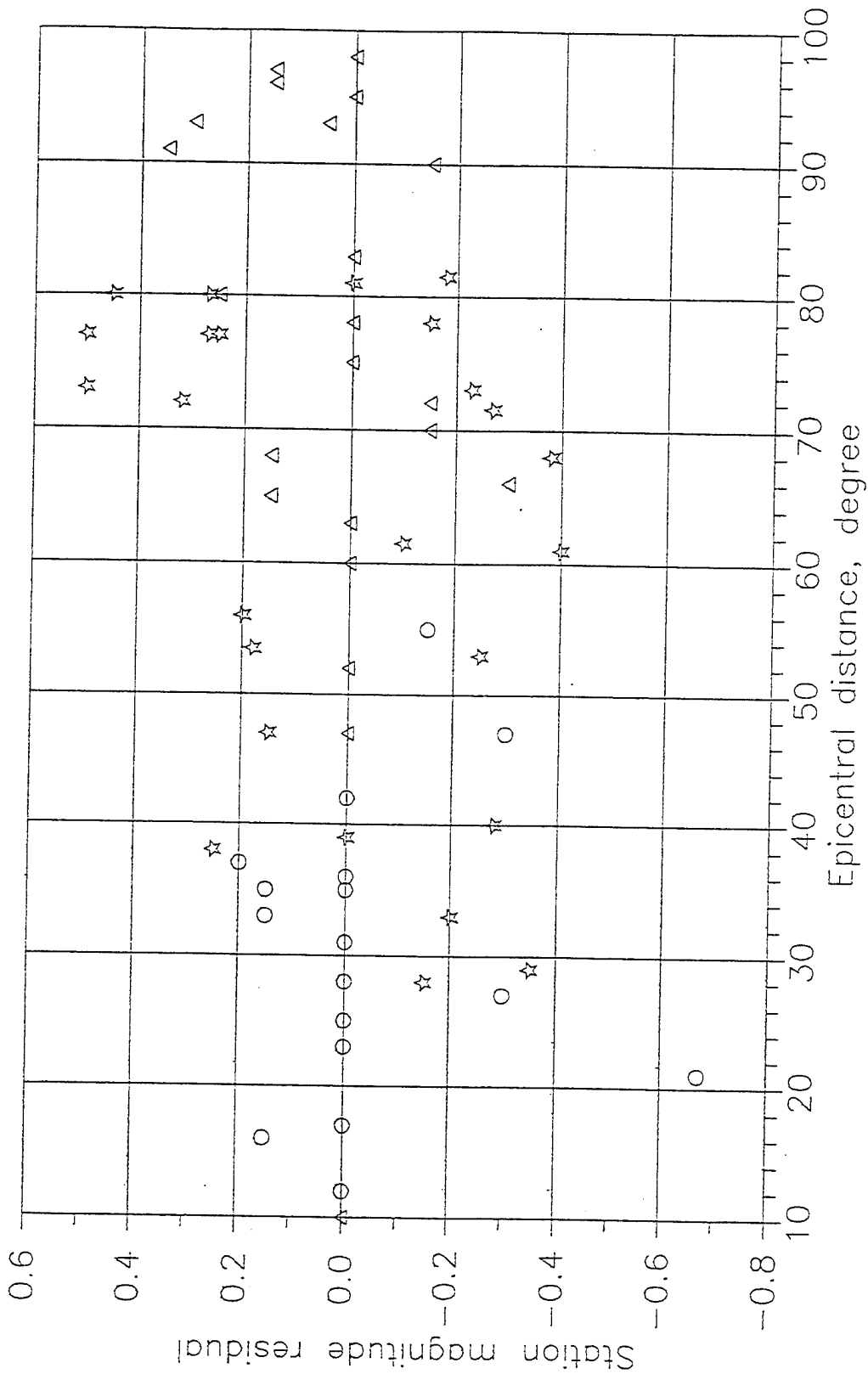


Figure 26c. The surface wave magnitude MLH station residuals versus distance for earthquakes from three zones : Central Asia, Alaska and Indonesia.

there is no dependence on the distance. Figure 26 shows it clearly. Here, the points are the station corrections for some epicentral zone versus their distance from this zone. For the Far East zones (Japan, the Aleutian, the Kuril, Alaska, the Philipines-Indonesia and the Mediterranean) the contact of the ocean-continent crusts is very close to the epicentral zones, so the distance is practically the distance from the station to this boundary.

To smooth out these diagrams for the Far East zones, we obtain curves which have great positive values for small distances going down to 3,000-4,000 km. Then the curves become practically flat and close to zero. The diagrams for the continental ray paths (Central Asian earthquakes) have station corrections scattered around zero for all distances. These curves can be regarded as  $C(D)$  - the first part of the total station corrections  $Cst$ . It is not constant for the station and is different for the same station depending on how far the epicentral zone is from the station. It exists only for the traces crossing the ocean-continent boundary.

The second part  $C(loc)$  is individual for each station and describes the influence of local conditions; it is the same for all epicentral zones. In Figure 26 this component assumes the form of the deviation from the smoothed out curve:

$$C(loc) = Cst - C(D).$$

The scattering of station residuals around the regional curves corresponds to the value of about 0.2. In some cases, the mean and regional corrections differ considerably (see, for example, the data for the stations ILT and MAG in Tables 19 and 20.

### 6.3. The Variations of the MLH Residuals Connected with the Black Sea Depression

A detailed analysis of similar dependencies was done for the Black Sea depression by Artemova and Khalturin [1990]. In this work the station residuals were used as a tool for localizing the territory - part of Black Sea, creating intensive change of surface wave amplitudes. The Black Sea was chosen for the study because it represents serious inhomogeneity having the oceanic type of crust in its deeper part. The Black Sea is surrounded by many stations and earthquake epicenters. Its geological structure is well studied.

The main source of data was the "Seismological Bulletin of ESSN". The maximum amplitudes of the surface waves and their period were borrowed from the Bulletin for 72 earthquakes, each of them was recorded by 6-12 stations. The

MLH magnitudes were calculated in a standard way from A/T. For each earthquake the average magnitude MLH and magnitudes residuals dMLH were determined. Then the station residuals for each station were averaged for a small group (4-10) of closely located earthquakes. The data obtained are shown in Table 23. The average residual for a small group of earthquakes was related to the line from the station to this small epicenter zone as shown in Figures 27 - 30. If the station is far away, only the ray trace is shown.

On the continental traces the residuals are positive (from 0 to 0.3) and are the same for the local and for the far away stations. For the traces passing along the Russian Platform the residuals slightly increased with the distance. That is due to the very high Q on this platform. When crossing the Main Caucasian Ridge, the amplitudes of the surface waves decrease approximately two times (0.2-0.3 magnitude units).

Table 23. The MLH Magnitude Residuals for Different Seismic Traces After the Data of the Earthquakes on the Alpine Band and the Number N of Traces Used

The Ray Trace	Seismic Stations			
	Close to the Sea		Far from the Sea	
	dMLH	N	dMLH	N
The ray traces passing out of the Black Sea:				
On the Western side	+0.10	8	+0.20	20
On the Northern side	+0.05	5	+0.05	4
On the Southern side	-0.05	15	-0.05	4
On the Eastern side (through the Great Caucasian Ridge)	-0.30	6	-0.15	6
On the Eastern side (out of the Great Caucasian Ridge)	0	13	0	16
The ray traces crossing the Black Sea:				
The Western part of the Sea	-0.40	14	-0.20	6
The Central part of the Sea	-0.55	15	-0.35	3
The Eastern part of the Sea	-0.55	13	-0.30	4
Laterally	-0.55	8	-0.25	3
The ray traces passing along the coast				
Along the Northern Shelf	-0.10	3	-	-
Along the Western Coast	-0.30	4	-	-
Along the Southern Coast	-0.50	3	-	-

When crossing the Black Sea depression, the amplitudes become significantly smaller. The station residuals in the stations situated close to the Sea are negative, and they are

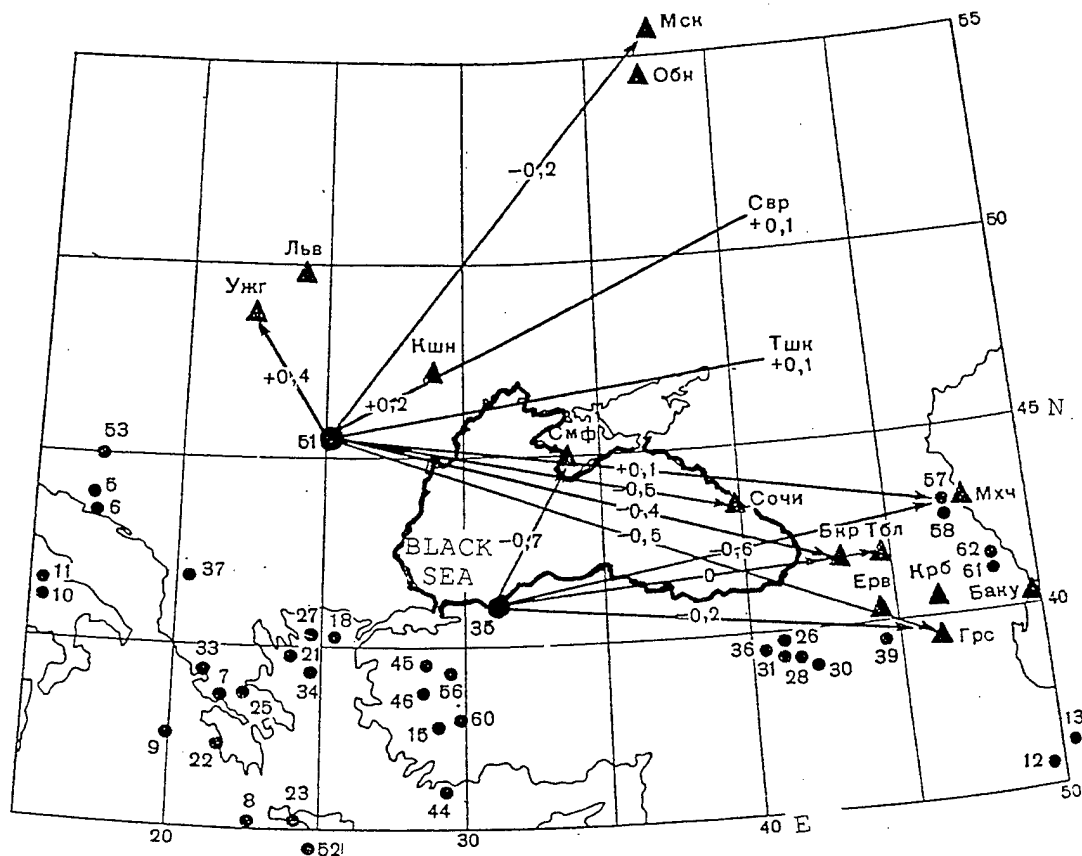


Figure 27. The map of the ray traces of Rg waves crossing and not crossing the Black Sea from two earthquakes : #35 in North - West Turkey and #51, Vrancea. The values of the residuals are shown in a middle of the ray traces, triangles are the seismic stations, solid circles are the epicenters used in this study. The residuals are great and negative when crossing the deep part of the sea.

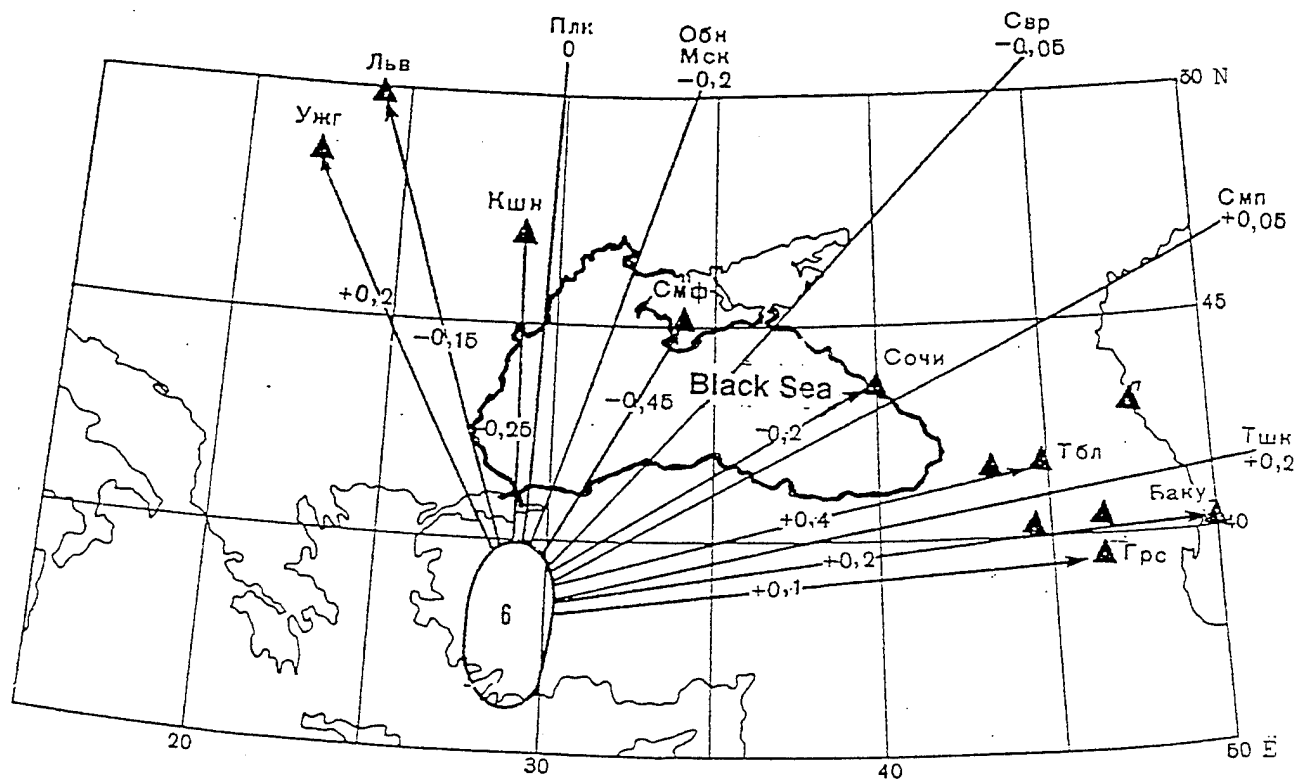


Figure 28. The map of the ray traces of Rg waves crossing and not crossing the Black Sea from the epicentral zone #6. The values of residuals are shown in a middle of the ray traces. The values of residuals are great and negative when crossing the deep part of the sea and small or positive when past.

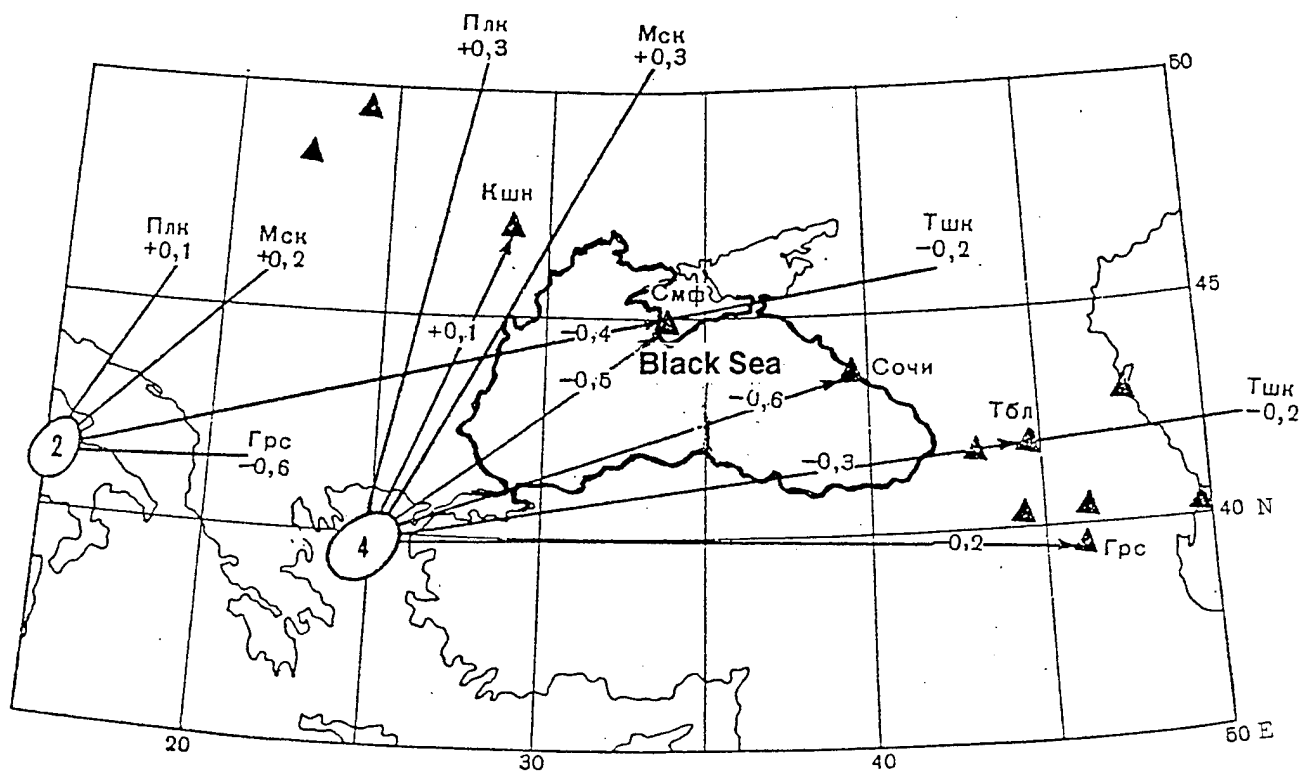


Figure 29. The map of the ray traces of Rg waves crossing and not crossing the Black Sea from the epicentral zone #2 and #4. The values of residuals are shown in a middle of the ray traces. The residuals are great and negative when crossing the deep part of the sea and small or positive when past.

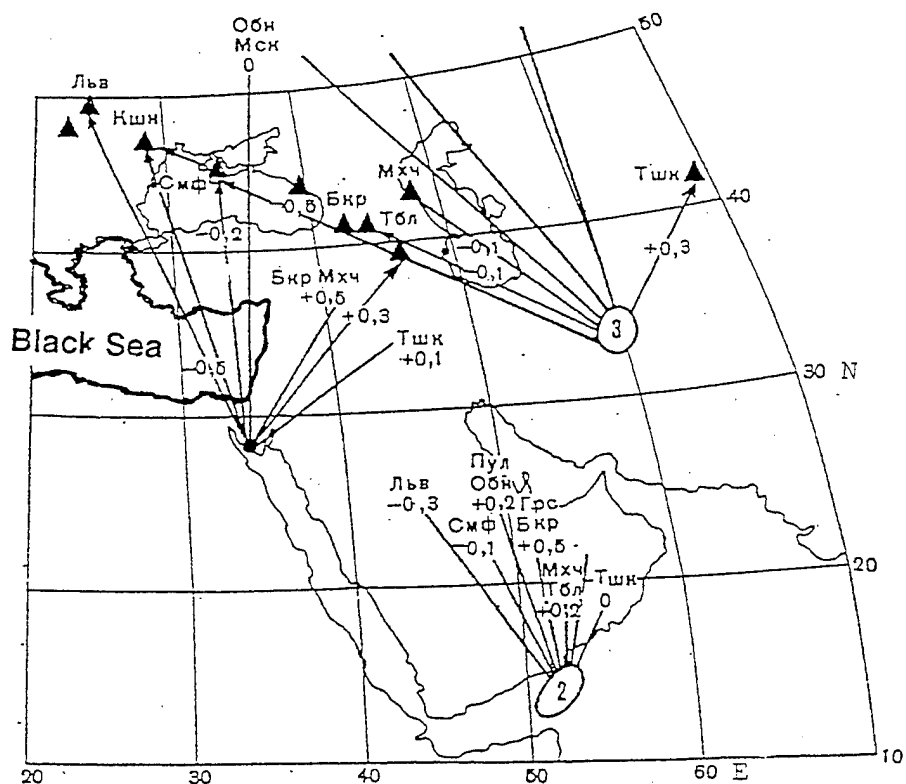
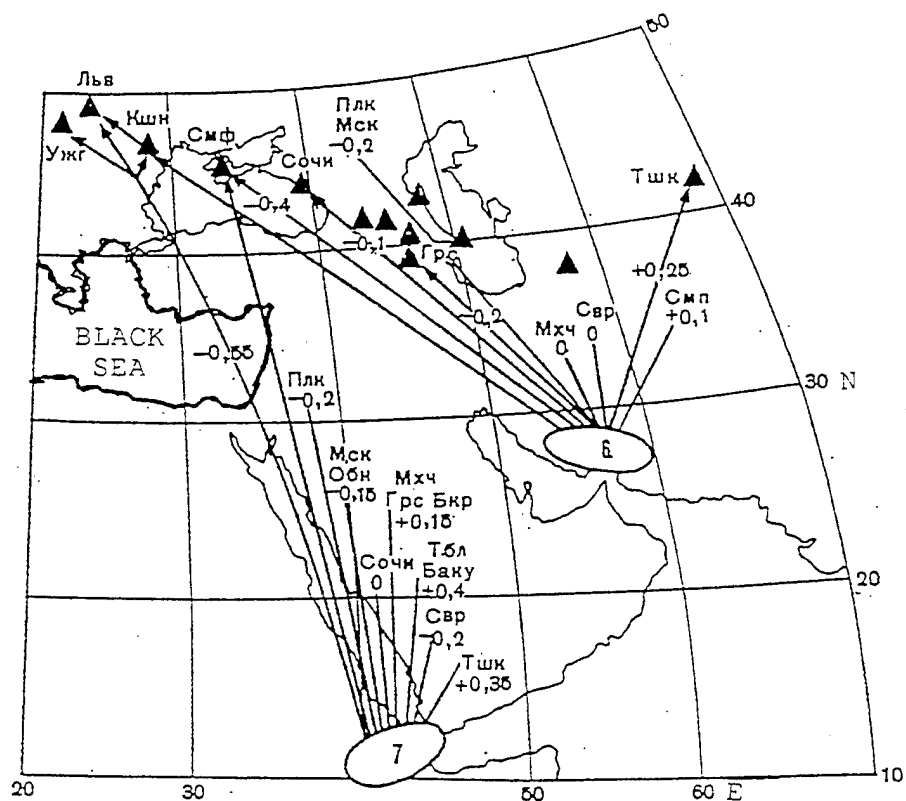


Figure 30. The map of the ray traces of Rg waves crossing and not crossing the Black Sea from the distant epicentral zones. The ray traces are not shown completely. The code of the station and the values of residual are shown near each ray trace. The negative residuals are at traces crossing the deep part of the Black Sea.

about 0.55. In Western stations, where a part of the traces crosses the shelf area of the sea, the residuals are negative too, only smaller, about -0.40. Note that the negative residuals decrease and disappear in distant stations, such as Obninsk (OBN). If distant epicentral zones are studied, one can see the same tendency as for the close ones (Table 24).

Outside the Black Sea the station residuals are positive and almost the same for the near and the distant stations. Crossing the Black Sea the amplitudes decrease sharply in the stations near the sea and much less in the distant ones. The values of the residuals are lower for distant epicenters than for the near epicenters.

From the data above it is clear that the inhomogeneity that is responsible for the observed results lies in the deep part of the Black Sea which is known as the suboceanic type of crust (without granite layer). A sharp decrease in amplitudes occur when the ray trace touches the deep part of the sea.

Table 24: The Magnitude Residuals  $\Delta MLH$  for Close and Distant from Black Sea Stations for Earthquakes from Distant Epicentral Zones with Two Types of Ray Traces

Ray traces	Close Stat.		Distant Stat.	
	$\Delta MLH$	N	$\Delta MLH$	N
East of the Black Sea	+0.1	20	+0.1	20
Crossing the Black Sea	-0.3	20	-0.1	20

The value of the magnitude residual does not depend on the length of the way inside the deep part of the sea (it is equal for all the rays crossing the Black Sea depression both in the North-South and East-West directions). It shows that the cause of the observed phenomena is not attenuation.

The study of the records allows to understand what happens with the waves. When crossing the Black Sea, the maximum phase corresponding to the group velocity of 3.0 km/s disappears. To determine MLH the stations situated near the sea, such as Simpheropol (the Crimea), measure the scattered waves without any clear arrival. Their maximum is very indefinite, weak and appears much later (a minute and more) than it is expected from the group velocity of 3.0 km/sec.

When inspecting the recordings of more distant stations, such as OBN, one will notice that they look much "better". The maximum of the amplitude has moved closer to the moment it is expected. Far from the sea the travel time of the scattered waves remains almost the same as it should be in the distance from the Black Sea.



Let us return to the problem of the magnitude correction associated with the known inhomogeneity, like that in the Black Sea region. Our opinion is that one must take for the basic magnitude only the estimates of the stations for which the ray traces are continental. For the station with traces crossing the sea the residuals (and corrections) should be considered as their deviation from the "continental mean magnitude".

If the earthquake is recorded by a very large number of stations, the regional inhomogeneity, such as for the Black Sea, does not modify the magnitude significantly. As regards to weaker events, the corrections that take into account a similar regional effect, can prevent serious errors.

In Table 25 we have shown the system of station corrections which are designed using the data above that refer to the continental paths for nine epicentral zones: 1 - the Persian Gulf, 2 - Iran, 3 - the Caucasus, 4 - East Turkey, 5 - Central Turkey, 6 - West Turkey, 7 - the Aegean Sea, 8 - Greece, 9 - Albania and Yugoslavia.

Table 25. Station Corrections dMLH for the Main Soviet Stations Which Should be Taken into Account the Black Sea Effect for Earthquakes from Nine Epicentral Zones

St.	Epicentral Zones								
	1	2	3	4	5	6	7	8	9
SIM	+0.5	+0.6	+0.7	+0.7	+0.7	+0.45	+0.4	+0.5	+0.3
SOC	+0.1	0.0		+0.3		+0.2	+0.6	+0.4	
LVV	+0.4		+0.1	+0.5		+0.15	-0.2	0.0	
KSH	+0.4	+0.5	0.0	+0.5		+0.25	-0.1	+0.1	
UZG			0.0			-0.2			
PUL	+0.2		0.0	0.0		0 0	-0.2	-0.2	-0.1
MOS	+0.2	+0.1	+0.1	0.0		+0.2	-0.2	-0.1	-0.1
OBN	+0.5	+0.2	+0.1	0.0	+0.7	+0.2	-0.2	0.0	
EKA	0.0	+0.2	+0.2	-0.1		0.0			-0.2
TBL			+0.2	+0.1		-0.4	+0.2	+0.1	
BKR	-0.2		+0.2	+0.1	0.0	-0.1	+0.1	+0.2	+0.6
GRS	+0.2			+0.1		-0.2	+0.2	+0.1	+0.7
TAS	-0.2	-0.3	-0.1	-0.1			+0.2		+0.1

#### 6.4. Small-Scale Variations of the MLH Residuals at the Epicentral Distances of 100 - 500 km

If the dMLH are studied in greater detail depending on the epicenter position, more local effects become visible. The examples are given on the map where the values of magnitude residuals dMLH are plotted at the epicenters. The data are taken from stations Garm (Figure 31) and Talgar (Figure 32).

In the Garm region we see great negative residuals for the nearby epicenters. Probably it is the result of crossing such different geological structures as mountain ranges, depressions and so on with the width about few tens or hundreds of kilometers.

#### 6.5. The MLH residuals connected with crossing Tibet

For the TLG station we find another regularity. On the map (Figure 33) the Talgar residuals averaged for several earthquakes are plotted inside their epicenter areas. We see an area of epicenters which have large negative residuals in TLG. The location of this area shows that it is the northern boundary of Tibet and destroys the surface waves crossing it.

This effect is extremely strong for the Lg waves [Molnar, Khalturin, 1977]. It is significant also for the surface (Rg) waves.

The data show that there are important inhomogeneities in the crust having an effect on the structure and amplitudes of the Rg wave. Thus, trying to achieve high accuracy one should take into account situations like that described above. It is important to use not only general corrections, but especially to correct the influence of each particular inhomogeneity.

The MLH residuals can be found even using a single station if the surface waves cross such a solid structure as Tibet. The map (Figure 32) shows the dMLH of the TLG stations. The average residual was calculated using the data of several nearby epicenters plotted on a small area of epicenters. The dMLH amplitudes abruptly decrease when crossing the northern border of Tibet [Molnar, Khalturin, 1977; Antonova, Khalturin et al., 1978]. It is not just the decreasing of amplitudes but a damaging to the group of maximum amplitudes (Figure 33). The maximum passes to a lower group velocity. It becomes 2.8-2.6 km/sec except the velocity is 3.0 km/sec when it passes left or right from Tibet.

We are not surprised at this result. Tibet extremely differs from the surrounding area. But the inhomogeneities, even of a smaller amount but strong enough, can be detected as changing amplitudes that damage the group of maximum amplitudes. An example is the Turfan depression which is as small as 50 - 100 km and where the same may happen when the

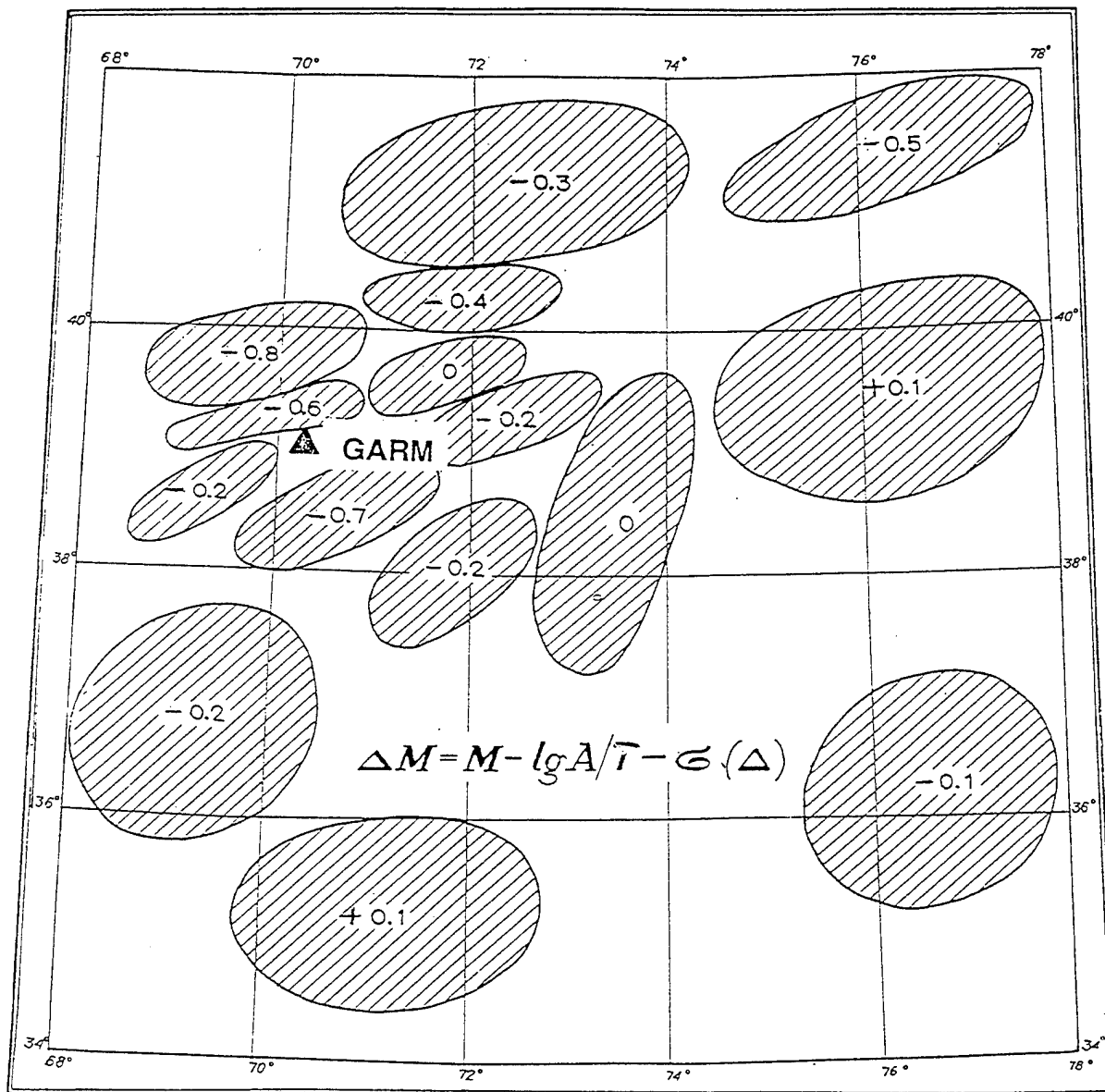


Figure 31. The small - scale dMLH residuals at Garm SKD station depending on the epicenter position.

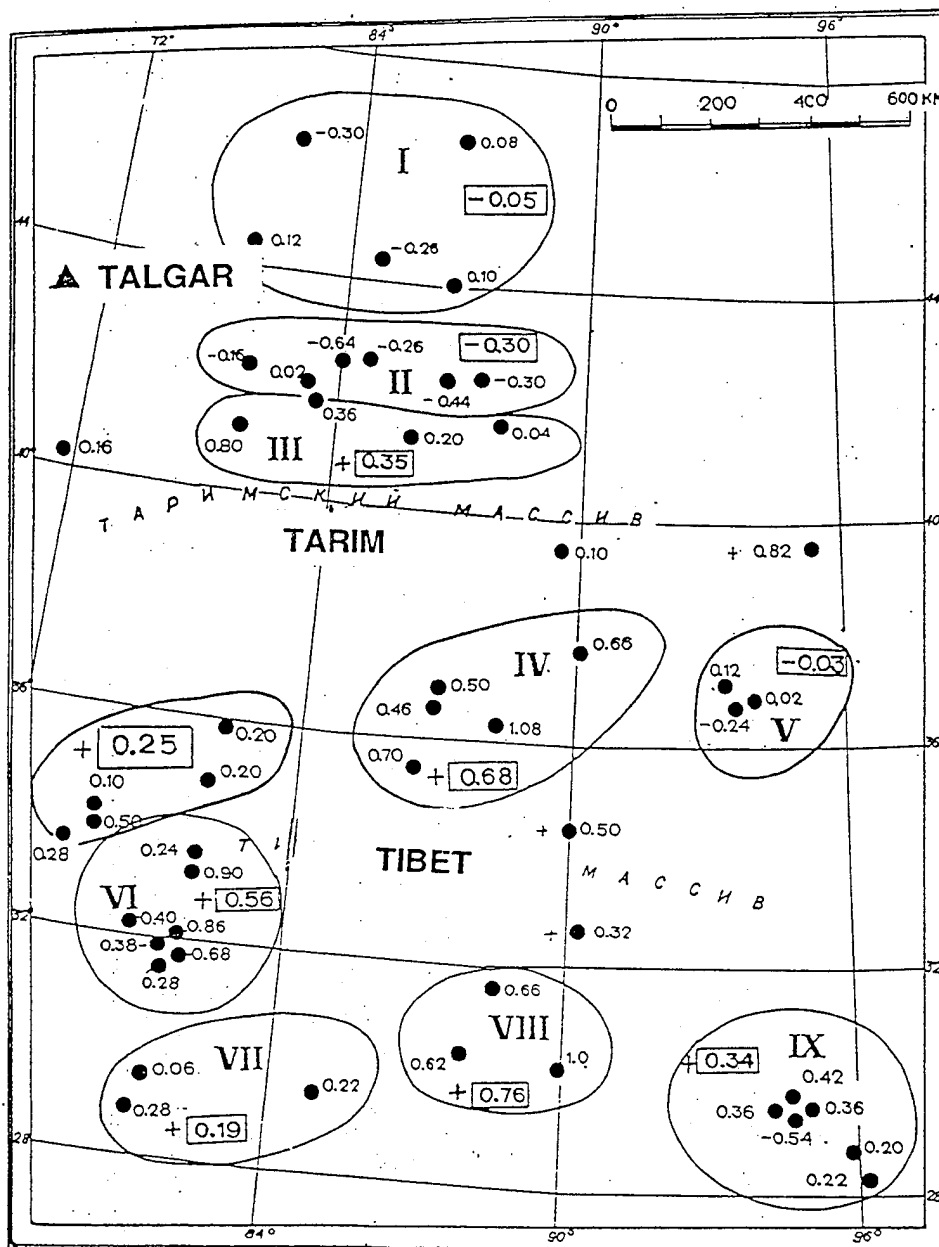


Figure 32. The small-scale dMLH residuals at Talgar SKD station depending on the epicenter position.

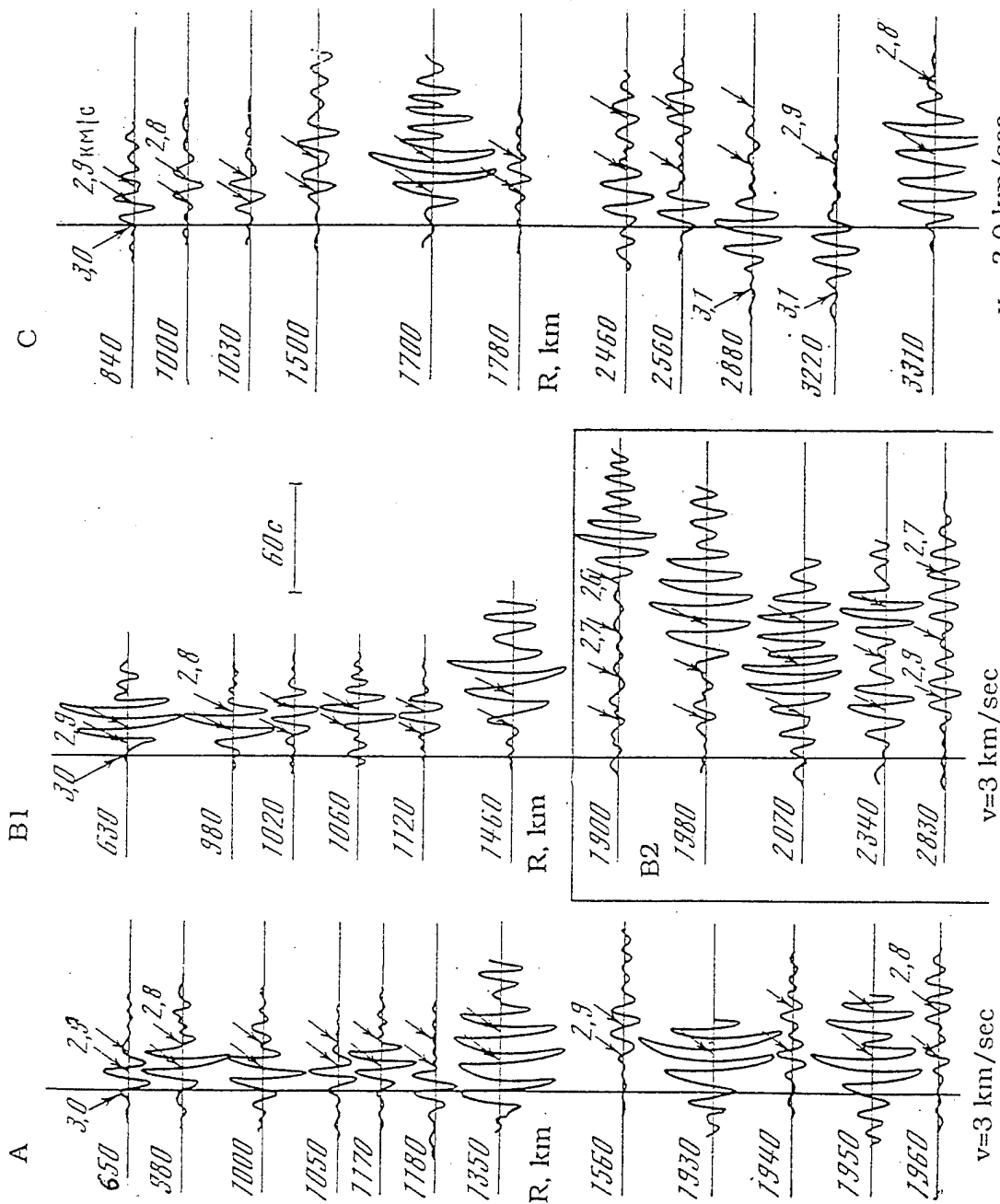


Figure 33. Example of damage of the surface wave train crossing the northern border of Tibet. The vertical line corresponds to the group velocity 3.0 km/sec. Records of Semipalatinsk ChISS station,  $f_c = 0.07 \text{ Hz}$ . A - traces, going westerly of Tibet; C - traces easterly of Tibet; B1 - traces, on the direction to Tibet, from epicenters localized northerly the Tibet border; B2 - epicenters localized inside Tibet, or southerly.

ray trace crosses exactly this small target.

## 7. THE USE OF SEISMIC CODA TO DETERMINE THE STATION CORRECTIONS FROM REGIONAL AND LOCAL OBSERVATIONS

Determination of station corrections and seismic event magnitudes from direct waves needs the special efforts to get well averaged data. The idea to use coda appears because the mechanism itself of seismic coda excitation and propagation averages the source pattern function as well as the path effect. So when measuring coda one need not trouble about the problem of averaging these effects: he will get it as a ready result.

It is clear that the station residuals of coda level can be applied for correcting the coda magnitude  $M_c$ . But does the coda residuals depend on local conditions, or on area one as well? Are the coda corrections equal to the corrections obtained from direct waves at regional distances? Is it the same as the residuals for P wave at teleseismic events?

Before we consider the station corrections from coda, let us discussed coda in general.

### 7.1. The Properties of Coda, Important When Using it for Determining the Station Correction

#### 7.1.1. The Basic Definition

Let us discuss definitions, important from this point of view. The word "seismic coda" is used in different senses. Someone calls "coda" the oscillation, which begins soon after the direct wave (P, S or Lg and Rg). These oscillations originated from scatterers localized close to the ray trace of direct wave so that coda consists of scattered wave, radiated from source at or near the same direction and propagated along near the same path as direct wave. It means that this coda depends on source radiation pattern in almost the same degree as direct waves. Moreover, this early coda influences by inhomogeneities, which localize close to the ray trace of direct waves. So the intensities of this coda depend on path effect too.

The coda, which is seen much later (2-3 times and more), then dominating direct wave, is of a different nature. The late seismic coda is waves, scattering and propagating in different directions from a source. As a result, the radiation pattern function becomes smooth by the mechanism of coda generation.

Let us look at coda by space domain. The energy of

seismic oscillation flow down from direct wave, fulfilling the volume of media inside the surface of wave front. Both epicenter and station are in a small central part of this volume. The size of that part is much (two or more times) bigger than epicentral distance, but several times smaller than radius of wave front. Scattered waves with the same travel times penetrate the volume of media everywhere and in all directions, smoothing the path differences. Inside the central part of volume smoothing is most perfect.

When the wave front spreads, the volume increases, and the energy density of scattered radiation falls, fulfilling larger volume and attenuating as well. In time domain the coda amplitudes decrease with lapse time. This decreasing use is described by the shape of coda envelope.

#### 7.1.2. Coda Envelope as a Calibration Curve for Coda Magnitude Scale

The calibration curve of coda-magnitude is the standard envelope of late coda. The "late" coda means the lapse time much more (no less than 2-3 times) than the time arrival dominating direct wave (Lg or Rg). In Figure 34, the envelopes of teleseismic events recorded at station Rio Carpintero, Cuba, by SKD instrumentation are shown. One can see that amplitudes of late coda fit well to standard curves, whereas the early coda amplitudes are much more than expected amplitudes of coda.

The curve  $A(t)$  is an approximating envelope of standard shape. For SKM-coda the level of this envelope (called  $A_{100}$ ), at a standard time 100 sec, was taken as a measure of coda intensity at the station record for certain event. For SKD-coda the measure of coda level was taken at  $A_{1000}$ .

The regions that differ in their geological structure and tectonics from each other, have a peculiar shape of coda envelope. The cold platforms differ from orogenic zones, these both differ from rifts zones with low  $Q$  in the crust and upper mantle. The shape of coda envelope  $A(t)$  is practically the same in a wide region around the station.

Figure 35 shows the regional coda envelopes compared with the one of Central Asia (dotted line). We see that the curves for some similar regions differ not so seriously, only in details, which can be neglected in practical use. In other cases the difference is significant. Compare, for example, the shape of coda envelope at Caucasus and one at Central Asia. Thus, the standard envelopes, if used for coda magnitude determination, must be made specific for each region. For example, platform, orogen, or rift have to be studied as separate regions.

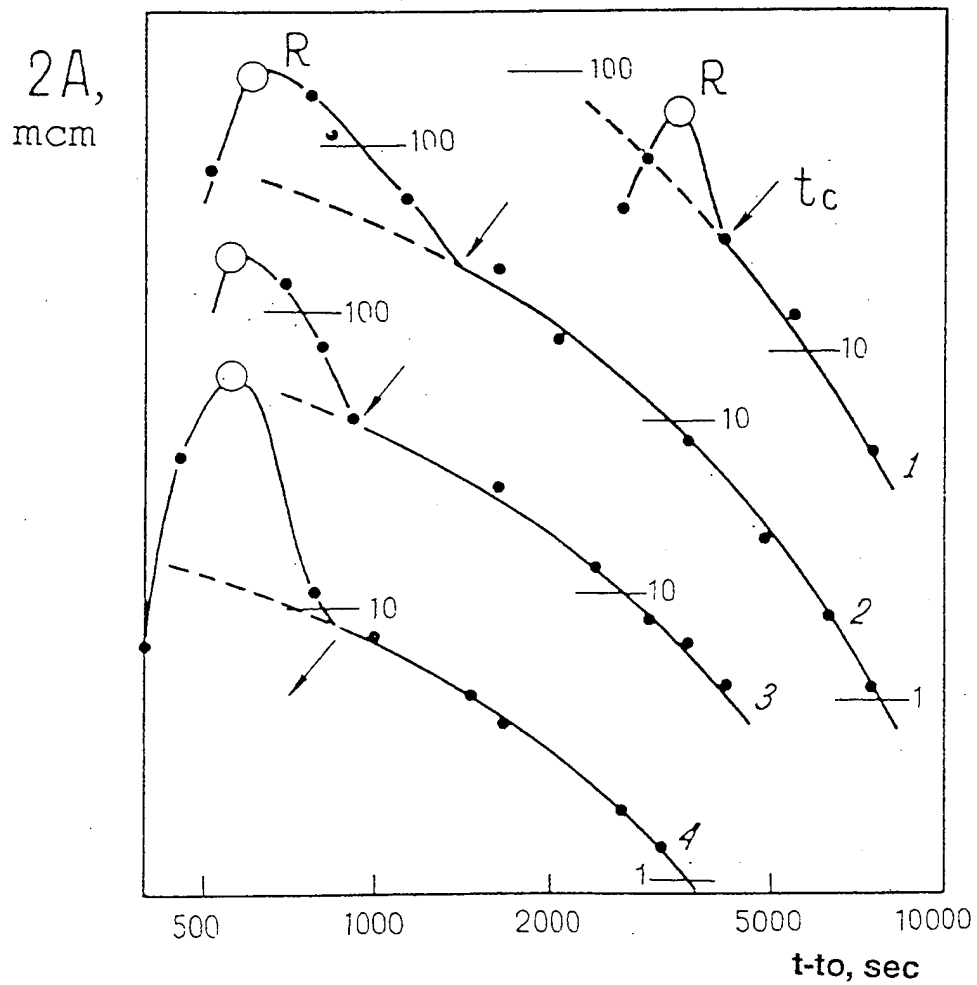


Figure 34. The examples of envelope on teleseismic events recorded by SKD station Rio Carpintero, Cuba.



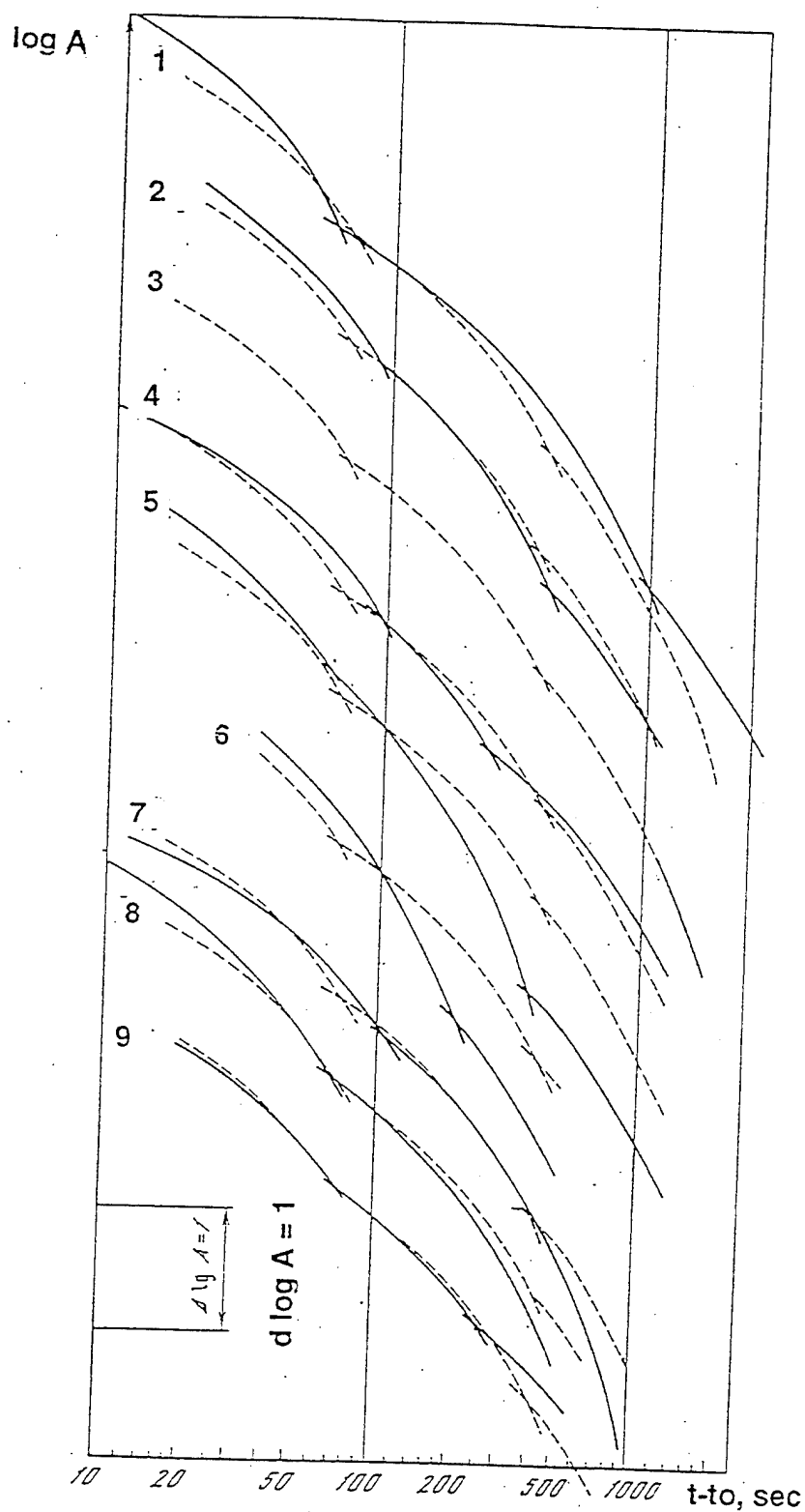


Figure 35. The regional SKM-coda envelopes : 1 - Altai and Sayans; 2 - Fergana Valley and Peter the Great Range; 3 - Southern and Central Tien Shan; 4 - Crimea; 5 - Caucasus; 6 - Kuril; 7 - Kamchatka; 8 - Cuba; 9 - Baykal. All curves are compared with Tien-Shan one (dotted line). Note that the curves for two regions (5 and 6) decrease much more than for others, exposing the low-Q zone beneath these regions.

## 7.2. The Method of the Determination the Station Magnitude Residual from Coda

The practical procedure for estimating the station residuals from coda is simple. We chose the records of the same earthquake at stations of network. The envelope of coda will be measured in several (about 10) moments of time. These points are approximated by curve with a standard shape.

Figure 36 shows an example of coda from the same earthquake at three stations: Talgar, Kaskelen and temporal station at the small distances between them. One can see how the difference of coda envelopes level looks like. Such station difference is very stable and practically not dependent on position of earthquake epicenter and on distance. We consider this difference as a measure of local site effect. In these examples the Talgar was taken as a basic station.

The level of coda can be estimated with accuracy about 0.1 log. unit even from one station record. It means that station correction can be obtained with accuracy about 0.05 from only several events records.

## 7.3. The Values of the Station Residuals Obtained from Coda

It is known that the local effect is some function of frequency. It means that if considering the site effect as a magnitude residual, it varies depending on spectral content of input seismic signal. If one needs to obtain correction, not only for magnitude but for spectral content, the correction must be studied for different frequencies separately. As a result, one obtains the spectral station correction  $C(f)$ . Obtaining the corrections separately for different types of instruments, as SKM and SKD, can be important, especially in the goal of discriminating the UNES from earthquakes using spectral criteria.

Here, the examples of station corrections determined will be shown beginning from the local case.

### 7.3.1. Station Residuals for Stations of Garm Network Determined by Coda Method

Look at residuals obtained for stations of Garm network. The size of area, where stations were installed is about 100x150 km. So the station corrections of Garm network shows the local effect only. Two kinds of instrumentations were used: SKD and SKM. At regular stations the seismometers were installed in tunnels with the instrumentation at the hard rocks, like granite, or on the mesa-cinozoic sediments, like limestone. RTS (Radio Telemetric Stations), operated at the tops of Peter the Great Ridge with the soft sediments on the surface. All residuals are referenced to the mean amplitudes

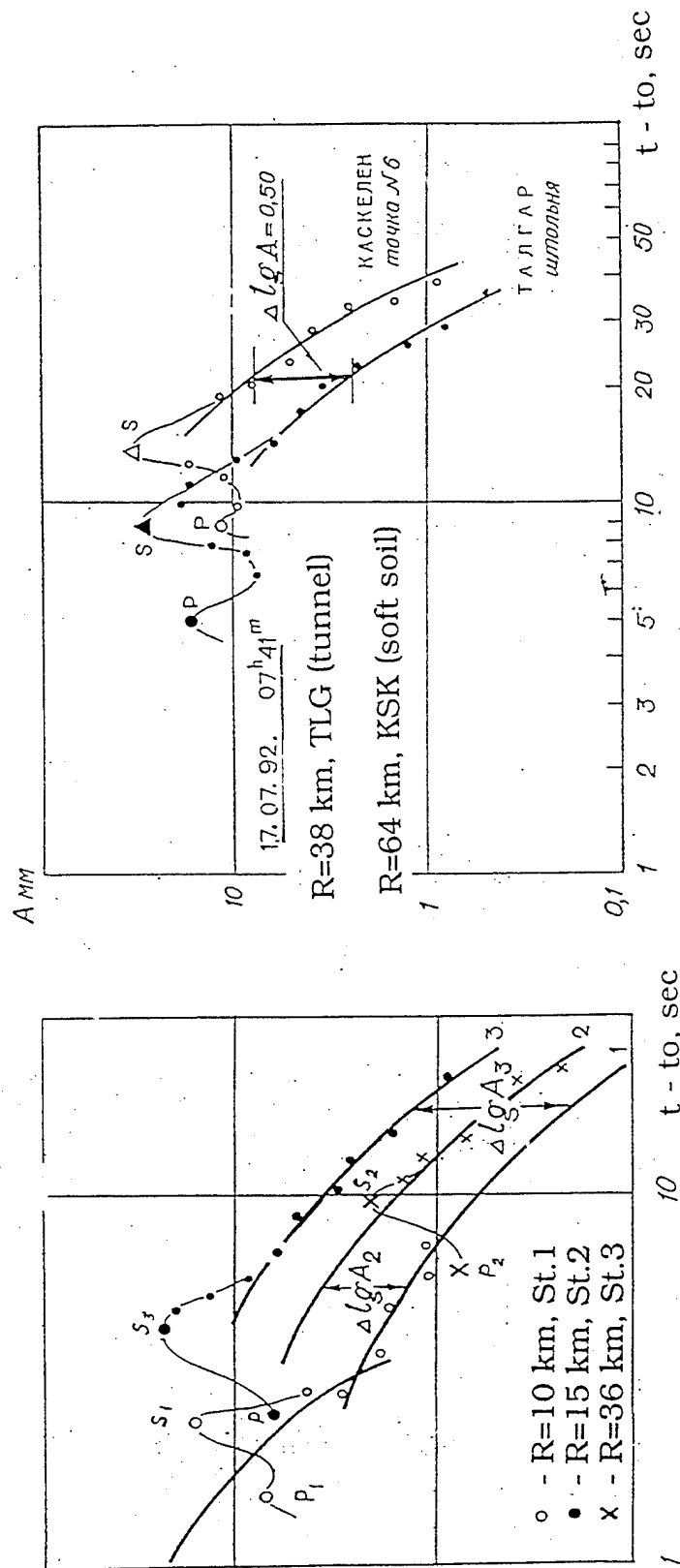


Figure 36. Examples of envelopes of the local earthquakes at stations with different site conditions. The lower curves correspond to station in the tunnel in hard rock, upper curves correspond to stations installed on the soft soil.

(see Table 26).

Table 26. The Log-Amplitude Residuals  $d\log A_c$  of Seismic Coda and their Standard Deviations  $s$  for Stations of Garm Network for Different Types of Instruments

Stat.	SKM		RTS		SKD	
	$d\log A_c$	$s$	$d\log A_c$	$s$	$d\log A_c$	$s$
The stations on hard rock						
GAR	-0.08	0.08			0.00	
YAL	-0.18	0.05				
JFR	-0.03	0.07				
CHS	-0.23	0.08			-0.06	0.15
TRT	-0.11	0.07				
SNG	-0.15	0.05				
Aver.	-0.13	0.07				
The station on hard sediments						
ISH	0.07	0.06				
KFG	0.11	0.13				
CHD	0.14	0.08			0.05	0.14
KHT	0.07	0.08				
Aver.	0.10	0.09				
The stations on soft sediments						
TDR	0.26	0.10				
LNG	0.26	0.07				
SFT			0.21	0.10		
BAL			0.26	0.09		
SKK			0.28	0.07		
KAU			0.38	0.09		
BAT			0.40	0.07		
MIO			0.43	0.0		
Aver.	0.26	0.09	0.35	0.08		

The significant increasing of amplitudes is mostly at RTS stations, installed at soft sediments. Small positive residuals are at stations, which are at the center of Peter the Great Ridge. The stations localized in South Tien Shan part of the Garm area with the instruments at the granite, like Chusal, Khait, Turatol, Sangikar, have smaller amplitudes of coda (negative residuals). For few stations, where long-period SKD instruments worked, we use Garm as a basic station. It was found, that all SKD stations are practically identical - the residuals are as small as 0.05.

### 7.3.2. Station Residuals of Three Local Networks of Short-Period Instruments SKM

Coda method for determination of the station residuals for local networks was also used at Altai, Uzbekistan and Crimea regions. These determinations were made in each network independently. In the Altai region, the residuals were calculated referencing the data to stations Tehely (TEL) and in Uzbekistan, to Nurata (NUR). The same method was applied to the three Crimea stations, the data were referenced to the average level of coda (Table 27).

In the Altai region, the standard deviation for each individual estimation was 0.07 - 0.12, so even 10 earthquakes are enough to get the small error of corrections: about 0.05 log.units. Only one station, (Ersin), has correction that exceeds the error. All stations in this rocky country are at or near the same good site conditions. At Crimea, the local site conditions vary more. Taking into account that the seismicity in Crimea is low and many earthquakes recorded by only 2-3 stations, the magnitude corrections are very important.

Table 27. The Station Magnitude Corrections dMc for Altai, Uzbekistan and Crimea Local Networks of SKM instruments Obtained from Seismic Coda

Altai		Uzbekistan		Crimea	
Stat.	dMc	Stat.	dMc	Stat.	dMc
TEL	0.00	NUR	0.00	ALS	0.00
ULG	-0.05	DGZ	0.08	YAL	0.30
ERS	0.21	KKL	0.08	SIM	-0.30
ETS	0.05	10T	0.15		
SGU	0.06	TAM	0.15		
UKN	-0.07	GAR	0.08		
NOV	0.03				
VBS	-0.05				
Average	0.03		0.090		0.00
Stand. dev.	0.085		0.051		0.25

The corrections for Uzbekistan network were obtained, referencing all data to Nurata station (Table 27). Garm referenced to Nurata has the same value of correction as inside the stations of Garm network.

#### 7.4. The Station Residuals of Direct S Waves and Coda

The important question is if station residuals obtained from coda are of the same value as for S or Lg waves. They were compared for Garm network stations (Figure 37) using the coda residuals (Table 26) and direct S waves residuals. About 100 local shallow earthquakes and deep ones from Hindu Kush zone were used with their amplitudes of S waves available at

# GARM NETWORK

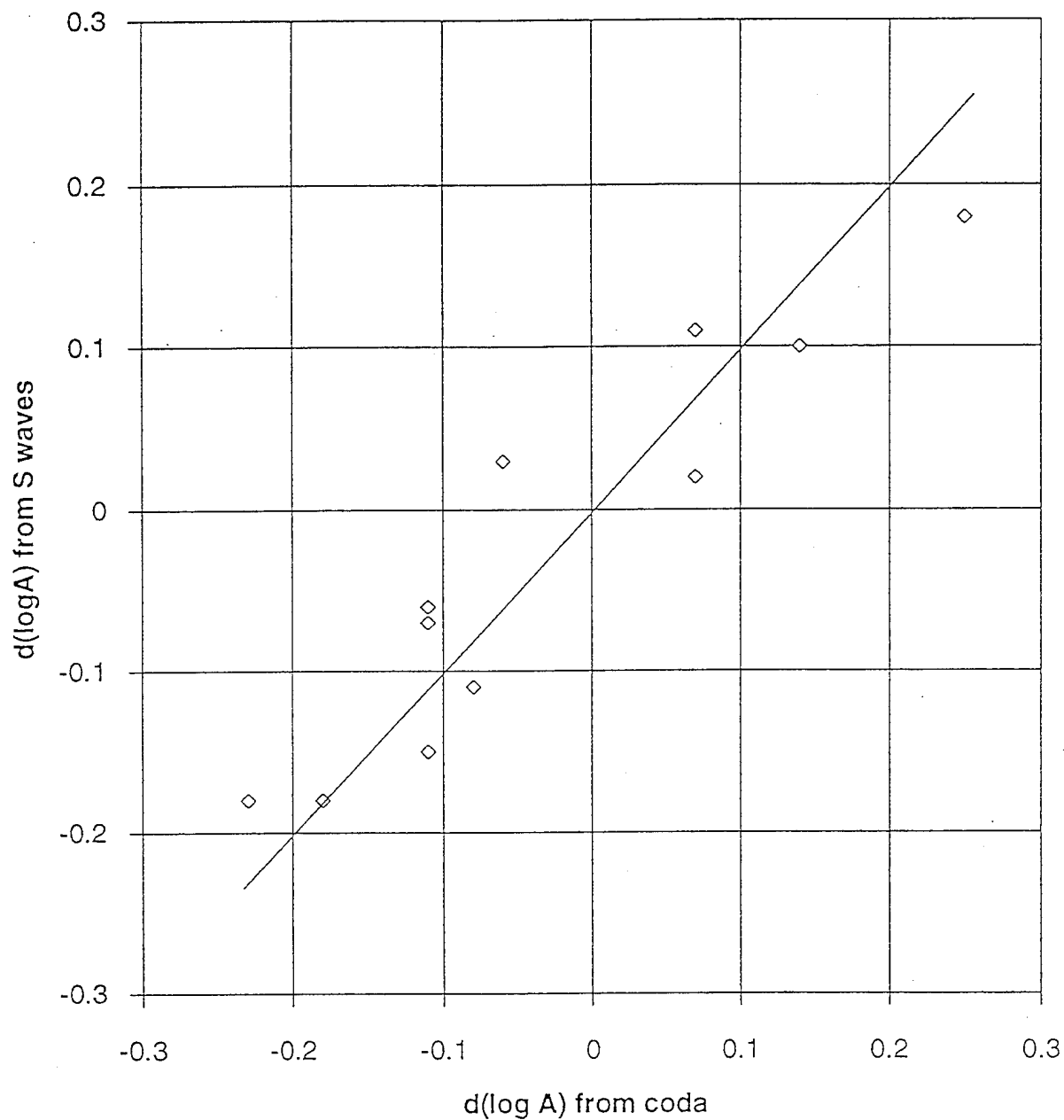


Figure 37. Comparison the station corrections for Garm network obtained from S wave and from coda SKM records of local and Hindu Kush earthquakes.

all stations. The station residuals  $d\log A$  were calculated from the deviation of  $\log$  amplitudes, normalized to standard distances. A good agreement between them was found (Table 28).

Table 28. The Comparing the Station Residuals  $d\log A$  and Their Standard Deviation  $s$  for Direct S Wave and Seismic Coda at Garm Network SKM-Stations

Stat.	Coda		Direct S Wave		Coda - S
	$d\log A$	$s$	$d\log A$	$s$	$d\log A$
TDR	0.26	0.10	0.18	0.20	0.08
ISH	0.07	0.05	0.11	0.20	-0.04
GAR	-0.08	0.08	-0.11	0.13	0.03
YAL	-0.18	0.05	-0.18	0.13	0.00
JFR	-0.06	0.07	0.01	0.14	-0.07
CHS	-0.23	0.07	-0.18	0.16	-0.05
TRT	-0.11	0.07	-0.06	0.14	-0.05
SNG	-0.11	0.04	-0.07	0.21	-0.04
KFG	-0.11	0.13	-0.15	0.18	0.04
CHD	0.14	0.08	0.10	0.19	0.04
KHT	0.07	0.08	0.02	0.21	0.05
LNG	0.25	0.07	0.18	0.22	0.07
Aver.	-0.008	0.074	-0.011	0.176	0.005
St. dev.	0.156		0.117		0.066

In the last column, the systematical difference between two sets of residual is shown; it is small. It seems that coda is a little more sensible to local condition than S waves; it is understandable. When using S or Lg waves, only one cycle of oscillation is measured. Coda feeds energy from all durations long of wave. The increasing of both amplitude and duration of direct wave results in coda to larger amplitudes.

Note, that individual variations for coda are 2.5 times smaller then for S waves. Thus, if using 15-20 earthquakes, one can expect to obtain from coda an error of local component of station correction as small as 0.02. We feel skeptical about the possibility of so high an accuracy in general. When approaching a small error, other factors unnoticeable before, begin to play some role. They cannot be random, but systematical in uncertain situations. Nature always has some jokes prepared to make people not believe too much in their power. We think that real lower level of error is about 0.05 and no less. Great efforts are necessary to obtain it.

#### 7.5. The Common System of Station Corrections for Whole Soviet Central Asia

#### 7.5.1. Data and Method Used for Estimation the Station Magnitude Correction

The use of coda allows us to obtain the corrections for many regional networks from East Kazakhstan to Caucasus. To obtain the common system of station corrections, we measured coda of the same earthquakes records from as many stations as possible. The events with magnitude were about 5.5-6.5, their intensity of coda were big enough to be measured practically for whole Central Asia. Their epicenters were in Central Asia, North Tien Shan, Kopet-Dag and at nearby areas of China, Afghanistan and Iran. For Caucasian stations, we took earthquakes from Southern Caucasus, Northern parts of Iran and Turkey.

The coda amplitude residuals were found for 42 seismic stations of Central Asia and 14 Caucasian stations. Most of those stations have only SKM instruments, but for a portion of them we can get corrections for both SKM and SKD instruments or SKD only. For most stations we used about 15 earthquakes; for stations of Tadjikistan, the number of events reach 45. Epicenter distances vary from 20 to 1500 km, depths from 3 to 250 km (Pamir-Hindu Kush under-crust earthquakes). The magnitude range was from 4.9 to 7.0.

There is an important problem - how to choose the basic magnitude. Some uncertainty appears when you take as a basic magnitude the average values. For example, in Kyrgyzstan almost all stations are in tunnels at hard rock; it is natural for this mountain country. In Turkmenia, only two stations, VAN and KRA are installed at hard rocks, whereas all others are at soft sediments of different thicknesses, from ten meters to kilometers. Thus, the mean magnitude, calculated by networks of each country turn out to be systematically different because of this methodical disagreement.

We prefer to use as a basic station one or a few stations with a "good" site condition, where instrumentations are installed on hard rocks in a tunnel. We compared seismic coda at distant stations with similar local conditions at records of common earthquakes. It was found that the coda level is practically the same for several of stations. For example, Garm (Tadjikistan) and Vitosha (Bulgaria), 3500 km between, both at good local conditions, have the same level of SKD-coda of the teleseismic events (Figure 38). The same is for Garm and Vannovskaya stations, 1200 km between, not only for SKM and SKD-coda, but for ChISS-coda as well. In Figure 39, the coda envelopes from two earthquakes are shown. One event is at Hindu Kush (close to Garm), another is from Kopet-Dag (close to Vannovskaya).

Thus, when determining residuals, we can use few stations localized in different regions as a basis in their areas, if they are installed at the crystalline rocks. For example,



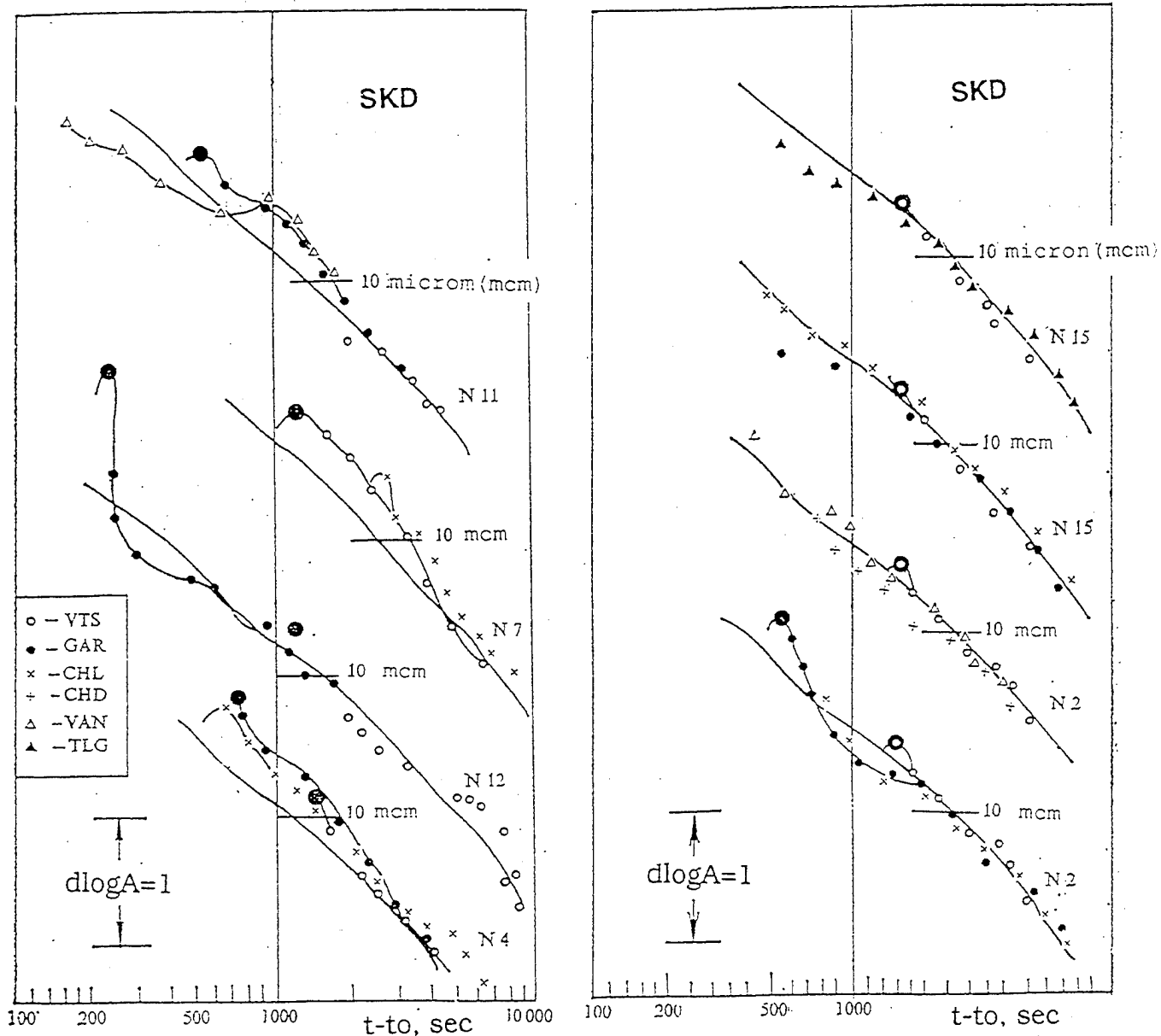


Figure 38. Envelopes of SKD-coda at VTS (Bulgaria) and Central Asian VAN, GRM, CHL, CHD and TLG stations. The earthquakes used are : #11-North Africa; #7-West Iran; #12-Hindu Kush,  $h=200$  km; #4-South Iran; #15-Gazli; #2-South Tien Shan. Note, that the late coda is close to the standard envelope (bold line), whereas the coda close to max  $R_g$  wave varies in shape. The distances from VTS to VAN - 2700 km, to GAR, CHL, CHD-3600 km, to TLG-4300 km.

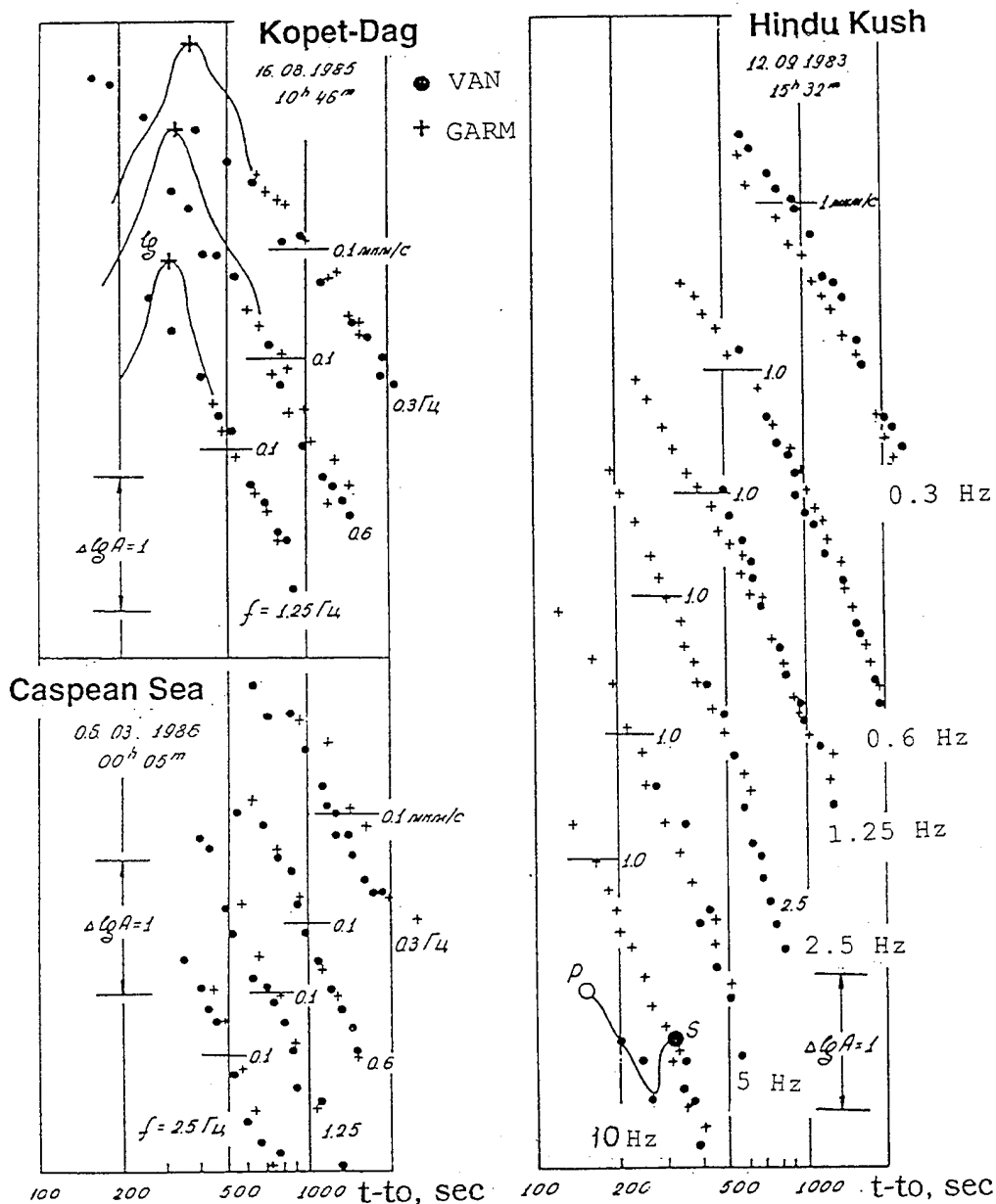


Figure 39. ChISS coda level at Garm and VAN stations, 1100 km between. Three events are taken : A - in Kopet-Dag, close to VAN; B - in the Caspian Sea; C-in Hindu Kush, close to Garm. Horizontal line indicate the absolute amplitude level (in micron/sec) for both stations data. Note that the level of coda on both stations is near the same at all frieqencies from 0.3 till 10 hz.

in Tadjikistan we use the Garm, Chusal and Gezan station; in Uzbekistan the Nurata was used; in Turkmenia - Vannovskaya. This way makes the absolute values of station residuals connected with geological and geophysical situations than with uncertain conditions at average station.

#### 7.5.2. Magnitude Station Residuals for Station Installed on Hard Rocks and on Sediments

The station residuals differ spectacularly for two groups of stations: installed on hard rocks and on soft sediments as is shown in Table 29 (Appendix 3).

The difference between hard rock stations and sediment stations in general is about 0.35. It is clear from Table 30, where the data from Table 29 are generalized. Here, the mean values of station corrections are shown for each region.

Table 30: The Mean Value of Residuals for Stations at Hard Rocks and at Sediments Depending on Region and Instrument

Region of Obs.	Number of St.	The Station Residuals				Difference	
		Sediments		Hard Rocks		Sed.-Hard R.	
		SKM	SKD	SKM	SKD	SKM	SKD
N. Tien Shan	14	0.48	-0.09	0.13	-0.17	0.36	0.08
S. Tien Shan	11	0.61	0.14	0.24	0.22	0.37	-0.08
Kopet-Dag	8	0.33	0.33	0.03	0.13	0.30	0.20
Average		0.47	0.12	0.03	0.06	0.34	0.07

The average difference in SKM-coda level for hard rock and sediments is remarkably constant in different regions.

#### 7.5.3. The Coda Level for Vertical and Horizontal Components

The amplitude ratio of horizontal H and vertical V components of coda is shown in Table 31. On average, the amplitudes for horizontal component of coda are 20-25 % (0.08 log.un.) bigger than for vertical component. For stations at hard rocks this value was a little less (0.07) than for stations at the sediments (0.09). For some stations that value was strongly different: Leninakan 0.45, Taldy-Kurgan 0.30, Samarkand 0.30, Tashkent 0.25. It is typical for cases when there is a very thick layer of soft sediments under the station.

Table 31: The Log-Difference (DlgA) of H and V Components of Coda Amplitudes at SKD and SKM Instruments Records, and Standard Deviations s of Individual Earthquake Data

St.	SKM		SKD		St.	SKM		SKD	
	DlgA	s	DlgA	s		DlgA	s	DlgA	s
KAZAKHSTAN									
ATA	0.00	0.05	0.15	0.13	TUR	0.05	0.08	0.05	0.08
TLG	0.00	0.09	0.15	0.10	KUR	0.05	0.07	0.00	0.07
KAS	0.05	0.07	0.10	0.09	TDK	0.30	0.11	0.05	0.09
=====									
KYRGYZIA									
FRU	0.00	0.06	0.15	0.11	SFK	0.00	0.06	0.00	0.06
OSH	0.05	0.04	0.05	0.10	ERK	0.10	0.07	0.00	0.08
KDZ	0.05	0.13	0.15	0.12	CHW	0.00	0.09		
BAT	0.05	0.08	0.05	0.07					
=====									
TADJIKISTAN									
DUS	0.00	0.08	0.00	0.08	CHG	0.15	0.07		
GIS	0.15	0.08	0.15	0.11	GEZ	0.15	0.07		
HOR	0.00	0.07	0.05	0.14	DZR	0.05	0.07		
MRG	0.00	0.04	0.20	0.15	SRT	0.00	0.07		
GAR	0.10	0.10	0.05	0.12	HRT	0.15	0.08		
=====									
UZBEKISTAN									
TAS	0.10	0.08	0.25	0.07	NUR	0.00	0.04		
FRG	0.00	0.07	0.05	0.12	ZRB	0.05	0.10		
SAM			0.30	0.08	HMS	0.00	0.03		
TST	0.05	0.08			TMB	0.05	0.05		
DGZ	0.05	0.08			NNK	0.05	0.05		
=====									
TURKMENIA									
ASH	0.15	0.08	0.10	0.09	GER	0.15	0.10		
VAN	0.10	0.10	0.05	0.07	KAU	0.10	0.11		
KRA	0.15	0.08	0.05	0.06	KRL	0.20	0.08		
NEB	0.20	0.12	0.05	0.09	GAU	0.12	0.06		
=====									
AZERBAIDJAN									
SHK	0.07	0.10	0.10	0.07	BAL	0.15	0.11	0.06	0.06
PKL	0.08	0.10	0.08	0.07	NHV	0.05	0.05	0.11	0.10
SHM	0.11	0.06	0.14	0.07	KRV	0.10	0.10	0.22	0.07
=====									
ARMENIA									
STE	0.07	0.06	0.14	0.12	LNK	0.47	0.14	0.44	0.16
YER	0.06	0.07	0.24	0.11	MTS	0.17	0.07		
KDG	0.13	0.08	0.04	0.06	IDG	0.11	0.06		

#### 7.5.4. Efficiency of Coda Method for Estimation the Station Corrections at Local Network and Seismic Arrays

The experience of using the coda residuals when determining coda magnitudes  $M_c$ , shows that station correction is very

effective for regional observations and especially for small local networks and arrays. It will be discussed in more detail in part 9. These data show that when using coda for magnitude determination, the station deviations are the main source of error. It means taking into account the station correction becoming a main condition for erasing the accuracy of magnitudes at the "regional" distances.

If station corrections have to be created for the recording of teleseismic signals, they can be different from the local corrections. We mentioned above that the teleseismic residuals for Baikal stations are negative for teleseismic signals because of low  $Q$  beneath this zone. The local Baikal signals are recorded normally. Thus, using coda for obtaining residuals one has to remember that it can show mostly local effect.

We believe that to obtain a good accuracy of magnitude, determination at regional distances (10-500 km) is possible only when using the coda-magnitude, and taking into account the station corrections.

The station corrections obtained from coda are the same as from shear waves. We saw it in the special study using data of local Garm network. We think that coda residuals, reflecting the local site conditions, are in good agreement in site effect at teleseismic observations and can be used as station corrections for teleseisms.

## **8. THE SPECTRAL ASPECT IN MAGNITUDE DETERMINATION AND CORRECTION**

The magnitude is not something absolute, existing independently, which we have to find by a most accurate method. It depends on what part of the spectrum of seismic signal is recorded and used for magnitude calculation. If this part corresponds to the maximum of source spectra or not, depends on both a source spectra and a frequency band pass of recording instrument.

In ESSN practice the MPV were obtained from both short-period SKM and long-period SKD instruments records. These two magnitude estimations differ depending on spectral content of earthquakes. There are different factors that play a significant role in spectral variation: the changing of earthquake magnitudes, a difference in tectonic situation in source volume, the attenuation in the crust and upper mantle beneath the epicentral zone.

The spectral difference is important as influencing on magnitude determination. From the other side, spectral content may be important itself; for example, as an event characteristic to discriminate earthquakes and UNES or QBs.

In this aspect, the spectral corrections are needed to correct the source spectrum. In this part of the report the problem will be considered for both of these aspects.

The residuals, found from broad-band instruments are referenced to uncertain frequency. Actually, the residuals are the functions of frequency depending on velocity cross-section beneath the station.

### 8.1. Amplitudes of P Wave and Coda on Short-Period (SKM) and Long-Period (SKD) Instruments Records and its Dependence on Magnitude

#### 8.1.1. A/T ratio of P waves on SKM and SKD Records

In practice of seismic services, people met the problem as the frequency dependence of magnitude residual. It looks as though there is a difference in seismic residuals from long- and short-period instrument records. In this part we discuss the difference of magnitudes, depending on the instrument, trying to see how it changes with magnitude, distance and conditions at ray path.

Both instruments, SKM and SKD, do record the displacement of ground oscillation; thus, measuring A/T of P wave is proportional to velocity of oscillation. Comparing the log A/T of P waves and MPV values measured on SKD and SKM instruments records at the same station show the difference between them called b :

$$b = \log(A/T)_{SKD} - \log(A/T)_{SKM}. \quad (8.1)$$

or

$$b = MPV(SKD) - MPV(SKM).$$

The b value is near zero for small and intermediate events at local distances till 200-300 km. Then b value increases slightly with distance in the interval 200 - 2000 km. Whereas in teleseismic zone it stays approximately constant and equal (0.25-0.30 magn. units) at Talgar, where natural period of SKM is equal to 1.2 sec, and 0.20-0.23 at Garm; the natural period of SKM is 2.0 sec (Figure 40). These numbers correspond to events in magnitude range MLH= 4.8-6.2.

One of the most important effects on b is connected with changing source spectra with magnitude. As a result, the tendency appears to increase b with magnitude:

$$b = b_0 + k \cdot (MLH - 5). \quad (8.2)$$

Parameters of eq. (8.2) depends on  $T_0$  of short-period SKM instrument. Figure 41 shows the relation between b and MLH for Talgar station, where  $T_0 = 1.2$  sec. In that case and for records of events at  $D > 2000$  km  $b_0 = 0.28$  and  $k = 0.16$ :

$$b = \log (A/T)_{SKD} - \log (A/T)_{SKM}$$

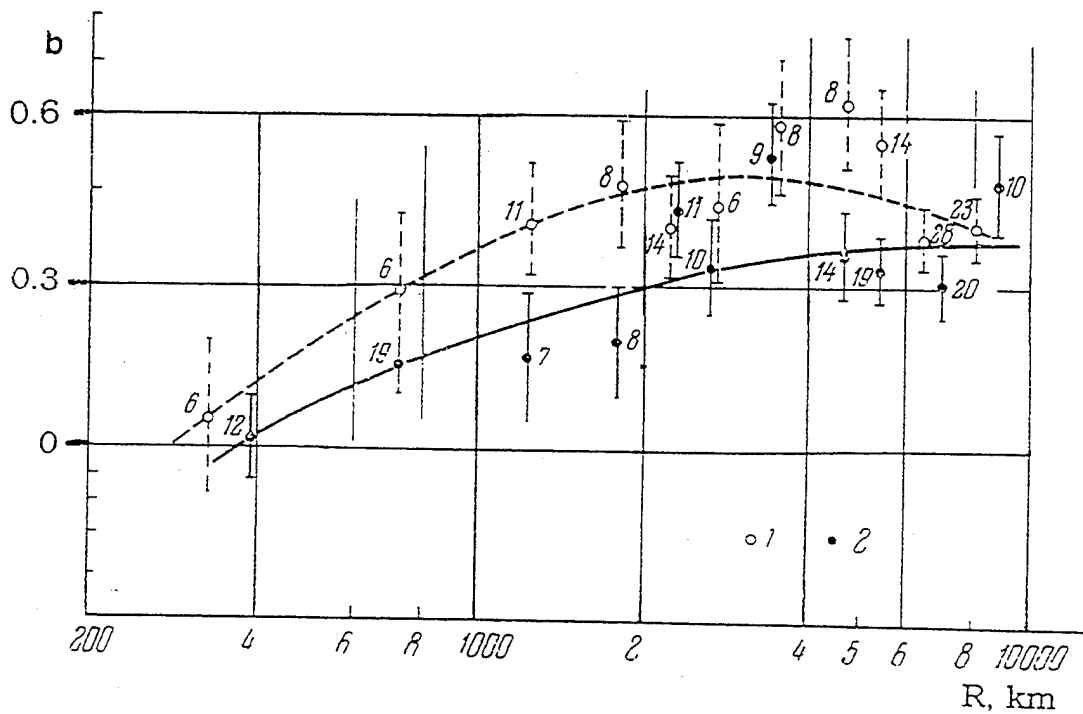


Figure 40. The dependence of  $b = (A/T)_{SKD} - (A/T)_{SKM}$  of P wave upon distance for Talgar (1) and Garm (2) SKM-stations. The period  $T_0$  of SKM instruments are 1.2 sec at Talgar and 2.0 sec at Garm. The numbers of individual measurements are shown near each point.

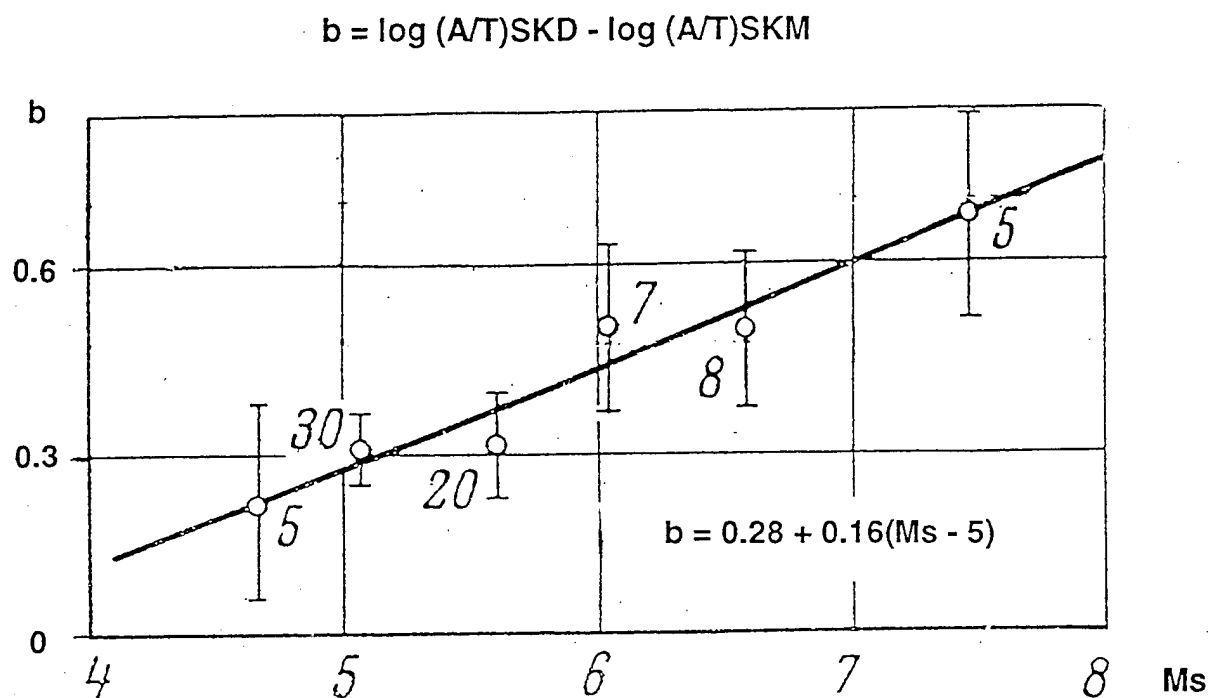


Figure 41. The dependence of  $b = (A/T)_{SKD} - (A/T)_{SKM}$  of P wave upon magnitude MLH for Talgar station.



$$b = 0.28 + 0.16(MLH - 5). \quad (8.2a)$$

Naturally,  $b$  will be more when comparing the magnitudes obtained from another pair of instruments. For example, comparing the SKD and Benioff records, with Benioff's  $T_0=0.8$  sec, less than at SKM (1.5 s), the magnitude difference should be more than in the previous case. Our comparison of the magnitude MPVA and MLH and  $m_b$  and MLH (Figure 42) shows that for the same MLH the  $m_b$  is less than MPVA, about 0.20-0.25 magn. units.

The relations, for (8.1)-(8.2) describe only the tendency, but the individual variations around these are great. As an example, look at the difference  $dm$  calculated by Korchagina and Moskwina [1974] as  $dm = m_b(\text{output}) - m_b(\text{input})$ . They used well corrected records of P wave for 7 real earthquakes at teleseismic distances (32-78 degrees) with magnitudes ranging from 6.0-7.0. They determined the magnitudes MPV before and after filtering the signals by frequency responses of SKM, SK and SKD instruments. The result is spectacular:

Instrument	$dm$	Stand. Dev.
SKD	-0.050	0.087
SK	-0.086	0.136
SKM	-0.486	0.242

The magnitudes, calculated from record of short-period SKM are not only significantly less than "real" magnitude, but vary strongly depending on spectral content of input signal. In our multifactor model these variations are considered as a part of random component. But when the spectral zoning is conducted, the spectral factor can be separated and corrected.

#### 8.1.2. The Difference Between SKM and SKD Coda Magnitudes as a Characteristic of Source Spectra

The difference between coda magnitudes  $M_c(\text{SKM})$  and  $M_c(\text{SKD})$  was taken by us as a parameter which is a measure of the difference in source spectra of earthquakes source spectra. The data from only one station (Garm) was used (Figure 43); thus, local effect did not take part in creating the variations of difference between  $M_c(\text{SKM})$  and  $M_c(\text{SKD})$ . The earthquakes on the wide region from Caspian Sea to East Kazakhstan were used. The relation between  $M_c(\text{SKM})$  and  $M_c(\text{SKD})$  was found:

$$M_c(\text{SKM}) = 0.87 \cdot M_c(\text{SKD}) + 0.70. \quad (8.3)$$

The significant scattering seems to be produced by the variations of the source spectra as well as a random variation. The standard variation of observed  $M_c(\text{SKM})$  around the expected one is 0.23. That is much more than the error of determination from the magnitude itself (about 0.1) by coda from a single station. It takes the random component about

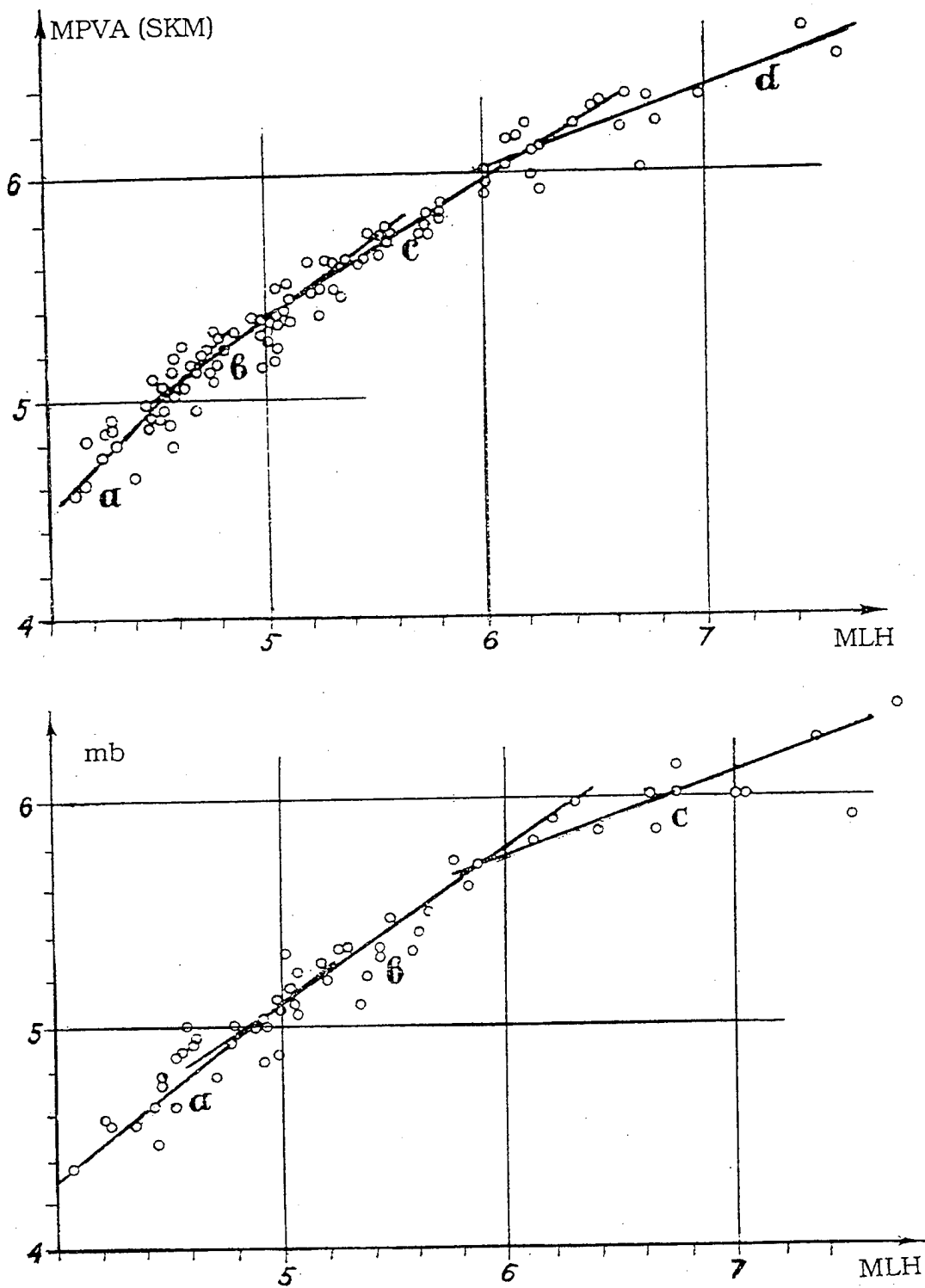


Figure 42. Comparison the MPVA (top) and mb (bottom) with surface wave magnitude MLH. Note the nonlinear character of the dependence for both cases. For the same MLH, the mb values are 0.20 - 0.25 smaller than MPVA.

CODA MAGNITUDES:  $M_{skm} = 0.87 \cdot M_{skd} + 0.70$

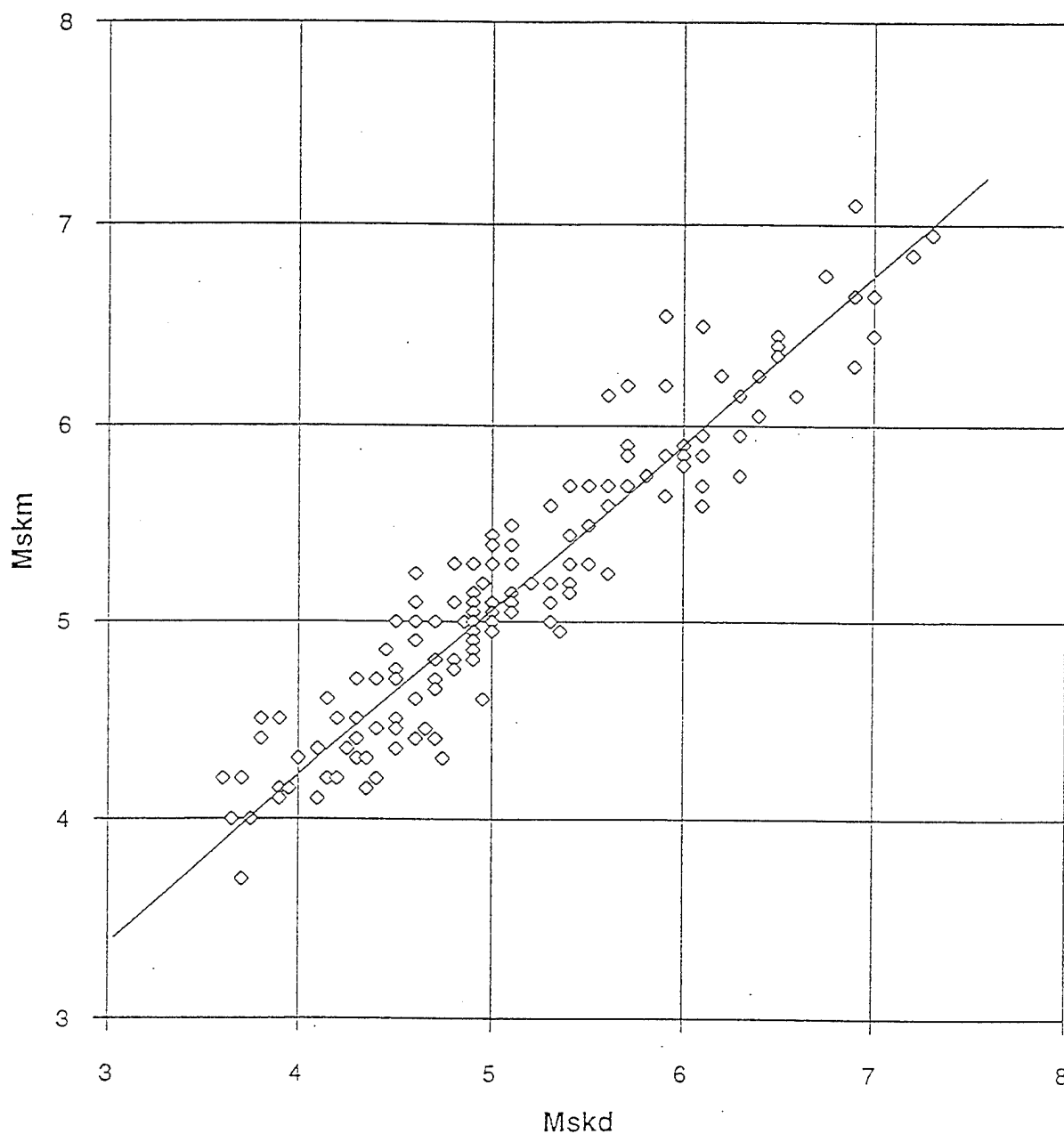


Figure 43. The correlation between the coda magnitudes  $M_c(SKD)$  and  $M_c(SKM)$  determined at single station Garm for shallow earthquakes. The relation between them is :  $M_c(SKM) = 0.91 + 0.83 M_c(SKD)$ .

0.14; an individual source spectrum variation creates the deviation component at about 0.18.

This result is important. It shows, that difference of seismic events, originating from their source spectra, can be recognized by using this two values of coda magnitudes from short- and long-period instrument records. When use the coda-magnitude, even single station data are of good confidence.

## 8.2. The Station Spectral Corrections Determination from ChISS Records of Coda Waves

### 8.2.1. CHISS Coda as an Instrument for Study a Very Local Site Effect (Local Spectral Residuals)

Even the soft sediments (thickness about tens meters) create the increasing of amplitudes of coda and direct waves as well in high frequency range (2.5-10 Hz). The thicker the sediments are, the lower the frequency, correspondent to the maximum of the site response spectral curve. That is only the general tendency. The shape of this curve depends on many details that can hardly be controlled.

The very local site effect was studied for the points of observations, as close to each other as 50-80 m, in small Chusal valley in Garm region. The ChISS instrument was used. The basic point was in the tunnel, 70 m deep, on the paleozoic crystal rocks. The instrument, worked permanently and installed in the concrete pier, 70 m deep in tunnel, was taken as a basic point. Point # 1 was installed close to the basic one, but on the ground. The point # 2 was also in the tunnel, at its mouth. Three other points (##3, 4, 5) were along the line crossing the valley. The total length of profile was 260 m. The soft sediments thickness changed from 30 m at #3 to 50 m at #4 and 60 m at #5. The slope of mountains surrounding the valley and in the basement of sediments consist of granite of Paleozoic age.

About 8-10 best records at each of the observation points were studied. The spectral amplitudes at each point were referenced to the ones at basic point for P, S and coda, for each frequency band from 0.62 to 27 Hz. The earthquakes used were mostly local ones (D=15-80 km) and deep Pamir - Hindu Kush events with hypocenter distances about 300 km.

In Figure 44, the coda envelopes of the same earthquakes are shown on two points of observation (basic point in the tunnel and point # 5 with the thickness of sediment of 60 m). The same is in Figure 45 for point of observation # 3 (30 m of sediments). In both examples, the envelopes are shown for several frequencies.

It was found that the spectral amplitudes increase with the

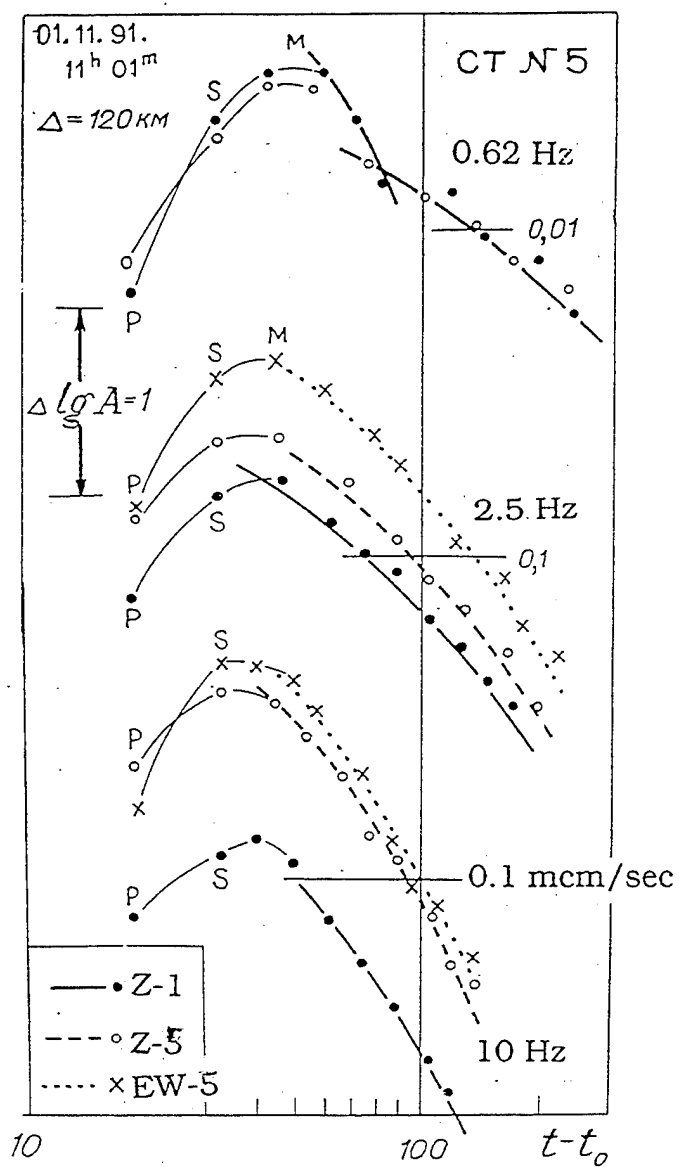


Figure 44. Comparison the level of ChISS coda envelopes of the same event at two close points of Chusal valley - at the tunnel in the granite (point #1, Z component, solid circle), and at the soft sediments 60 m thickness (point # 5, Z - open circle and EW - crosses). The frequency from top-to-bottom:  $f=0.62$ , 2.5 and 10 Hz.

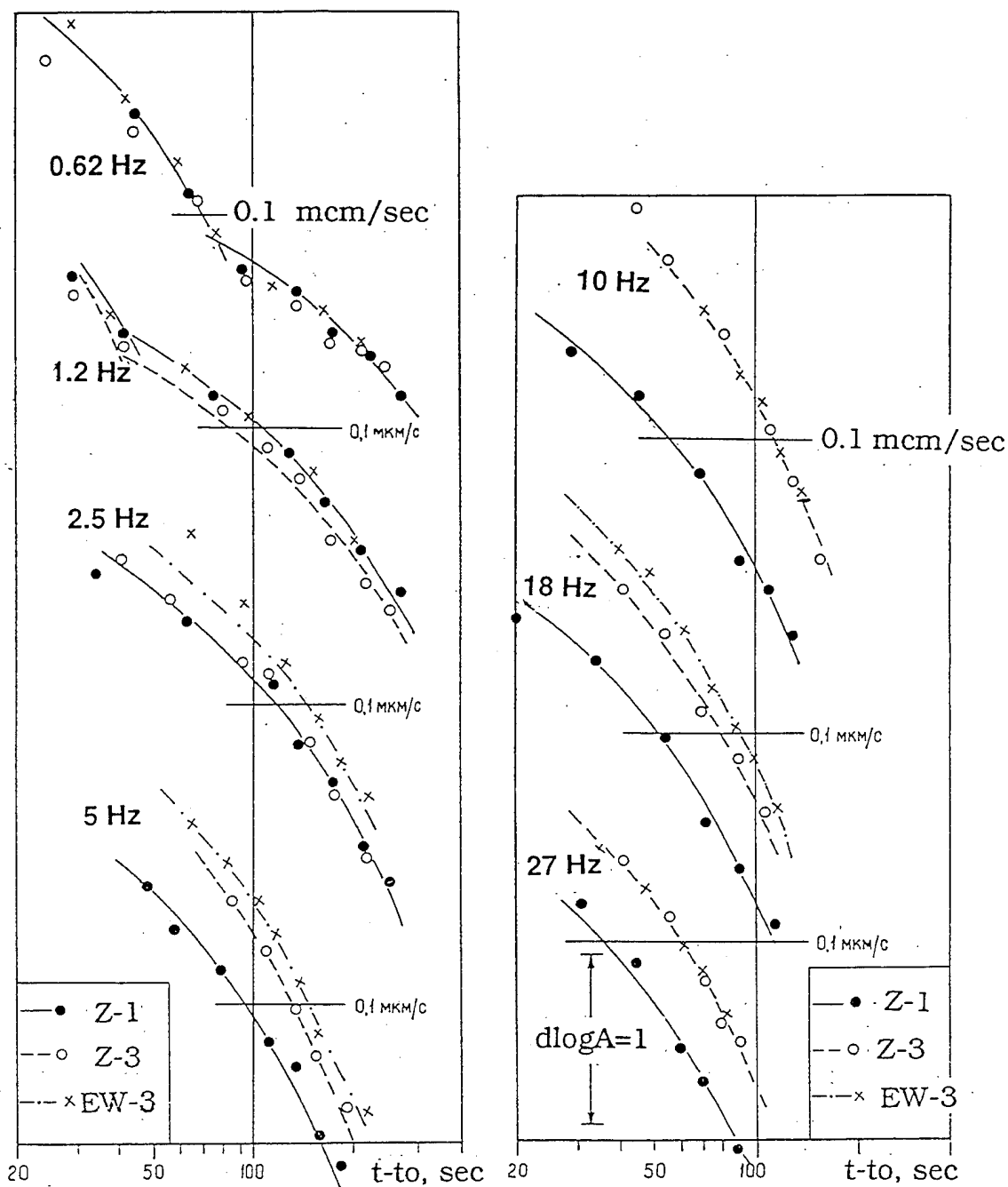


Figure 45. Comparison the level of ChISS coda envelopes of the same event at two close points of Chusal valley - at the tunnel in the granite (point #1, Z component, solid circle), and at the soft sediments 40 m thickness (point # 3, Z - open circle and EW - crosses). The frequency from top-to-bottom - at left: 0.62, 1.25, 2.5, 5 Hz and at right: 10, 18 and 27 Hz.

thickness of sediments, depending on frequency (Figure 46). When thickness is 30 m (point # 3), the amplitudes do not increase at frequencies lower than 5 Hz. After increasing the thickness the amplification appears at 5 Hz and increases at 18-40 Hz. Maximum amplification (10 times) is at 10 Hz.

The spectral ratios were determined for P, S, coda and microseismic noise, and were founded approximately similar. The coda and S wave have near the same log-difference of spectra in each couple of observation points. As for P waves, they have a similar tendency of spectral residuals, but the deviation of data is significantly larger.

Note that ratios of two points in tunnel (#2 & #1) look unexpectedly different (Figure 46). The amplitudes in the tunnel mouth are increased two times at 10 Hz in comparison with the ones at point #1, but are less for 18 Hz. It seems that the deformation of signal spectra can be influenced by the tunnel itself or by contact conditions of instrument with its basement. This result is important, showing, that the observation point, taken as a basic one to calculate the spectral corrections for several stations of group, must be checked if it is good for that goal. Some independent criteria must be taken into account. For example, the station can be taken as "good" if the spectra of signals by this station are of "normal" shape.

#### 8.2.2. Spectral Station Residuals for ChISS Stations at Central Asia and Kazakhstan Obtained by Coda Method

The ChISS network was operated in Tadjikistan, Kyrgyzstan, Turkmenistan, Kazakhstan, Caucasus and some sites in Russia. To use these data for determination of source spectra, the system of spectral station correction was necessary. The station corrections as a function of frequency for all ChISS stations were obtained. Garm station was taken as a basis. The spectral residuals were obtained for each frequency channel separately.

The error of corrections is small. Figure 47 shows the ratios of individual measurement of the coda level on two stations (Chusal/Garm) versus time series during the years 1988 (top) and 1989 (bottom) for 18 Hz. The pictures like that were built for each frequency during each year to check the stability of the ratios. For example, to catch some rough mistake, (for example, a wrong position of decimal point).

The examples of shape of spectral residuals of two stations, Chusal (top) and Chil-Dora (bottom) are shown in Figure 48. Garm was taken as a basic station. It is not so easy to explain these spectral ratios. Garm and Chusal seems to be at the same local conditions, the seismometers were installed in the tunnels, on hard rock. It is difficult to say why the the amplitude ratio at Chusal/Garm at 27 Hz is equal 2. It is

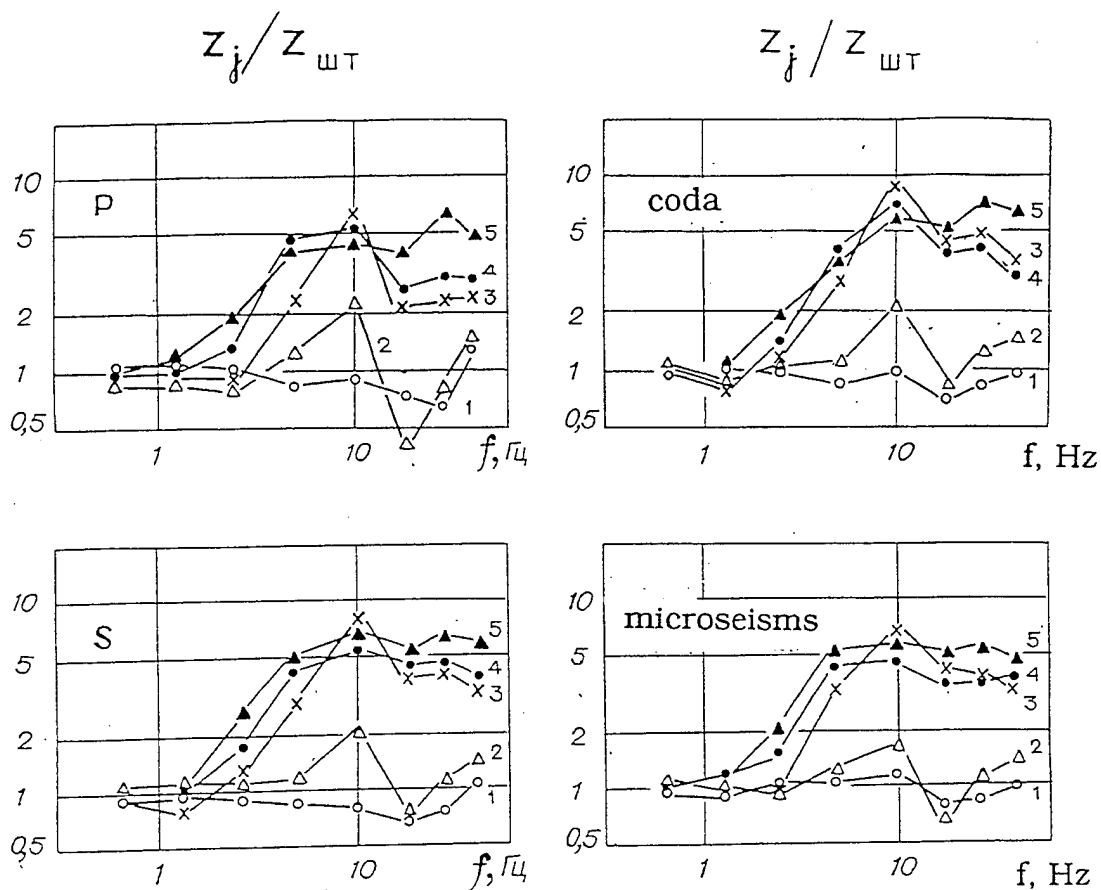


Figure 46. The amplitude spectral ratio of different types of seismic waves in several points of observation (## 1 - 5) in the Chusal valley, referenced to the basic point. The vertical components were used. Note that the spectral ratios are near the same for P, S, coda and microseismic noise.



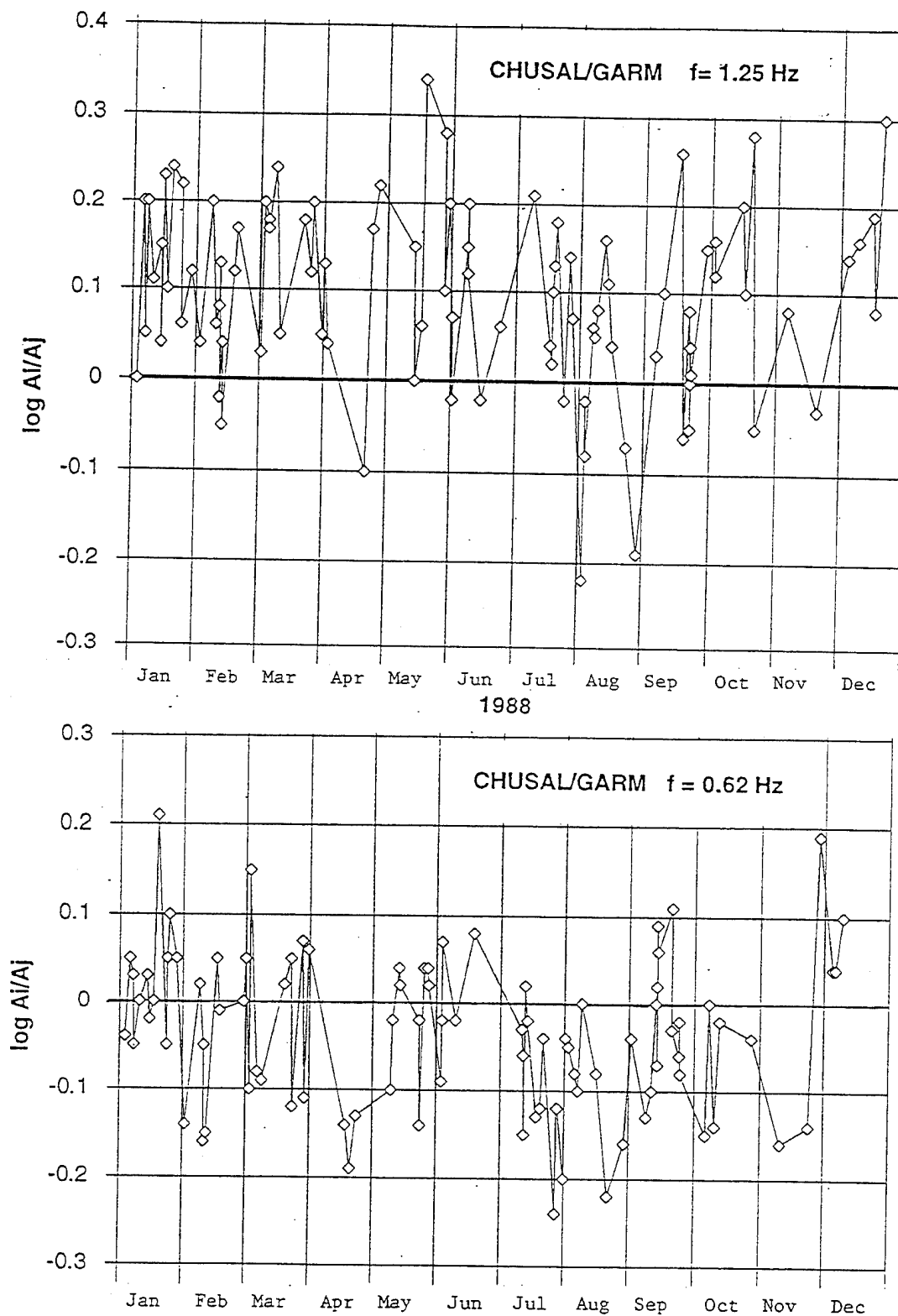


Figure 47. The monitoring of spectral ratio of coda level of the same earthquakes at two stations: Chusal and Garm during the 1988 at 1.25 Hz (top) and 0.62 Hz (bottom). Note the small scattering of individual ratios: standard deviation is 0.10 log. units.

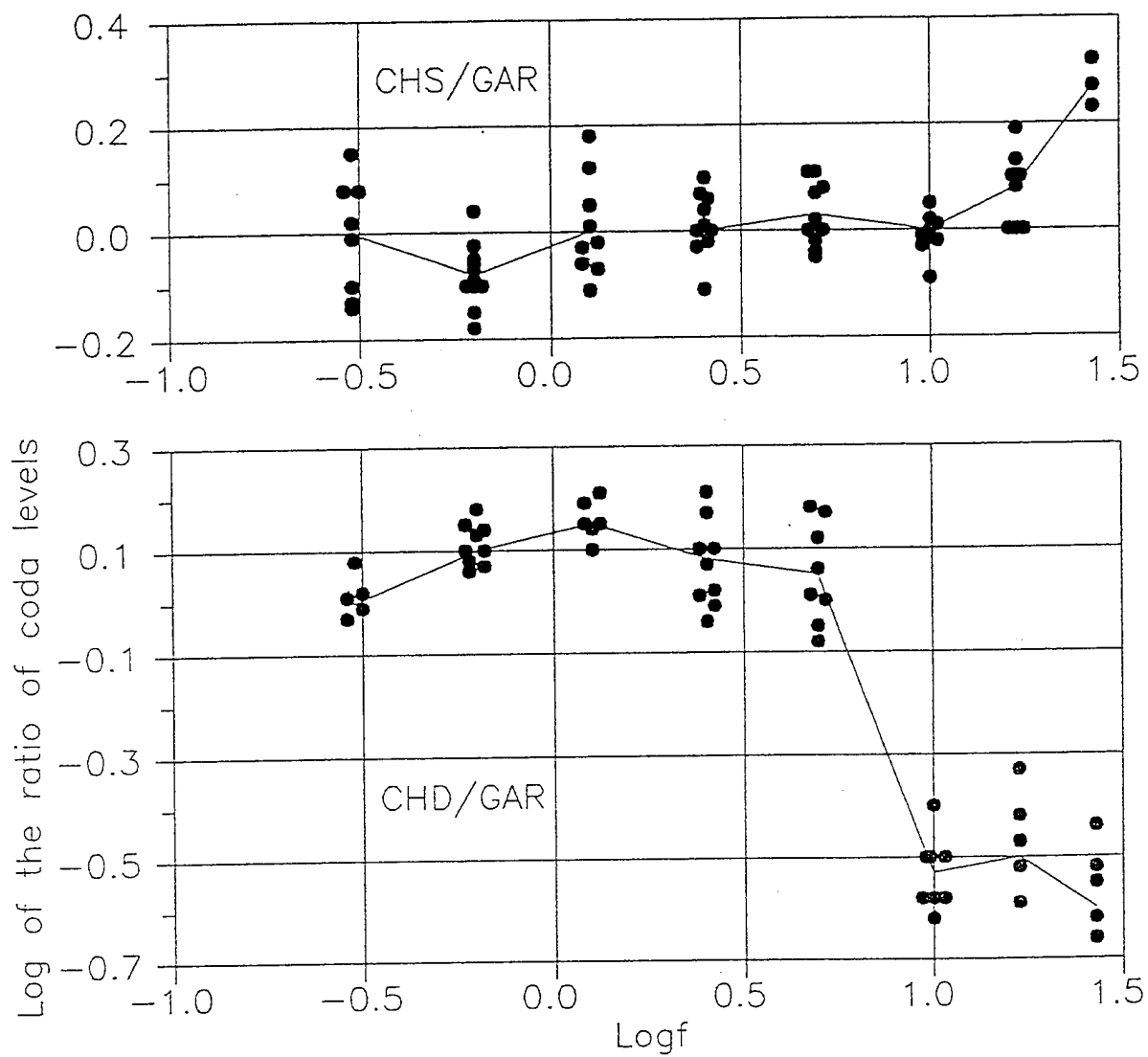


Figure 48. The spectral ratios of coda level of the same events on the records of two ChISS stations of the Garm network : Chusal and Garm (top) and Chil-Dora/Garm (bottom). The solid circles are the data from individual earthquakes.

probably due to a different response of the relief or of the tunnel itself, or contact between the seismometer and pier. What is the reason - the difference like that exist as systematical error and its correction is necessary.

The bottom graph appears as a result of attenuation. But it is not as simple. First, the seismometer in Chil-Dora was installed in the tunnel, but in limestone of Mesozoic age. If the shape of the ratio was due to attenuation, the value of ratio at 18 and 27 Hz will be less than at 10 Hz. Thus, the existing ratios have to be studied and corrected to obtain a good source spectra.

Table 32 shows the spectral residuals for different ChISS stations in Central Asia. The coda spectral content of all these stations were used to obtain the source spectra, so the good corrections were very important.

Table 32. Station Spectral Residuals of Seismic Coda Level for Central Asia and Kazakhstan ChISS Stations; Garm was Taken as a Basic Station

St.	Frequencies, Hz							
	0.14	0.30	0.62	1.25	2.5	5	10	18 27
Thick Sediments								
CHD		0.00	0.16	0.18	0.00	-0.04	-0.54	-0.68 -0.70
SRZ		0.60	0.45	0.37	0.10	-0.16	-0.10	-0.52 -0.60
BGZ		1.15	0.92	0.72	0.60	0.52	0.18	
SUF	0.40	0.17	0.17	0.0	-0.15	-0.05		
GIS		0.32	0.22	0.14	0.28	0.28	0.00	-0.14
LNG		0.50	0.60	0.40	0.20	0.10	0.0	0.04
Hard Rocks								
GZN		0.20	-0.00	0.10	0.22	0.22	0.22	0.25 0.06
CHG		0.28	0.20	0.13	-0.04	-0.00	0.00	0.18 0.67
ARZ		0.44	0.20	0.16	0.05	0.12	0.16	0.24 0.58
VAN		0.20	0.00	-0.03	-0.08	-0.27	-0.28	-0.28
TLG	-0.05	0.15	0.00	-0.29	-0.42	-0.56		

The spectral residuals were found for all ChISS stations. There are examples of spectral station residuals in Figures 49 - 52.

The spectral residual curves for stations at sedimentary rocks are similar. The max is at low frequencies, but the levels are different. The residual at low frequency vary from 0.16 in Chil-Dora to 1.15 in Bogi-Zagon. For high frequencies the residuals became small or negative, reaching -0.5 or even -1.0 for frequencies about 5-10 Hz. Such site responses are typical for stations with local conditions similar to

# SPECTRAL STATION RESIDUALS

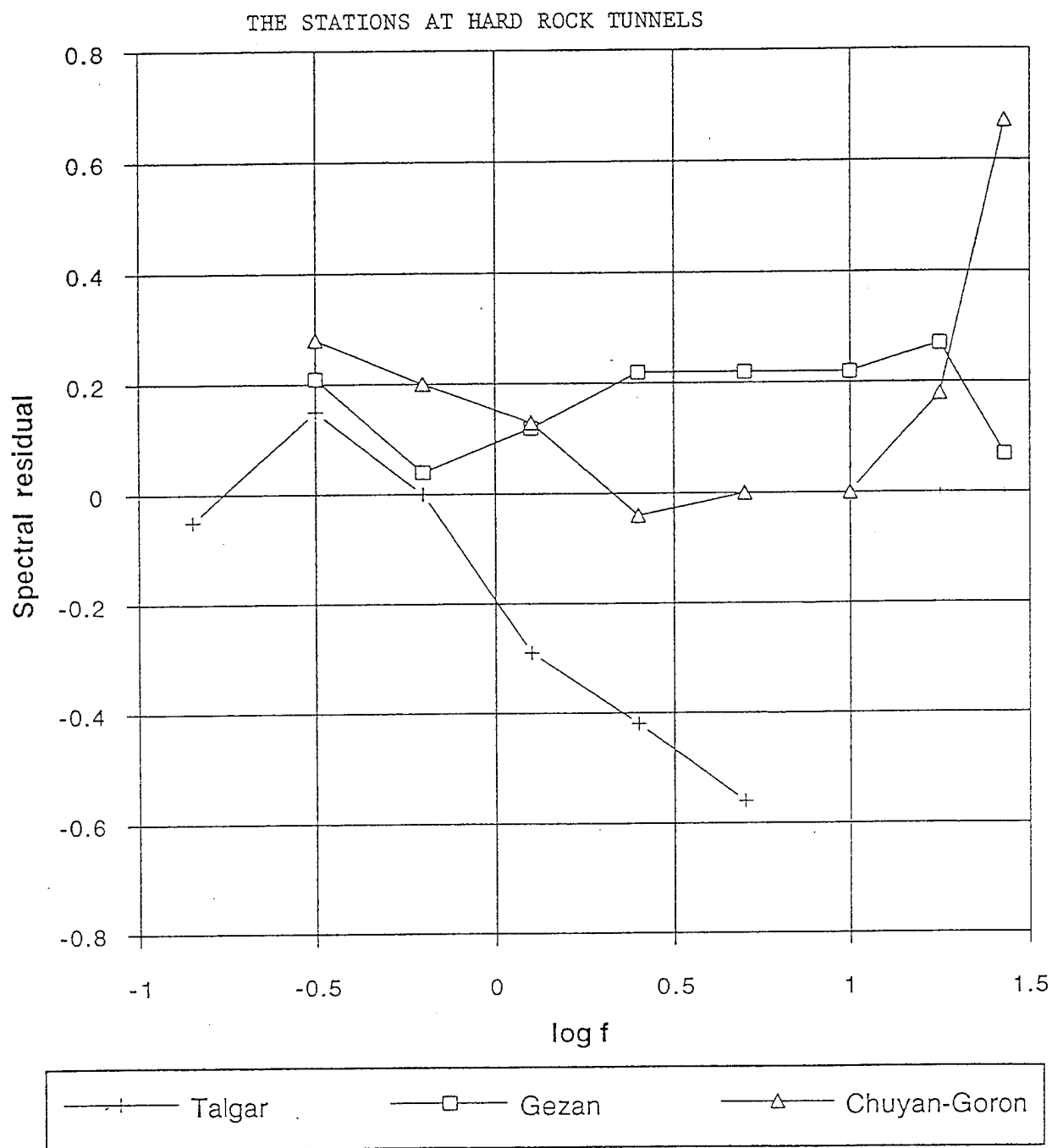


Figure 49. The spectral station residuals for three ChISS stations installed in tunnel on Paleozoic rocks : Gezan and Chuyan-Goron (Tadjikistan), and Talgar (North Tien Shan).

# SPECTRAL STATION RESIDUALS

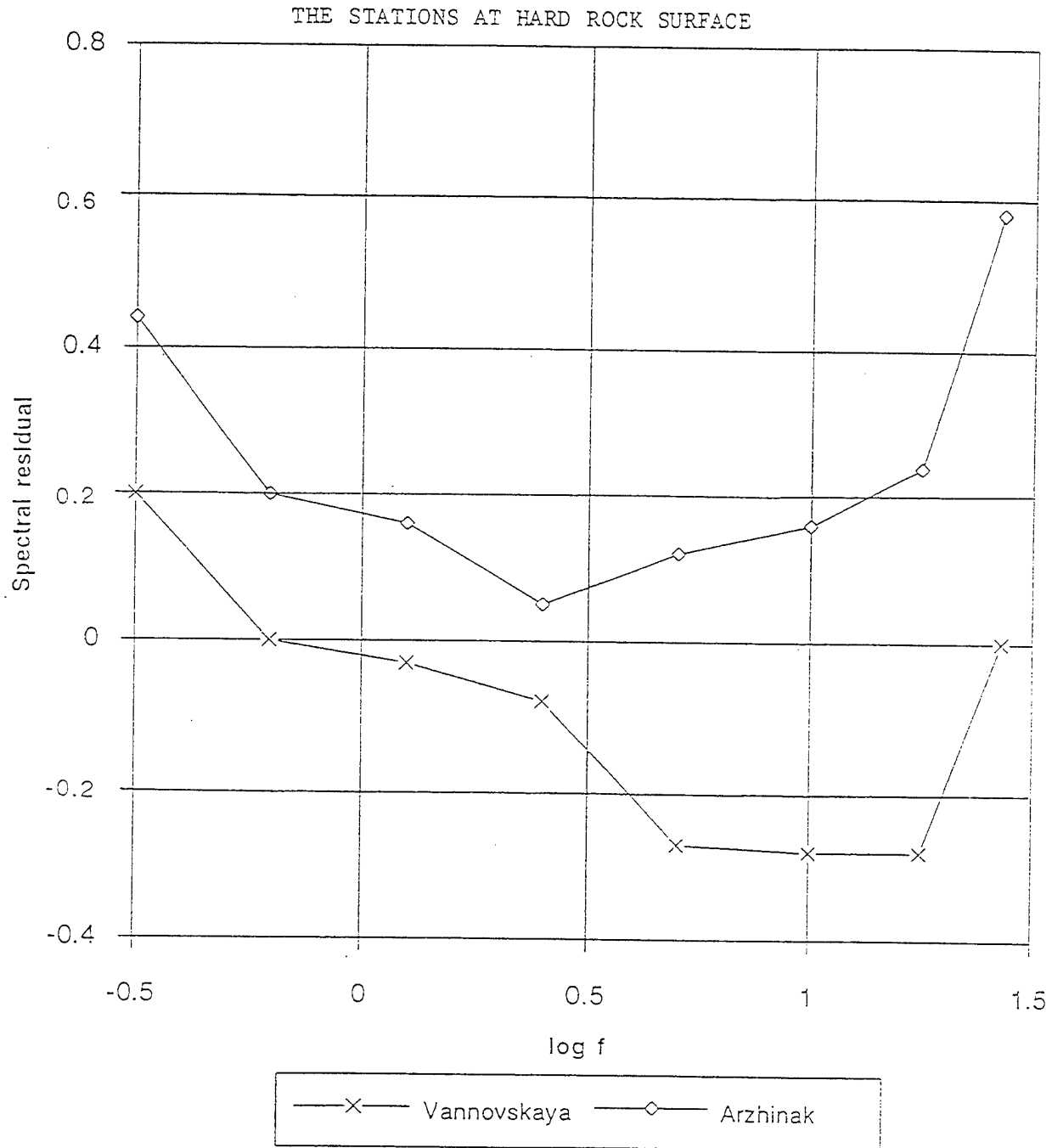


Figure 50. The spectral station residuals for two ChISS-stations: Arzhinak (Tadjikistan), Vannovskaya (Mesozoic limestone, Kope Dag).

# SPECTRAL STATION RESIDUALS

THE STATIONS ON MESOZOIC ROCKS

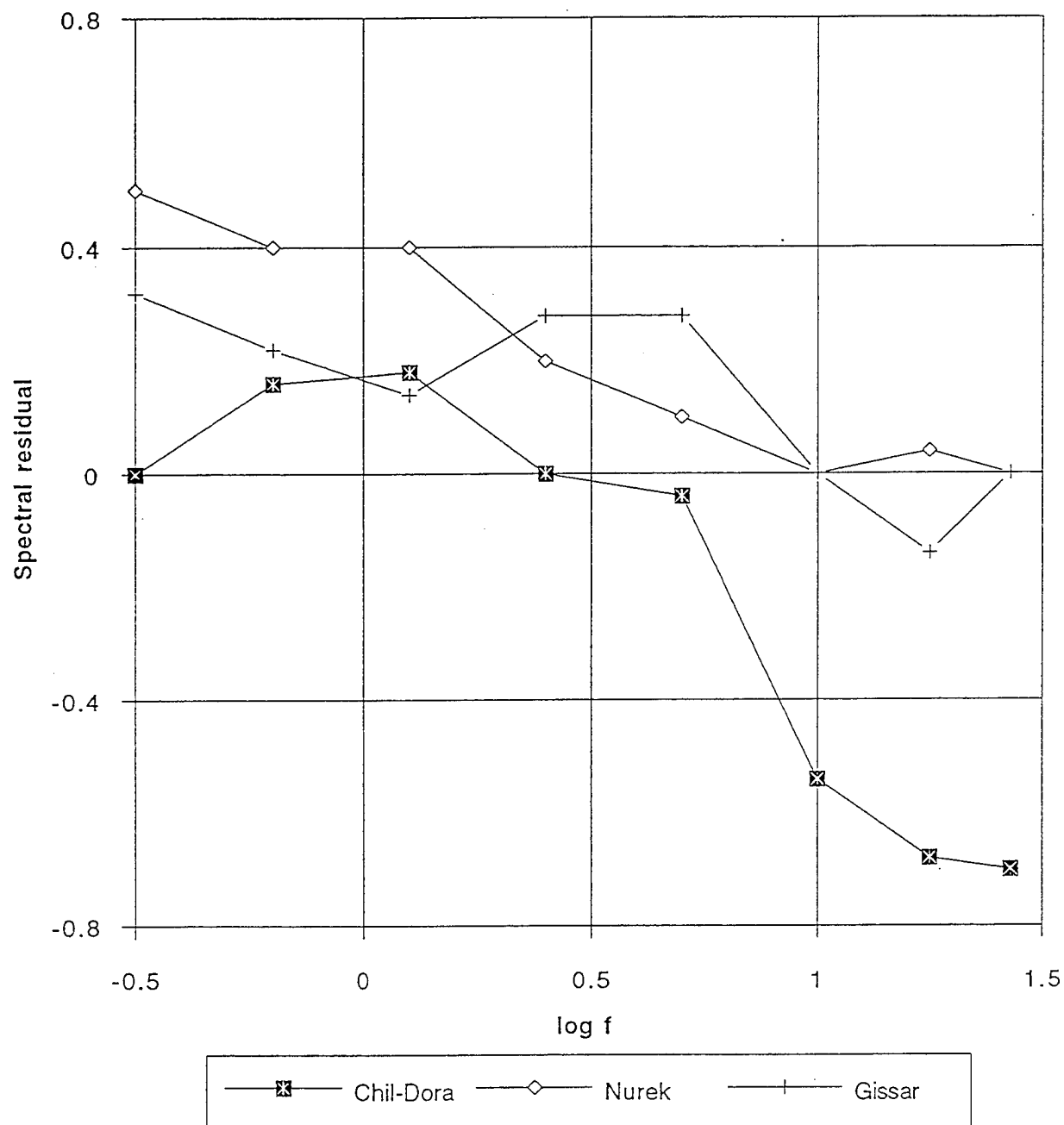


Figure 51. The spectral station residuals for three ChISS stations installed in tunnel on Mesozoic sedimentary rocks: Nurek, Gissar, Chil-Dara (Tadjikistan).

# SPECTRAL STATION RESIDUALS

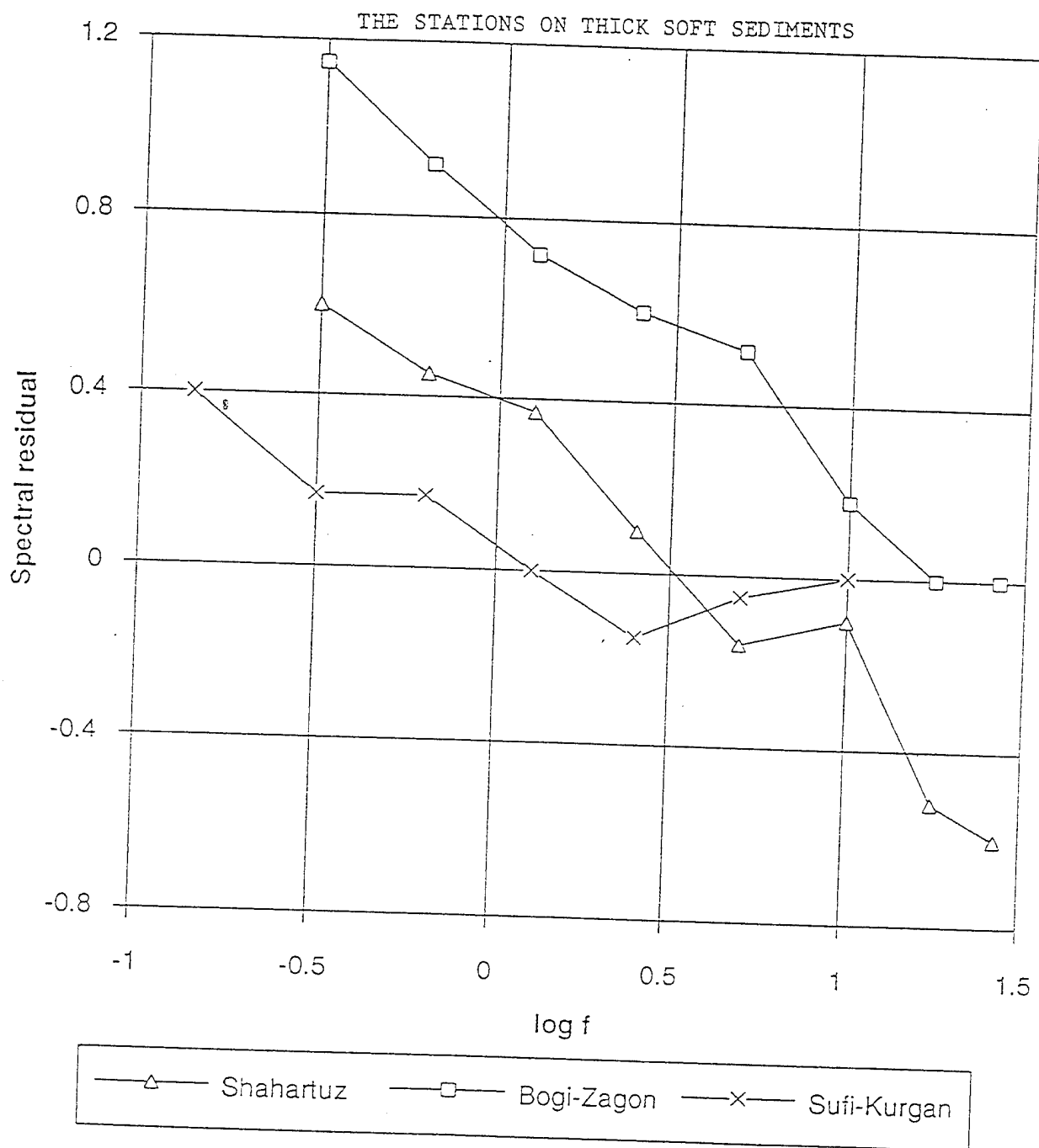


Figure 52. The spectral station residuals for three ChISS stations installed on thick sediments: Shahartuz and Bogi-Zagon (Tadjik Depression) and Sufi-Kurgan (Alai Valley).

Bogi-Zagon: Shahartuz, Dushanbe, Alma-Ata.

Other stations have different shapes of spectral residuals. These are stations installed at hard rocks (Chuyan-Goron, Chusal, Arzhinak). These residuals are much less. At high frequencies their residuals sometimes are too large and hardly understandable; but they exist, and we must correct them.

Talgar is special. It is installed on a high rock tunnel. The  $Q$  in crust around Talgar is high, about 460 for 1 Hz. The residual, obtained from late coda correspondent to lapse times, is big enough to touch the low- $Q$  volume beneath the Talgar area. We believe that these negative residuals from coda originate due to the "dark hole". The same effect observed for teleseismic records, with ray traces, penetrated this low- $Q$  volume. As for local seismicity with the distances less than 100 km, the residual for direct waves is about zero for all frequencies.

Let us look at spectral results from the point of view of the station corrections for broad band instrument records. The spectral site responses similar to CHD, SRT, BGZ make a different station residual for short- and for long-period seismic signal. If the low-frequency signal is arrived, the residual on SKM records will be positive; if the signal has high frequencies, it will be negative. It is known that the deep earthquakes of Pamir - Hindu Kush zone, usually having high-frequency spectra, are known for having the negative residuals at DUS, TAS, BGZ, SRT and other stations installed at the sediments. But if an earthquake with a low-frequency content is recorded, the residuals at these stations is positive.

The use of coda allows us to obtain a common system of station spectral corrections for stations, even as far from each other as 500 - 1000 km. From our experience of determination with the spectra of large ( $M > 5$ ) earthquakes, these corrections provide the coincident spectral amplitudes from distant stations and from stations with different local conditions as well.

## 9. THE SOURCE SPECTRA AND SPECTRAL ZONING

The spectral zoning is an important part of developing the UNE/EQ discriminator. The spectral content of seismic signal is one of the most confident information sources to build the spectral discriminator. There are different factors influenced on the spectrum of seismic signal:

- a) The source spectrum, depending on the conditions in the particular volume of media including the source;
- b) The existence or absence of low- $Q$  block beneath the



epicentral zone or observation area;

c) The "normal" attenuation along the path. In this section we show some data about influence for the two first factors.

#### 9.1. The Mapping of Low- and High-Frequency Earthquakes Based on Spectral Content of Coda

The simplest way to see very roughly the spectral difference of two events is to compare the difference between their coda magnitudes from short- and long-period instruments. Let us return to Figure 53. Because of the small error of magnitude determination from coda, the difference  $dM$  observed between  $M_c(SKM)$  and expected from formula (8.3) is not exclusively noise. This variation  $dM$  may be considered as the effect of real difference in source spectra. If so, one can expect, that earthquakes with low-frequency spectra (small  $dM$ ) will separate in their epicenter positions from high frequency earthquakes (large  $dM$ ).

Figure 53 is a mapping of  $dM$ . Here, the diamonds are the low-frequency earthquakes ( $dM < -0.13$ ), crosses are the epicenters of high-frequency ones ( $dM > 0.13$ ). To make the results clearer, the earthquakes with intermediate  $dM$  are not shown on this map. The bend of high seismic activity with a strongly fractured crust between the South Tien Shan and Pamir, consists of epicenters with both kinds of  $dM$ . Almost all of North Pamir's earthquakes have the low  $dM$ . All events in West Tien Shan, Turan Platform (Gazli) and Kazakh platform have high-frequency spectra.

It is clear from data, as shown in Figure 53, that when trying to create the discriminator, one must use earthquakes from the same zone where the UNE are conducted (or expected).

The discriminator, based on earthquake data from different zones may appear exiting, but do not work in some particular zone. For example, in a work [Zfang et al., 1992], where the spectral discrimination was proposed, the only earthquake showing the same value of the discrimination parameter was of the epicenter in Altai, where the high-frequency earthquakes are regular.

#### 9.2. The Method of Determination of the Source Spectra from ChiSS-Coda

The difference between a pair of magnitudes,  $M_c(SKM)$  and  $M_c(SKD)$  is an extremely rough parameter. A more detailed description of spectral content can be done from ChiSS-coda. The method of determination of the source spectra from ChiSS-coda was proposed in [Rautian, Khalturin, 1978]. Measuring the coda envelopes at several channels, corresponding to certain frequencies, one can see the spectral content of coda as

# THE EARTHQUAKES OF CENTRAL ASIA

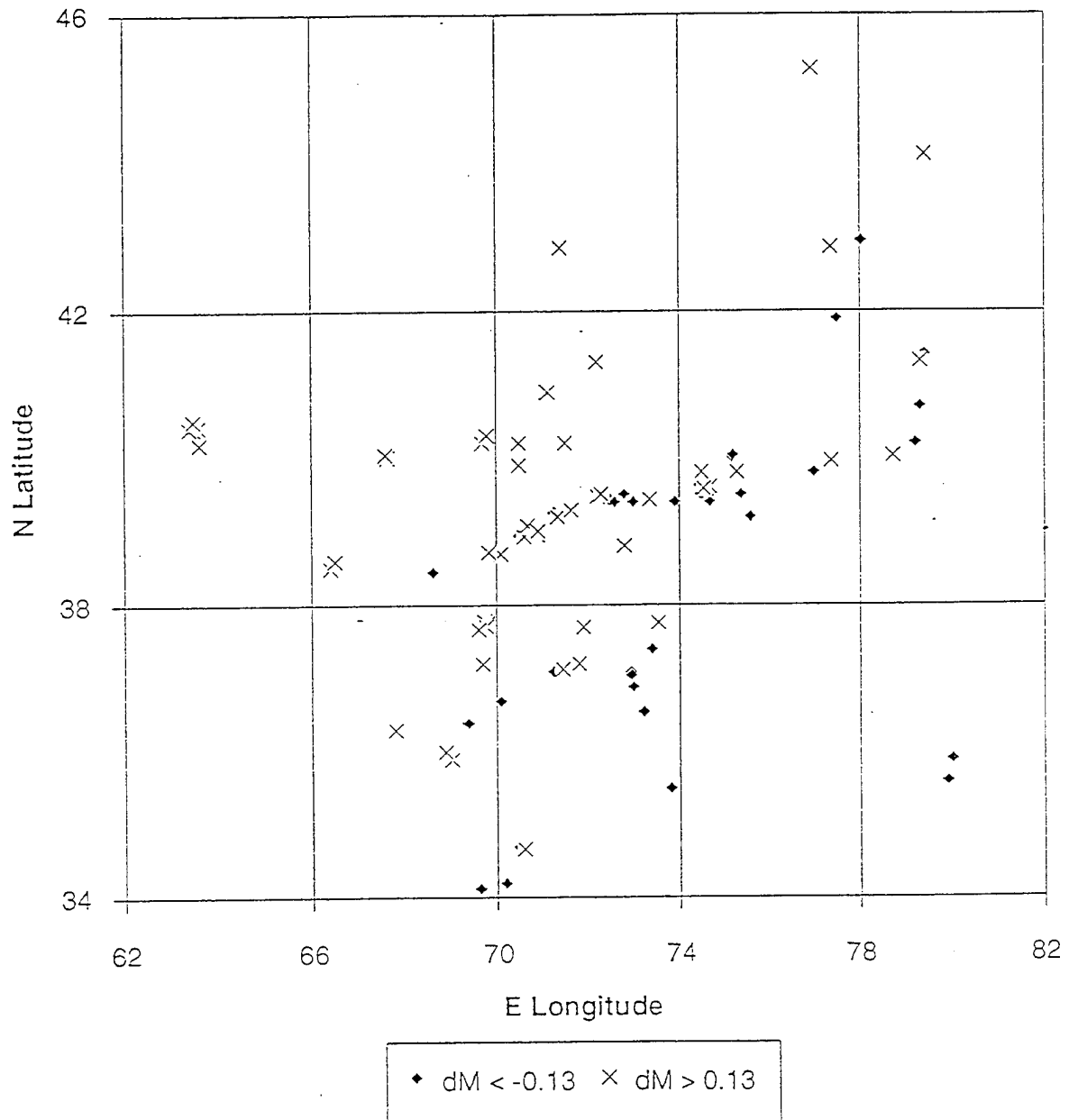


Figure 53. The map of  $dM = M_c(SKM) - M_c(SKD)$  for Central Asiain earthquakes. The diamonds are epicenters of low-frequency events, with  $dM < -0.13$ ; the crosses are high-frequency ones, with  $dM > 0.13$ .

A100(f). The source spectrum can be found in a form of displacement spectrum DIS(f), using the transform function d(f):

$$\log \text{DIS}(f) = \log \text{A100}(f) + d(f),$$

velocity spectrum VEL(f) as :  $\log \text{VEL}(f) = \log \text{A100}(f) + v(f)$ ,

acceleration spectrum ACC(f):  $\log \text{ACC}(f) = \log \text{A100}(f) + a(f)$ .

The transform function, found from ChISS-observation of both direct waves and coda at the small epicentral distances is shown in Table 33.

Table 33. The Transform Functions d(f), v(f) and a(f) which are Used for Calculation the Source Spectrum from Coda Spectrum at 100 sec

f, hz	d(f)	v(f)	a(f)	f, hz	d(f)	v(f)	a(f)
0.02	8.70	7.84	6.98	1.25	5.00	5.90	6.80
0.04	7.80	7.25	6.70	2.5	4.62	5.82	7.02
0.07	7.20	6.84	6.50	5.0	4.25	5.75	7.25
0.14	6.40	6.35	6.30	10.0	4.14	5.94	7.84
0.30	5.80	6.10	6.40	18.0	4.10	6.15	8.20
0.62	5.40	6.00	6.60	27.0	4.06	6.29	8.52
				40.0	4.03	6.44	8.84

The d(f) means the logarithm of spectral content of coda at lapse times 100 sec if seismic source radiates the delta-pulse. DIS(f) is proportional to spectrum of seismic moment M(f). Using this method the determination of source spectra was conducted for both earthquakes and UNES.

The high precision can be reached when taking into account the spectral corrections (see Table 32). In Tables 34 there are the regular examples of calculating the source spectra from ChISS-coda at several stations. The logarithms, measuring A100 for each station at each frequency channel, are shown in the upper part of the table. These are uncorrected data; one can see the serious difference between station data for the same frequency.

Then spectral corrections were added. Later, all stations data were averaged and standard deviations were calculated. These results are shown at the bottom of the table. After correcting station difference, the standard deviation became as small 0.05-0.12 log units.

Table 34. The Example of Coda Spectral Content  $\log A_{100}(f)$  at Different Stations Before Correcting and Average Value and its Standard Deviation After Adding the Station Spectral Corrections for Earthquake Feb 20, 1988

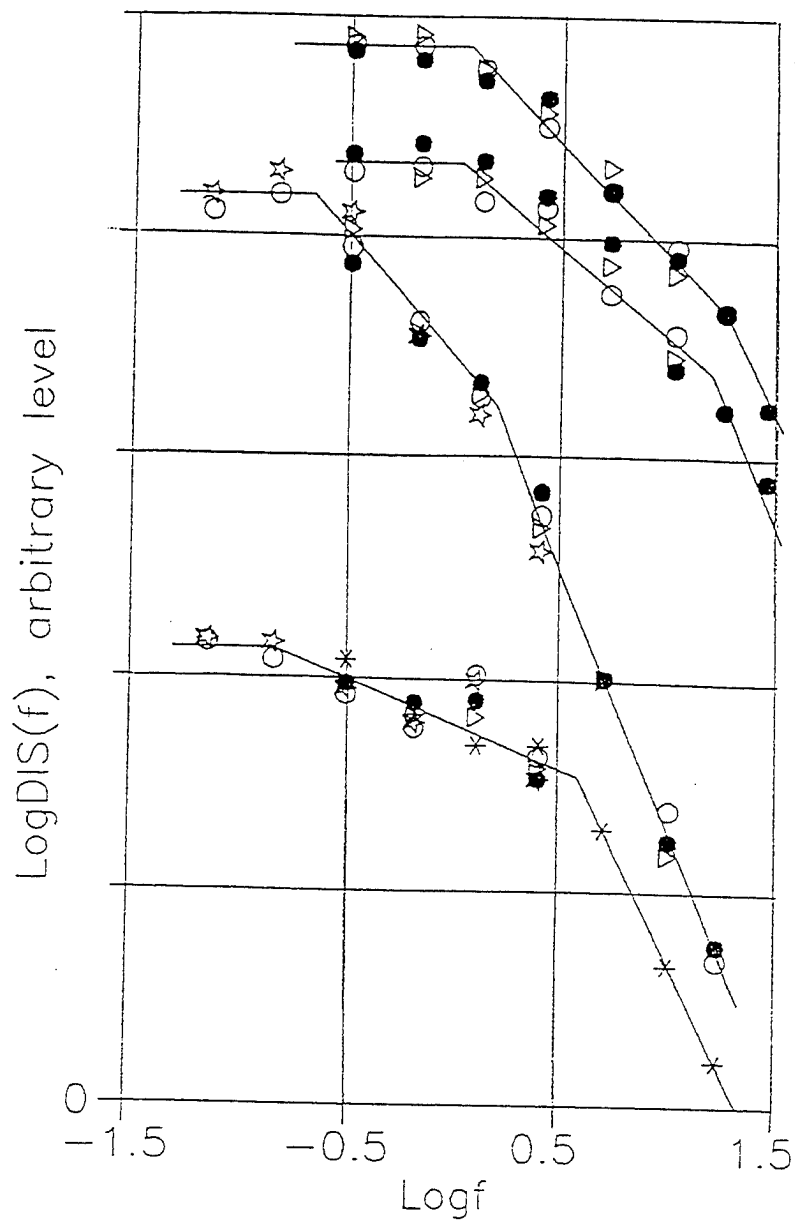
Date	Time	Zone	Latit.	Long.	h	MPVA	K		
20.02.88	01-51	Darvaz	38.58	70.50	7	5.0	12.2		
f, hz	0.14	0.30	0.62	1.25	2.5	5	10	18	27
Uncorrected Data logA100(f)									
GAR	-0.85	-.62	-.39	-.30	-.30		-1.05	-1.52	
CHS		-.68	-.43	-.13	-.10	-.29	-.88	-1.53	-2.10
CHD		-.34	-.15	-.17	-.08	-.31	-1.30		
GIS				-.23	.03	.10	-.75		
BGZ		.00	.07	-.17	-.37	-.42	-1.45		
GZN		-.77	-.51	-.23	-.56	-.64			
GRG		-.88	-.72	-.74	-.64	-.67	-1.00	-1.48	-2.20
Average		-.55	-.36	-.28	-.29	-.37	-1.07	-1.51	-2.15
Stan. dev.		.30	.34	.19	.43	.34	.18	.02	.05
Aver. st. dev. before correcting is 0.231									
After adding the station spectral corrections:									
Aver.logA100	-.60	-.41	-.21	-.16	-.21	-.21	-.90	-1.53	-2.07
Stand. dev.	.12	.06	.08	.11	.15	.12	.12	.00	.04
Aver. st. dev. after correcting is 0.085									

Avoiding any discussion of the spectra themselves from Table 34 one can notice that after correcting the station deviations decreased 2-5 times.

Figure 54 shows the source spectra  $DIS(f)$  of four earthquakes recorded by 5 stations. The absolute level of each event is marked by horizontal lines with the values of  $\log DIS(f)$  (m3) near it. The scattering of the station data (after correcting) for the same event is small.

Figures 55-57 give additional examples of the variety of individual source spectra, which are determined with a good confidence due to high accuracy of coda method and the efficiency of spectral station corrections. Note that the shapes of spectra are in a good agreement with the theoretical models; there are the flat low-frequency parts and the high-frequency slope is proportional to the  $f$  squared. Note the spectacular difference of the shape of the spectra of each earthquake. In their corner frequencies  $f_1$  and  $f_2$ , show the slope of spectra in their intermediate part (between  $f_1$  and  $f_2$ ). It evidenced the fruitfulness for both the coda method and station corrections in the problem of studying the source spectra of seismic events at regional distances.

### 9.3. The Regional Difference of the Source Spectra



●●●●● Chusal  
 ○○○○○ Garm  
 ☆☆☆☆☆ Sufi-Kurgan  
 \*\*\*\*\* Vannovskaya  
 ▷▷▷▷▷ Chil-Dora

Figure 54. The source spectra  $\log \text{DIS}(f)$  of four earthquakes obtained by coda method, using the data of 3 - 5 stations for each. The station spectral corrections were used. Note the small scattering of the different stations data.

1.11.78 19-48 39.50 72.60 H=13 MPVA=6.7 MLH=6.8 K=16.0

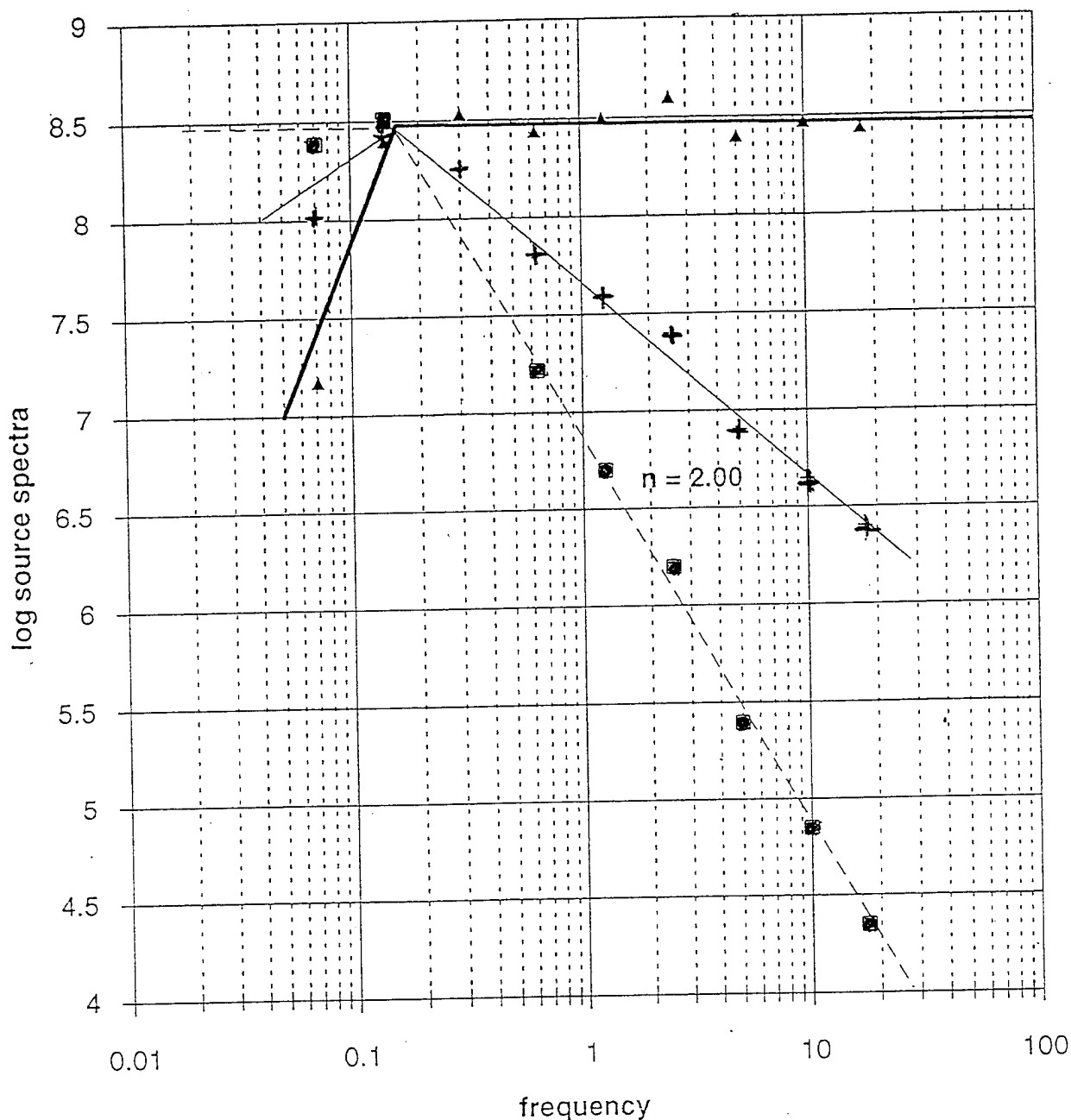


Figure 55. Source spectra of displacement (squares), velocity (crosses) and acceleration (triangles) for Alay earthquake (Nov 1, 1978, 38.5N, 72.6E,  $M_s=6.8$ ) obtained by Rautian method from record of Garm station ( $R=200$  km). Spectrum has simple shape with single corner frequency. The  $f$ -square slope observed between 7 sec and 18 Hz without  $f_{max}$ . Source parameters are:  $\log M_0 = 19$  (in  $N \cdot m$ ),  $T_0=6$  sec,  $\log E = 15.7$  (in J), apparent stress is 170 bars.

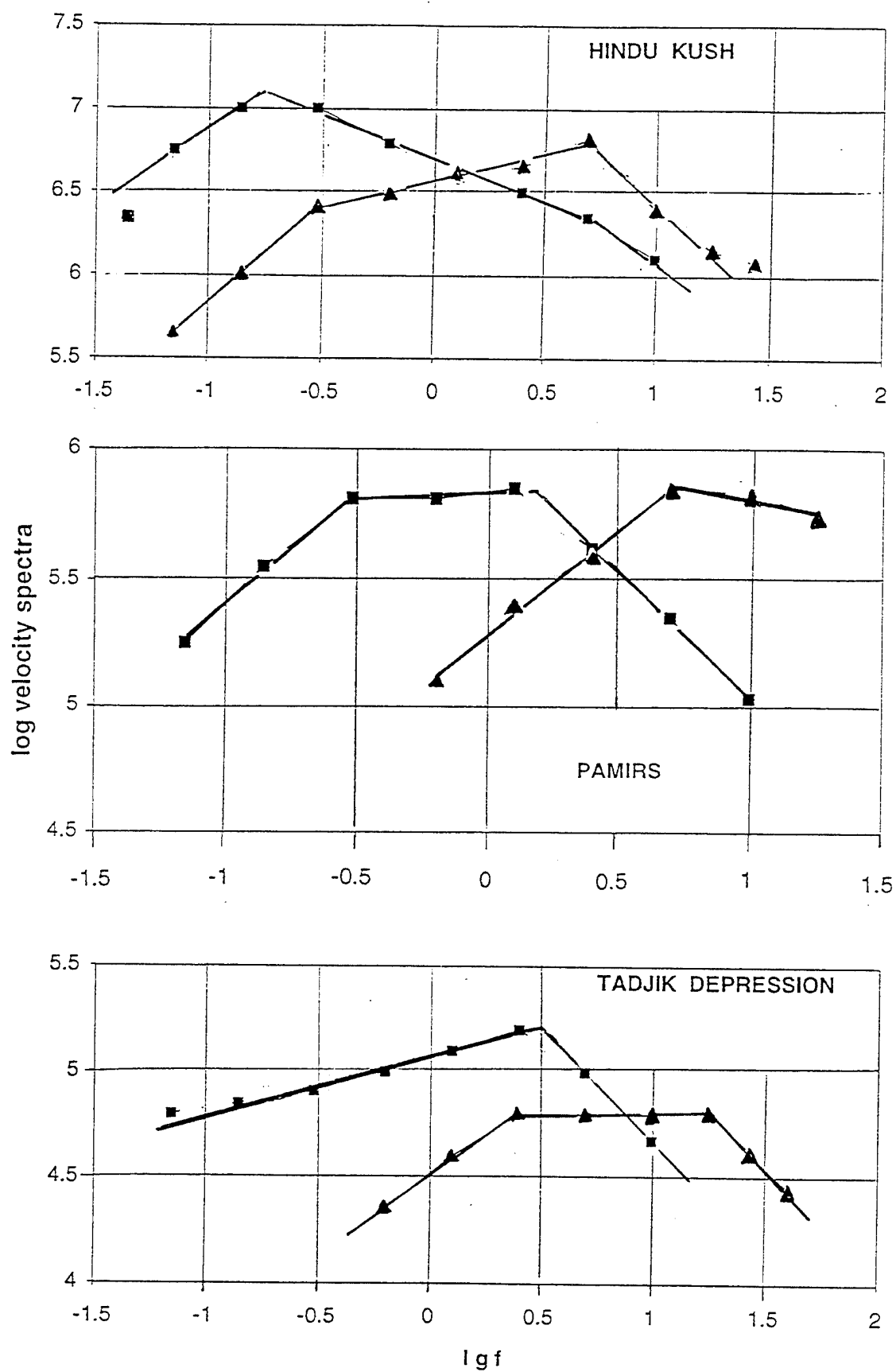
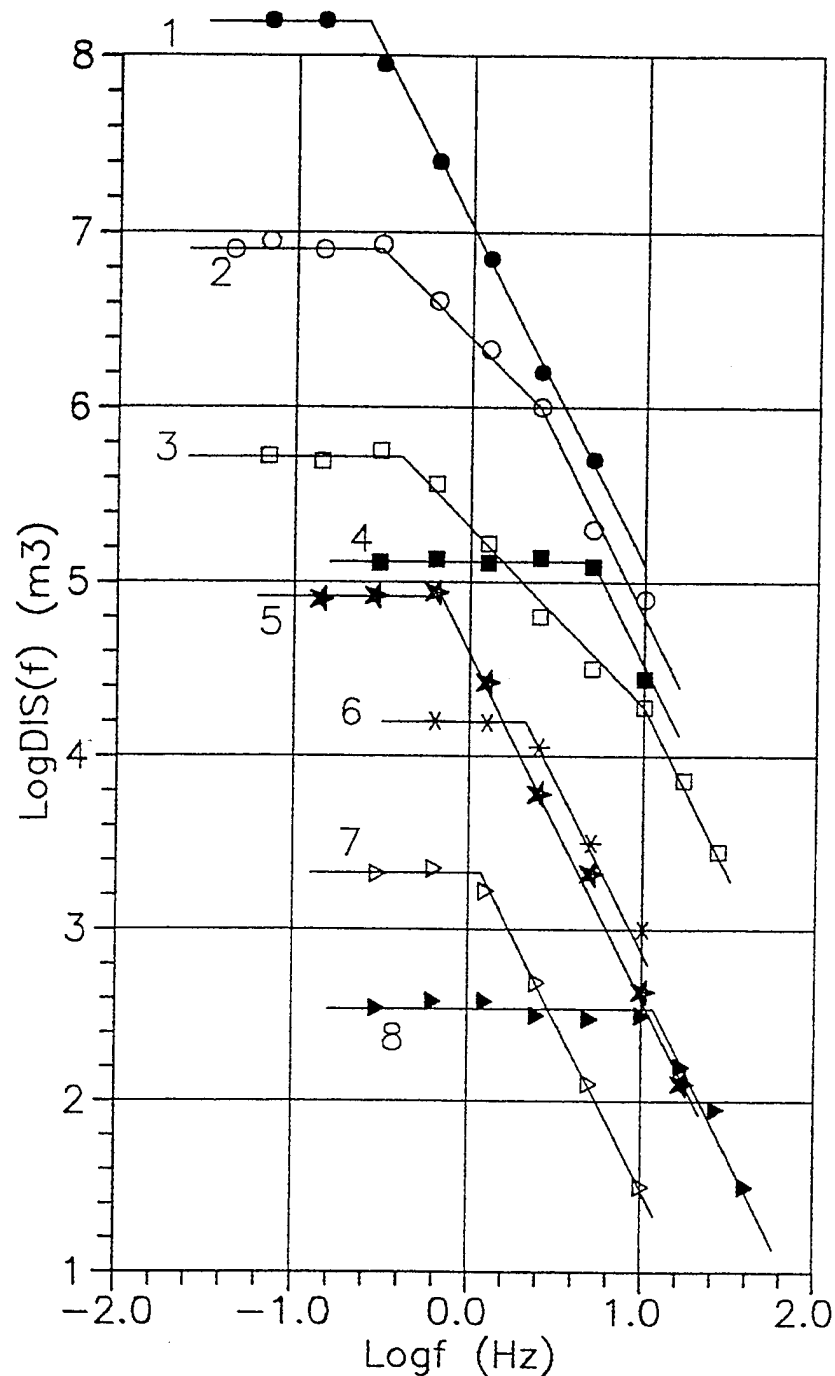


Figure 56. The velocity source spectra for shallow (squares) and deep (triangles) earthquakes. Deep events are deeper than 100 km in Pamir and Hindu Kush and more than 12 km in Tadjik Depression).



1. Mar. 24, 1978, 21:05, N.Tien Shan,  $M_s=7.1$ ;
2. Nov. 27, 1976, 21:42, Hindu Kush,  $M_P=6.6$ ;
3. Jan. 11, 1974, 02:03, Hindu Kush,  $M_P=5.2$ ;
4. Apr. 04, 1976, 01:56, Gazli,  $M_s=4.5$ ;
5. Jun. 19, 1977, 22:15, S.Tien Shan,  $K=11$ ;
6. Jan. 9, 1972, 02:55, Tashkent,  $K=10$ ;
7. Dec. 1, 1978, 12:12, Nurek,  $K=8.6$ ;
8. Dec. 8, 1973, 09:01, Garm,  $K=8.2$ .

Figure 57. The displacement source spectra of eight Central Asian earthquakes obtained by Rautian's method from data of one-four stations each. Station spectral correction were used. Note the clear flat part of spectra and high frequency slopes agree to the omega-square model.



From our study of source spectra using ChISS-coda method we found that there is extremely wide individual variations of source spectra, even if they are near the same location and magnitude. That is not errors, but natural variation of sources. But nevertheless there is some regularity of spectral content of source radiation for zones with different tectonic situation. Table 35 shows the typical values of apparent stress

$hs = E/M_0$  ,  
calculated from source spectra.

Table 35. Apparent Stress Values (Minimum, Average and Maximum) of Earthquakes From Some Epicentral Zones

Epicentral Zones	N	lgE (J)	Apparent Stress, Bars		
			Minim	Average	Maxim
Gazli	16	12.5-14.5	50	250	1000
Caspian Sea	3	13.0-15.5	170	320	400
West Hindu Kush	16	14.0-15.0	1.6	33	130
Xingjiang	10	12.0-13.9	12	30	80
	8	11.1-11.7	1	10	48
North Tien Shan	2	12.0-13.9	80	150	280
	18	10.0-11.9	5	32	80
South Tien Shan	3	12.1-13.9	21	43	130
	5	11.1-11.7	8	25	78
Darvaz & Peter I	11	10.0-13.5	2	8	32

Similar differences were found from another characteristic of source spectra, so-called dynamic stress. It can be taken as a value, responsible for the short-period part of source spectra.

Table 36. The Upper Limits of Dynamic Apparent Stress  $hs$  at Some Epicentral Zones of Central Asia

Zone	$hs$ , bars	Zone	$hs$ , bars
Gazli	4000	Tashkent Area	210
Caspian Sea	2500	Darvaz Ridge	200
West Hindu Kush	2000	Zaalai Ridge	200
West Elburs	1000	South Pamir	180
Kazakh platform	950	Gerat	162
Kashgar	880	South Elburs	160
West Tien-Shan	760	Central Tien Shan	140
Djungaria	700	Zerafshan Ridge	100
Great Balkhan	700	Kopetdag Ridge	99
North Tien Shan	600	Nurek Area	70
Isfara (Fergana Valley)	530	Toktogul Area	68
Alai Valley	530	North Pamir	66

Table 36. (continued)

Zone	hs, bars	Zone	hs, bars
Wakhsh Ridge	480	Illyak fault	30
Peter 1 Ridge (h>12 km)	340	Pre-Kopet-Dag Trough	24
Peter 1 Ridge (h<12 km)	200		

Analysis of this value obtained by coda method for the earthquakes of Central Asia was conducted. The significant difference exists for the upper limits of the dynamic apparent stress. The upper limits do not depend on the magnitude of earthquake, but on the effective strength and tectonic stress in the zone. For the Central Asia region that upper limit changes from 20 - 30 bars at normal and strike-slip faults (Kopet-Dag, Illyak fault near Dushanbe), to 1000-5000 bars (Gazly), being about 330-500 bars at thrust orogen tectonics in Tien-Shan. Some detail data are shown in Table 36.

#### 9.4. The Effect of Attenuation in Epicentral Area on the Teleseismic Data

The b value (eq. 8.1) and the spectrum of seismic signal depend not only on source, but on the geological structure beneath the epicentral zone and the area of observation as well. The most important is the absence or existence of low-Q volume beneath the observation area and/or epicentral zone. At regional distances the source spectra differences are seen clearly and looks like the most important factor. But when looking at very wide regions from teleseismic distances, the source differences seems smoothed and the ray traces influence became more important, being systematical.

When looking at P waves at teleseismic distances, the attenuation in epicenter area seems to be the stronger factor, responsible for spectra of signals. The map of spectral ratios for 2.5/0.5 Hz at ChISS-spectra of P waves is shown in Figure 58. More than 700 earthquakes of  $m=4.5-5.5$  were used. All data was obtained mostly from Semipalatinsk ChISS station. The values of these ratios were referenced to epicenters and then smoothed. The low values -0.6 to -0.8 are localized in East Africa (-0.82), the Western parts of both Americas (-0.72), Tibet (-0.70) Iran, Caucasus, New Guinea (0.60), Mediterranean (-0.55). The higher values were found from earthquakes of Philippines (0.33), Central Asia, Altai, Sayans, (-0.20); Kommandores, Aleutian, Hokkaido and Kamchatka (0.16).

The detail mapping allows separating the smaller area with extreme values of spectral ratios: -1.4 for Tibet, -1.0 for South Iran, from 0.2 to -0.2 Kazakh platform and

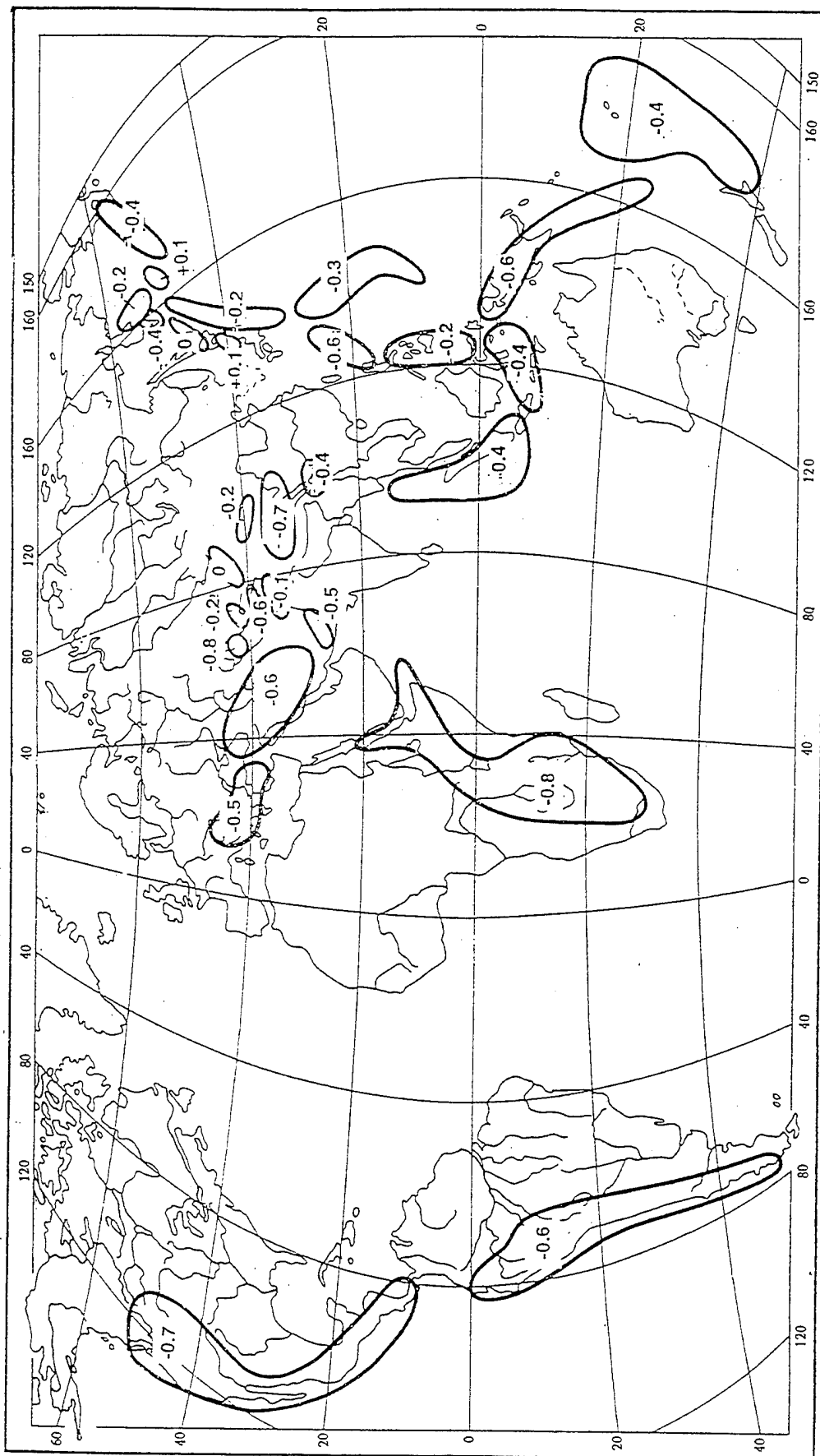


Figure 58. Map of spectral ratios 2.5/0.5 Hz at ChISS-spectra of teleseismic events P wave records of Semipalatinsk ChISS station. More than 700 earthquakes of  $m_b = 4.5 - 5.5$  were used. The values of these ratios were referenced to epicenters and then smoothed.

Siberia. For Baikal earthquakes, they are known as high-frequency radiated from local observation. But when using the teleseismic records of events from this zone, they turn out to be low-frequency ones. These regional difference are created by low-Q volume beneath this epicentral zone.

One can see that spectral parameters display the difference of spectral content of earthquakes depending on epicentral zone. So when building some spectral criteria for discriminating UNEs from earthquakes, the earthquakes used must be taken from the zone, for which the monitoring of UNE supposed to be conducted. In the case of Kazakhstan, for example, it is known that local earthquakes are mostly of very high-frequency spectra.

## 10. THE ESTIMATION OF REALISTIC ERRORS OF MAGNITUDES AND MAGNITUDE CORRECTIONS

### 10.1. Values of Standard Deviations Correspondent to Main Factors and Total Deviation of Magnitude Determination

In previous sections of this study, the contribution of the factors in the deviation of magnitude were estimated. They are described as components of magnitude deviations. I Table 37 shows the summary of the results we will use to calculate the examples of error in different situations.

Table 37. The Standard Deviations, Correspondent to Different Factors Responsible for Total Magnitude Deviation

Type of Deviation	The Value of Dev.	Type of Deviation	The Value of Dev.
Local	0.12	Random (EQ)	0.27
Area	0.15	Random (UNE)	0.18
Zone	0.15	Total obs. (EQ)	0.38
Path	0.18	Total obs. (UNE)	0.32

The "total observed" deviation here is determined without the deviation due to zone effect (which can not be seen from teleseismic observation). So the "real total" deviation is a little more than it is seen from observation: 0.41 for EQ and 0.35 for UNE.

To obtain the realistic estimation of errors of magnitude and of station correction at any particular case, one needs to take into account the values of each partial deviation and the numbers of realization for each factor taking part in that case: the numbers  $N(\text{loc})$ ,  $N(\text{area})$ ,  $N(\text{zone})$ ,  $N(\text{path})$ ,  $N(\text{rand})$ .

### 10.2. Estimation the Station Correction Error dB

The first example is the error dB for the station correction B which is determined from records of N(eq) earthquakes. In this case N(rand)=N(eq), N(path)=N(zon), thus the error dB is estimated as follows:

$$dB = \frac{S(rand)^2}{N(eq)} + \frac{S(zone)^2 + S(path)^2}{N(zone)} \quad (10.1)$$

When using many earthquakes, but from only a few zones, the zone and path effects will not be smoothed enough and are responsible for the error. Let us take the N(eq) as large as 100, but all these are from only 5 zones. The dB in this case is:

$$dB = \frac{0.27^2}{100} + \frac{0.15^2 + 0.18^2}{5} = 0.027 + 0.067 + 0.08 = 0.108$$

If taking even 500 earthquakes from the same 5 zones, the first term only will decrease and became 0.012, but the total error stays practically the same, 0.105. It means that the station correction calculated from data of a few epicentral zones will not be precise for events from other zones.

### 10.3. Calculation the Precision of Magnitude Determination

Another example is when the magnitude M is determined, and the records of N(st) were used. In this case N(rand) = N(st); N(path)=N(area). The error of magnitude dM will be calculated as:

$$dM = \frac{S(rand)^2}{N(st)} + \frac{S(loc)^2}{N(st)} + \frac{S(area)^2}{N(area)} + \frac{S(path)^2}{N(area)} + S(zone) \quad (10.2)$$

For individual measurement (only one station record is available and no station correction was used) the error will be equal to the value of total deviation, 0.41 for EQ. If the station correction was taken into account, the error of correction dB will replace the S(loc) and S(area). In this case the dM became slightly smaller, but not significantly.

$$dM = 0.27 + 0.10 + 0.18 + 0.15 = 0.37$$

If 20 stations were used from 5 areas without station corrections, the error dM from formula (10.2) will be:

$$dM = \frac{0.27^2}{20} + \frac{0.12^2}{5} + \frac{0.15^2}{5} + \frac{0.18^2}{5} + 0.15^2 =$$

$$= 0.06 + 0.054 + 0.067 + 0.08 + 0.15 = 0.200$$

If the station correction is available, its errors dB(loc) and dB(area) must be placed in second and third terms. If local and area components of dB are not known separately, they can be found formally and roughly from their general ratio (0.12/0.15). In this case it is easy to obtain for the same case:

$$dM = \frac{S(rand)^2}{N(st)} + dB \left( \frac{0.39^2}{N(st)} + \frac{0.61^2}{N(area)} \right) + \frac{S(path)^2}{N(area)} + S(zone)^2 \quad (10.3)$$

If the dB=0.10, we see the dM practically the same as without station correction:

$$dM = 0.06 + 0.037 + 0.08 + 0.15 = 0.196$$

If the stations are in a very few areas, the area effect as well as the path one and especially the zone effect stay as main sources of error. In this situation, using a large number of stations does not help to diminish the error dM, it will stay approximately constant for any number of stations:

$$dM = 0.61 \frac{dB^2}{N(area)} + \frac{S(path)^2}{N(area)} + S(zone)^2 \quad (10.3a)$$

#### 10.4. Zone Effect, Strategy of Diminishing and Lower Limit of the Magnitude Error

Even when many areas of observation were used, the zone effect stays constant and can be considered as limiting the possible precision of magnitude. Remember the real situation (UNEs from Nevada and Semipalatinsk). Thus, studying the zone effect and determining the zone correction is an important step to reaching the precise magnitude. If zone correction Z is known with its error dZ, the limit of dM becomes equal to that dZ.

The estimations of dB and dM for a typical situation give the errors about 0.10-0.15, the dM is more than dB because of not diminishing the zone effect. It seems to be realistic and is in good agreement with the observed discrepancies. The calculation of errors this way for a

particular situation gives the realistic values and helps to optimize the strategy of diminishing the error. This strategy needs efforts to make each term of equation smaller. It doesn't make sense to make one small term smaller and smaller. One has to pay attention to the large term.

For example, when the goal is monitoring some small zone, the station correction must be found for each station especially for that area. This correction includes the local area and pass effects and will be effective till the station and path effects remain smaller than zone effect. Later, the main source of error becomes the zone effect. The next effort must be not increasing the number of stations or using more accurate station correction, but the determination of the zone effect and its correction.

## CONCLUSIONS

1. In trying to obtain high accuracy of magnitude, individuals obtained the station corrections  $B$ . The errors of corrections  $\delta B$ , as well as errors of magnitudes  $\delta M$  (calculated from numerous stations records and using this corrections) are announced as about 0.01 or even less. These estimations are based on the assumption that magnitude deviations are random and do not depend on any factors.

When comparing the magnitudes for the same event, but from different sets of data the discrepancy varies from 0.07 to 0.17. The same is true when comparing the station correction for the same station obtained from different sets of data. The discrepancy between different sets of data vary from 0.00 to 0.45 with its standard deviation from 0.07 to 0.25. It shows that there are some factors creating station residual which are not random in the simple sense.

2. The multi-factor model of station residuals is proposed. The total magnitude deviation  $S$  consists of partial deviations, which originate from five independent factors. They are:

- a) Local station condition  $S(\text{loc})$ ;
- b) Observation area condition  $S(\text{area})$ ;
- c) Epicentral zone conditions  $S(\text{zone})$ ;
- d) Path effect  $S(\text{path})$ ;
- e) Random scattering of data  $S(\text{rand})$ .

These partial deviations describe the contribution of each factor into the total deviation.

3. The factors appear random or systematical depending on the situation. When studying the station residuals at stations localized in a small area, the local effect is random, but the area residual is systematical and identical for all stations of the area. Thus, the area residual cannot be

found from comparing the local data only.

When determining the magnitude of event, the epicentral zone effect is systematical. It cannot be found from data of distant stations only, without independent information about typical residual for earthquakes of this particular zone. The error due to uncorrected zone effect stays systematical but unknown for all events in the same epicentral zone. It becomes random when using the magnitudes for events from wide territory including many different zones.

4. The "areas" and "zones" are recommended to choose from a geological point of view as a territory which can be considered as more or less homogeneous. The most important difference between different areas (or different zones) is the existence or absence of low Q in the crust and upper mantle.

5. The area residual was taken as an average station residual calculated from all stations in this area. The local residuals were calculated as the difference of each particular station residual from area residual.

6. The zone effect is invisible from teleseismic observation, but originated from the same cause as area effect. There are two important examples showing the values of difference between two zones as large as 0.35. The "zone" component of deviation must be taken equal to the "area" deviation. The residual for a particular zone is supposed to be equal to area residual for stations localized in this zone.

If no area residual is known for some territory, it can be taken from a very general opinion of similarity from the area under consideration with other well-studied territories. For example, for shields and platforms the expected residual is about +0.20; for volcanic territory, where the low-Q is known or likely exists, the zone residual expects to be -0.20; for orogenic territory like Tien Shan, Altai, etc the residual is probably about zero. The assumption like that is very useful when monitoring some new zones.

7. The path effect creates the difference between the A/T-D for any particular couple "source-receiver" and the standard calibration function. The most serious difference is observed at distances less than 2000 km and more than 8500 km. The latter probably originates from complexity of the boundary between the low-mantle and the core. It creates the small-scale variations which do not connect with local site conditions.

8. The values of factor components of magnitude deviations were found:

Local	0.10	Random (EQ)	0.28
Area	0.14	Random (UNE)	0.18



Zone	0.14	Total (EQ)	0.40
Path	0.19	Total (UNE)	0.34

9. To obtain the realistic estimation of errors  $dM$  or  $dB$  one needs to take into account the values of each partial deviation, and the numbers of realization for each factor taking part in a particular case:  $N(loc)$ ,  $N(area)$ ,  $N(zone)$ ,  $N(path)$ , and  $N(rand)$ . Based on the simplified multi-factor model of magnitude deviation, the formulas for calculating errors  $dB$  of station corrections and errors  $dM$  of magnitude are proposed.

10. Calculating the errors for some examples make the values (0.10-0.20) significantly larger, than announced errors (0.03-0.003), but are in good agreement with the observed discrepancy of station corrections (or magnitudes) determined from different sets of data.

11. As it follows from this study of the errors, the efficiency of station correction is not important in most cases. But they are important to prevent the systematical error due to threshold effect.

12. When monitoring some small zones, the special station correction including path effect must be found for this particular zone. In such cases the main source of error will be zone effect. The zone effect correction is the main way to diminish the "unpredictable" magnitude error.

13. The "random component" of deviation includes the effects which cannot be easily diminished. These effects are, for example, a spectral content of source radiation, depending on the tectonic situation; an effect of geological structure in the vicinity of the source, transforming the time-history (symmetric to the local effect of structures in vicinity of the station). Some artifacts play a serious role too; these are systematical overestimations of magnitude for small events, the instability of instrument magnification, etc.

14. Our opinion is that to be realistic, 0.07 is the lower limit of a magnitude error.

15. It is a special situation when monitoring small events.

First, the observations on the regional distances began playing an important role. Second, the data of only a small number of stations are available. In this situation the special station correction must be used for each station and for the particular epicentral zone. Such correction includes local, area and path effects. Thus, a zone effect remains an important source of systematic errors for all events of this zone.

Our successful experience shows that a random component of magnitude deviation can be diminished including the different waves existing at the regional distances (Pg, Sn, Lg and coda) separately for several frequency bands. It is equivalent to increasing the number of stations. In doing so, the random component became as small as 0.05 even for a few stations.

The analysis of data must be conducted keeping in mind the possible threshold effect. North's consideration of this problem is very useful to correct it. Comparing his data with mb from ISC (which did not take this effect into account) shows, that the threshold effect became notable even for magnitudes of UNE 5.0-5.5!

16. The problem of influence zone effect is not unsoluble, but one needs to pay special attention to a basic magnitude in a globe scale. When comparing the station residuals and magnitudes calculated from different sets of data, the discrepancy sometimes is too important. The different idea of choosing the basic magnitude probably plays an important role.

Our opinion is that the basic magnitudes must be taken for earthquakes localized out of the zones with low-Q beneath them. The stations used to calculate magnitude must be taken out of that area as well. If so, the magnitudes calculated from different but similar areas will not have a geophysically created discrepancy. The station residuals must be calculated as difference from that basic magnitude. If using this method, the area residuals can be taken as zone residual for earthquakes, localized at the same territory.

17. There is a method to diminish the random component on the single station. It is convenient at the regional networks and consists in the using of more parameters. The Pn, Pg, Lg waves and especially coda amplitudes at several frequency bands are equivalent to several stations data of P wave. Using only coda from few stations allows reaching the the random error as small as 0.05-0.07 magn.units.

18. The problem of discriminating underground nuclear explosions from quarry blasts (QB) and earthquakes (EQ) makes the spectral aspect of correction to be an important part of the problem of accuracy. The discrimination is usually based on the ratio of short- and long-period amplitudes. It can be the ratio of short-period P wave and long-period Rg or Lg waves, the ratio of short- and long-period coda or ratio of P-wave, recorded on different frequency bands. Two parts of the problem are important. First, using the spectral correction to obtain the precise information of spectral parameters of event. Second, studying the regularity of spectral characteristics of EQ and QB depending on epicentral zone; we call it spectral zoning.

19. The residual of surface wave magnitude is specific. It appears as a shadow from large inhomogeneities (for example, like Black Sea with its oceanic crust). The length of the shadow is about 2-3 times the size of the inhomogeneity. Thus, residual depends not on the station or position of epicenter themselves, but on crossing the deep part of the Black Sea. The values of residual reaches 0.50-0.70. The boundary between the Pacific oceanic crust and continental crust of Asia creates the shadow as long as 4000 km. A similar effect, but not as strong, is for earthquakes from the Mediterranean recorded in East Europe.

The station correction for surface wave magnitude has to be considered as consisting of two parts,  $B(st)$  is usual station correction, the other,  $b(D)$  depends only on distance from structure, creating the shadow and has the same value for all stations at the same distance :

$$B = B(st) + b(D) .$$

The special system of correction must be used in each particular case.

## REFERENCES

- Antonova L.V., V.I. Khalturin, T.G. Rautian et al. (1968). The main experimental regularities of dynamics of seismic waves. Nauka Publ. House, Moscow, 173 pp. (in Russian).
- Antonova L.V., Z.I. Aranovich, N.V. Kondorskaya (1974). Magnitude and optimization of seismic observations problem. In "Magnitude and Energy of Earthquakes". Institute Earth Physics, Moscow, v.2, pp.195-202, (in Russian).
- Antonova L.B., T.G. Rautian, V. I. Khalturin, et al. (1978). The experimental study of the Earth interior. Moscow, Nauka Publ. House, (in Russian). 155 pp.
- Dotsev N.T., V.I. Khalturin, M. Shomakhmadov (1989). The comparing of the coda envelopes on SKD-records on the stations about 4000 km between. Bulgar. Geophys. Proc., 15, no 1, Sofia. (in Russian), pp.56-59.
- Feofilaktov V.D. (1970). About the instrumentation and station magnitude corrections in "Geophysical Observations in Obninsk", (in Russian), pp.17-26.
- Gutenberg B. (1945). Amplitudes of P, PP, and S waves and magnitudes of shallow earthquakes. Bull. Seism. Soc. Am. 35, no3.
- Khalturin V.I. (1974). The relations between the magnitude scales, expected and observed ones. In "Magnitude and Energy of Earthquakes", v.1, Acad. Sci. USSR, (in Russian), pp.145-153.
- Khalturin V.I., T. G. Rautian, P. Molnar (1977). The spectral content of Pamir-Hindu Kush earthquakes: evidence for a high Q zone in the mantle, J. Geophys. Res., 82, pp.2931-2944.
- Khalturin V.I. (1989). The regional variation of shape of the coda envelopes as a function of frequency. The 25th General Assembly IASPEI, Aug.21 - Sept.1 1989. Abstracts. Istanbul, p.533.
- Khalturin V.I., T.G. Rautian, A. M. Shomakhmadov (1989). The magnitude scale, based on seismic coda. In "Earthquakes of Central Asia and Kazakhstan in 1985". Donish Publ. House, Dushanbe (in Russian), pp.137-173.
- Khalturin V.I., T.G. Rautian (1991). The source spectra of earthquakes, in "The Earthquakes and the Process of its Preparation". Nauka Publ. House, Moscow (in Russian), pp.82-93.
- Khalturin V.I., E. V. Artemova (1992). The magnitude corrections and their relation with the Earth crust structure in a region of Black Sea. The Seismic Wave Fields. Moscow, Nauka Publ. House, 1992, pp.68-78.

Khalturin V.I. (1992). The amplitudes and attenuation of surface waves. Seismic wave fields. Moscow, Nauka Publ. House, 1992, pp.79-96.

Khalturin V.I., A. I. Ruzaikin (1992). The dependence of surface wave intensity on the source depth from the records of frequency band pass filters station (ChISS) at distances up to 2,000 km. Seismic Wave Fields. Moscow, Nauka Publ. House, (in Russian) pp.55-67.

Khalturin V.I., T.G.Rautian, P. Richards (1993). The study of the small magnitude seismic events at and near Semipalatinsk Test Site. EOS, Abstracts of Fall Meeting of AGU, San Francisco, Dec. 5-9, 1993, p.449.

Kirichenko V.P. (1993). Results of the calibration seismic yield estimation methods for UNEs at Balapan Test Site. 15th Annual Seismic Research Symposium. Vail, Colorado. PL-TR-93-2160, ADA271458.

Korchagina O.A., A. G. Moskwina (1974). The magnitude, calculated from in-put and out-put seismic signal. In "The Magnitude and Energy of Earthquakes", Acad.Sci. USSR, Moscow v.1 (in Russian), pp.214-219.

Landyreva N.S. (1967). Determination MLH when processing the Bulletin of Basic Seismic Stations of USSR. Information Bulletin of ESSN, Moscow, (in Russian), pp.37-43.

Landyreva N.S. (1974). Estimation the MLH value for Seismological Bulletin of ESSN. In "The Magnitude and Energy of Earthquakes", Acad. Sci. USSR, Moscow, v.2, (in Russian), pp. 9-18.

Marshall P.D., D.L. Springer, and H. C. Rodean (1979). Magnitude correction for attenuation in the upper mantle. Geophysical J. Royal Astr. Soc., 57, pp.609 - 638.

North R.G. (1977). Station magnitude bias - its determination, causes, and effects. MIT Lincoln Lab, Technical note, 1977-24.

Pasechnik I.P. (1962). The connection between seismic magnitude and seismogeological structure of the region of observation. Izvestia of Acad. Sci. USSR, Geophys. Seria, n11. (in Russian).

Pisarenko V.F., T.G. Rautian (1965). The effect of a station and a source location at an accuracy of the seismic parameters determination. In "The Computational Seismology", no 1, (in Russian). pp.160-186.

Rautian T.G., V.I.Khalturin, M.Zakirov, et al. (1981). The experimental study of seismic coda, Nauka Publishing House, Moscow, (in Russian), 142 pp.

Rautian T.G., V.I.Khalturin (1982). The source spectra and the source parameters of the earthquakes from Central Asia. In "Earthquakes in the USSR in 1979". Nauka Publ. House, Moscow (in Russian), pp. 95-103 and 222-227.

Rautian T.G. (1960) The energy of earthquakes. In "Methods of Detail Study of Seismicity". Transactions of the Geophysical Institute Acad. Sci. USSR, no. 9(176), (in Russian). pp. 85-109.

Rautian T.G. (1964). The determination of the energy of seismic waves at the distances up to 3500 km. Transactions of the Geophysical Institute Acad. Sci. USSR, no 32, (in Russian), pp.88-93,

Rautian T.G. (1974). The problem of determination of the earthquake energy. In "Magnitude and Energy of Earthquakes" v.2, (in Russian). pp.107-112.

Rautian T.G., V.I.Khalturin (1978). The use of the coda for determination of the earthquake source spectrum. Bull. Seism. Soc. Am, 68, no 4, pp.923-948.

Rautian T.G. (1991). The seismo-active media and sources of earthquakes. In "The Study of Earthquakes and its Modelling" Nauka Publ. House, Moscow, (in Russian), pp. 35-48.

Richards P.G. (1993). Station magnitude bias-its existence and problems of estimation. Lamont-Doherty Earth Observatory, 23 pp.

Ringdal F. (1985). Study of magnitudes, seismicity and earthquake detectability using a global network. In the VELA Program, DARPA, pp.611-624.

Ruprechtova L. (1958). Dependence of amplitude of seismic body waves on the distance. Studia geophysica et geodeatica, v.2, n4.

Ruprechtova L. (1961). Travel - time curves and amplitude-distance curves of the P and S waves at distances smaller than 30 degrees. Geofisikalni sbornik, n 106.

Shomakhnadov A.M., V.I. Khalturin (1990). The station corrections for the seismic stations of Garm Network. C.S.E, Inst. Phys. Earth, Moscow (in Russian), pp.64-70.

Solovyev S.L. and Solovyeva O.N. (1964). The comparison amplitude - distance curves from Kuril - Kamchatka and Mediterranean earthquakes. Izvestia Acad. Sci. USSR, geophys. seria, n 4, (in Russian).

Zapolsky K.K. (1971). The frequency band pass filter seismic station, in "Experimental Seismology", Nauka Publishing House, Moscow, (in Russian), pp.20-36.

Zapolsky K.K., I. L. Nersesov, T. R. Rautian, V.I. Khalturin (1974). The physical basis of magnitude and of earthquakes. In "Magnitude and Energy of Earthquakes", v.1, Acad. Sci. USSR, Moscow, (in Russian), pp.79-131.

Zapolsky K.K. (1973) Temporal-frequency fields and dynamic characteristics of the source functions of the large earthquakes. DAN USSR, 210, n 6. (in Russian).

Vanek J., A. Zatopek, K. Karnik, N. Kondorskaya et al. (1962) Standardization of the magnitude scale, Izvestia of Acad. Sci. USSR, ser. geophys., no 2. (in Russian).

Vanek J. and A. Tskhakaya (1967). The station corrections for determination of the magnitude. Izvestia of Acad. Sci. USSR, The Physics of the Earth N 4, Moscow, (in Russian).

Vanek J., N. V. Kondorskaya, I. B. Fedorova (1974). The problem of homogeneous station system to determinate the magnitude of earthquakes. In "The Magnitude and Energy of Earthquakes", v.1, Acad. Sci. USSR, Moscow, (in Russian), pp. 154-162.

Vanek J., N. V. Kondorskaya, et al. (1983). The station corrections for P, S and surface waves in the homogeneous magnitude system of Eurasian continent. The Physics of the Earth, No 6, Moscow, (in Russian), pp. 50-58.

Vanek J., N. V. Kondorskaya, L. Christoskov (1992). The homogeneous magnitude system of Eurasia continent for seismological processing of data. The Physics of the Earth, no 6, Moscow, (in Russian), pp. 50-58.

# APPENDIX 1

Table 1: The List of Seismic Stations Used for Estimate Station Corrections

Station	Code	Latit.	Long.	Instruments	
Bulgaria					
Kyrdzali	KDG	41.6	25.4	SKD	
Pavlikeni	PAV	43.2	25.3	SKD	SKM
Sofiya	SOF	42.7	23.2	SKD	
Vitosha	VTs	42.6	23.2	SKD	SKM
Poland					
Krakov	KRA	50.0	19.9	SKD	
East Germany					
Collmberg	CLL	51.3	13.0	SKD	
Moxa	MOX	50.6	11.6	SKD	
Czecho-Slovakia.					
Kashp.gory	KHC	49.1	13.6	SKD	
Pruhonice	PRU	50.0	14.5	SKD	
FUSSR					
Kola Peninsula					
Apatity	APA	67.6	33.3	SKD	
Urals					
Ekaterinburg	EKT	56.8	60.6	SKD	
Carpathian					
Kishinev	KSH	47.0	28.7	SKD	
Lvov	LVV	49.8	24.0	SKD	
Uzhgorod	UZH	48.6	22.3	SKD	SKM
Russian Platform					
Moscow	MOS	55.7	37.6	SKD	
Obninsk	OBN	55.1	36.6	SKD	
Pulkovo	PUL	60.0	30.0	SKD	SKM
Crimea					
Alushta	ALU	44.7	34.4		VGK
Simpheropol	SIM	45.0	34.1	SKD	
Yalta	YAL	44.5	34.2	SKD	SKM
North Caucasus					
Pyatigorsk	PYA	44.0	43.0	SKD	SKM
Grozni	GRO	43.3	45.7	SKD	
Makhach-Kala	MAK	42.9	47.5	SKD	
Sochi	SOC	43.6	39.7	SKD	SKM
Georgia					
Tbilisi	TBL	41.7	44.7	SKD	
Bakuriani	BKR	41.7	43.5	SKD	SKM
Goris	GRS	39.5	46.3	SKD	
Abastumani	ABS	41.8	42.8	SKD	SKM
Lagodekhi	LGD	41.8	46.3	SKD	SKM
Oni	ONI	42.6	43.5	SKD	SKM
Bagdadi	BGD	41.5	44.8		SKM
Akhalkalaki	AHL	41.4	43.5		SKM
Gori	GOR	42.0	44.1	SKD	
Dusheti	DST	42.1	44.7	SKD	
Gegechkori	GGK	42.3	42.4	SKD	



Table 1 (Continued)

Station	Code	Latit.	Long.	Instruments		
Armenia						
Leninakan	LEN	40.8	43.8	SKD	SKM	ChISS
Metsamor	MTS	40.1	44.1		SKM	
Idjevan	IDV	40.6	45.1		SKM	
Stepanavan	STE	41.0	44.4	SKD	SKM	
Yerevan	YER	40.1	44.3	SKD	SKM	
Kadjaran	KDR	39.1	46.1	SKM	SKD	
Azerbaijan						
Baku	BKU	40.4	49.9	SKD		CHISS
Balabur	BAL	38.7	48.8	SKD	SKM	
Gebrail	GEB	39.4	47.0	SKD	SKM	
Kirovabad	KRV	40.7	46.3	SKD	SKM	
Nahichevan	NAH	39.2	45.4	SKD	SKM	
Pirkuli	PIR	40.8	48.6	SKD	SKM	
Sheki	SHK	41.2	47.2	SKD	SKM	
Shemakha	SHE	40.6	48.6	SKD	SKM	
Turkmenia						
Ashgabad	ABD	37.9	58.4	SKD	SKM	ChISS
Gaudan	GAU	37.7	58.4		SKM	
Germab	GER	38.0	57.7		SKM	
Kara-Kala	KAR	38.4	56.3		SKM	
Kaushut	KAU	37.5	59.5		SKM	
Krasnovodsk	KRS	40.0	53.0	SKD	SKM	
Kyzyl-Arvat	KZA	39.0	56.2	SKD		
Nebitdag	NBD	39.5	54.4	SKD	SKM	
Vannovskaya	VAN	38.0	58.1	SKD	SKM	
Uzbekistan						
Andizhan	AND	40.8	72.4	SKD	SKM	
Djizak	DJK	40.1	67.8		SKM	
Fergana	FRG	40.4	71.8	SKD	SKM	
Humsan	HUM	41.7	69.9		SKM	
New-Nikolaevka	NNK	42.4	70.6		SKM	
Namangan	NMG	41.0	71.7		SKM	
Nurata	NUR	40.6	65.7		SKM	
Samarkand	SAM	39.7	67.0	SKD	SKM	
Tamdy-Bulak	TMD	41.8	64.5		SKM	
Tashata	TSH	40.6	72.6		SKM	
Tashkent	TAS	41.3	69.3	SKD	SKM	
Zarabad	ZAR	37.8	66.7		SKM	
Tadjikistan						
Arjinak	ARJ	38.74	68.62			CHISS
Bogi-Zagon	BGZ	38.492	69.817			ChISS
Bolgzuan	BLD	38.313	69.668			ChISS
Chuan-Garon	CNG	38.652	69.162		SKM	ChISS
Gissar	GIS	38.470	68.567	SKD	SKM	ChISS
Djerino	GJR	38.783	68.843		SKM	ChISS
Dushanbe	DUS	38.6	68.8	SKD	SKM	
Gesan	GSN	39.290	67.790		SKM	ChISS

Table 1 (continued)

Station	Code	Latit.	Long.	Instruments		
Hura-tube	URT	39.9	69.0		SKM	
Khorog	KHO	37.5	71.5	SKD	SKM	
Murgab	MRG	38.4	73.9	SKD	SKM	
Nurek	NRK	38.400	69.350	SKD	SKM	ChISS
Shahartuz	SRT	37.575	68.100		SKM	ChISS
Ragun	RGN	38.700	69.783			ChISS
Garm Network						
Balkh	BAL				SKM	
Batyr	BAT				SKM	
Chil-dora	CHD	38.78	70.31	SKD	SKM	ChISS
Chussal	CHS	39.11	70.76	SKD	SKM	ChISS
Garm	GAR	39.007	70.317	SKD	SKM	ChISS
Ishtion	ISH	38.84	70.77		SKM	
Jaffr	JFR	39.10	70.59		SKM	
Kaudal	KAU				SKM	
Kaftar-Gusor	KFG	38.84	70.16		SKM	
Khait	KHT	39.17	70.89		SKM	
Langar	LNG	38.90	71.06		SKM	
Miyonadu	MIO				SKM	
Tavil-dora	TDR	38.42	70.48		SKM	
Turatol	TRT	39.25	70.78		SKM	
Safetoron	SFT				SKM	
Sangikar	SNG	39.04	70.14		SKM	
Siyokukh	SKK				SKM	
Yaldimich	YAL	39.06	70.44		SKM	
Afghanistan						
Kabul	KBL	34.5	69.0	SKD	SKM	
Kyrgyzia						
Batken	BAT	40.7	70.8	SKD	SKM	
Bishkek	FRU	42.8	74.6	SKD	SKM	
Chauway	CHW	40.1	79.1		SKM	
Erkinsai	ERK	42.7	73.8	SKD	SKM	
Kadjisai	KDS	42.1	77.2	SKD	SKM	
Naryn	NRN	41.4	75.8	SKD		
Osh	OSH	40.5	72.8	SKD	SKM	
Przevalsk	PRZ	42.3	83.2	SKD		
Rybachye	RYB	42.4	76.1	SKD		
Sufi-Kurgan	SFK	40.0	73.5	SKD	SKM	ChISS
S.Kazakhstan						
Alma-Ata	ATA	43.3	76.9	SKD	SKM	
Chimkent	CHM	42.3	69.6		SKM	
Kastek	KAS	43.0	76.0	SKD	SKM	
Kurty	KUR	43.9	76.3	SKD	SKM	
Medeo	MDO	43.17	77.05		SKM	ChISS
Stchel Dalnaya	STL	43.24	77.36	SKD		
Taldy-Kurgan	TDK	45.0	78.4	SKD	SKM	
Talgar	TLG	43.23	77.23	SKD	SKM	ChISS
Turgen	TUR	43.30	77.63	SKD	SKM	
Kazakh. platform						
Semipalatinsk	SEM	50.4	80.3	SKD	SKM	ChISS

Table 1 (Continued)

Station	Code	Latit.	Long.	Instruments	
Zerenda	ZRN	52.9	69.1		ChISS
Baikal					
Zakamensk	ZAK	50.4	103.3	SKD	SKM
Kyachta	KYA	50.4	106.7	SKD	
Mondy	MOY	51.7	101.0		SKM
Irkutsk	IRK	52.2	104.3	SKD	SKM
Bodon	BDN	53.7	110.1		SKM
Kabansk	KAB	52.1	106.7	SKD	
Altai					
Chagan-Usun	CUR	50.1	88.4		SKM
Novosibirsk	NOV	54.9	83.2		SKM ChISS
Eltsovka	ELT	53.1	86.3		SKM
Ersin	ERN	50.3	95.2		SKM
Verkh-basa	VEN	53.3	90.3		SKM
Ust-Elegest	UER	51.6	94.1		SKM
Ust-Kan	USK	50.9	84.8		SKM
Tehely	TEL	51.0	90.2		SKM
North-East Siberia					
Yakutsk	YAK	62.0	129.7		SKM
Magadan	MAG	59.5	150.8	SKD	
Tiksi	TIK	71.6	128.8	SKD	SKM
Arctic					
Kheis	KHE	80.6	58.2	SKD	SKM
Iultin	ILT	67.8	178.7	SKD	SKM
Kamchatka					
Petropavlovsk	PET	53.0	158.6	SKD	SKM
Kluchi	KLC	56.7	160.9	SKD	
Far East					
Vladivostok	VLA	43.1	131.9	SKD	SKM
Yuzh.Sakhalinsk	YSS	47.0	142.8	SKD	SKM
Okha	OKH	53.6	142.9	SKD	
Uglegorsk	UGL	49.1	142.1	SKD	SKM

## APPENDIX 2

Table 19: Regional Station Corrections dMLH (Horizontal Component) by Landireva [1974] for Six Epicentral Zones

Stat.	Aleuts	Kamchatka	Kuril	Japan	Anatolia	Caucasus
ABD	-0.40	-0.60	-0.40	-0.30		0.00
AND					0.12	-0.35
APT	0.10	00.00	-0.10	-0.10	-0.09	-0.12
BKR					0.03	0.03
BKU					-0.20	0.14
DUS						-0.13
EKA	0.00	-0.10	0.10	-0.20	0.09	0.19
FRU	-0.10	-0.10	-0.10	00.00	0.13	0.00
GAR					0.40	0.17
GRS	0.00	0.10	0.00	0.10	-0.03	0.02
IRK	0.10	0.10	0.00	-0.20	0.07	
IUL					0.07	0.00
KHE	0.10	0.20			-0.22	-0.10
KHR	0.10	0.00	0.00	0.00	0.40	0.40
KLC		0.50				
KRV					-0.16	0.23
KSH	-0.10	-0.10	-0.10	-0.10	0.34	0.40
KZA					0.00	
LVV	-0.10	-0.20	-0.20	-0.30	0.20	0.08
MAG	0.30	0.60	0.70	0.60	-0.21	
MAK					-0.09	-0.27
MOS	0.00	0.00	0.00	0.00	0.33	0.11
OBN					0.21	0.15
OKH		0.30	0.50			
PET	0.50	0.70	0.50	0.50	-0.19	-0.20
PRZ					0.10	
PUL	0.10	0.10	0.20	0.00	0.08	0.07
SEM	-0.20	0.00	0.00	0.00	0.35	0.15
SIM	-0.10	-0.20	0.00	0.10	0.60	0.50
SOC					0.42	0.30
TAS	-0.10	-0.10	-0.10	0.00	0.11	-0.04
TBL	-0.60	-0.40		-0.40	0.03	0.00
TIK	0.30	0.40	0.20	0.40	-0.09	0.10
TLG					0.30	0.20
UGL	0.40	0.40	0.50	0.50		
VLA	0.40	0.30	0.40	0.50	-0.12	-0.20
UZG	0	0	0	0	0.02	0.06
YAK	0.20	00.00	0.20	0	-0.21	
YAL	0	0	0	0		
YER	0	0	0	0	-0.27	
YSS	0.50	0.50	0.60	0.50	-0.24	

Table 20: Regional Station Corrections dMLH (Horizontal Component) by Landyrevva [1974] for Seven Epicentral Zones

Stat.	Iran	Central Asia	Baikal	Alaska	Philip-pines	Mediterranean	Kopet-Dag
ABD		-0.10	-0.20	-0.50	-0.20	-0.06	-0.01
AND		-0.28			-0.10	-0.17	-0.39
APT	0.00	-0.20		0.20	-0.10	-0.12	-0.07
ATA		-0.08		-0.40		-0.10	
BKR		0.20				0.08	0.27
BKU		0.10				-0.20	0.40
DUS		0.00				0.30	-0.25
EKA	0.10	-0.08	0.10	0.10	0.00	0.03	0.14
FRU	-0.20	0.08	-0.10	-0.60	-0.10	0.00	-0.12
GAR		0.13					0.17
GRO				-0.60			
GRS	0.20	0.60	0.60	0.00	0.20	0.20	0.26
IRK	-0.20	0.20		-0.20	0.00	-0.12	-0.17
IUL		0.00				0.11	-0.14
KHE		0.12		0.20	-0.30	-0.16	-0.05
KHR	0.00	0.20	0.10	-0.20	0.20	0.31	0.30
KRV		0.40				-0.07	0.50
KSH		-0.04			0.00	0.18	0.34
KZA		0.00	-0.20			0.04	
LVV	-0.10	-0.07		0.20	-0.10	0.19	0.11
MAG					0.30	-0.11	-0.22
MAK		-0.15				0.13	0.26
MOS	0.30	-0.09	0.10	0.30	-0.10	0.02	0.30
NRN		0.24					
OBV		0.06				0.10	0.33
PET		0.16	0.03	0.10	0.00	-0.25	-0.20
PRZ		0.11					-0.27
PUL	0.10	-0.07	0.00	0.30	-0.10	-0.01	0.14
SEM	0.30	0.00			0.00	0.07	-0.03
SIM	0.30	0.30		0.10	0.00	0.36	0.40
SOC	-0.10	0.30		0.10		0.37	0.24
TAS	-0.20	-0.12	0.30	-0.30	0.20	0.13	-0.18
TBL		0.14	0.00	-0.30	-0.30	0.10	0.09
TIK	-0.30	0.07		0.10	0.10	-0.18	-0.18
TLG		0.26				0.14	0.00
UGL						-0.12	
UZG		-0.14				0.12	0.15
VLA	-0.30	0.04		-0.20	0.00	-0.24	-0.28
YAK		0.16		-0.30	0.10	-0.11	-0.31
YAL						0.60	
YER		0.40		0.10		0.20	0.12
YSS	-0.40	0.00	0.20	0.00	0.00	-0.36	-0.38

Table 21: Regional Station Corrections dMLH (Horizontal component) from Vanek et al.[1980] for Five Epicentral Zones

Stat.	Mean	Alaska	Japan	Philip.	Asia	Mediterr.
BKR	.11	-.01	.11	.11	.37	.11
CLL	.02	.22	.02	-.07	.02	.02
FRU	-.16	-.16	-.01	-.16	-.16	-.16
GRO	-.49	-.59	-.49	-.49	-.49	-.49
GRS	.53	.19	.53	.53	.53	.53
ILT	.17	.17	.42	.17	-.18	.17
IRK	.08	-.08	.08	.08	-.03	.08
KHE	.06	.06	.06	-.24	-.23	.06
KRA	.17	.37	.17	.17	.17	.17
KRV	.22	-.03	.22	.22	.55	.22
MAG	.17	.17	.80	.17	-.09	.17
MAK	-.24	-.35	-.24	-.24	-.24	.24
MOX	.05	.31	.05	-.06	.05	.05
OBN	0.00	0.00	0.00	0.00	0.00	0.00
PET	.15	.15	.53	.15	-.02	.15
PRU	.06	.24	.06	.06	.06	.06
PRZ	-.32	-.32	-.32	-.32	-.32	-.32
PUL	.15	.15	.15	-.15	-.06	.15
PYA	-.04	-.04	-.04	-.04	-.04	-.04
SEM	.08	-.09	.08	.08	.08	.08
SIM	.07	-.04	.07	.07	.24	.07
SOC	.09	.09	.09	.09	.20	.09
SOF	.02	.02	.02	.02	.21	.02
TAS	-.17	-.17	-.17	-.17	-.17	-.17
TIK	.01	.01	.34	.01	-.17	.01
VLA	.17	.17	.17	.17	-.02	-.15
YSS	.08	.29	.08	.08	-.04	.08
ZAK	.11	-.06	.11	.11	.11	.11

Table 22: Regional Station Magnitude Correction dMLV  
(Vertical Component) from Vanek et al.[1980] for Five Zones

Stat.	Mean	Alaska	Japan	Philip.	Asia	Mediterr.
BKR	.47	.32	.47	.47	.47	.47
CLL	.09	.09	.09	-.12	-.03	.09
FRU	-.11	-.11	.07	-.11	-.11	-.11
GRO	.06	-.10	.06	.06	.06	.06
GRS	.76	.76	.76	.76	.76	.76
ILT	.20	.20	.46	.20	-.17	.20
IRK	.08	-.06	.08	.08	-.19	.08
KHE	.11	.11	.11	-.21	-.12	.11
KRA	.17	.17	.17	.17	.17	.17
KRV	.45	.08	.45	.45	.45	.45
MAG	.32	.21	.77	.32	.25	.32
MAK	.10	-.08	.10	.10	.10	.10
MOX	.07	.24	.07	-.09	-.02	.07
OBN	0.00	0.00	0.00	0.00	0.00	0.00
PET	.26	.26	.60	.26	.26	.26
PRU	.47	.47	.47	.47	.47	.47
PRZ	-.10	.03	.03	.03	-.09	.03
PUL	.18	.18	.18	-.09	.03	.18
PYA	.15	.15	.15	.15	.15	.15
SEM	.15	-.16	.15	.15	.15	.15
SIM	.13	-.07	.13	.13	.36	.13
SOC	.35	.27	.35	.35	.35	.25
SOF	-.01	-.01	-.01	.15	.19	-.01
TAS	.05	.05	.05	.05	.31	.05
TIK	0.00	0.00	.39	0.00	0.00	0.00
VLA	.28	.28	.28	.28	.07	.28
YSS	.30	.33	.72	.30	.05	.30
ZAK	.04	-.22	.04	.04	.04	.04

# APPENDIX 3

Table 29: Station Magnitude Residual dM and Their Standard Deviation s for Horizontal (H) and Vertical (V) Components from SKM and SKD Records at Hard Rocks and Sediments Obtain by Coda Method for Stations of Regional Networks at Central Asia and Caucasus

Station	SKM				SKD			
	H		V		H		V	
	dM	s	dM	s	dM	s	dM	s
KAZAKHSTAN								
Hard rocks								
TLG	0.00	0.15	0.05	0.14	-0.05	0.19	-0.15	0.14
KAS	0.25	0.12	0.20	0.12	-0.10	0.15	-0.25	0.11
TUR	0.20	0.19	0.10	0.19	-0.05	0.17	-0.10	0.18
KUR	0.05	0.17	0.00	0.18	-0.20	0.21	-0.20	0.21
Aver.	0.12	0.16	0.09	0.16	-0.10	0.18	-0.18	0.16
Sediments								
ATA	0.60	0.10	0.60	0.11	0.15	0.16	0.00	0.18
TDK	0.35	0.17	0.10	0.13	-0.15	0.14	-0.20	0.16
Aver.	0.48	0.14	0.35	0.12	0.00	0.15	-0.10	0.17
=====								
KYRGYZSTAN								
Hard rocks								
OSH	0.25	0.13	0.20	0.15				
KDZ	0.00	0.20	0.00	0.17	-0.15	0.15	-0.30	0.18
SFK	0.10	0.15	0.10	0.16	-0.40	0.14	-0.40	0.15
CHW	-0.10	0.12	-0.10	0.16				
BAT	0.35	0.14	0.30	0.13	-0.20	0.12	-0.20	0.13
Aver.	0.12	0.15	0.12	0.16	-0.25	0.14	-0.30	0.15
Sediments								
OSH					-0.25	0.15	-0.35	0.21
FRU	0.45	0.13	0.45	0.13	-0.05	0.20	-0.20	0.14
ERK	0.50	0.13	0.40	0.16	-0.25	0.15	-0.25	0.13
Aver.	0.48	0.13	0.42	0.15	-0.18	0.17	-0.27	0.16
=====								



Table 29 (Continued)

Station	SKM				SKD			
	H		V		H		V	
	dM	s	dM	s	dM	s	dM	s
TADJIKISTAN								
Hard rocks								
HRG	0.25	0.09	0.20	0.12	-0.30	0.19	-0.25	0.20
GAR	0.25	0.10	0.10	0.09	-0.10	0.15	-0.15	0.15
CHG	0.25	0.10	0.05	0.11				
GZN	0.25	0.10	0.10	0.12				
DJR	0.20	0.10	0.15	0.14				
HRT	0.35	0.14	0.20	0.12				
Aver.	0.25	0.11	0.14	0.12	-0.20	0.16	-0.20	0.16
Sediments								
DUS	0.75	0.10	0.75	0.12	0.15	0.11	0.10	0.12
GIS	0.65	0.11	0.50	0.12	0.20	0.12	0.05	0.14
KLB					0.10	0.12		
SRT	0.50	0.13	0.45	0.12				
Aver.	0.65		0.56	0.12	0.15	0.12	0.08	0.13
=====								
UZBEKISTAN								
Hard rocks								
TST	0.20	0.12	0.10	0.15				
DGZ	0.20	0.12	0.15	0.19				
NUR	0.25	0.15	0.25	0.14				
ZRB	0.10	0.14	0.05	0.12				
TMB	0.25	0.11	0.20	0.11				
HBS	0.25	0.11	0.20	0.13				
NNK	0.35	0.09	0.30	0.11				
Aver.	0.23	0.12	0.18	0.14				
Sediments								
TAS	0.85	0.13	0.80	0.13	0.30	0.09	0.05	0.11
FRG	0.30	0.13	0.30	0.12	0.00	0.15	0.00	0.10
SAM					0.05	0.11	-0.30	0.10
Aver.	0.58	0.13	0.55	0.13	0.12	0.12	-0.08	0.10
=====								
TURKMENISTAN								
Hard rocks								
VAN	0.10	0.16	-0.05	0.09	0.15	0.09	0.05	0.13
KRA	-0.05	0.23	-0.15	0.25	0.10	0.12	0.00	0.10
Aver.	0.03	0.20	-0.10	0.18	0.13	0.11	0.02	0.12

Table 29 (Continued)

Station	SKM				SKD			
	H		V		H		V	
	dM	s	dM	s	dM	s	dM	s
Sediments								
ASB	0.70	0.19	0.55	0.16	0.50	0.19	0.40	0.20
KAU	0.50	0.14	0.40	0.17				
KKL	0.40	0.12	0.35	0.23				
GAU	0.05	0.17	-0.10	0.14				
NEB	0.15	0.15	-0.00	0.18	0.15	0.14	0.05	0.17
GER	0.15	0.19	-0.05	0.17				
Aver.	0.33	0.17	0.19	0.18	0.33	0.17	0.22	0.19
=====								
AZERBAIDJAN								
Hard Rocks								
BAL	0.14	0.12	0.00	0.08	0.06	0.04	-0.22	0.05
KRV	-0.04	0.13	-0.15	0.10	-0.11	0.12	-0.32	0.13
Aver.	0.05	0.13	-0.08	0.09	-0.03	0.08	-0.27	0.09
Sediments								
SHK	0.20	0.13	0.13	0.15	-0.22	0.15	-0.38	0.05
NCV	0.25	0.15	0.18	0.07	-0.06	0.14	-0.16	0.10
PRK	0.47	0.16	0.33	0.05	0.14	0.17	-0.05	0.12
SHM	0.69	0.13	0.56	0.12	0.51	0.13	0.39	0.14
Aver.	0.43	0.14	0.33	0.10	0.12	0.15	-0.05	0.13
=====								
ARMENIA								
Hard Rocks								
STE	0.25	0.11	0.20	0.13	0.25	0.08	0.00	0.11
KDG	-0.15	0.10	-0.30	0.12	0.10	0.13	0.00	0.13
IDG	0.05	0.09	0.00	0.09				
MEZ	0.00	0.10	0.00	0.12				
Aver.	0.15	0.10	-0.02	0.12	0.18	0.11	0.00	0.12
Sediments								
LEN	1.40	0.13	0.95	0.19	0.89	0.21	0.50	0.21
YER	0.45	0.10	0.40	0.12	0.60	0.08	0.40	0.08
Aver.	0.93	0.12	0.67	0.16	0.75	0.15	0.45	0.15
=====								

Table 29 (Continued)

Station	SKM				SKD			
	dM	H	s	V	dM	H	s	V
GEORGIA Hard Rocks								
ABA	0.05			-0.10	0.10			0.00
LAG	-0.10			0.05	-0.10			0.00
ONI	0.05			-0.10	0.10			-0.15
BGD	-0.04			0.00				
AKH	0.00			-0.05				
GOR					-0.15			0.10
DST					-0.05			0.00
GEG					-0.20			0.15
Aver.	0.01			0.04	0.05			0.02

Prof. Thomas Ahrens  
Seismological Lab, 252-21  
Division of Geological & Planetary Sciences  
California Institute of Technology  
Pasadena, CA 91125

Prof. Keiiti Aki  
Center for Earth Sciences  
University of Southern California  
University Park  
Los Angeles, CA 90089-0741

Prof. Shelton Alexander  
Geosciences Department  
403 Deike Building  
The Pennsylvania State University  
University Park, PA 16802

Prof. Charles B. Archambeau  
University of Colorado  
JSPC  
Campus Box 583  
Boulder, CO 80309

Dr. Thomas C. Bache, Jr.  
Science Applications Int'l Corp.  
10260 Campus Point Drive  
San Diego, CA 92121 (2 copies)

Prof. Muawia Barazangi  
Cornell University  
Institute for the Study of the Continent  
3126 SNEE Hall  
Ithaca, NY 14853

Dr. Jeff Barker  
Department of Geological Sciences  
State University of New York  
at Binghamton  
Vestal, NY 13901

Dr. Douglas R. Baumgardt  
ENSCO, Inc  
5400 Port Royal Road  
Springfield, VA 22151-2388

Dr. Susan Beck  
Department of Geosciences  
Building #77  
University of Arizona  
Tucson, AZ 85721

Dr. T.J. Bennett  
S-CUBED  
A Division of Maxwell Laboratories  
11800 Sunrise Valley Drive, Suite 1212  
Reston, VA 22091

Dr. Robert Blandford  
AFTAC/TT, Center for Seismic Studies  
1300 North 17th Street  
Suite 1450  
Arlington, VA 22209-2308

Dr. Stephen Bratt  
ARPA/NMRO  
3701 North Fairfax Drive  
Arlington, VA 22203-1714

Dale Breeding  
U.S. Department of Energy  
Recipient, IS-20, GA-033  
Office of Arms Control  
Washington, DC 20585

Dr. Lawrence Burdick  
C/O Barbara Wold  
Dept of Biology  
CA Inst. of Technology  
Pasadena, CA 91125

Dr. Robert Burridge  
Schlumberger-Doll Research Center  
Old Quarry Road  
Ridgefield, CT 06877

Dr. Jerry Carter  
Center for Seismic Studies  
1300 North 17th Street  
Suite 1450  
Arlington, VA 22209-2308

Dr. Martin Chapman  
Department of Geological Sciences  
Virginia Polytechnical Institute  
21044 Derring Hall  
Blacksburg, VA 24061

Mr Robert Cockerham  
Arms Control & Disarmament Agency  
320 21st Street North West  
Room 5741  
Washington, DC 20451,

Prof. Vernon F. Cormier  
Department of Geology & Geophysics  
U-45, Room 207  
University of Connecticut  
Storrs, CT 06268

Prof. Steven Day  
Department of Geological Sciences  
San Diego State University  
San Diego, CA 92182

Dr. Zoltan Der  
ENSCO, Inc.  
5400 Port Royal Road  
Springfield, VA 22151-2388

Dr. Dale Glover  
Defense Intelligence Agency  
ATTN: ODT-1B  
Washington, DC 20301

Dr. Stanley K. Dickinson  
AFOSR/NM  
110 Duncan Avenue  
Suite B115  
Bolling AFB, DC 20332-6448

Dr. Indra N. Gupta  
Multimax, Inc.  
1441 McCormick Drive  
Landover, MD 20785

Prof. Adam Dziewonski  
Hoffman Laboratory, Harvard University  
Dept. of Earth Atmos. & Planetary Sciences  
20 Oxford Street  
Cambridge, MA 02138

Dan N. Hagedorn  
Pacific Northwest Laboratories  
Battelle Boulevard  
Richland, WA 99352

Prof. John Ebel  
Department of Geology & Geophysics  
Boston College  
Chestnut Hill, MA 02167

Dr. James Hannon  
Lawrence Livermore National Laboratory  
P.O. Box 808, L-205  
Livermore, CA 94550

Dr. Petr Firbas  
Institute of Physics of the Earth  
Masaryk University Brno  
Jecna 29a  
612 46 Brno, Czech Republic

Dr. Roger Hansen  
University of Colorado, JSPC  
Campus Box 583  
Boulder, CO 80309

Dr. Mark D. Fisk  
Mission Research Corporation  
735 State Street  
P.O. Drawer 719  
Santa Barbara, CA 93102

Prof. David G. Harkrider  
Division of Geological & Planetary Sciences  
California Institute of Technology  
Pasadena, CA 91125

Prof. Donald Forsyth  
Department of Geological Sciences  
Brown University  
Providence, RI 02912

Prof. Danny Harvey  
University of Colorado, JSPC  
Campus Box 583  
Boulder, CO 80309

Dr. Cliff Frolich  
Institute of Geophysics  
8701 North Mopac  
Austin, TX 78759

Prof. Donald V. Helmberger  
Division of Geological & Planetary Sciences  
California Institute of Technology  
Pasadena, CA 91125

Dr. Holly Given  
IGPP, A-025  
Scripps Institute of Oceanography  
University of California, San Diego  
La Jolla, CA 92093

Prof. Eugene Herrin  
Geophysical Laboratory  
Southern Methodist University  
Dallas, TX 75275

Dr. Jeffrey W. Given  
SAIC  
10260 Campus Point Drive  
San Diego, CA 92121

Prof. Robert B. Herrmann  
Department of Earth & Atmospheric Sciences  
St. Louis University  
St. Louis, MO 63156

Prof. Lane R. Johnson  
Seismographic Station  
University of California  
Berkeley, CA 94720

Dr. William Leith  
U.S. Geological Survey  
Mail Stop 928  
Reston, VA 22092

Prof. Thomas H. Jordan  
Department of Earth, Atmospheric &  
Planetary Sciences  
Massachusetts Institute of Technology  
Cambridge, MA 02139

Mr. James F. Lewkowicz  
Phillips Laboratory/GPE  
29 Randolph Road  
Hanscom AFB, MA 01731-3010( 2 copies)

Prof. Alan Kafka  
Department of Geology & Geophysics  
Boston College  
Chestnut Hill, MA 02167

Prof. L. Timothy Long  
School of Geophysical Sciences  
Georgia Institute of Technology  
Atlanta, GA 30332

Robert C. Kemerait  
ENSCO, Inc.  
445 Pineda Court  
Melbourne, FL 32940

Dr. Randolph Martin, III  
New England Research, Inc.  
76 Olcott Drive  
White River Junction, VT 05001

U.S. Dept of Energy  
Max Koontz, NN-20, GA-033  
Office of Research and Develop.  
1000 Independence Avenue  
Washington, DC 20585

Dr. Robert Masse  
Denver Federal Building  
Box 25046, Mail Stop 967  
Denver, CO 80225

Dr. Richard LaCoss  
MIT Lincoln Laboratory, M-200B  
P.O. Box 73  
Lexington, MA 02173-0073

Dr. Gary McCartor  
Department of Physics  
Southern Methodist University  
Dallas, TX 75275

Dr. Fred K. Lamb  
University of Illinois at Urbana-Champaign  
Department of Physics  
1110 West Green Street  
Urbana, IL 61801

Prof. Thomas V. McEvelly  
Seismographic Station  
University of California  
Berkeley, CA 94720

Prof. Charles A. Langston  
Geosciences Department  
403 Deike Building  
The Pennsylvania State University  
University Park, PA 16802

Dr. Art McGarr  
U.S. Geological Survey  
Mail Stop 977  
U.S. Geological Survey  
Menlo Park, CA 94025

Jim Lawson, Chief Geophysicist  
Oklahoma Geological Survey  
Oklahoma Geophysical Observatory  
P.O. Box 8  
Leonard, OK 74043-0008

Dr. Keith L. McLaughlin  
S-CUBED  
A Division of Maxwell Laboratory  
P.O. Box 1620  
La Jolla, CA 92038-1620

Prof. Thorne Lay  
Institute of Tectonics  
Earth Science Board  
University of California, Santa Cruz  
Santa Cruz, CA 95064

Stephen Miller & Dr. Alexander Florence  
SRI International  
333 Ravenswood Avenue  
Box AF 116  
Menlo Park, CA 94025-3493

Prof. Bernard Minster  
IGPP, A-025  
Scripps Institute of Oceanography  
University of California, San Diego  
La Jolla, CA 92093

Prof. Brian J. Mitchell  
Department of Earth & Atmospheric Sciences  
St. Louis University  
St. Louis, MO 63156

Mr. Richard J. Morrow  
USACDA/IVI  
320 21st St. N.W.  
Washington, DC 20451

Mr. Jack Murphy  
S-CUBED  
A Division of Maxwell Laboratory  
11800 Sunrise Valley Drive, Suite 1212  
Reston, VA 22091 (2 Copies)

Dr. Keith K. Nakanishi  
Lawrence Livermore National Laboratory  
L-025  
P.O. Box 808  
Livermore, CA 94550

Prof. John A. Orcutt  
IGPP, A-025  
Scripps Institute of Oceanography  
University of California, San Diego  
La Jolla, CA 92093

Prof. Jeffrey Park  
Kline Geology Laboratory  
P.O. Box 6666  
New Haven, CT 06511-8130

Dr. Howard Patton  
Lawrence Livermore National Laboratory  
L-025  
P.O. Box 808  
Livermore, CA 94550

Dr. Frank Pilotte  
HQ AFTAC/TT  
1030 South Highway A1A  
Patrick AFB, FL 32925-3002

Dr. Jay J. Pulli  
Radix Systems, Inc.  
201 Perry Parkway  
Gaithersburg, MD 20877

Dr. Robert Reinke  
ATTN: FCTVTD  
Field Command  
Defense Nuclear Agency  
Kirtland AFB, NM 87115

Prof. Paul G. Richards  
Lamont-Doherty Earth Observatory  
of Columbia University  
Palisades, NY 10964

Mr. Wilmer Rivers  
Teledyne Geotech  
1300 17th St N #1450  
Arlington, VA 22209-3803

Dr. Alan S. Ryall, Jr.  
ARPA/NMRO  
3701 North Fairfax Drive  
Arlington, VA 22203-1714

Dr. Chandan K. Saikia  
Woodward Clyde- Consultants  
566 El Dorado Street  
Pasadena, CA 91101

Dr. Richard Sailor  
TASC, Inc.  
55 Walkers Brook Drive  
Reading, MA 01867

Prof. Charles G. Sammis  
Center for Earth Sciences  
University of Southern California  
University Park  
Los Angeles, CA 90089-0741

Prof. Christopher H. Scholz  
Lamont-Doherty Earth Observatory  
of Columbia University  
Palisades, NY 10964

Dr. Susan Schwartz  
Institute of Tectonics  
1156 High Street  
Santa Cruz, CA 95064

Mr. Dogan Seber  
Cornell University  
Inst. for the Study of the Continent  
3130 SNEE Hall  
Ithaca, NY 14853-1504

Secretary of the Air Force  
(SAFRD)  
Washington, DC 20330

Office of the Secretary of Defense  
DDR&E  
Washington, DC 20330

Thomas J. Sereno, Jr.  
Science Application Int'l Corp.  
10260 Campus Point Drive  
San Diego, CA 92121

Dr. Michael Shore  
Defense Nuclear Agency/SPSS  
6801 Telegraph Road  
Alexandria, VA 22310

Dr. Robert Shumway  
University of California Davis  
Division of Statistics  
Davis, CA 95616

Dr. Matthew Sibol  
Virginia Tech  
Seismological Observatory  
4044 Derring Hall  
Blacksburg, VA 24061-0420

Prof. David G. Simpson  
IRIS, Inc.  
1616 North Fort Myer Drive  
Suite 1050  
Arlington, VA 22209

Donald L. Springer  
Lawrence Livermore National Laboratory  
L-025  
P.O. Box 808  
Livermore, CA 94550

Dr. Jeffrey Stevens  
S-CUBED  
A Division of Maxwell Laboratory  
P.O. Box 1620  
La Jolla, CA 92038-1620

Prof. Brian Stump  
Los Alamos National Laboratory  
EES-3  
Mail Stop C-335  
Los Alamos, NM 87545

Prof. Jeremiah Sullivan  
University of Illinois at Urbana-Champaign  
Department of Physics  
1110 West Green Street  
Urbana, IL 61801

Prof. L. Sykes  
Lamont-Doherty Earth Observatory  
of Columbia University  
Palisades, NY 10964

Dr. Steven R. Taylor  
Los Alamos National Laboratory  
P.O. Box 1663  
Mail Stop C335  
Los Alamos, NM 87545

Prof. Tuncay Taymaz  
Istanbul Technical University  
Dept. of Geophysical Engineering  
Mining Faculty  
Maslak-80626, Istanbul Turkey

Prof. Clifford Thurber  
University of Wisconsin-Madison  
Department of Geology & Geophysics  
1215 West Dayton Street  
Madison, WI 53706

Prof. M. Nafi Toksoz  
Earth Resources Lab  
Massachusetts Institute of Technology  
42 Carleton Street  
Cambridge, MA 02142

Dr. Larry Turnbull  
CIA-OSWR/NED  
Washington, DC 20505

Dr. Gregory van der Vink  
IRIS, Inc.  
1616 North Fort Myer Drive  
Suite 1050  
Arlington, VA 22209

Dr. Karl Veith  
EG&G  
5211 Auth Road  
Suite 240  
Suitland, MD 20746



Prof. Terry C. Wallace  
Department of Geosciences  
Building #77  
University of Arizona  
Tuscon, AZ 85721

Phillips Laboratory  
ATTN: GPE  
29 Randolph Road  
Hanscom AFB, MA 01731-3010

Dr. Thomas Weaver  
Los Alamos National Laboratory  
P.O. Box 1663  
Mail Stop C335  
Los Alamos, NM 87545

Phillips Laboratory  
ATTN: TSML  
5 Wright Street  
Hanscom AFB, MA 01731-3004

Dr. William Wortman  
Mission Research Corporation  
8560 Cinderbed Road  
Suite 700  
Newington, VA 22122

Phillips Laboratory  
ATTN: PL/SUL  
3550 Aberdeen Ave SE  
Kirtland, NM 87117-5776 (2 copies)

Prof. Francis T. Wu  
Department of Geological Sciences  
State University of New York  
at Binghamton  
Vestal, NY 13901

Dr. Michel Bouchon  
I.R.I.G.M.-B.P. 68  
38402 St. Martin D'Herès  
Cedex, FRANCE

Prof Ru-Shan Wu  
University of California, Santa Cruz  
Earth Sciences Department  
Santa Cruz, CA 95064

Dr. Michel Campillo  
Observatoire de Grenoble  
I.R.I.G.M.-B.P. 53  
38041 Grenoble, FRANCE

ARPA, OASB/Library  
3701 North Fairfax Drive  
Arlington, VA 22203-1714

Dr. Kin Yip Chun  
Geophysics Division  
Physics Department  
University of Toronto  
Ontario, CANADA

HQ DNA  
ATTN: Technical Library  
Washington, DC 20305

Prof. Hans-Peter Harjes  
Institute for Geophysics  
Ruhr University/Bochum  
P.O. Box 102148  
4630 Bochum 1, GERMANY

Defense Technical Information Center  
8725 John J. Kingman Road  
Ft Belvoir, VA 22060-6218  
(2 copies)

Prof. Eystein Husebye  
NTNF/NORSAR  
P.O. Box 51  
N-2007 Kjeller, NORWAY

TACTEC  
Battelle Memorial Institute  
505 King Avenue  
Columbus, OH 43201 (Final Report)

David Jepsen  
Acting Head, Nuclear Monitoring Section  
Bureau of Mineral Resources  
Geology and Geophysics  
G.P.O. Box 378, Canberra, AUSTRALIA

Phillips Laboratory  
ATTN: XPG  
29 Randolph Road  
Hanscom AFB, MA 01731-3010

Ms. Eva Johannisson  
Senior Research Officer  
FOA  
S-172 90 Sundbyberg, SWEDEN

Dr. Peter Marshall  
Procurement Executive  
Ministry of Defense  
Blacknest, Brimpton  
Reading FG7-FRS, UNITED KINGDOM

Dr. Bernard Massinon, Dr. Pierre Mechler  
Societe Radiomana  
27 rue Claude Bernard  
75005 Paris, FRANCE (2 Copies)

Dr. Svein Mykkeltveit  
NTNT/NORSAR  
P.O. Box 51  
N-2007 Kjeller, NORWAY (3 Copies)

Prof. Keith Priestley  
University of Cambridge  
Bullard Labs, Dept. of Earth Sciences  
Madingley Rise, Madingley Road  
Cambridge CB3 0EZ, ENGLAND

Dr. Jorg Schlittenhardt  
Federal Institute for Geosciences & Nat'l Res.  
Postfach 510153  
D-30631 Hannover, GERMANY

Dr. Johannes Schweitzer  
Institute of Geophysics  
Ruhr University/Bochum  
P.O. Box 1102148  
4360 Bochum 1, GERMANY

Trust & Verify  
VERTIC  
Carrara House  
20 Embankment Place  
London WC2N 6NN, ENGLAND